MOLECULAR MECHANISMS UNDERLYING TDP-43 AND C9ORF72 TOXICITY IN AMYOTROPHIC LATERAL SCLEROSIS

Baskaran, Pranetha

Awarding institution:
King's College London

MOLECULAR MECHANISMS UNDERLYING TDP-43 AND C9ORF72 TOXICITY IN AMYOTROPHIC LATERAL SCLEROSIS

PRANETHA BASKARAN

4 YEAR NEUROSCIENCE PHD

2015

Acknowledgement

I would like to express my sincere gratitude to my supervisors Prof. Sarah Guthrie and Prof. Chris Shaw for their guidance and support throughout my PhD study. Thank you Dr. Poopalasundaram, Ms. Dopplapudi, Dr. Poparic, Ms. Hunter, Dr. Montague, Mr. Austen, Dr. Carretero Rodriguez for all the help, advice and the good times.

My sincere thanks to Ms. Vinu Priya, Mr. Glady Dhinakaran and Mr. Sujendra Vijayagiri. Without their love and precious support it would not be possible to have completed my study. Thank you for staying through it all.

Last but not the least; I would like to thank my family for making all of this possible and for giving me the courage to reach for the stars. Thank you Mummy, Daddy, Perips, Jhansima, Pri, Eugi and Hari for all the love.

Abstract

Amyotrophic lateral sclerosis (ALS) is a late onset adult neurodegenerative disease characterised by progressive muscular paralysis, reflecting degeneration of upper and lower motor neurons in the primary motor cortex, corticospinal tracts, brainstem and spinal cord. This project investigates the molecular mechanisms underlying toxicity in ALS. The presence of ubiquitinated misfolded protein inclusions in the cytoplasm/nucleus of neurons is the key feature of most neurodegenerative diseases. Several research groups have shown that mutations in the gene encoding TDP43 are causative in ALS. TDP43 has DNA and RNA binding properties, and is involved in RNA splicing, transport and stability. Local translation of mRNA plays a key role in axonal guidance to targets, synapse formation and maintenance and neuronal survival – processes which may misfunction in ALS. Genetic studies have also identified expansion repeat number as a key factor in several degenerative diseases. The GGGGCC (G4C2) intronic repeat expansion within C9ORF72 has been identified as the most common genetic cause of amyotrophic lateral sclerosis and frontotemporal dementia (FTD). Intranuclear neuronal RNA foci have been observed in ALS and FTD tissues, suggesting that G4C2 RNA may be toxic to neurons. Here I use the rat primary cortical neurons in vitro and the chick embryonic system in vivo to model the acute effects of TDP43 and the G4C2 repeats. My in vitro experiments show that overexpression of mutant and wild-type TDP43 is toxic to cortical neurons and that TDP43 mis-localizes to the cytoplasm over time. Neuronal disintegration through mRNA mislocalization and cytoskeletal disorganization by TDP43 could be an underlying pathological mechanism in ALS. G4C2 repeats initiate apoptotic cell death in chick embryonic motor neurons in vivo. Increase in repeat number increases cytotoxicity. RNA and protein toxicity play a key role in the G4C2 disease mechanism. We propose that aberrant regulation of RNA processing, protein sequestering and disruption of cytoskeletal integrity may contribute to neurodegeneration.

Molecular mechanisms underlying TDP-43 and C9ORF72 toxicity in Amyotrophic lateral sclerosis

Contents

Abbreviations

ActB	β – actin
ALS	Amyotrophic lateral sclerosis
ALSbi	ALS with behavioural impairment
ALSci	ALS with cognitive impairment
ALS-FTD	Amyotrophic lateral sclerosis - frontotemporal dementia
ANG	Angiogenin
ANOVA	Analysis of variance
APEX1	Apurinic endonuclease
ATXN2	Andataxin-2
BCIP	5-bromo-4-chloro-3-indolyl-phosphate
BSA (fraction V)	Bovine Serum Albumin - Fraction V
bvFTD	Behavioural variant frontal temporal dementia
C9ORF72	Chromosome 9 open reading frame 72
CBD	Corticobasal degeneration
CBS	Corticobasal syndrome
CFTR	Cystic fibrosis transmembrane conductance regulator
CHMP2B	Charged multi vesicular body protein 2B
CNS	Central nervous system
CT	Computed tomography
CTE	Chronic traumatic encephalopathy
DAB	Diaminobenzidine
DCTN1	Subunit of dynactin
DENN	Differentially expressed in normal and neoplastic cell
DEPC	Diethylpyrocarbonate
DGCR8	DiGeorge critical region 8
DLDH	Dementia lacking distinctive histopathology
DM1	Myotonic dystrophy type I

DM2	Myotonic dystrophy type 2
DNA	Deoxyribonucleic acid
DPR	Dps- like peroxide resistance
EDTA	Ethylenediaminetetraacetic acid
EGFP	Enhanced Green Fluorescent Protein
ESC	Embryonic stem cell
ESCRTIII	Endosomal sorting complex III
ESCRTs	Endosomal sorting complexes required for transport
fALS	Familial Amyotrophic lateral sclerosis
FBS	Fetal bovine serum
FTD-ALS	Frontal temporal dementia with ALS
FTLD/FTD	Frontotemporal lobar Dementia
FTLD-U	FTD with Ubiquitin positive inclusions
FUS	Fused in sarcoma
fvFTD	Frontal variant or behavioural variant FTD
FXTAS	Fragile X Tremor/Ataxia Syndrome
GA	GlyAla
GEMs	Gemini of coiled bodies
GFP	Green Fluorescent Protein
GGGGCC / G4C2	Hexanucleotide repeat expansion
GP	PolyGlyPro
GPAS	Antisense GP protein
GR	GlyArg
H1/H2	Haplotype influences
HBSS	Hanks' Balanced Salt Solution
HDAC6	Histone deacetylase 6
HH	Hamburger-Hamilton stages
HITS- CLIP	Highthroughput sequencing of RNA isolated by crosslinking immunoprecipitation

HIV	Human immunodeficiency virus
HnRNP	Heterogeneous nuclear ribonucleoprotein
hnRNPA1 and *hnRNPA2/B1*	Heterogeneous nuclear ribonucleoprotein A1 and A2/B1
IBMPFD	Inclusion body myopathy with Paget disease of the bone
Kif2A	Kinesin Heavy Chain Member 2A
LMN	Lower motor neuron
LPA	Logopenic progressive aphasia
MABT	Maleic acid buffer containing Tween 20
Map1B	Microtubule associated protein 1B
Map2	Microtubule associated protein 2
MAPT	Microtubule associated protein tau
MFN1	Mitochondria fission/fusion proteins
miRNA	MicroRNA
MND	Motor neuron disease
MRI	Magnetic resonance imaging
MT	Microtubule
MVB	Multi vesicular bodies
NBT	Nitro blue tetrazolium
NCI	Nuclear cytoplasmic inclusions
ncRNAs	Non coding RNA
NEALS	Northeast ALS
NEK1	NIMA related kinase 1
NES	Nuclear export domain
NF	Neurofilament
NFL	Neurofilament light chain
nfvPPA	Nonfluent variant PPA
NIH	National Institute of Health
ND1-L	Novel Kelch family protein Nd1-L
NLS	Nuclear localisation domain

NTMT solution	Sodium, Tris-HCl, Magnesium Cholride, Tween 20 Buffer
OPCD	Olivopontocerebellar degeneration
OPTN	Optineurin
PA	PolyProAla
PBS-T	Phosphate buffered saline Tween
PD	Parkinson disease
PFA	Paraformaldehyde
PGRN	Progranulin
PiD	Pick's disease
PNFA	Progressive nonfluent aphasia
PPA	Primary progressive aphasia
PR	polyProArg
Pri- miRNA	Primary miRNA transcript
PSP	Progressive supranuclear palsy
Rab-GEF	Rab guanine- diphosphate/triphosphate exchange factor
RAN	Repeat associated non ATG translation
RBP	mRNA binding protein
RISC	RNA induced silencing complex
RLU	Relative light unit
RNA	Ribonucleic acid
sALS	Sporadic amyotrophic lateral scelerosis
SCA8	Spinocerebellar ataxia type 8
SD	Semantic dementia
SMN	Survival motor neuron
SOD1	Superoxide dismutase gene
SQSTM1	Sequestosome 1
SSC	Saline-sodium citrate buffer
SSRI	Selective serotonin reuptake inhibitors
STAMBP also known as	STAM binding protein

AMSH	
svPPA	Semantic variant PPA
TARDBP / TDP-43/ TDP	TAR DNA Binding Protein
TBK1	Tank binding Kinase 1
TE Buffer	Tris-EDTA Buffer
TMEM106B	Transmembrane protein 10 6B
TUB4a	Tubulin Alpha 4A
TUNEL	Transferase dUTP Nick End Labeling
UBI	Ubiquinated inclusion
UBQLN	Ubiquilin 1
UBQLN2	Ubiquilin2
UCSF	University of California, San Francisco
UMN	Upper motor neuron
UPR	Unfolded protein response
UPS	Ubiquitin proteasome system
UTR	Untranslated region
UV CLIP	Ultraviolet Cross linking and Immunoprecipitation
VAPB	Vesicle associated membrane protein B
VCP	Valosin containing protein
VEGF	Vascular endothelial growth factor
VSM-20	Vancouver, San Francisco and Mayo family 20
WFN	World Federation of Neurology
WPRE	Woodchuck hepatitis virus posttranscriptional regulatory element
WT	Wild-type

List of Figures

List of Tables

1 INTRODUCTION

1.1 Amyotrophic Lateral Sclerosis

1.1.1 Introduction

The term ‘motor neuron disease’ was introduced into the neurological literature by Brain in 1933 to encompass the spectrum of clinical presentations of patients with degeneration of the upper and the lower motor neurons. This spectrum collectively includes progressive muscular atrophy (Lower motor neuron (LMN) involvement), Charcot ALS, primary lateral sclerosis (Upper Motor Neuron (UMN) involvement) and progressive bulbar palsy (bulbar involvement) (Katirji et al., 2013). In the United States, the term ‘amyotrophic lateral sclerosis’ (ALS) is collectively used to refer to the entire spectrum of patients whereas in Britain, ‘motor neuron disease’ (MND) is more commonly used. MND is frequently used as an all-encompassing term to collectively define a broad category of conditions of various etiologies.

Amyotrophic lateral sclerosis (ALS) is a fatal, late onset progressive motor neurodegenerative disease. The disease is characterized by progressive muscular paralysis reflecting degeneration of motor neurons in the primary motor cortex, corticospinal tracts, brainstem and spinal cord. The word ‘amyotrophic lateral sclerosis’ was coined in 1874 by Charcot, to emphasize the involvement of the lateral corticospinal tract in the disease (Rowland and Shneider, 2001). The term “amyotrophic” refers to the loss of muscle mass while the term “lateral” refers to the tract where nerves run down both sides of the spinal cord which is one of the sites where neurons undergo degeneration. Finally, the term “sclerosis” refers to the scar tissue-like appearance of the spinal cord after degeneration of the descending cerebrospinal tracks. In North America, it is also referred to as ‘Lou Gehrig’s disease’, named after the famous baseball player who was affected by ALS.

1.1.2 Epidemiology

Several factors such as date of disease onset, duration between pathological changes and manifestation of clinical symptoms have complicated epidemiological studies in ALS. (ALS is quite rare in occurrence even though it is the third most common neurodegenerative disease after Alzheimer's and Parkinson's diseases (Kiernan et al., 2011). Population based studies have established that the incidence of ALS in Europe is fairly uniform at 2 per 100,000 population per year. Different populations having similar ALS phenotype may exhibit different clinical presentations across European registries (Logroscino et al., 2010). There is increasing evidence of ethnic variation in the incidence of MND. These studies show that the incidence of ALS is lower in individuals with mixed ancestral origin than in individuals of single origin (Cronin et al., 2007). Epidemiological studies suggest that the incidence of MND is highest in the Caucasian population (Rechtman et al., 2015). Males are usually affected more than females (ratio about 1·6:1), although the incidence between men and women is about the same in familial disease. Peak age at onset is 58–63 years for sporadic disease and 47–52 years for familial disease. Incidence decreases rapidly after 80 years of age (Logroscino et al., 2010). Death occurs in most patients within two to five years after diagnosis.

1.1.3 Aetiology

Most cases are sporadic (sALS) (90-95%), whereas 5-10% is familial (fALS), with a Mendelian pattern of inheritance. MND is a disorder of unknown aetiology, wherein each individual may be affected by a different combination of triggers, both genetic and environmental. The causes of most cases of ALS are as yet undefined. In sporadic or non-inherited ALS, environmental, toxic, viral, or genetic factors may be implicated.

ALS can be inherited in an autosomal dominant, autosomal recessive or X-linked manner (Kinsley and Siddique, 2012). Considerable progress has been made in comprehending the genetics of ALS in the past decade. The pathobiology of ALS is predicted largely based on studies of ALS-associated gene mutations. Linkage analysis,

candidate gene studies and genome wide association studies have revealed 1/3 of fALS and a small number of sALS genes involved in ALS. Several genes have been implicated in fALS and sALS. The discovery of eleven disease-associated mutations in the superoxide dismutase (SOD1) gene marked the beginning of the study of ALS pathogenesis (Rosen et al., 1993). Several genes have been implicated in ALS viz., TAR DNA-Binding Protein (TARDBP), fused in sarcoma (FUS), Ubiquilin2 (UBQLN2), Chromosome 9 open reading frame 72 (C9ORF72). Some of the sALS mutations include apurinic endonuclease (APEX1), charged multivesicular body protein 2B (CHMP2B), neurofilaments, paraxonase, survival motor neuron (SMN), vascular endothelial growth factor (VEGF), progranulin (PGRN) andataxin-2 (ATXN2). Mitochondrial genes have also been suggested in ALS(Lin and Beal, 2006).

There is a great heterogeneity for genetic spectrum of fALS and sALS. Mutations in the *C9orf72* gene are responsible for 30- 40% of fALS in the United States and Europe. Worldwide, *SOD1* gene mutations cause about 20% of fALS, while *TARDBP and FUS* mutations account for about 5% and *ANG* gene mutations account for around 1%. The other genes that have been associated with fALS each account for a small proportion of cases. It is estimated that 60 percent of individuals with fALS have an identified genetic mutation. The cause of ALS in the remaining individuals remains unknown. Since sALS and fALS share similar clinical and pathological profiles, insights from studies of ALS-causing gene mutations apply to sALS. More than twenty genes have been implicated in ALS, and large scale sequencing studies have identified new risk genes and pathways like Tubulin Alpha 4A (TUB4a)(Smith et al., 2014), Tank binding Kinase 1 (TBK-1) and NIMA related kinase 1 (NEK1) (Cirulli et al., 2015). It is important to investigate the link between the gene-environment connections as 90% of the cases are sporadic. The identification of novel genes and molecular pathways caused by aberrant genes will help broaden our understanding of ALS genetics and pathogenesis and identify strategic approaches to uncover new treatments.

1.1.4 Pathology of ALS

ALS is characterized by degeneration of the corticospinal tracts and extensive loss of lower motor neurons (LMNs) or anterior horn cells, degeneration and loss of Betz cells and other pyramidal cells in the primary motor cortex and reactive gliosis in the motor cortex and spinal cord (Wijesekera and Leigh, 2009). The presence of intracellular ubiquinated inclusions (UBIs) in the LMNs of spinal cord and brain stem and the corticospinal UMNs is a hallmark feature of ALS. The compositions of ubiquitinated inclusions are unknown and can be composed of different type of proteins such as ubiquitin, SOD-1 and peripherin. TDP-43 inclusions, FUS inclusions, Bunina bodies, Hyaline conglomerate inclusions are also found in ALS. Non-motor pathology in ALS comprises of posterior column demyelination and reduced density of myelinated sensory fibres. (Kwong et al., 2008, Ferrari et al., 2011, Hortobágyi et al., 2000, Neumann et al., 2006a)

1.1.5 Pathological Mechanisms of ALS

In the last two decades several experimental models *in vitro* and *in vivo* have shed light into the pathogenesis of the disease. A single mutation can manifest several presentations, suggesting that varying mechanisms influence outcome, and different mutations can present similar ALS phenotypes, implying that different causes sharing similar pathophysiological pathways cause ALS (Ravits et al., 2013). Therefore, ALS is not considered to be a single disease entity. Several potential mechanisms have been implicated in ALS. Pathophysiological mechanisms that contribute to cell death after disease-onset include aberrant RNA function, oxidative stress, excitotoxicity, mitochondrial dysfunction, protein aggregation, generation of free radicals, disrupted axonal transport, mis-regulation of growth factors, non-cell autonomous mechanisms, inflammation, and caspase-mediated cell death (apoptosis)(Chen et al., 2013, Rossi et al., 2013). Despite such research, no direct mechanism for ALS has been identified. Most investigators and clinicians agree that various factors, possibly a combination of some or all of the above processes, may lead to development of the disease(Strong,

2001, Wilson et al., 2001, Bruijn et al., 2004, Shaw, 2005). Whether these mechanisms intertwine, work in parallel or in sequence to cause neuronal death remains to be investigated.

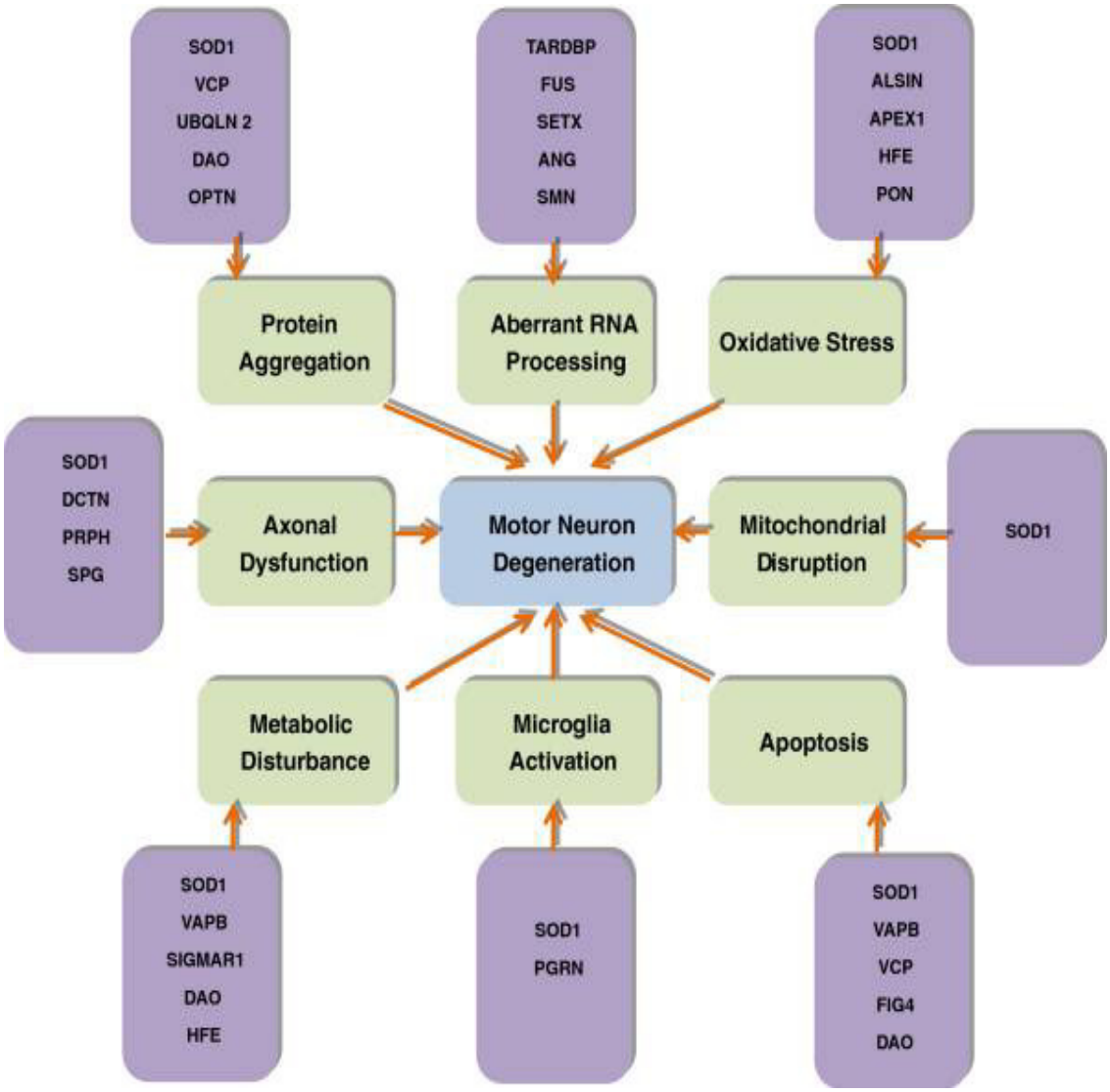

Figure 1.1 ALS genes and mechanism
ALS is caused by interplay of various molecular pathways in motor neurons and an interaction with neighbouring non-neuronal cells like microglia (Taken from (Chen et al., 2013))

1.1.6 Clinical features of ALS

ALS leads to progressive degeneration of the motor neurons that supply voluntary muscles. ALS is relentlessly progressive, 50% of patients die within 30 months of symptom onset and about 20% of patients survive between 5 years and 10 years after symptom onset (Kiernan et al., 2011). The classic presentation of ALS is insidious, progressive, asymmetric muscular weakness and atrophy along with neurologic signs, particularly fasciculations and hyper-reflexia (Walling, 1999). The clinical manifestations depend on the area of the nervous system that is damaged. Disease onset can be upper or lower limb or Bulbar. Symptoms in patients with lower limb onset includes tripping, stumbling and awkwardness while walking or running; while those with upper limb onset may first notice difficulty in actions such as buttoning clothes, picking up small objects or turning keys. Speech problems, such as slurring, hoarseness or decreased volume are the most common presentations in the bulbar form of ALS. LMN degeneration causes fasciculation, cramps, muscle atrophy, spasticity, and hyper-reflexia. Bulbar signs and symptoms include dysarthria, dysphagia, sialorrhea (drooling), tongue atrophy, and tongue fasciculation. Patients with ALS often experience fear, anxiety, depression and weight-loss. The disabilities progress until eventually ventilatory and nutritional assistance is required. Death is usually caused by respiratory failure.

Cognitive impairment is frequently recognised in ALS. Subtle subclinical cognitive defects and frontal lobe dysfunction is seen in up to half of MND patients (Lomen-Hoerth et al., 2003, Ringholz et al., 2005)In spite of the widespread devastating effects of ALS, certain functions are conspicuously unaffected; extraocular muscle movement, bladder and bowel control, sensory function and skin integrity are usually preserved. Recent studies of the various clinical manifestations of ALS have shown that the classical concept that ALS only affects the motor system is obsolete. ALS is now considered to be a multisystem neurodegenerative disease.

1.1.7 Diagnostics, Treatment and Management of ALS

ALS is a difficult disease to diagnose as it requires a series of tests and through clinical examination to rule out other diseases that mimic ALS. The World Federation of Neurology (WFN) has developed an algorithm called El Escorial criteria for diagnosis of ALS. There is no cure yet for ALS, so care is aimed at maintaining quality of life and prolonging life as much as possible. Riluzole, a glutamate antagonist, is the only drug approved by the Food and Drug Administration for the treatment of ALS. Symptomatic and supportive treatments are available to help people be more comfortable while maintaining their quality of life.

1.2 Frontotemporal Lobar Dementia

1.2.1 Introduction

Frontotemporal lobar degeneration (FTLD) refers to a clinically and pathologically group of non Alzheimer form of dementia. FTLD results from degeneration of the cortex of the frontal and temporal lobes, often in conjunction with the degeneration of subcortical brain regions. This gives rise to a spectrum of behavioural, language, and movement disorders. FTLD is characterized by progressive changes in behaviour, executive dysfunction and/or language impairment. The spectrum of FTLD collectively includes behavioural variant frontal-temporal dementia (bvFTD), Pick's disease (PiD), primary progressive aphasia (PPA) and semantic dementia (SD) (Snowden et al., 2002).

Arnold Pick, a Professor of Neuropsychiatry at the German University in Prague was the first to describe lobar cortical atrophy. Formerly, the term Pick's Complex grouped several frontal lobe-temporal lobe dementias such as frontal dementia, primary progressive aphasia, semantic dementia, cortical basal ganglionic degeneration, frontal-temporal dementia with motor neuron disease (FTD-MND), and dementia with ALS (ALS-FTD); the grouping included Pick's disease as a specific type (Riedl et al., 2014). During the 90s, the term Pick's disease was dropped in favor of FTLD with or without Pick bodies. PiD is currently considered as a subgroup of FTLD, which consist of abnormal three-repeat tau protein (FTLD-tau)(Ittner et al., 2011).

1.2.2 Epidemiology

FTLD are a frequent cause of dementia and account for 5% to 10% of all dementia patients and 10% to 20% of patients under 65 years of age (Graff-Radford and Woodruff, 2007). It is the second most common form of neurodegenerative dementias in adulthood, after Alzheimer's disease. It has been difficult to obtain accurate estimates about the incidence and prevalence of FTLD in the general population due to the rarity of the disease, accuracy of diagnosis and variation in diagnostic criteria. The prevalence of FTLD in persons aged between 45 and 64 years in the US is estimated to

be between 15 and 22 cases per 100,000, 15 per 100,000 in the UK, 4 per 100,000 in Netherlands and 22 per 100,000 in Italy. Although estimates vary widely, a positive family history is observed in up to 40% of patients, suggesting a strong genetic component to the disease; but only 10% of cases are inherited in a dominant manner (Coyle-Gilchrist et al., 2016). Onset occurs most commonly between the ages of 45 and 65 years, although the disorder can present before the age of 30 years as well as in the elderly (Snowden et al., 2002). There is no significant difference in the mean age of symptom onset between clinical variants of FTLD. There is an equal incidence in men and women. The mean duration of illness is 7 to 13 years from onset in cases that do not have motor neuron disease, and may be shorter in bvFTD than in PNFA and semantic dementia (Onyike, 2011). The median survival is considerably shorter (3 years) in FTLD cases with concomitant motor neuron disease, although, a subset survive for up to 5 years (Hales and Hu, 2013).

1.2.3 Genetics of FTLD

Genetic background is not only crucial in disease pathogenesis, but it also modulates disease course. While scientists have found gene mutations that are linked to FTLD, most cases of FTLD are sporadic, meaning that there is no known family history of FTLD. Current genetic research shows that if a diagnosed individual has no family history of FTLD or related neurological conditions, there is less than a 10% chance that they carry a mutation in a currently known FTLD gene. FTLD may present an autosomal dominant pattern of inheritance, and mutations within progranulin (PGRN) (Le Ber et al., 2007) and microtubule-associated protein tau (MAPT) are recognized as the most common forms of known genes (Filippi et al., 2016). It has been demonstrated that MAPT H1/H2 haplotype influences clinical FTLD presentation and short-term prognosis in FTLD spectrum (Borroni et al., 2010); on the other hand, apolipoprotein E (APOE) genotype, beyond being the most recognized genetic risk factor for late-onset Alzheimer's disease, might modulate the FTLD clinical picture (Borroni et al., 2006). More recently, vascular endothelial growth factor (VEGF) polymorphisms have been associated with increased risk of FTLD (Borroni et al., 2008). The C9orf72 mutation can also cause FTLD and is currently the most important genetic cause of familial FTLD

accounting for 25.9% of all cases (Renton et al., 2011, DeJesus-Hernandez et al., 2011). VCP mutations are associated with a specific condition called inclusion body myopathy with Paget disease of the bone and FTD (IBMPFD) and they account for a very small percentage of FTLD cases, but only in families with the specific constellation of symptoms. Affected individuals may develop FTD, IBM, Paget disease of the bone or any combination of the three conditions (Kimonis and Watts, 2005). The other genes associated with rare FTLD cases include Charged multi vesicular body protein 2B (CHMP2B), TAR DNA-binding protein (TARDBP), Fused in sarcoma (FUS).

1.2.4 Pathology of FTLD

Pathologically, two major types of changes are observed in FTLD: gross morphologic atrophy in the frontal and anterior temporal lobes, and microscopic changes, including any or all of the following: gliosis, inclusion bodies, swollen neurons, and microvacuolation. FTLD is characterized by a severe decrease in overall brain weight due to frontal and temporal lobar atrophy and atrophy may extend into the parietal lobes, amygdala, hippocampus, thalamus and basal ganglia. Ventricular enlargement, pallor of the substantia nigra, atrophy of the anterior nerve roots and discoloration of the lateral funiculus in the spinal cord are some of the morphological changes observed. The gross atrophy results from synapse loss, dendritic atrophy and neuron loss.

The remaining neurons show two distinctive histologic features: swelling (called "ballooned" or "Pick cell") and an inclusion within the perikaryon, most often in layer II (Pick body). Pick bodies are distinct spherical argyrophilic inclusions (seen with silver staining) that accumulate in neurons of the frontal lobes. Pick bodies are usually found in limbic (greatest concentration is in the amygdala and hippocampus, including the dentate gyrus), paralimbic, and ventral temporal lobe cortex, but may also be seen in anterior frontal and dorsal temporal lobes. They are rarely found elsewhere in the brain. Pick bodies are composed of randomly arranged filaments of the tau protein (Piguet et al., 2011).

About 40% of FTLD patients are pathologically characterized by inclusions of hyperphosphorylated tau (FTLD-tau) (Goedert et al., 2012). FTLD patients with tau negative inclusions were referred to as FTLD-U. FTLD-TDP (with TDP-43 inclusions) and FTLD-FUS (with FUS inclusions) account for the majority of cases of FTLD-U. Some inclusions are negative for FUS and TDP-43 but positive for components of the Ubiquitin-proteasome system (UPS) (Mackenzie et al., 2009). Tau, TDP-43 and FUS are the major proteins in patients with FTLD. However, in some cases, especially in older patients, there may be an accumulation of more than one type of protein, including proteins that are associated with other neurodegenerative diseases, such as Alzheimer disease.

1.2.5 Pathogenic Mechanism in FTLD

The disease mechanism in FTLD is not very clear and studies suggest that loss/gain of the relevant protein functions might contribute to FTLD. Tau is a member of the microtubule (MT)-associated protein family. The main function of these proteins is to stabilize the MTs and to promote MT assembly by binding. Tau may have additional functions, including the regulation of kinesin-dependent transport of vesicles and organelles along the MTs (Avila et al., 2004). Mutations in MAPT are expected to cause disease by a toxic gain of function mechanism, likely related to splicing regulation mutations that disturb the normal 4R/3R tau ratio thereby leading to aggregation, resulting in the formation of tau filaments and associated cellular dysfunction (Goedert and Spillantini, 2001). In contrast, the identification of null mutations in PGRN indicated that a loss of function is the primary disease mechanism involved in this form of FTLD-U (Mackenzie et al., 2006). PGRN appears to regulate cell cycle progression and cell migration in a range of tissue remodeling processes including development, wound repair/inflammation, and tumorigenesis (He and Bateman, 2003). Because all pathogenic PGRN mutations described to date are expected to reduce the levels of functional PGRN and granulins, a role for PGRN in maintaining neuronal survival has been suggested (Mackenzie et al., 2006). VCP acts as a molecular chaperone in a range of cellular activities, including ubiquitin-dependent protein degradation, cell-cycle regulation, and apoptosis. VCP mutations are likely to cause a loss or alteration of the

normal function of VCP, leading to impaired ubiquitin-proteasome system activity and the accumulation of ubiquitinated proteins within cells (Kimonis et al., 2008). Human CHMP2B belongs to the charged multivesicular body protein family. The exact function of CHMP2B is unknown, but its yeast ortholog Vps2 is a component of the endosomal sorting complex III (ESCRTIII), which is involved in the degradation of surface receptor proteins and formation of endocytic multivesicular bodies (MVB) (Skibinski et al., 2005). Thus, endosomal trafficking dysfunction might be an important factor leading to the neurodegeneration. Exactly how the loss of the proteins mutated in FTLD-U triggers the formation of abnormal neuronal inclusions containing ubiquitinated TDP-43 remains unknown. For PGRN, which is best known as a secreted growth factor involved in cell signalling, a functional link with TDP-43 has not been identified yet. It therefore remains to be determined whether a loss of TDP-43 function, rather than the formation of aggregates, contributes to the FTLD-U phenotype. Future clinicopathological studies, including neuroimaging and genetics, are necessary to improve the prediction of the underlying pathology of FTLD.

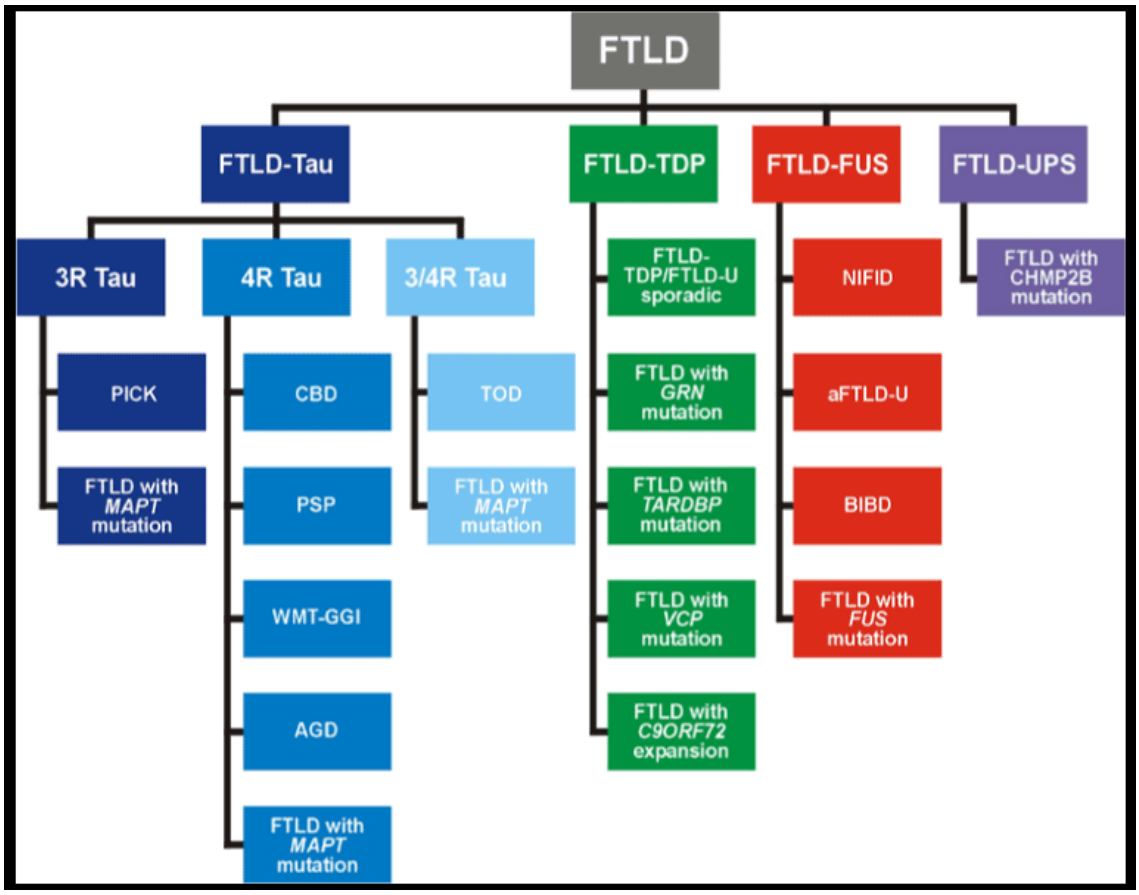

Figure 1.2 The molecular and genetic classification of frontotemporal lobe degeneration
(Taken from Goedert et al., Cold Spring Harb Perspect Med, 2012).

1.2.6 Clinical features of FTLD

The onset and progress of FTLD is slow. The most striking symptoms of FTLD are behavioural and personality changes. There are three main clinical variants of FTLD. These three syndromes are the behavioural variant of FTD (bvFTD), and two language variants: Progressive nonfluent aphasia (PNFA), and semantic dementia (SD) (Neary et al., 1998). The language variants (SD and PNFA) are sometimes grouped together under the term "primary progressive aphasia" (PPA). PPA has since been split into three subgroups: progressive non-fluent aphasia, semantic dementia and logopenic progressive aphasia (LPA) (Gorno-Tempini et al., 2011). At autopsy, patients with LPA are often found to have Alzheimer's disease, not FTLD.

The behavioural presentation of FTD is often referred to as ''frontal variant'' FTD (fvFTD). Each clinical variant is associated with distinct regional patterns of brain

atrophy and varying degrees of histopathological characteristics. There is an overlap of clinical characteristics, particularly during the later stages, when the disease progresses across the frontal and temporal lobes. The predominant impairment in these subtypes is in behaviour, expressive language or receptive language, respectively. Whether the prevalence of depression differs between these clinically distinct variants remains unclear. Verbally inappropriate sexual comments and gestures are common in FTLD. Despite this inappropriate behaviour, sexual drive is often reduced with impotence common in the FTLD prodrome in men. Other socially inappropriate behaviours sometimes seen in FTLD include theft, assault, inappropriate or offensive speech, and public urination or masturbation. Many FTLD patients exhibit stereotyped or perseverative behaviours such as repetitive cleaning, pacing, organizing objects into groups, use of catch phrases, impulse buying, hoarding, and counting. Dietary changes, especially cravings for sweets, are common in FTLD. Decreased satiety and food cravings often lead to a weight gain in many patients (Achi and Rudnicki, 2012). The insidious onset of personality changes and behavioural abnormalities is initially the most prominent feature of fvFTD. Poor insight, loss of personal awareness, loss of social awareness, and blunting of affect are common behavioural changes that are seen early in fvFTD. Increased submissiveness, a lack of empathy, self-centeredness, emotional coldness, and decreased concern about family and friends is also common. The patients may undergo dramatic changes in beliefs, attitudes, and/or religious sentiment, leading to the emergence of a new personality as the disease progresses. Orbitobasal (ventromedial) frontal lobe dysfunction leads to disinhibition, poor impulse control, antisocial behaviour, and stereotyped behaviours. Disinhibition or distractibility may manifest as restlessness, pressured speech, impulsivity, irritability, aggressiveness, violent outbursts, or excessive sentimentality. Obsessive-compulsive disorder, delusions, euphoria and apathy are other features seen in patients with fvFTD. As the disease progresses, patients develop language dysfunction as seen in PNFA. Impairment on tests of executive function or working memory is the most common deficit in fvFTD. Memory and visuospatial function are relatively spared. (Boxer and Miller, 2005, Hodges, 2001)

Semantic dementia (SD) is a syndrome of progressive loss of knowledge about people, objects, facts, and words (Snowden et al., 1996). The most common presenting

complaint in SD involves language, and is often described as a loss of memory for words or a loss of word meaning. Repetition, prosody, syntax, and verb generation are preserved. Associative agnosia may lead to difficulty with object recognition. Many of the disinhibited and compulsive behaviour seen in fvFTD are also present in SD, as both groups have measurable damage to the orbitofrontal cortex (Liu et al., 2004). An emergence of artistic talent has been observed in some patients with SD who have significant language impairment, but preserved visuospatial skills. PNFA patients present with changes in fluency, pronunciation, or word finding difficulty. Anomia in progressive PNFA is more significant for verbs than for nouns. Unlike fvFTD and SD, PNFA patients do not display typical behavioural abnormalities until later in the disease (Neary et al., 1998). Episodic memory, semantic memory, and visuospatial function are preserved in PNFA. Executive function and working memory are often impaired. Language difficulties include agrammatism, phonemic paraphasias, and anomia. Other language problems may include stuttering, impaired repetition, apraxia of speech, alexia, and agraphia. As the disease progresses, motor impairments often arise in subjects who are destined to develop motor neuron disease (FTD-MND), corticobasal degeneration (CBD), or progressive supranuclear palsy (PSP). Ocular motor impairment is an early feature of PSP and CBD, and is associated with FTD-MND. (Boxer and Miller, 2005)

1.2.7 Diagnosis, Treatment and Management of FTLD

There are many potential causes that may explain changes in cognition, behaviour and motor skills. No single diagnostic test exists to confirm or rule out a diagnosis of FTLD. This often results in a long and frustrating process of testing for other disorders with symptoms similar to FTLD to rule them out. The individuals need to be evaluated by a neurologist experienced with FTLD and related neurodegenerative conditions. The diagnosis of FTLD generally involves: medical history and detailed neurological examination; neuropsychological examination to assess language, behaviour, memory, executive and visual-spatial functions and neuroimaging to determine the focus and extent of brain atrophy**.** In 1998, Neary and colleagues published consensus guidelines

for the clinical diagnosis of bvFTD that have since been widely adopted for use in research and clinical practice.

Rational treatments for frontotemporal dementia are currently limited. Since the causes of FTLD are unknown, there is no way to prevent it, slow down disease progression, or cure it. Drugs used for Alzheimer's disease, such as Aricept, are not effective in treating FTLD and may even make symptoms worse. The treatment aims to lessen the effects of the symptoms and increase the quality of life. Behavioural therapy may be helpful in reinforcing positive behaviour in patients showing challenging symptoms. Speech therapy may help with language problems. Patients with FTD-MND are often started on riluzole, which is generally well tolerated and has low drug-drug interactions with antidepressants and memantine. A combination of pharmacological therapy with behavioural, physical and environmental modification techniques is necessary for the appropriate management of the behavioural symptoms of FTLD.

1.3 ALS-FTLD

1.3.1 Introduction

For several years, it was thought that in ALS, the body was wasted but the mind was spared. Pathological investigations and genetic screening have helped us understand the pathology and genetic variability associated with FTLD and ALS. Improved knowledge regarding the molecular pathogenesis underlying ALS and FTLD; and sophisticated diagnostic measures has made it clear that dementia is seen in patients with ALS (Ravits et al., 2013, Ferrari et al., 2011). Thus, ALS is now considered to be a multi-system neurodegenerative disorder (Strong, 2001). Over the last 150 years, and especially in the last two decades, there has been growing evidence that FTLD signs can be seen in patients primarily diagnosed with ALS, implying clinical overlap among these two disorders. Both FTLD and ALS are heterogeneous at the clinical, neuropathological and genetic levels and, even though they come across as distinct progressive disorders, there is increasing evidence of the fact that they share some clinical, neuropathological and genetic features. This implies that either they share the same neurodegenerative pathway or that they may be a part of a common spectrum.

1.3.2 Epidemiology

FTLD can be detected in up to 50% of ALS patients (Strong, 2008, Liscic et al., 2008, Lomen-Hoerth et al., 2003). Based on two large epidemiologic studies, the occurrence of mild cognitive impairment has been reported in 36% and 51% of patients with ALS (Massman et al., 1996, Ringholz et al., 2005). Several studies have shown that ALS patients with frontotemporal impairment have significantly shorter survival compared with FTLD or ALS patients (Ferrari et al., 2011). Patients with ALS-FTD typically have onset of symptoms in their 50's, and like ALS without dementia, it is slightly more common in men than women. Both sporadic and familial cases of adult onset ALS–FTD have been reported in the literature.

1.3.3 Genetics of ALS-FTD

ALS–FTD is a genetically heterogeneous disorder. Genetic analysis of this disorder has helped us unravel the common links between FTLD and ALS, since individuals from ALS– FTD-linked pedigrees may have clinical features of ALS, FTLD, or both.

Table 1.1 Genes in ALS, FTD and ALS-FTD

Genes	Involvement in ALS-FTD spectrum	Putative protein function
Causal ALS		
PGRN	FTD	Growth factor
MAPT	FTD	Cytoskeleton
SOD1	ALS	Superoxide metabolism
TARDP	ALS/ ALS-FTD	RNA metabolism
FUS	ALS/ ALS-FTD	RNA metabolism
UBQLN2	ALS/ ALS-FTD	Proteasome
SQSTM1	ALS/ ALS-FTD	ubiquitination/autophagy
VCP	ALS/ ALS-FTD/ FTD	Proteasome. vesicle trafficking
OPTN	ALS	Autophagy
CHMP2B	ALS/FTD (rare)	Vesicle trafficking
MATR3	ALS/ ALS-FTD	RNA metabolism
hnRNPA1	ALS/ ALS-FTD/FTD	RNA metabolism
hnRNPA2B1	ALS/ ALS-FTD/FTD	RNA metabolism
ATXN2	ALS	RNA translation, endocytosis
C9orf72	ALS/ ALS-FTD/FTD	DENN protein
NFH	ALS	Axonal transport
DCTN1	ALS/ ALS-FTD	Axonal transport
PFN 1	ALS	Cytoskeleton
VAPB	ALS	Vesicle trafficking
Alsin	Juvenile ALS	Vesicle trafficking
TUBA4A	ALS	Cytoskeleton
CHCHDIO	ALS/ ALS-FTD/ FTD	Oxidative phosphorylation
PPARGC1A	ALS	Mitochondrial biogenesis
Peripherin	ALS	Cytoskeleton
FIG4	ALS	Vesicle trafficking
SPGI1	Juvenile ALS	Axonal maintenance , Vesicle trafficking
SETX	ALS	DNA/RNA metabolism
EWSRI	ALS	RNA metabolism
TAF15	ALS	RNA metabolism
ANG	ALS/ ALS-FTD	Angiogenic factor
TBK1	ALS	Autophagy

Genes	Involvement in ALS-FTD spectrum	Putative protein function
Modifiers, Susceptibility genes		
ATXN2	ALS	RNA translation. Endocytosis
EPHA4	ALS	Axon guidance
UNC13A	ALS/ ALS-FTD	Neurotransmitter release
ELP3	ALS/ ALS-FTD	RNA metabolism
SSI8L1	ALS	Chromatin regulation
APOE	ALS/ FTD	Lipid homeostasis
KIFAP3	ALS	Axonal transport
VEGF	ALS	Angiogenic factor
SMN1	ALS	Survival factor
ZNF5 12B	ALS	Positive regulator of TGF-β signalling
SPAST	ALS	Cytoskeleton
PON 1,2,3	ALS	Detoxifying enzyme
HFE	ALS	Iron metabolism
TMEM106B	FTD	Endolysosomal pathway

(Table adapted from Eykens and Robberecht; 2015)

There is a clinical and pathological overlap between ALS and FTLD. The understanding of the link between FTLD and ALS was rapidly accelerated by the identification of TDP-43 pathology (Neumann et al., 2006b). TDP-43 co-localized with ubiquitin and appeared to be the major component of nuclear, cytoplasmic and dendritic inclusions that characterise ALS and frontotemporal lobar degeneration with ubiquitin inclusions (FTLD-U). However, in most patients with ALS and FTLD, only TDP-43 aggregates, and no TDP-43 mutations, are present. Mutations in other genes such as PGRN, VCP, and C9orf72 also trigger TDP-43 inclusion formation in ALS– FTD, although the mechanism is not known (Janssens and Van Broeckhoven, 2013b, Ling et al., 2013a). Missense mutations in TDP-43 can be a rare cause of ALS and sometimes FTLD (Sreedharan et al., 2008, Kabashi et al., 2008), strongly supporting the idea that ALS and FTLD represent a continuum of a broader TDP-43-mediated neurodegenerative disorder. Interestingly, a related RNA-binding protein, FUS, has also been genetically and pathologically implicated in both ALS and FTLD, further supporting the ALS–FTD spectrum concept (Neumann et al., 2009b, Vance et al., 2009).

Two major genes were described in 2011, which cause FTLD and/or ALS within extended kindreds: C9orf72 and Ubiquilin2. A set of five adult-onset ALS–FTD families

were linked to chromosome 9q21– q22 (Hosler et al., 2000), but no additional families have been published and the gene remains unknown. Several groups have reported linkage of an autosomal dominant adult-onset ALS–FTD locus to chromosome 9p (van Blitterswijk et al., 2012a). In these pedigrees, individual patients present with behavioral variant FTD, ALS, or a combined phenotype. Collectively, these reports suggested that there is a major locus on chromosome 9p21, which causes both ALS and FTLD.

A hexanucleotide repeat expansion (GGGGCC) in the first intron of c9orf72 gene on chromosome 9p21 has been found to be the most common cause of familial and sporadic cases with ALS, ALS-FTD, or FTLD (Majounie et al., 2012, Renton et al., 2011, DeJesus-Hernandez et al., 2011). Ubiquilin2 (UBQLN2) is responsible for X-linked FTD/ALS. In 2011, a series of families with X-linked ALS carried mutations in the UBQLN2 gene, encoding ubiquilin2 (Deng et al., 2011). One hundred and eighty-eight ALS families without evidence of male to male transmission were analysed, identifying four further mutations that all affected a conserved PXX repeat region in the UBQLN2 gene. Twenty-three percent (8/35) of affected individuals in the UBQLN2 families had both FTLD and ALS, meaning that overlap FTLD/ALS syndromes were much more common among these families than in kindreds with GRN, TARDP, FUS, or VCP mutations. Given that X-linked ALS is rare, it was anticipated that UBQLN2 will be a rare cause of familial ALS and further families will be needed to delineate pathogenic and nonpathogenic variants. Mutations are observed at variable frequencies in ALS, FTD–ALS or FTLD patients in progranulin (*GRN*) (Cruts et al., 2006), angiogenin (*ANG*) (Greenway et al., 2006), subunit of dynactin (*DCTN1*) (Münch et al., 2005), heterogeneous nuclear ribonucleoprotein A1 and A2/B1 (*hnRNPA1* and *hnRNPA2/B1*) (Kim et al., 2013), optineurin (*OPTN*) (Maruyama et al., 2010), sequestosome 1 (*SQSTM1*) (Fecto et al., 2011) and valosin-containing protein (*VCP*) (Kimonis et al., 2008), charged multivesicular body protein 2B or chromatin modifying protein 2B (*CHMP2B*) (Skibinski et al., 2005) and vesicle-associated membrane protein-associated protein B (VAPB) (Nishimura et al., 2004).

1.3.4 Pathological features of ALS-FTD

Frontal temporal dementia ALS (FTD-ALS) is a neurodegenerative disorder associated with ALS wherein in addition to the typical signs of neuronal degeneration in ALS, neuropathological changes in ALS-FTD consist of cortical atrophy: including the frontal and temporal lobes, hippocampus and amygdala, spongiform change in the neocortex and ubiquitinated inclusions (UBIs) in the substantia nigra (Mackenzie, 2007). The frontal and temporal lobes, including the motor regions of the cerebral cortex, show loss of neurons and gliosis (scar tissue in the brain), and many of the remaining neurons are shrunken or abnormally shaped. There is also degeneration of motor neurons in the brain stem and spinal cord. Patients with FTLD pathologically may demonstrate a tau positive pathology or a tau negative pathology. Patients with tau negative pathology have ubiquitin positive inclusions (FTLD-U). TDP-43 was found to co-localise with ubiquitin and is a major component of ubiquitinated inclusions in both ALS and FTLD. Burden and distribution of the TDP-43 varied depending upon the clinical phenotype. Patient with pure ALS have TDP-43 pathology primarily in the spinal cord, those with pure FTLD have TDP-43 pathology primarily in the cortex, while those with FTD-ALS have TDP-43 pathology in both area (Giordana et al., 2011). However, TDP-43 inclusions are not only found in the expected areas for ALS and FTLD, but can also be seen in the cerebellum, parietal, and even occipital lobes although to lesser degrees, suggesting TDP-43 is part of a multisystem neurodegenerative process (Geser et al., 2009b). TDP-43 levels in cerebrospinal fluid are higher in patients with ALS or FTLD, but there is overlap between the patient groups as well as with controls (Steinacker et al., 2008). In patients with ALS-FTD, the density and the distribution of the ubiquitylated inclusions was higher than in ALS patients. In addition to the dentate gyrus, frontal and parietal neocortices, anterior cingulate gyrus, and hippocampus, UBIs were also found in the temporal, occipital and entorhinal cortices, posterior cingulate gyrus, caudate, and the putamen in patients with ALS-FTD. The substantia nigra subgroup of UBIs were distributed heterogeneously amongst the dentate gyrus, parahippocampal gyrus, amygdala, neostriatum, and anterior horn cells in ALS patients, whilst they were numerous and almost uniformly present in patients with ALS-FTD. In particular, the number of SCIs in the second and third layers of the

parahippocampal gyrus and amygdala was significantly higher in those with ALS-FTD than ALS.

1.3.5 Common pathogenic-mechanisms in ALS and FTLD

Multiple pathways are involved in disease initiation and progression in ALS and FTLD. ALS and FTLD are linked clinically, pathologically and mechanistically, and the diseases are now properly recognized as representatives of a continuum of a broad neurodegenerative disorder, with each presenting a spectrum of overlapping clinical symptoms. RNA and protein homeostasis pathways are intimately linked and their dysfunction is fundamentally involved in disease pathogenesis. Perturbation of either pathway can amplify an initial abnormality through a feed-forward loop, which may underlie relentless disease progression. With the identification of TDP-43 and FUS ubiquitinated inclusions and rare mutations in the respective genes in both ALS and FTLD, errors in RNA binding were considered to be the linking mechanism for ALS and FTLD. TDP-43 and FUS/TLS are RNA binding proteins with functional roles in several aspects of RNA metabolism (Lagier-Tourenne et al., 2010). The fact that TDP-43 is the major component of ubiquitinated inclusions in ALS, ALS-FTD and FTLD has led to the speculations that errors in RNA processing could be a key factor in neurodegeneration. The identification of a large intronic hexanucleotide expansion in the previously uncharacterized gene C9ORF72 in families with ALS, FTLD or both led to two other disease mechanisms: RNA mediated toxicity and haploinsufficiency. This was based on previous studies of other repeat expansion diseases (La Spada and Taylor, 2010). Other ALS-FTD genes like *UBQLN2*, *VCP*, *VAPB*, *SQSTMI*, *CHMP2B*, *OPTN* are associated with protein clearance pathways or maintaining proper protein homeostasis; implying that disruption in protein homeostasis (or proteostasis) is a key characteristic of both diseases. Protein aggregation and degradation in ALS-FTD suggests that disruption of either of the two major protein clearance pathways: the ubiquitin-proteasome system and autophagy might also be underlying mechanisms in neurodegeneration. One of the key features of prion diseases is the conformational conversion of a native state to an infectious, misfolded and pathological state of the prion protein. The infectious cycle comes from the perpetuating conversion of the normal prion protein into a

pathological conformation and spreading to other cells. Both TDP-43 and FUS/TLS contain prion-like domains (Gitler and Shorter, 2011), which may facilitate seeding and aggregation. This suggests that a prion-like seeding and spreading mechanism could underlie TDP-43 and FUS/TLS-mediated disease (Polymenidou and Cleveland, 2011). Errors in RNA and protein homeostasis accumulate and may eventually lead to failure in autoregulation, deregulation of ALS-linked genes, proteo-toxic stress, and loss of neuroprotection.

1.3.6 Clinical features of ALS-FTD

Strong and colleagues proposed five categories with which to classify ALS patients along a continuum: (1) ALS patients cognitively and behaviourally intact; (2) ALS patients with mild cognitive impairments; (3) ALS patients with mild behavioural impairments; (4) ALS with a full-fledged FTD; (5) ALS with other non FTD-forms of dementia (Strong et al., 2009). The terms ALSci (ALS with cognitive impairment), ALSbi (ALS with behavioural impairment), ALS-FTD (amyotrophic lateral sclerosis-frontotemporal dementia) and ALS non-FTD dementia, are concepts that aim to capture the key differences between the various clinical phenotypes. Cognitive and behavioural deficits in ALS may, range from mild to-moderate impairment to FTD (Strong et al., 2003). According to the diagnostic guide proposed by Strong et al. (2009), the ALSci and ALSbi acronyms refer to patients with cognitive limitations or changes in affect and social behaviour that do not meet the criteria for dementia. Frontal variant or behavioural variant FTD (fvFTD), nonfluent variant PPA (nfvPPA), semantic variant PPA (svPPA) have been described within the ALS population, although varied frequencies of FTD subtypes have been reported (Ringholz et al., 2005, Lomen-Hoerth et al., 2003). Currently, there are no reported cases of lvPPA, the most recently and least studied PPA variant, in association with ALS. Behavioural, cognitive, and linguistic symptoms may overlap, but aphasic symptoms can be an early and dominant feature for a long time in ALS, independently from dementia (Bak, 2010). The term ‘ALS dementia’ has commonly been adopted to designate the clinical syndrome.

Clinical features of ALS-FTD may be varied depending on the affected region. Some of the varying symptoms seen in patients include writing errors consisting of

paragraphias such as substitutions, omissions, or syntactic errors, dysgraphia, defects in recognition of familiar people and severe behavioural. ALS/FTD patients may present as socially disinhibited, with excessive sociability, unaware or unconcerned by disability or conversely lacking appropriate emotions, apathetic, inert, and emotionally blunted. The most commonly reported behavioural change in ALS/FTD was an increase in self-centeredness and irritability. However, behaviour impairment in ALS/FTD patients remains an under-investigated area (Zago et al., 2011). Generally in ALS-FTD, the clinical manifestations of FTLD antedated the appearance of motor signs and the disease shows a more rapid and tumultuous course in comparison to the one observed in patients with FTLD or ALS alone. The motor symptoms arising from motor neuron disease in FTD/MND are the same as those seen in ALS. Not all of these symptoms will be seen in every patient. Rather the symptoms depend on which parts of the nervous system are involved. Motor difficulties may include: Muscle weakness, which can involve the arms, legs, face, tongue or neck, clumsiness with fine movements of the hands, tripping or falling (due to weak or stiff legs), shortness of breath (due to weak breathing muscles), muscle atrophy, fasciculations, muscle cramps, dysphagia, dysarthria, spasticity, hyperreflexia. Overall, memory is relatively preserved in patients with ALS-FTD, and the memory problems reported are believed by most neurologists to be related to frontal dysfunction.

1.3.7 Diagnosis, Treatment and management of ALS-FTD

Diagnosing cognitive and behavioural impairment in ALS requires a comprehensive neuropsychological evaluation. When comprehensive neuropsychological evaluation is not possible, screening measures for cognitive and behavioral function can be useful. Strong and his colleagues, have developed a novel criteria for diagnosis of frontotemporal dysfunction in ALS.

The treatments and management of ALS-FTD patients are the same as in ALS and FTLD. The treatments aim to increase the quality of life. Patients with this diagnosis usually experience a rapid decline in both physical and cognitive abilities and have shorter survival rates. Physical therapy, speech therapy and behavioural therapy may help patients with ALS-FTD. There are five types of strategies used with patients and

families in managing negative behaviour: environmental, behavioural, pharmacological, physical and those internal to the family carer. Clinics also can provide resources and support for caregivers and families.

1.4 TAR DNA binding protein

The presence of ubiquitinated misfolded protein inclusions is the key feature of most neurodegenerative diseases. In 2006, several years after the discovery of the SOD1 mutation, TAR DNA-binding protein 43 (TDP-43), a highly conserved nuclear protein, was identified as the major disease protein in ALS and in the most common variant of FTLD, FTLD-U, which is characterized by cytoplasmic inclusions that stain positive for ubiquitin but negative for tau and α-synuclein (Neumann et al., 2006b, Arai et al., 2006). TDP-43 was first identified in a screen for protein factors that were capable of binding the long terminal repeat transactive response element of HIV-1 (Ou et al., 1995).

1.4.1 TDP-43 gene structure and functions

TDP-43 is an RNA/DNA binding protein. TDP-43 is found in all higher eukaryotes including *Drosophila melanogaster*, *Xenopus laevis*, and *Caenorhabditis elegans* (Wang et al., 2004). The *TARDBP* gene encoding TDP-43 is located on human chromosome 1p36 and has 6 exons, five of which encode the predominant 43 kDa protein, TDP-43. However, *TARDBP* can undergo alternative splicing to generate up to 11 protein isoforms (Wang et al., 2004). In addition to full-length TDP-43, three protein isoforms of TDP-43 are identified in human brain and spinal cord, but the biological significance of these isoforms is not known and their presence in other species has not been identified (Strong et al., 2007). TDP-43 is ubiquitously expressed in all tissues examined, including heart, lung, liver, spleen, kidney, muscle and brain (Buratti and Baralle, 2001) and localizes primarily to the nucleus of cells. TDP-43 is a member of the heterogeneous nuclear ribonucleoproteins (hnRNPs) family, a group of proteins that bind RNAs (Sephton et al., 2012). Along its 414 amino acid sequence, there are two highly conserved RNA recognition motifs in the N- terminus, which are involved in RNA/DNA binding (Buratti and Baralle, 2001, Ou et al., 1995). Additionally, the N-terminus of TDP-43 can mediate the formation of homodimers (Kuo et al., 2009). TDP-43 contains a bipartite nuclear localization signal sequence and a nuclear export signal

which allows nucleocytoplasmic shuttling (Winton et al., 2008a). The C-terminal glycine-rich region of TDP-43 is less conserved among species (Wang et al., 2004) and is involved in protein-protein interactions and influences it's solubility and cellular localization (Ayala et al., 2008).

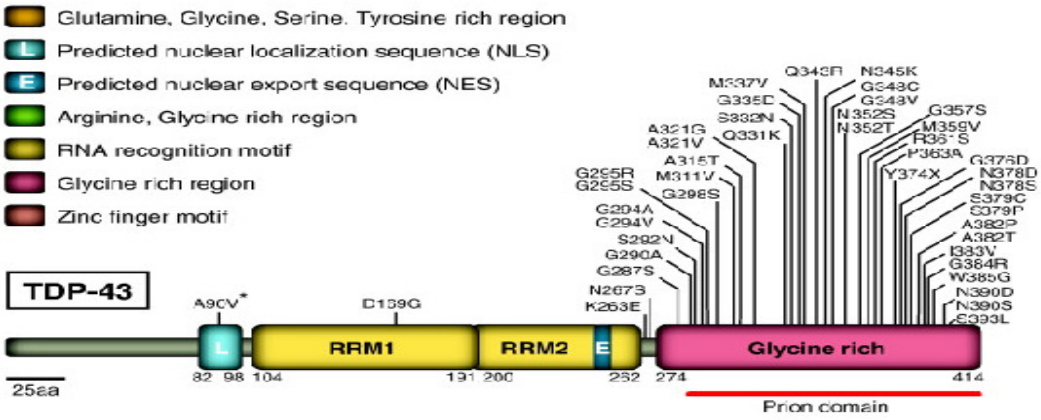

Figure 1.3 Structure of TDP43 protein

TDP-43 is 414 AA long with two RNA recognition motifs (RRM1 and RRM2); Nuclear localization region (L); Nuclear Export region (E) and a Glycine rich C-terminal. Most mutations are found in the Glycine rich region (Taken from Tourenne and Cleveland; 2009)

1.4.2 Mutations in TDP-43

Several groups have identified various mutations in the highly conserved region of *TARDBP* in sporadic and familial ALS cases and have provided evidence of a direct link between TDP-43 dysfunction and neurodegeneration (Gitcho et al., 2008, Kabashi et al., 2008, Sreedharan et al., 2008). To date, 38 nonsynonymous TARDBP mutations have been identified in both familial and sporadic ALS, most clustering in the region encoding the C-terminus, and accounting for approximately 1–2 % of total cases. Nearly all of the described ALS-associated TDP43 mutations are dominant missense mutations within the glycine-rich domain, suggesting that altering the function of this domain is sufficient to induce neurodegeneration. Thus exon 6 and its encoded glycine-rich domain are critical components of the TDP-43 protein.

In familial ALS cases, the mutations segregate with the disease and no mutations have been found in unaffected family members. This indicates a high degree of penetrance for *TARDBP* mutations in these families, although further studies are needed as mutations in TDP-43 have been identified in patients with apparent sporadic ALS. Several lines of evidence support the pathogenicity of missense mutations in different disease models. Recently two patients with FTD-MND were shown to have TARDBP mutations, illustrating that *TARDBP* mutations are not restricted to ALS alone (Benajiba et al., 2009). Discovery of *TARDBP* mutations in both ALS and FTD-TDP patients reflects a recurring theme that these diseases are linked within a broad spectrum of neurodegenerative TDP-43 proteinopathies.

The TDP-43 mutants that were used in this study are missense mutations located on exon 6 which encodes the highly conserved glycine rich C-terminus of TDP-43 (Sreedharan et al., 2008). This region mediates interactions with proteins, including the heterogeneous ribonucleoproteins. The M337V is a familial mutation where valine is substituted for methionine at codon 337. The Q331K is a sporadic mutation wherein glutamine is substituted for lysine at codon 331. When these two TDP-43 mutants were electroporated into the neural tube of developing chick embryos, there was a reduction in rate of maturation of the neural tube with an increase in apoptotic nuclei, suggesting a toxic gain of function or dominant negative effect (Sreedharan et al., 2008). These two mutants were also shown to provoke age-dependent, mutant-dependent, progressive motor axon degeneration and motor neuron death when expressed in mice at levels similar to endogenous TDP-43 (Arnold et al., 2013).

1.4.3 TDP-43 pathology

TDP-43 is predominantly a nuclear protein, though it is actively shuttled between the nucleus and the cytoplasm (Fallini et al., 2012). However, under physiolodical and pathological conditions, TDP-43 is depleted from the nucleus and accumulates in the cytoplasm in both neurons and glia (Van Deerlin et al., 2008, Igaz et al., 2009). Thus TDP-43 proteinopathies could be caused by a loss of function (depletion of TDP-43 from the nucleus) or by a gain of function (aggregation of TDP-43 in the cytoplasm) or a combination of both (Neumann et al., 2006b, Vance et al., 2009, Wegorzewska et al.,

2009, Lagier-Tourenne and Cleveland, 2009). Pathological TDP-43 is abnormally ubiquinated, hyperphosphorylated and N-terminally cleaved to generate C-terminal fragments (20-25 kDa) (Arai et al., 2006). Under normal circumstances, ubiquitinated and hyper-phosphorylated TDP-43 cannot be found in brain tissue, thus the modifications of TDP-43 are disease specific but it is not clear whether TDP-43 aggregation is causative or if it is a secondary effect of another pathological mechanism.

Based on the pattern of TDP-43 aggregates in the brains and spinal cords from 76 people who died of ALS, researchers have defined four different stages for TDP-43 proteinopathy: stage 1- TDP-43 aggregates only in the motor cortex, brainstem, and spinal cord; stage 2 -prefrontal neocortex, precerebellar nuclei, and the red nucleus - a midbrain structure involved in motor control; stage 3 - postcentral neocortex and striatum and stage 4 - temporal lobe. Overall, TDP-43 pathology appeared to start in the motor cortex at the top of the brain and radiate downward to the spinal cord, as well as forward to the frontal cortices. The same pattern was found in patients with GGGGCC repeat expansion in the C9ORF72 gene. The predictable spread of TDP-43 indicates that this misfolded protein, like others (misfolded Aβ, tau, and α-synuclein), transfers pathology down the axon and across synapses through connected neural networks (Brettschneider et al., 2012).

1.4.4 TDP-43 relevant neurodegenerative disease

TDP-43 pathology can be found in many neurodegenerative diseases. The pathology of TDP-43 can be a primary or secondary histopathological feature. ALS, FTLD-TDP, ALS-FTD, and rare disorders (Perry syndrome, FTLD–inclusion body myopathy–Paget syndrome) have TDP-43 pathology as the primary histopathological feature. ALS cases are mostly sporadic, and many of them harbour TDP-43 inclusions. TDP-43 inclusions are also found in patients with familial ALS, with the exception *SOD1, TAU* and *FUS* mutations. Although TDP-43 pathology in ALS can be found throughout the brain; the most severely affected areas of the CNS are the motor cortex, the spinal cord, the basal ganglia, and the thalamus. TDP-43 is the main protein component of the ubiquitinated inclusions found in most cases of ALS and FTLD-U. In FTLD-TDP, TDP-43

pathology is found throughout the CNS, although the occipital cortex and cerebellum remain relatively unaffected (Geser et al., 2009a). A small proportion of FTLD-U cases does not harbour TDP-43 pathology and instead have ubiquitinated inclusions for FUS (FTLD-FUS) or an unknown protein (FTLD-UPS). TDP-43 pathology is found in sporadic and familial cases of FTD involving *PGRN* and *VCP* mutations and in FTD with or without MND with *C9ORF72* hexanucleotide repeat expansions.

TDP-43 pathology has also been observed in VCP mutations associated with a syndrome complex consisting of FTLD, inclusion body myopathy and Paget disease of the bone (Kimonis et al., 2008). Other syndromes that harbour TDP-43 pathology include: inclusion body myositis and Perry syndrome, Parkinson disease, Alzheimers disease, and related disorders (PD with dementia, dementia with Lewy bodies plus Alzheimers disease), Huntington disease, Chronic traumatic encephalopathy (CTE) and rare disorders (Guam ALS, Guam ALS–PD). These diseases show TDP-43 pathology as secondary pathological features (Hasegawa et al., 2008, Geser et al., 2010). The presence of TDP-43 aggregates/inclusions in numerous disorders suggests a pathogenic role for TDP-43 and is collectively grouped together as TDP-43 proteinopathies.

1.4.5 Normal TDP-43 functions

Numerous functions have been proposed for TDP-43 through studies in cell culture experiments, animal models and biochemical assays. TDP-43 plays an important role in RNA processing. The RRM1 domain of TDP-43 is critical for its binding to single-stranded RNA (Buratti et al., 2005, Buratti and Baralle, 2001, Ou et al., 1995, Polymenidou et al., 2011). TDP-43 preferentially binds UG repeats, but can also bind to non UG repeat sequences. High-throughput sequencing of RNA isolated by crosslinking immunoprecipitation (HITS-CLIP) revealed that TDP-43 binds to a large proportion of the transcriptome (>6,000 RNA species), preferentially localizing to introns (including deep intronic sites), 3’ untranslated regions (UTRs) and non-coding RNAs. TDP-43 binds to both 3’-untranslated regions (3’UTR) of mRNAs and long non-coding RNAs (ncRNAs). The former affects stability or transport while the latter influences their regulatory roles. TDP-43 regulates a number of proteins linked to neurodegenerative diseases viz.

progranulin, sortilin and FUS/TLS. TDP-43 regulates its own expression levels by binding to the 3' UTR of its own mRNA, providing a mechanism for the autoregulation (Polymenidou et al., 2011, Ayala et al., 2011, Tollervey et al., 2011b). UV-CLIP studies revealed that TDP-43 binds to different proteins that play an important role in vesicle transport, protein trafficking, ubiquitin ligase molecules, signalling molecules, transcriptional regulators, RNA processing molecules, ion receptor channels and cytoskeletal proteins (Xiao et al., 2011).

TDP-43 associates with members of the heterogenous nuclear ribonucleoprotein (hnRNP) family of proteins (Ling et al., 2010, Freibaum et al., 2010, Buratti et al., 2005). The interactions of TDP-43 with hnRNPs are dependent on its C-terminal glycine-rich domain. hnRNP complexes are known to regulate splicing, and TDP-43 regulates the splicing of human cystic fibrosis transmembrane conductance regulator, survival of motor neuron (SMN), apolipoprotein A2 (APOA2) and serine/arginine-rich splicing factor 2 (SC35) (Buratti and Baralle, 2001). Transcriptome-wide analysis indicates that the splicing of many additional transcripts is probably mediated by TDP-43 (Polymenidou et al., 2011, Tollervey et al., 2011b). TDP-43 also influences mRNA turnover: it regulates mRNA levels of cyclin-dependent kinase 6 (Ayala et al., 2008), Futsch (Feiguin et al., 2009), low molecular weight neurofilament (Strong et al., 2007) and histone deacetylase 6 (Fiesel et al., 2011). The localization of TDP-43 in RNA granules within neuronal processes also suggests that TDP-43 is involved in RNA trafficking (Wang et al., 2008b). Aside from its role in mRNA pathways, TDP-43 is also thought to regulate microRNA (miRNA) biogenesis (Kawahara and Mieda-Sato, 2012). Knockdown of TDP-43 alters the level of several miRNAs (Buratti and Baralle, 2010, Buratti et al., 2010, Sreedharan et al., 2008).

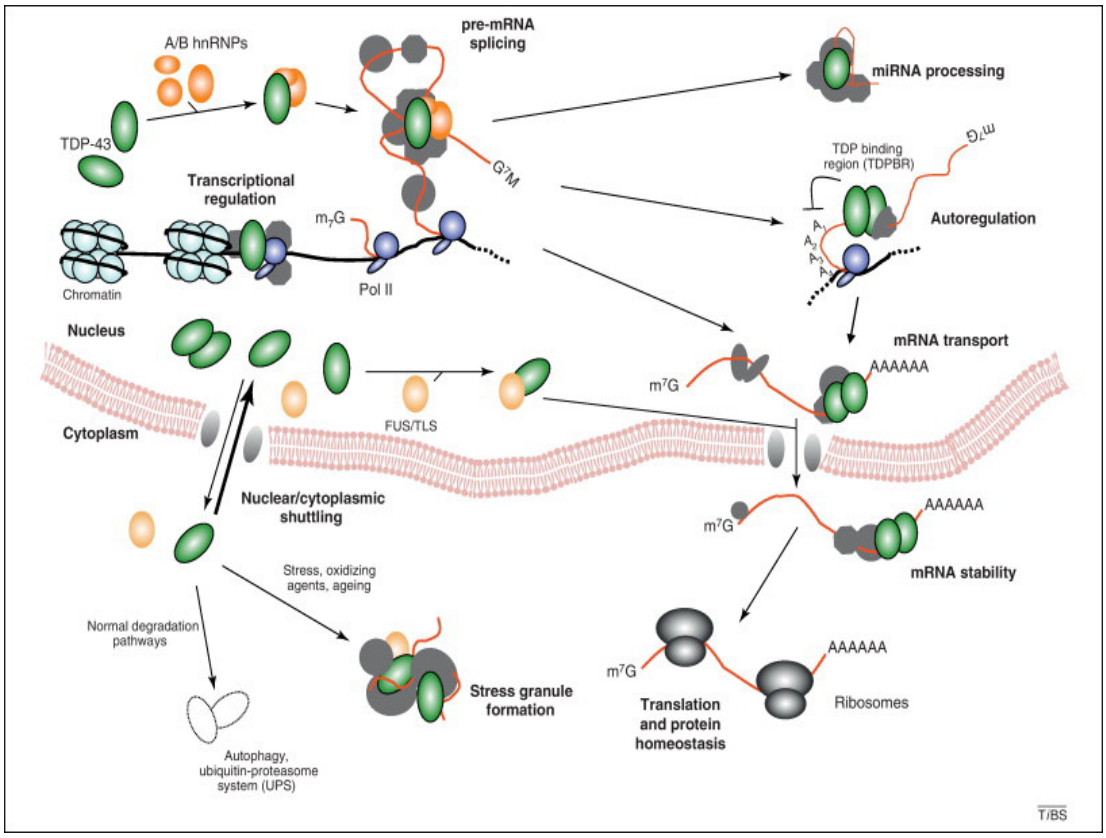

Figure 1.4 Nuclear and cytoplasmic processes of TDP-43

RNA processing pathways controlled by TDP-43. The major nuclear and cytoplasmic processes in which TDP-43 has been shown to play a role (Taken from Buratti and Baralle, 2012)

TDP-43 also interacts with DNA: in particular, single-stranded DNA. A variety of stressors cause TDP-43 to be redistributed from the nucleus into the cytoplasm, where it resides within stress granules. (Wang et al., 2008b, Freibaum et al., 2010, Volkening et al., 2009). Transgenic animal models have shown that TDP-43 is essential for early embryonic development, but the biochemical pathways and genes affected are unknown (Kraemer et al., 2010, Sephton et al., 2010). TDP-43 can act as a transcriptional repressor and is associated with proteins involved in transcription (Sephton et al., 2011). TDP-43 is also known to play an important role in regulation of protein homeostasis (Chen et al., 2012, Ling et al., 2013a), neurite outgrowth (Fallini et al., 2012; Fiesel et al., 2011), localized protein synthesis (Diaper et al., 2013a, Diaper et al., 2013b), cell division (Ayala et al., 2008), apoptosis(Sreedharan et al., 2008), axonal transport (Fallini et al., 2012, Alami et al., 2014). Thus, TDP-43 plays an essential role in

several molecular and cellular processes. Although the role of TDP-43 in RNA processing is well established, the full range of TDP-43 function has yet to be understood.

1.4.6 Disease mechanism for TDP-43

TDP-43 pathology is defined by cytoplasmic mislocalisation, aggregation, and post-translational modification. It is not clear as to which of these mechanisms are directly linked to neurodegeneration and which are secondary to the disease pathology or are epiphenomena. The disease mechanism in TDP-43 revolves around three scenarios: TDP-43 mislocalisation forms inclusions that have acquired novel toxic properties that are independent of the normal function of TDP-43 ('novel toxic gain of function'); the toxicity due to increased normal activity of TDP-43 ('gain of normal function') and finally, loss of nuclear TDP-43 due to its redistribution to the cytoplasm ('loss of normal function'). Evidence for all the 3 mechanism has been reported and a combination of these gain- and loss-of-function mechanisms cannot be excluded (Arnold et al., 2013). The fundamental question as to whether TDP-43 mediates neurodegeneration via a gain of function or a loss of function remains unanswered. TDP-43 gain- and loss-of-function animal models have been generated in species ranging from worms to rodents because of its strong evolutionary conservation. Gain-of-function models are usually achieved by gene overexpression and loss-of-function models by gene knockout or knockdown. *In vivo* and *in vitro* studies have shown that both proteinopathic and preproteinopathic pathways mediate TDP-43 toxicity. Some of the proposed mechanisms are described below.

1.4.6.1 Loss of nuclear TDP-43

Nuclear clearance in TDP-43 is a mechanistically unexplained aspect of TDP-43 loss of function mechanism. In patients with ALS, nuclear clearance of TDP-43 was observed in the majority of inclusion-bearing cells. This led to the hypothesis that some of the adverse effects of abnormal TDP-43 metabolism may reflect a loss of TDP-43 nuclear function (Neumann et al., 2006; Igaz et al., 2008). Transgenic mice expressing human WT-TDP-43, shows nuclear clearance in the affected neurons in the absence of TDP-43

cytoplasmic inclusions (Wegorzewska et al., 2009). Loss of TDP-43 has seen to cause motor defects in transgenic mice and *Drosophila (Feiguin et al., 2009, Sephton et al., 2010)*. Nuclear clearance seems to be an early event in ALS and FTLD-TDP because they occur in cells harbouring pre-inclusions or ubiqutin-negative inclusions (Neumann et al., 2006b, Mori et al., 2008). Thus it has been speculated that the localization of TDP43 within specific nucleoplasmic domains is required for its normal function and loss of normal function of TDP-43 causes its mislocalisation. The contribution of nuclear loss of function mechanism remains unclear. Given the known physiological roles of TDP-43, it is easy to speculate that their loss of function may have profound effects on RNA processing with detrimental consequences for the cell.

1.4.6.2 TDP-43 cytoplasmic localization

Although normal TDP-43 is predominantly nuclear, it shuttles between the cytoplasm and nucleus (Ayala et al., 2005; Wang et al., 2004; Fallini et al., 2012). Thus low levels of TDP-43 can be detected in the cytoplasm. *D. melanogaster* model of mutant VCP-mediated neurodegeneration has shown that VCP mutations redistribute TDP-43 from the nucleus to the cytoplasm (Ritson et al., 2010). The NES and NLS motifs within TDP-43 are the major *cis* elements regulating nuclear localisation. TDP-43 A90V mutant results in increased cytoplasmic partitioning, presumably because the mutation is located between the two NLS motifs (Winton et al., 2008c). TDP-43 or its 35kDa CTFs are re-distributed to the cytoplasm in response to a variety of stressors and co-localise with stress granules (Volkening et al., 2009). Thus, both genetic and environmental factors seem to influence TDP-43 localization. The prevalence of cytoplasmic TDP-43 pathology in a variety of neurodegenerative diseases other than ALS and FTD-TDP suggests that a variety of stressors or insults may lead to cytoplasmic localization and aggregation. Several studies using cell lines and animal model have attempted to address whether cytoplasmic TDP-43 causes neurodegeneration. Mutations of one or both NLS motifs render TDP-43 predominantly cytoplasmic, resulting in cytoplasmic aggregates both in cultured cells and transgenic (Igaz et al., 2011, Winton et al., 2008b). TDP-43 cytoplasmic aggregates can recruit non-mutated nuclear TDP-43 into the cytoplasm of cultured cells (Winton et al., 2008). Transgenic mice expressing TDP-

43 with an NLS mutation resulted in cytoplasmic TDP-43 and rare cytoplasmic inclusions (Igaz et al., 2011). TDP-43 mislocalisation is seen in various models like yeast, cultured spinal and cortical neurons, chick embryos, certain transgenic mice mutants (Barmada et al., 2010, Johnson et al., 2008, Tripathi et al., 2014, Zhang et al., 2009), suggesting that these abnormalities may play a role, at least in part, in TDP-43-mediated neurodegeneration. Increased cytoplasmic localisation of TDP-43 is associated with the formation of intracellular aggregates in the affected areas in patients and in animal models including *Drosophila*, rats, chick, mice (Lee et al., 2012). In cell culture systems, increased cytoplasmic localisation of TDP-43 was proposed to facilitate the formation of intracellular aggregates. Although several cell culture models indicate that cytoplasmic TDP-43 is toxic, animal models have yielded mixed results, and further work is required to determine the mechanistic importance of cytoplasmic versus nuclear TDP-43.

1.4.6.3 TDP-43 Aggregation

The appearance of granular cytoplasmic TDP-43 aggregates, designated as pre-inclusions has been postulated to be an early event in the formation of TDP-43 inclusions (Lee et al., 2012). Pre-inclusions in neurons are accompanied by the characteristic absence of normal nuclear TDP-43. Mature aggregates in ALS are characteristically dense, round inclusions or filamentous skeins in the cytoplasm of affected motor neurons. A variety of TDP-43 cytoplasmic, neuritic and intranuclear inclusions can be seen in the forebrain neurons in FTLD-TDP. The importance of this diversity is unknown.

Purified TDP-43 synthesized in bacteria is intrinsically aggregation prone. Purified full length TDP-43 or C-terminal fragments form amorphous aggregates lacking amyloid properties (Baloh, 2011). This is similar to inclusions formed in ALS/FTLD patient tissues, which likewise appear amorphous and non-amyloid. TDP-43 mutations linked to ALS, increases the aggregation potential of purified TDP-43 illustrating that the tendency to aggregate must be an important property of mutant TDP-43. TDP-43 is highly aggregation prone when overexpressed in yeast, and this property is dependent on the presence of the C-terminal domain (Johnson et al., 2009). In contrast to the

strong tendency of exogenously expressed TDP-43 to form cytoplasmic aggregates in yeast, TDP-43 in cultured mammalian cells (endogenous or overexpressed) remains predominantly soluble, and in the nucleus. However, in cultured mammalian cells, detergent insoluble aggregates of TDP-43 can be formed through several manipulations. These include mutating the RNA binding domain or the nuclear localization signal, or expressing truncation mutants containing only the C-terminal domain (Wang et al., 2004; Ayala et al., 2008; Winton et al., 2008; Igaz et al., 2009). This suggests that altered TDP-43 RNA binding, nuclear localization or proteolytic cleavage can promote TDP-43 aggregation.

One aspect common to all of the models is that overexpression of TDP-43 (wild-type or disease causing mutants) in worms, flies, zebrafish, mice or rats, is toxic in a dose dependent manner and able to produce neurodegeneration. Unfortunately beyond that point of universal agreement, many of these models differ from one another with respect to whether TDP-43 forms insoluble aggregates, is mislocalized to the cytoplasm, or shares other core features of human TDP-43 pathology. TDP-43 inclusions or insolubility is found only in a subset of invertebrate and fish models despite producing similar toxicity and neurodegeneration (Liachko et al., 2010, Li et al., 2010). Therefore, a recurrent theme in these studies is that TDP-43 inclusions are not necessary to promote neurotoxicity. However, these models required the presence of the functional RNA binding motif (RRM1) to promote toxicity. This suggests that in these animal models, TDP-43 toxicity is not through formation of inclusions, but instead via direct modulation of TDP-43 RNA binding partners.

Quantification of TDP43-positive inclusions in transgenic mice revealed no correlation between the number of inclusions and neurodegeneration (Igaz et al., 2011). In rodent models, insoluble TDP-43 inclusions are a minor component of the pathology and are produced as a consequence of TDP-43 overexpression. Although TDP-43 inclusions are a minor component of the pathology in rodent models, they recapitulate most other key features of human TDP-43 pathology, including nuclear clearing, C-terminal fragmentation, and phosphorylation (Tian et al., 2011, Wegorzewska et al., 2009, Shan et al., 2010, Xu et al., 2011). While detergent insoluble inclusions were the key feature leading to the connection between TDP-43 and neurodegeneration, existing animal

models clearly demonstrate that TDP-43 toxicity (at least in the context of overexpression) can occur without the formation of TDP-43 inclusions.

1.4.6.4 Prion like mechanism of TDP-43

A number of recent studies have demonstrated the cellular, prion like nature of TDP-43 (Udan and Baloh, 2011, Nonaka et al., 2013) Purified TDP-43 protein is prone to aggregation *in vitro*. TDP-43 inclusions with amyloid characteristics were found in a subset of ALS spinal cord samples and CNS tissue from ALS and FTD-TDP patients (Bigio et al., 2013, Neumann et al., 2007). Misfolded TDP-43 has been detected in the spinal cord of ALS patients (Shodai et al., 2013). Bioinformatics studies have identified that TDP-43 is the 69th protein most likely to have a prion domain out of 27,879 proteins (Udan and Baloh, 2011). Transducing recombinant pre-formed TDP-43 aggregates into the cytoplasm of TDP-43 overexpressing cells can also induce TDP-43 aggregates (Furukawa, 2012), presumably through a 'seeding' reaction, similar to that recently observed for tau and α-synuclein (Guo et al., 2011). In numerous neurodegenerative disorders, amyloid deposits composed of α-synuclein protein (Parkinsons), tau protein (dementia) are found. Though TDP-43 seeding reactions have been demonstrated *in vitro* (Nonaka et al., 2013), their role in disease pathogenesis is still unclear. The identification of a prion-related glutamine/asparganine (Q/N) rich domain on the C-terminus of TDP-43 has led to the speculation that this prion-like domain has been implicated in aggregation of TDP-43 in cultured cells, and it is thought to confer biochemical properties associated with prions including aggregation, protease resistance and cell-to-cell propagation (but not necessarily infectivity) (King et al., 2012, Gitler and Shorter, 2011). Alternatively the aggregates formed could be a response to cellular stress mediated by prion like domain. Substantial evidence for the seeding and propagation of TDP-43 supports the clinical observation on the prion like behaviour of ALS. The evidence for prion-like behaviour of TDP-43 needs further characterization. Clarity on this concept for TDP-43 proteinopathies could advance understanding of how TDP-43 aggregation contributes to the anatomic spread and clinical progression of these diseases.

1.4.6.5 Phosphorylation and C-terminal fragmentation of TDP-43

C-terminal TDP-43 fragments of ~25 and ~35 kDa were recovered in the sarkosyl-insoluble fraction of affected brain regions of ALS-TDP and FTD-TDP patients (Neumann et al. 2006), and it is suspected that they seed the aggregation of TDP-43 into inclusions. The 25 kDa CTFs recapitulate some of the pathological features of TDP-43 proteinopathy such as increased cytoplasmic accumulation, hyperphosphorylation, insolubility, polyubiquitination and cytotoxicity (Zhang et al., 2009; Igaz et al., 2008). 25 kDa CTFs were found to increase in number in transgenic mice expressing wild-type or mutant TDP-43, arguing for a pathogenic role. However the 25 kDa CTF was solely nuclear as opposed to being cytoplasmic in patients and cell culture (Wegorzewska et al., 2009). Accumulation of 35 kDa CTFs was found in lymphoblastoid cell lines derived from patients with TDP-43 mutations (Kabashi et al., 2008), but the 35 kDa fragments were either low or undetectable in the CNS tissues of patients (Neumann et al., 2006), suggesting that this fragment is not pathologic.

Caspase- 3 is considered to be the main protease generating the 25 kDa CTFs. Since caspase-3 is activated during apoptosis, generation of CTF is considered to be a late event in neurodegeneration. Downregulation of progranulin, a secreted growth factor can also mediate the proteolytic cleavage of TDP-43 (Zhang et al., 2007). However, this was not replicated in other studies (Dormann et al., 2009). It is not clear if TDP-43 CTFs confer a gain or loss of function. One group found that TDP-43 CTFs impair neurite growth during differentiation of cultured rodent neurons, and that full-length TDP-43 rescues this phenotype, suggesting that TDP43 CTFs act by a dominant-negative mechanism. However, expression of full-length TDP-43 in *D. melanogaster* was toxic to a variety of neuronal cell types, whereas expression of TDP-43 CTFs did not result in neurotoxicity (Voigt et al., 2010, Yang et al., 2010)

Phospho-specific antibodies have been used to study the role of phosphorylation of TDP-43 in FTD-U and ALS patients. S409/410 has been identified as the major site of phosphorylation on TDP-43 (Neumann et al., 2009a). TDP-43 CTFs or cytoplasmic TDP-43 is phosphorylated in a variety of cell lines that are engineered to overexpress TDP-43 (Zhang et al., 2010; Igaz et al., 2011). Phosphorylated TDP-43 proteins exhibit a

longer half-life than non-phosphorylated proteins. This suggests that phosphorylation may inhibit UPS-mediated degradation and contribute to aggregate. Alternatively, as TDP-43 phosphorylation is associated with TDP-43 insolublility, it remains possible that aggregation may render TDP-43 CTFs less vulnerable to UPS-mediated degradation and that phosphorylation is merely a marker of aggregation. It is not clear whether phosphorylation of TDP-43 and its CTFs are a primary event, or an epiphenomenon following earlier pathogenic events. Although a correlation between insolubility and phosphorylation of TDP-43 has been reported, phosphorylation is not required for C-terminal cleavage, aggregation or toxicity in cellular models (Zhang et al., 2009, Igaz et al., 2009). There is some evidence that TDP-43 phosphorylation may result in differential degradation and/or toxicity of the protein, but the precise role of TDP-43 phosphorylation in disease mechanism remains unclear.

1.4.6.6 Ubiquitination, the ubiquitin-proteasome system and the autophagic system

The accumulation of ubiquitinated proteins in many neurodegenerative disorders strongly suggests that components of the protein degradation machinery are defective. The ubiquitin proteasome system (UPS) and the autophagy–lysosome system (hereafter called 'autophagy') play an important role in proteolysis. They monitor protein quality and protect cells from dysfunctional or misfolded proteins (unfolded protein response, UPR). Ubiquitination of the pathologic CTFs (Igaz et al., 2009) in cells suggests that cellular degradation machineries play an important role in removing TDP-43 aggregates. Thus, disruption of the UPS might contribute to increased levels of ubiquitylated TDP-43 in ALS and FTD-TDP. The role of ubiquitination of TDP-43 in disease pathogenesis remains unknown, although it is likely to be a late event, since most of the TDP-43 pre-inclusions have weak or no ubiquitination (Giordana et al., 2010, Mori et al., 2008). Inhibition of UPS or the autophagic system in cell culture systems, showed an increase in cytoplasmic TDP-43 accumulation and the formation of intracellular aggregates (Lagier-Tourenne et al., 2010).

TDP-43 interacts with a variety of proteins that are involved in autophagy or related pathways, including the endosomal sorting complexes required for transport (ESCRTs),

ubiquilin 1 (UBQLN), sequestosome 1, histone deacetylase 6 (HDAC6), VCP and STAM-binding protein (STAMBP; also known as AMSH), ubiquilin 2 (UBQLN2) (Janssens and Van Broeckhoven, 2013a). ESCRTs are required to traffic proteins into multivesicular bodies, and depleting cells of ESCRT subunits inhibits autophagy and results in increased ubiquitylated, cytoplasmic TDP-43. UBQLN was found to mediate TDP-43 autophagosomal degradation in cultured cells. TDP-43 was also shown to affect the expression of histone deacetylase 6 (HDAC6), another protein associated with autophagosomal degradation. HDAC6 promotes the aggregation of polyubiquitinated proteins and their autophagic degradation (Fiesel et al., 2010). Genetic ablation of HDAC6 resulted in ubiquitinated protein aggregate accumulation and neurodegeneration in *Drosophila* and in mice (Lee et al., 2010). VCP acts as a molecular chaperone in a range of cellular activities, including ubiquitin-dependent protein degradation, cell-cycle regulation, and apoptosis. UBQLN2 is thought to be involved in protein degradation. TDP-43 inclusions were found in the CNS tissue of patients with *UBQLN2* mutations, suggesting that perturbation of protein degradation pathway is mechanistically linked to the formation of TDP- 43 inclusions. These findings indicate that both the UPS and autophagy play a key role in TDP-43 turnover. However, whether this role includes modifying or inducing TDP-43 patho-mechanisms requires further examination.

1.4.6.7 TDP-43 repression of cryptic exons is compromised

Ling et al., 2015 have reported a new function for normal TDP-43: the repression of cryptic exon inclusion in the pool of translation-ready mRNAs. They found that depletion of TDP-43 expression in mouse ES cells and human HeLa cells resulted in the identification of a battery of cryptic exons using RNA sequencing. HIT-CLIPS showed that TDP-43 binds directly to the cryptic exons leading to the hypothesis that TDP-43 plays an important role in their repression. They found that expression of an artificial protein comprising the RNA binding motif of TDP-43 rescued cell death associated with TDP-43 depletion and also dampened inclusion of cryptic exons in many of the transcripts previously identified (Ling et al., 2015).

1.4.6.8 RNA metabolism

Defects in RNA processing have been implicated in the pathogenesis of many human diseases (Cooper et al., 2009). The high frequency of alternative splicing in the brain suggests that neurodegenerative disorders might be clinical manifestation of defects in RNA processing. TDP-43 has been implicated in RNA biology, suggesting that disturbances in RNA regulation may play a major role in ALS and FTD.

1.4.6.8.1 mRNA splicing

Increased levels of wild-type TDP-43 were reported to lead to an increased number of intranuclear structures called GEMs (Gemini of coiled bodies) in mice (Shan et al., 2010). GEMs are small punctate nuclear structures that are enriched with survival motor neuron (SMN) protein and play a role in small nuclear ribonucleoprotein maturation and pre-RNA splicing. Mutations in *SMN* can cause a paediatric form of MND called spinal muscular atrophy (Lefebvre et al., 1995). Like TDP-43, SMN forms part of a complex that is involved in pre-mRNA splicing. TDP-43 has been shown to be involved in the exon splicing of SMN (Wang et al., 2004). TDP-43 was also shown to enhance exon 7 inclusion and stability of SMN2 in cultured cells (Bose et al., 2008). Assembly of the SMN complex takes place in the cytoplasm and transported into the nucleus for maturation of the small nuclear ribonucleoproteins (Tsao et al., 2012). Similarities in function and cellular distributions of TDP-43 and SMN, suggest that abnormal RNA processing especially RNA splicing, might be an important common mechanism underlying various types of MND. While the role of increased GEMs in TDP-43-induced toxicity remains to be determined, these findings suggest that TDP-43 overexpression impacts pathways that control RNA metabolism.

The most studied pre-mRNA splicing effect of TDP-43 occurs on cystic fibrosis transmembrane conductance regulator (CFTR). CFTR is a multi-domain integral membrane glycoprotein that belongs to the 'adenosine nucleotide binding cassette transporter family'. Mutations in *CFTR* cause the genetic disorder cystic fibrosis in an autosomal-recessive fashion (Riordan, 2008). TDP-43 binds to the (UG) repeats of CFTR, to promote exon 9 skipping. TDP-43 overexpression enhanced the skipping of

CFTR exon 9, whereas silencing of TDP-43 resulted in exon 9 inclusion (Buratti et al., 2001). TDP-43 also mediates exon skipping of ApoA2 exon 3 by binding to a (GU)16 repeat in intron 2. *ApoA2* encodes for apolipoprotein AII, a protein abundant in high-density lipoprotein complexes. Knockdown of TDP-43 leads to constitutive exon 3 inclusion independent of any *cis*-acting elements (Mercado et al., 2005). Thus TDP-43 can inhibit or enhance splicing functions. Recent screens have yielded many novel splicing-related protein interaction partners of TDP-43. This further emphasizes the importance of TDP-43 for the mRNA maturation process (Friebaum et al., 2010; Sephton et al., 2011).

1.4.6.8.2 mRNA stability

As a member of the hnRNP family, the main distinguishing feature of TDP-43 is its ability to bind RNA in a single-stranded and sequence-specific manner. This is facilitated by its two RRM motifs. The RNA-binding function of TDP-43 is essential for most of its RNA-processing steps. It is estimated that mRNA stability regulates the expression of 5–10% of human genes and thus represents an important regulatory mechanism. TDP-43 binds to the 3'UTR of its target mRNA and stabilizes them (Strong et al., 2007). In addition to its effects on RNA splicing, TDP-43 also influences mRNA turnover: its expression regulates mRNA levels of cyclin-dependent kinase 6 (Ayala et al., 2008), histone deacetylase 6 (Fiesel et al., 2010), Futsch (Godena et al., 2011), MAP1B (Coyne et al., 2014) and low molecular weight neurofilament (Strong et al., 2007)

1.4.6.8.3 Transcriptional Regulation

TDP-43 was described as a protein associated with HIV transcription (Ou et al., 1995). TDP-43 binds to pyrimidine-rich sequences together with other factors via its two RNA recognition domains and represses gene expression. TDP-43 regulates the testis-specific expression of the mouse *SP-10* gene (Abhyankar et al., 2007). TDP-43 interacts with subunits of the mediator complex which binds to the C-terminal tail of RNA polymerase II (pol II) and stimulates initiation as well as re-initiation of transcription (Fiesel and Kahle, 2011). The termination of pol II is important for regulation of gene

expression. If termination is not stopped, pol II remains bound to DNA and is not available for another round of transcription. In some transcripts, elongation of pol II pauses after the poly-A signal, slowing down transcription rate. This provides enough time for the 5'-3' exonuclease Xrn2 to attach to the 3' cleavage product and to degrade it while catching up with RNA pol II. In a yeast study, TDP-43 was identified as an Xrn2 protein-interactor suggesting a possible role for TDP-43 in transcriptional regulation via interference with the termination process (Wang et al., 2008a). Thus, TDP-43 may exert positive as well as negative effects on transcription depending on the context (Fiesel and Kahle, 2011).

1.4.6.8.4 mRNA Quality Control

RNA quality control is emerging as an important step in RNA processing. Nucleus is the centre for quality control after which the correctly processed mRNAs are exported to the cytoplasm. Exosomes in the nucleus play an important role in the degradation of aberrant pre-mRNAs that result from mutations in factors important for 3' end processing, splicing and export (Vanacova and Stefl, 2007). The The nonsense mediated decay (NMD) is the most characterized pathway. This surveillance mechanism prevents the accumulation of non-functional mRNAs bearing a premature termination codon (Isken and Maquat, 2007). NMD degradation involves two different mechanisms: 5' decapping followed by 5'-3' exonuclease activity or 3' deadenylation and 3'-5' exonuclease activity. Final RNA degradation is accomplished by the exosome auxiliary factor 5'-3' exonuclease Rrp6 or by the cytoplasmic 3'-5' exonuclease Xrn1. TDP-43 was shown to interact with Rrp6 in a yeast study indicating a potential involvement of TDP-43 in the nuclear or cytoplasmic RNA quality control (Buratti and Baralle, 2009).

1.4.6.8.5 MicroRNA biogenesis

miRNAs are short, endogenous non-coding single-stranded RNAs that control gene expression. In vertebrates, miRNA encoding genes are the most abundant class of regulatory genes. The regulatory functions of microRNAs are accomplished through the RNA-induced silencing complex (RISC). MiRNAs assemble into RISC, activating the

complex to target messenger RNA (mRNA) specified by the microRNA. miRNA biogenesis starts with the transcription into a primary miRNA transcript (pri-miRNA). The pri-miRNA is endonucleolytically cleaved by the microprocessor complex, which consists of the RNase III enzyme Drosha and DGCR8 protein (DiGeorge critical region 8; also known as Pasha (partner of Drosha)). TDP-43 was identified as a component of the large Drosha complex in mouse and human cells by mass spectrometry (Buratti et al., 2010). Human and mouse Drosha complexes were able to process pri-miRNA to pre-miRNA *in vitro* suggesting a putative role for TDP-43 in the biogenesis of (pre-)miRNA. Buratti *and colleagues* (Buratti et al., 2010) reported that specific miRNAs are regulated upon knockdown of TDP-43 in Hep-3B, HeLa and SH-SY5Y cells. These miRNAs were either downregulated or upregulated suggesting different activities of the TDP-43 protein on these miRNAs.

1.4.6.8.6 mRNA translation/export

TDP-43 has not been described to affect RNA export and translation directly; however, it might have indirect effects. All mRNA precursors are retained in the nucleus until maturation is completed. Thus, inappropriate RNA maturation may also impair RNA export and subsequent translation into functional proteins. This aspect of putative TDP-43 biology remains to be investigated (Fiesel et al., 2011).

1.4.6.8.7 TDP-43 Autoregulation

The TDP-43 protein is normally expressed through transcription and translation, and once produced, it regulates its own expression by a feedback mechanism, i.e., upregulating its own expression when the protein level is too low and inhibiting its expression when the protein level is too high (Polymenidou et al., 2011; Ayala et al., 2011; Sephton et al., 2009). Autoregulation of TDP-43 seems to occur through a particular region of its 3'UTR that is called the TDP-43 binding region (TDPBR). This region contains several non-UG sequences, which are essential for autoregulation of TDP-43 mRNA levels. When TDP-43 nuclear levels rise, increased binding to the TDPBR promotes mRNA instability and increased exosome degradation and vice versa when there are low levels of TDP-43 (Ayala et al., 2011). By this auto-regulatory mechanism,

the intracellular level of TDP-43 is maintained within a narrow range. This tightly maintained TDP-43 level may be important because TDP-43 functions in multiprotein/RNA complexes, where a proper structure and function of the complex requires a certain stoichiometric ratio between TDP-43 and its protein and RNA partners. Overexpression of exogenous TDP-43 leads to a decrease in endogenous TDP-43 mRNA and protein in cultured cells and transgenic mice (Igaz et al., 2011; Kabashi et al., 2008). Based on this, a hypothetical 'loss of autoregulation' model has been proposed wherein export of TDP-43 to the cytoplasm and its sequestration into insoluble aggregates may well stimulate the autoregulatory system to attempt a major increase in the levels of TDP-43 to nullify the loss of nuclear TDP-43. This energetic expenditure of TDP-43 production may lead to a certain degree of cell suffering and will lead to increased aggregate formation. This would feed forward through a vicious cycle leading to cell death (Polymenidou et al., 2007). The detailed mechanism underlying auto-regulation is unresolved. Regardless, self-regulation of TDP-43 expression seems to be an important contributor to ALS pathogenesis following an initiating event that yields reduction in nuclear TDP-43 levels (by mutation and/or cytoplasmic aggregation), thereby driving elevated TDP-43 synthesis.

1.4.6.9 Mitochondrial Dysfunction

TDP-43 wild-type transgenic mice show large perinuclear accumulation of mitochondria in TDP-43 negative cytoplasmic aggregates. This phenomenon was attributed to impaired mitochondrial trafficking reflected by a marked reduction of mitochondria at nerve terminals (Xu et al., 2010; Shan et al., 2010). However, mitochondrial inclusions are not observed in human cases and their relevance to human disease is unknown. Although not fully characterized, TDP-43 promotes neuron survival or neuroprotection via increased HDAC6 (microtubule associated deacetylase) expression. HDAC6 has recently been implicated in mitophagy and the clearance of misfolded protein aggregates (Lee et al., 2010). TDP-43 aggregation could directly cause mitochondrial defects or indirectly through improper regulation of HDAC6. Other TDP-43 regulated targets could also indirectly compromise

mitochondrial integrity. Transgenic mice expressing human TDP-43 wild-type showed abnormal expression of the mitochondria fission/fusion proteins MFN1 and Fis1 (Xu et al., 2010). NSC-34 cells expressing TDP-43 show mitochondrial dysfunction and oxidative stress. Additionally, the expression of TDP-43 in yeast, leads to the formation of perimitochondrial TDP-43 aggregates that causes mitochondrial-dependent oxidative stress and cytotoxicity (Braun et al., 2011). Abnormal mitochondria accumulate in presynaptic axosomatic terminals of motor neurons in ALS (Gendron and Petrucelli, 2011) and cytoplasmic granules in motor neurons contain mitochondria with TDP-43 immunoreactivity (Mori et al. 2008). TDP-43 also disrupts ER-mitochondria interactions and this is associated with disruption in cellular Ca2+ homeostasis (Stoica et al., 2014). Disturbance of mitochondrial Ca2+ transport in ALS have been widely described in SOD1 models *in vitro* and *in vivo*. Together, these findings implicate mitochondrial abnormalities in TDP-43-induced toxicity and provide a potential convergence between TDP-43 and SOD1 in the pathogenesis of ALS (Carri et al., 2015).

1.4.7 Disease models of TDP-43

1.4.7.1 Loss of function mechanisms

Loss of function mechanisms has not been fully characterized. In rodents, knocking down TDP-43 was shown to cause early embryonic lethality. Inducible knockout in adult mice causes a rapid loss of fat tissue and lethality (Xu, 2012). In mouse embryonic stem cells, conditional knockout of TDP-43 causes cell death (Chiang et al., 2010). knockdown of TDP-43 in cultured neurons causes morphological abnormalities and cell death (Guo et al., 2011, Tsai et al., 2010, Yang et al., 2010, van Eersel et al., 2011) and a large change in gene expression in cells of the CNS (Polymenidou et al., 2011; Tollervery et al., 2011). In *C. elegans*, TDP-43 deletion mutants are viable, but show slow growth, locomotor defects and low fertility. TDP-43 knockout in *Drosophila*, causes abortive embryonic development and lethality and those that survive to adulthood, display severe locomotor defects, abnormal neuronal morphology and

premature death. Adult TDP-43 knockdown flies show progressive axonal degeneration and locomotor defects (Li et al., 2010). TDP-43 knockdown during embryonic development causes selective defects in motor axonal growth and results in motor behavioural abnormalities in zebrafish (Kabashi et al., 2010). These results do not show any conclusive evidence of a role for TDP-43 dysfunction in neurodegeneration in ALS and FTLD, but they do indicate the importance of TDP-43 in the development and functioning of the nervous system.

Rapid lethality without motor neuron disease was seen with ubiquitous postnatal removal of TDP-43 (Chiang et al., 2010). Selective removal of TDP-43 from motor neurons produced age-dependent progressive motor neuron degeneration with ALS-like pathology. However, in one study, the removal of TDP-43 did not cause any symptoms and the mice lived a normal life span (Iguchi et al., 2013) whereas in another study only the male mice developed pathology and phenotype (Wu et al., 2012). Recent studies have shown that ALS linked TDP-43 mutants can produce aberrant RNA splicing and adult-onset MND without loss of nuclear TDP-43 (Arnold et al., 2013). This shows that although neuronal loss of function of TDP-43 may contribute to disease development and progression, it may be insufficient to produce fatal MND.

1.4.7.2 Gain of function mechanisms

Several TDP-43 wild-type and mutant over-expression models have been generated in worms, flies, zebrafish, chick, mice, rats etc. to study ALS. Almost all of the overexpression models show neurodegeneration accompanied by several phenotypes such ad motor deficits, decreased locomotion, paralysis, motor neuron loss and reduced life span. The diversity and severity of the phenotypes correlates with the levels of transgene accumulation in the neurons. In worms, flies and zebrafish, expression of human TDP-43 carrying ALS-linked mutations uniformly produces greater toxicity than wild-type TDP-43. Mice expressing human wild-type TDP-43 in the CNS has consistently shown a dose and threshold dependent toxicity (Igaz et al., 2011, Shan et al., 2010, Stallings et al., 2010, Xu et al., 2011). Diverse phenotypes including motor abnormalities, growth retardation, cognitive impairments and lethality were reported. Overexpression of mutant TDP-43 in mice resulted in gait abnormalities and death

within 150 or 75 days (Stallings et al., 2010; Wegorszewska et al., 2009). TDP-43 fragmentation, astrogliosis, Ubiquitin accumulation microgliosis, axonal degeneration, neuronal loss, motor function impairments, and shortened lifespan are observed in many of the transgenic animals. However, it is not clear how the toxicity mediated by wild-type TDP-43 in these organisms relates to the situation in human disease. To date copy number variation of the *TARDBP* gene has not been found in humans nor are brain mRNA levels changed in most patients with various TDP-43 proteinopathies (Lagier-Tourenne et al., 2010). The comparison of TDP-43 transgenic models indicates that both wild-type and mutant TDP-43 are neurotoxic upon overexpression. However, the threshold of TDP-43 expression required to induce toxicity appears to be lower for mutant TDP-43 than for wild-type TDP-43. That mutant TDP-43 may be more toxic than wild-type TDP-43 in rodents is consistent with some studies conducted in other model organisms, including yeast, chicken embryos, *Drosophila melanogaster* and mammalian cells.

In yeast, aggregation of TDP-43 is accelerated by certain mutations (Johnson et al., 2008), similar to cultured cells (Guo et al., 2011). In response to stressful stimuli, TDP-43 mutations alter TDP-43 stress granule formation, leading to increased TDP-43 inclusion formation (Dewey et al., 2012, Liu-Yesucevitz et al., 2010). Mutant TDP-43 is reportedly more prone to mislocalise to the cytoplasm of primary neurons, where it induces a toxic gain-of-function and cell death (Barmada et al., 2010). Some mutations increase the tendency of TDP-43 to become cleaved into CTFs (Rutherford et al., 2008, Kabashi et al., 2008, Sreedharan et al., 2008) and produce higher amounts of protease-resistant fragments of 10–11 and 24–25 kDa (Guo et al. 2011). Altered RNA expression and splicing are likely contributors to TDP-43 toxicity in rodent TDP-43 transgenic models.

These studies emphasize that TDP-43 interacts with a diverse spectrum of RNA targets with important functions in the brain. A greater understanding of the pathomechanisms of TDP-43 is absolutely necessary. This information will help us understand the characteristic traits of ALS-TDP and FTLD-TDP, such as TDP-43 mislocalisation, aggregation, truncation, phosphorylation, ubiquitination and RNA metabolism.

1.5 Chromosome 9 open reading frame 72

1.5.1 *C9ORF72* Expansion Discovery

Linkage analysis of kindreds involving multiple cases of ALS, FTD and ALS-FTD reported an important locus for the disease on the short arm of human chromosome 9 (Boxer et al., 2010, Morita et al., 2006, Pearson et al., 2011, Vance et al., 2006). Using the genome-wide association (GWAs) approach, a locus on chromosome 9p21 was found to be accountable for nearly half of familial ALS and nearly one quarter of all ALS cases in a cohort of 405 Finnish patients and 497 controls (Laaksovirta et al., 2010). Next-generation sequencing technology identified a hexanucleotide repeat expansion (GGGGCC) within the C9ORF72 gene as the cause of chromosome 9p21-linked ALS-FTD, and confirmed the presence of this large expansion in a substantial proportion of familial ALS and FTD cases. Overall, the GGGGCC (G4C2) hexanucleotide repeat expansion was found in nearly one half of Finnish familial ALS cases and in more than one third of familial ALS cases of wider European ancestry (Renton et al., 2011). At the same time De-Jesus Hernandez et al., provided evidence that disease in the 'Vancouver, San-Francisco and Mayo family 20' (VSM-20: a large ALS-FTD family) was caused by an expanded hexanucleotide repeat in a non-coding region of chromosome 9 open reading frame 72 (*C9ORF72)* and that this repeat expansion is the most common cause of familial FTD and ALS identified to date. They identified a total of 75 unrelated expanded GGGGCC repeat carriers from 722 patients with FTD, ALS or a combination of both (DeJesus-Hernandez et al., 2011). Results from these two independent studies showed that *C9ORF72* repeat expansions are the most common cause of sALS and fALS and that *C9ORF72* repeat expansion is more than twice as common as mutations in the SOD1 gene as a cause of familial ALS and more than three times as common as TARDBP, FUS, OPTN and VCP mutations combined.

1.5.2 *C9ORF72* gene and protein

The C9ORF72 gene comprises 12 exons, including two non-coding exons (1a and 1b). Alternative splicing results in multiple transcript variants encoding different isoforms: V1, V2 and V3, with exons 1a and 1b to be differentially incorporated into RNA. The three transcripts are predicted to express two alternative C9ORF72 protein isoforms of varying amino acid length. Transcript variants 1 and 3 are predicted to express the long amino acid (481) C9ORF72 while transcript variant 2 is predicted to express the short amino acid (222) C9ORF72 protein (DeJesus-Hernandez et al., 2011). The functions of the C9ORF72 protein isoforms are yet to be characterized though they have been implied to play a role in the regulation of endosomal trafficking. Bioinformatic studies suggest that C9ORF72 belongs to a poorly characterised protein family that is highly conserved throughout evolution, with marked loss or divergences in certain species such as the fruit fly *Drosophila*. Protists, a eukaryotic ancestor common to plants, fungi and animals have been known to express C9ORF72. C9ORF72 orthologues have been identified in *C. elegans*, zebrafish and mice which are therefore ideal model systems for studying loss of C9ORF72 protein function (Stepto et al., 2014b).

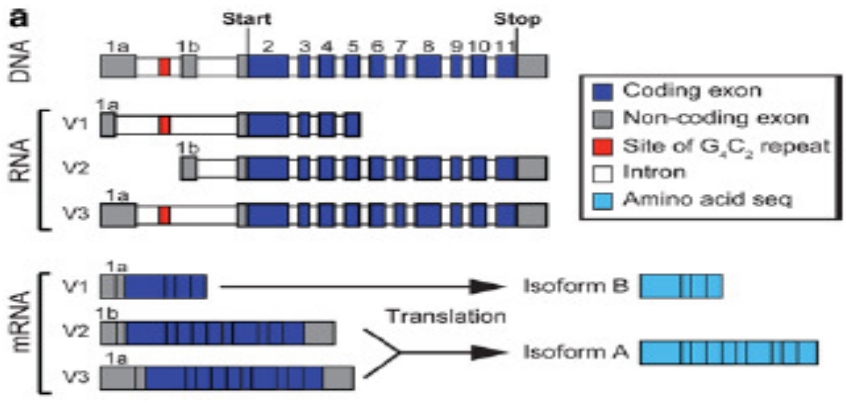

Figure 1.5 C9orf72 gene and protein isoforms
(Taken from Stepto et al., 2014)

RT-PCR analysis shows that all the C9ORF72 transcripts are expressed in various tissues and that C9ORF72 is mostly a cytoplasmic protein (DeJesus-Hernandez et al., 2011). C9ORF71 is expressed in the CNS with the highest expression in the cerebellum. Expression was also observed in the frontal cortex, hippocampus, hypothalamus and spinal cord (Renton et al., 2011). C9ORF72 was expressed throughout neurons in cortical cultures (Atkinson et al., 2015). A recent study showed increased expression of the non-repeat-containing transcript in motor neurons and frontal cortex of transgenic mice and in human embryonic stem cell-derived motor neurons. This study also identified that the mouse C9ORF72 orthologue is most readily expressed in neurons associated with FTLD and ALS, but almost absent in spinal microglia and astrocytes suggesting that neuron-specific expression patterns of C9ORF72 may explain cell type-specific neurodegeneration (Suzuki et al., 2013).

Sequence homology identifies C9ORF72 as a member of the highly conserved family of 'differentially expressed in normal and neoplastic cell' (DENN) proteins. Proteins with DENN regions regulate Rab GTPases. DENNs are Rab guanine-diphosphate/triphosphate (GDP-GTP) exchange factors (Rab-GEFs). GTPases function in vesicular formation and membrane trafficking and are therefore crucial for synapse formation and function (Stepto et al., 2014b). Since DENN's control membrane based processes, it is speculated that C9ORF72 is likely to be involved in some trafficking event of membranes within the cell.

1.5.3 GGGGCC hexanucleotide expansion repeats

A GGGGCC hexanucleotide repeat expansion intronic to chromosome 9 open reading frame 72 (C9ORF72) was identified in 2011 as the most common genetic cause of ALS and FTLD with or without concomitant (Renton et al., 2011, DeJesus-Hernandez et al., 2011). Pathologic expansion of C9ORF72 is the most common genetic cause of ALS, estimated at around 34% of familial and 6% of sporadic ALS cases and 7% sporadic of FTLD, and 25% of familial FTLD cases (Majounie et al., 2012). The highest mutation frequencies were observed in Caucasian populations of Europe and North America, and were markedly elevated in ALS patients of Finland, Sweden and Denmark (Renton et al., 2011, Majounie et al., 2012). By contrast, in Asian populations *C9orf72* repeat

expansions were generally rare (Jang et al., 2013, Tsai et al., 2012). Patients with a family history of disease showed significantly higher mutation frequencies compared to non-familial patients.

1.5.4 *C9orf72* repeat expansions are associated with wide clinical diversity.

An individual carrying a pathological C9orf72 repeat expansion can develop FTLD or ALS, or both. Clinical data from patients with *C9ORF72* mutations show that males are much more susceptible (55.8%) than females; and the mean age at onset is 56.1 years, and the mean disease duration is 49.9 months. The age at onset and disease duration are highly variable, even within a single family. Juvenile ALS was not associated with C9orf72 repeat expansions. The age of onset ranges from 27 to 83 years, and the disease duration varies between 3 and 264 months. Patients with C9ORF72 have a tendency towards younger age at onset and shorter disease duration when compared to patients without them (van Blitterswijk et al., 2014).

Patients with C9ORF72 mutations also show mutations in other ALS/FTLD related genes viz. *TARDBP*, *FUS*, *SOD1*, *ubiquilin-2* (UBQLN2), *Progranulin* (PNR) *vesicle-associated membrane protein B* (VAPB), *angiogenin* (ANG), *optineurin* (OPTN), *D-amino-acid oxidase* (DAO), peripherin (PRPH), and *presenilin-2* (PSEN2). However, some of these mutations are also seen in control patients. Thus the mechanisms underlying multiple mutations are not clear (van Blitterswijk et al., 2012b, Cooper-Knock et al., 2015).

The ALS phenotype associated with G4C2 repeat expansion of *C9ORF72* is representative of the whole clinical spectrum of ALS (Cooper-Knock et al., 2012, Murray et al., 2011). Bulbar onset has been found to be more frequently associated with *C9ORF72*-related ALS, than with non-*C9ORF72* ALS (van Rheenen et al., 2012). The predominant FTLD phenotype associated with *C9ORF72* mutations is that of bvFTD. PNFA was the second most common FTLD variant associated with *C9ORF72* expansions whilst SD has been seen more rarely associated with *C9ORF72* expansions. Additional symptoms seen in patients with C9ORF72

mutations include psychotic phenomena and signs of Parkinsonism (Boeve et al., 2012, Cooper-Knock et al., 2012, Snowden et al., 2013). C9ORF72 mutations have been detected in patients with clinical diagnoses of Multiple sclerosis, Alzheimer's disease, Parkinson disease, sporadic Creutzfeldt–Jakob disease, corticobasal syndrome (CBS), and olivopontocerebellar degeneration (OPCD); but they appear to be rare, and may be put down to clinical misdiagnoses (Majounie et al., 2012). All these findings highlight the substantial clinical heterogeneity that is detected in patients with C9ORF72 mutations.

TDP-43 pathology is associated with repeat expansions in *C9ORF72* in various neuroanatomical regions. In addition to the TDP-43 positive inclusions, p62 positive TDP-43-negative neuronal intranuclear (NII) and cytoplasmic inclusions (NCIs) were found in the cortex, hippocampus and cerebellum. These inclusions are unique to C9ORF72 mutations (Stepto et al., 2014a). Several research groups are trying to identify the nature of these TDP-43 negative ubiquitinated protein, as it may shed light on the disease mechanisms associated with *C9ORF72* expansions.

1.5.5 Somatic heterogeneity of G4C2 hexanucleotide repeat expansions

In general population, the vast majority of the *C9ORF72* alleles contain two to thirty GGGGCC hexanuceotide repeats. Affected individuals with *C9ORF72* mutations harbour one normal allele and one expanded allele with hundreds to thousands of these repeats. The size of the G_4C_2 hexanucleotide repeats in *C9orf72* alleles ranges from two repeats to more than 4000 repeats, although the exact number of repeats and hence the precise threshold for disease is still unclear due to difficulties in accurately handling and sequencing DNA with such a high GC content (van Blitterswijk et al., 2013, Buchman et al., 2013). Consequently, a cut-off of thirty repeats is commonly used to differentiate between pathogenic and non-pathogenic repeat sizes (Renton et al., 2011). The pathologic cut-off for *C9orf72* repeat expansions remains debatable since repeat sizes of thirty or more are also present in approximately 0.17% of the control subjects. However, relatively small repeat sizes are reportedly

pathogenic in FTLD (Gómez-Tortosa et al., 2013) and the clinical phenotype of ALS cases with 20–30 repeats are similar to those with over 30 repeats (Byrne et al., 2014).

So far, in a pure ALS group, there has been no correlation between phenotype and repeat length (van Blitterswijk et al., 2013). A study group detected substantial variation in repeat sizes between samples from the cerebellum, frontal cortex, and blood in FTLD patients with C9OR72 mutations. They found that the frontal cortex had the longest repeat numbers while the cerebellum had the shortest repeats. The repeat length in the frontal cortex correlated with age of onset and age of sample collection whereas the longer repeats within the cerebellum correlated with survival. Their findings indicated that expansion size did affect disease severity. It is hypothesised that repeat expansions can increase in size through a human lifetime resulting in significant somatic heterogeneity, implying that the minimum repeat length in the CNS is more reflective of the germline repeat number. One study used a small group of patients with a variety of neurodegenerative phenotypes (FTLD, ALS and Alzheimer's disease), identified a positive correlation between repeat length and age of onset in C9ORF72-related patients (Beck et al., 2013). A clear relationship between *C9ORF72* expansion size and disease severity is yet to be found, particularly in ALS. Myotonic dystrophy type I (DM1) is caused by a repeat expansion in a non-coding region of DMPK. In DM1, the correlation between repeat size and phenotype is apparent, but only when a large number of cases (>100) are considered. In comparison, only small groups of patients have been studied in C9ORF72-ALS. Thus a bigger study group of C9ORF72 patients are needed to identify a correlation.

Measuring the G4C2 repeat length has proved to be technically challenging as it is not amenable to PCR-based sequencing. In most settings, a pathogenic G4C2 hexanucleotide repeat expansion is detected using a repeat-primed PCR assay (RP-PCR), ideally accompanied with a PCR amplicon fragment length assay. RP-PCR detects an expanded repeat allele as being larger than 60 repeats, without further indication of the exact repeat length. PCR amplicon fragment length assay provides the exact repeat length of alleles for up to 80 repeats (Akimoto et al., 2014, van der Zee et al., 2013). Several groups have optimised Southern hybridisation-based techniques for measuring the repeat length. However, it requires biomaterials, expertise and equipment that are

not commonly available in clinical laboratories. Instability of large G4C2 hexanucleotide repeats, may result in somatic mosaicism, as observed by smeared instead of discrete bands on Southern blots. C9orf72 repeat expansion mutation carriers are somatically heterogenic with variations in repeat numbers between tissues (van Blitterswijk et al., 2013).

1.5.6 The transcribed GGGGCC repeat forms nuclear RNA foci

Intracellular accumulation of expanded nucleotide repeats as RNA foci in the nucleus and/or cytoplasm of affected cells has emerged as an important disease mechanism for the growing class non-coding repeat expansion disorders (Todd and Paulson, 2010). In diseases such as Myotonic Dystrophy type 1 and 2 (DM1 & DM2) and Fragile X Tremor/Ataxia Syndrome (FXTAS), the major pathogenic function of repeat-expanded RNA arises from the formation of nuclear RNA foci (Wojciechowska and Krzyzosiak, 2011, Cooper et al., 2009). Expanded GGGGCC hexanucleotide repeat forms nuclear RNA foci in human brain and spinal cord (DeJesus-Hernandez et al., 2011). Numerous studies have now presented evidence for both sense and antisense intranuclear RNA foci in disease-relevant CNS regions of C9+ patients, including frontal cortex, cerebellum, hippocampus, and spinal neurons as well as in non-neuronal cells (Gendron et al., 2013, Lagier-Tourenne et al., 2013, Mizielinska et al., 2014, Zu et al., 2013). Double labelling of sense and antisense foci showed that the majority of cells in the brain and the blood express either sense or antisense foci with only a minority of cells positive for both (Lagier-Tourenne et al., 2013, Zu et al., 2013, Mori et al., 2013a).

1.5.7 RAN translation in G4C2 expansion repeats

Microsatellite-expansion diseases are caused by the expansion of short stretches of repetitive DNA. These repeat mutations can be bi-directionally transcribed and can be translated in the complete absence of a starting ATG (Repeat associated non ATG translation). RAN translation was first discovered in spinocerebellar ataxia type 8 (SCA8) (Zu et al., 2011). RAN proteins have been reported in a growing number of diseases, including Fragile-X tremor ataxia syndrome (FXTAS), spinocerebellar ataxia type 8 (SCA8), myotonic dystrophy type 1 (DM1) and C9ORF72 amyotrophic lateral

sclerosis (ALS)/frontotemporal dementia (FTD). The mechanism of RAN-translation initiation is unclear.

RAN translation of the sense GGGGCC expansion results in the expression of three sense dipeptide proteins: GlyPro (GP), GlyArg (GR) and GlyAla (GA). Immunostaining shows evidence that RAN proteins accumulate in neuronal inclusions in the cerebellum, hippocampus and other brain regions of C9ORF72 ALS/FTD but not in control autopsy tissue. The dipeptide inclusions were similar in abundance and shape to the ALS/FTD inclusions. They co-localise with the p62-positive/phospho-TDP-43 negative inclusions but not with TDP-43. Studies have shown that GA and GP dipeptides occur more commonly than GR. Several groups have shown that the dipeptides are toxic but the results are conflicting as to which didpetide is the most toxic with all the three sense dipeptides shown to be the most toxic (Ash et al., 2013, Mori et al., 2013a, Zu et al., 2013). The G4C2 expansion repeats can be translated bidirectionally. The 3 antisense dipeptide repeats are polyProArg, (PR), polyProAla (PA) and polyGlyPro (GP). Brain autopsy of *C9ORF72* patients show an accumulation of antisense dipeptides (Gendron et al., 2013, Mori et al., 2013a, Mann et al., 2013, Zu et al., 2013). A unique C-terminal end flanks the sense GP and is not found in the antisense GP protein (GP_{AS}). Five of the six C9-RAN proteins are predicted to contain completely different C-terminal flanking sequences that may also affect their function and pathogenicity. Similar to the observation for RNA foci, sense and antisense RAN proteins have been infrequently detected in the same cell, although in one study all six proteins were shown to be expressed in the same brain region. The dipeptide expression in affected *C9ORF72* patient brains is strikingly different, both within the patient and between the patients. The reason for this variability is unknown and the functional and distributional variation could explain the differential toxicity (Zu et al., 2013).

Two mechanisms have been proposed for the RAN translation of dipeptides viz. Initiation from alternative start codons with a kozak sequence or through the formation of hairpin structures (Mori et al., 2013). The hairpin structures fold in to G-quadruplex structure under specific conditions. The GGGGCC sense strand can form the G-quadruplex while the CCCCGG anti-sense strand cannot. Thus the anti-sense

strands form only the hairpin structures that are less stable than the G-quadruplex. This difference in stability might affect the didpeptide expression (Wojciechowska et al., 2014). The increased propensity of longer repeat tracts to adopt RNA structures may explain why longer G4C2 repeat tracts are typically associated with higher levels of RAN protein accumulation and expression of RAN proteins in multiple reading frames (Mori et al., 2013, Zu et al., 2013). It remains unclear how the products of RAN translation play a toxic role in disease progression.

1.5.8 Disease mechanism underlying C9ORF72 mediated neurodegeneration.

Several cell and animal models have been generated to gain insights into C9ORF72-related ALS and FTLD. Based on other microsatellite expansion disorders, the three primary models have been proposed for toxicity (1) Happloinsufficiency or loss of C9ORF72 protein function (DeJesus-Hernandez et al., 2011, Renton et al., 2011); (2) accumulation of toxic RNA foci (Polymenidou et al., 2012), which sequester RNA-binding proteins and result in dysregulation of RNA splicing, trafficking and translation; (3) RAN translation of the sense and antisense hexanucleotide expansion repeats form dipeptides (Ash et al., 2013, Mori et al., 2013a). In addition to these three major mechanisms, other factors could modify disease pathogenesis viz., Variation in the G4C2 repeat length and independent genetic modifiers that mediates factors that could lead to neurodegeneration. Studies have suggested a non-neuronal role to *C9ORF72* toxicity wherein they first affect astrocytes and the toxicity subsequently spread to neurons (Meyer et al., 2014). The large degree of clinical heterogeneity observed within the *C9ORF72* patient population could either be a result of distinct pathogenic mechanisms or combinations thereof.

1.5.8.1 Haploinsufficiency of C9ORF72 protein

Studies have shown that G4C2 expansion repeats abolished the expression of the C9ORF72 variant 1 (DeJesus-Hernandez et al., 2011). Thus several loss of function mechanisms have been proposed for *C9ORF72*. Failed translation of mRNA leads to loss of protein expression in repeat expansions within non-coding regions. Studies

have shown a reduction in variant-specific and total C9ORF72 mRNA in Post-mortem tissue from *C9ORF72* patients, including cerebellum, motor cortex, frontal cortex, and cervical spinal cord, as well as in patient-derived iPSNs, lymphoblast cell lines and in blood samples (Xi et al., 2015, Donnelly et al., 2013, Mori et al., 2013a).

Reduced C9ORF72 mRNA expression in the disease condition may occur through suppression of gene expression via epigenetic changes. Expanded G4C2 repeats were shown to interact with trimethylated, but not non-trimethylated lysine residues within histones H3 and H4 (Belzil et al., 2013). Expanded G4C2 repeats may also suppress C9ORF72 mRNA expression through hypermethylation of a cytosine-phosphate–guanine (CpG) island upstream of C9ORF72, a phenomenon that was reported in the blood of C9+ patients with repeat expansion greater than 43 repeat units, but not in controls (Xi et al., 2013).

In contrast, substantial increases in sense and antisense transcripts containing C9ORF72 intron 1 (the site of the expansion) have been described in C9ORF72 patient cerebellum, relative to controls. This indicates that although overall C9ORF72 expression may be reduced in C9+ carriers, transcript variants containing intron 1, or spliced intron 1 fragments, may be stabilised, suggesting that an RNA gain-of-function mechanism could also be at play (Mori et al., 2013a). Thus, it remains unclear whether G4C2 repeat expansion in C9 ALS/FTLD represents a loss or gain of C9ORF72 function in disease.

To determine the loss of function mechanism, C9ORF72 orthologues have been knocked down in zebrafish, mouse and human cell lines. These data produced contradictory results at two extreme ends, suggesting that C9ORF72 protein is either dispensable or essential for normal nervous system development and function (Ciura et al., 2013, Lagier-Tourenne et al., 2013). In FTLD patient carrying a *C9ORF72* homozygous hexanucleotide expansion, the levels of all three C9ORF72 transcript variants were reduced when compared to heterozygous cases wherein only levels of V1 and V2 were reduced. Although the loss of all three transcripts resulted in severe clinicopathological features, their severity was within the range of hetereozygous effects. Since a true loss of function mechanism did not produce lethal effects, the study ruled out haplosufficiency and leaned more towards a dominant gain of function

(Fratta et al., 2013). Small expansions of approximately 50 repeats did not affect transcription possibly because smaller expansions do not lead to hypermethylation of a CpG island 5' to the repeat sequence (Xi et al., 2013). If smaller repeat lengths are pathogenic, then haploinsufficiency is not the responsible mechanism. Taken together, the available studies so far neither rule out, nor confirm reduced expression of C9ORF72 as a pathogenic mechanism in C9 ALS/FTLD**.**

1.5.8.2 RNA mediated toxicity

Repeat expansions form hairpin structures within pre-mRNA and mRNA molecules, which in turn can lead to aggregation of mutated RNA and sequestration of RNA binding proteins (RBPs) into these foci. Among other effects, foci-bound RBPs are unable to regulate their RNA targets, including alternative splicing of pre-mRNAs, leading to diminished cellular viability (Todd and Paulson, 2010). RNA foci formation and resulting RNA metabolism abnormalities are well-characterised mechanisms for trinucleotide repeat-related RNA diseases as seen in DM1&2 as well as in FXTAS. The available studies on G4C2-related neurodegeneration suggest that C9 ALS/FTLD hexanucleotide repeat expansion shares similarities with these other RNA diseases. Screening for point mutations in *C9ORF72* in ALS samples did not render any pathogenic variants, suggesting that C9ORF72 pathogenesis is caused by a toxic gain of function due to RNA foci resulting from the noncoding expansion (Harms et al., 2013).

A significant correlation between RNA foci burden and age of disease onset has been reported, suggesting that increased RNA foci load may directly correlate with disease pathogenesis (Mizielinska and Isaacs, 2014). Repeat length-dependent formation of RNA foci have also been observed in numerous cell types, primary neurons and zebrafish embryos ectopically expressing G4C2 sequences. RNA foci were observed with a repeat length of 38 (~6 foci per cell) or 72 (~12 foci per cell), but not with 8 repeats in neuronal and non-neuronal cells. *In vivo* studies in *Drosophila* and zebra fish show more age–related neurodegeneration (motor defects and apoptosis) with the longer repeats than the shorter ones (Lee et al., 2013a). Experimental evidence from cell and animal models suggests that expression of G4C2 hexanucleotides can cause

repeat length-dependent formation of RNA foci which directly and progressively correlate with cellular toxicity that is mediated by caspase-dependent cell death.

To gain insights into the pathogenic mechanisms underlying repeat-mediated toxicity, several pulldown experiments have been carried out to identify interacting partners of G4C2 repeats (Xu et al., 2013). All studies so far have consistently identified RBPs including hnRNPs as the major interacting proteins of G4C2 repeats, thereby revealing a striking similarity to other nucleotide repeat expansion diseases (Cleary and Ranum, 2013, Todd and Paulson, 2010). Another screen for G4C2 RNA-binding proteins identified hnRNP A3, which forms p62+/ TDP-43- neuronal cytoplasmic and intranuclear inclusions in hippocampus, as well as cerebellum in a subset of C9+ (Mori et al., 2013b). hnRNP A3 cycles between the nucleus and cytoplasm and is involved in alternative pre-mRNA splicing, nuclear import and cytoplasmic trafficking of mRNA, as well as mRNA stability, turnover and translation (He and Smith, 2009). Several RBPs involved in RNA metabolism, translation and transport were identified.

Experimental evidence from C9+ patient-derived iPSNs, transfected cells and transgenic *Drosophila* suggest that direct binding of a specific subset of RBPs and hnRNPs to disease-related G4C2 repeats and their sequestration into RNA foci might be causally related to cellular toxicity and apoptotic cell death. G4C2 binds the RNA binding protein Pur α, and overexpression of Pur α rescues G4C2-mediated neurodegeneration in *Drosophila*. Pur α is involved in modulation of gene transcription, translation, controls cell cycle and differentiation and is a component of RNA-transport granules .The putative disease mechanism would thus be a loss of function of Pur α due to binding to G4C2 (Xu et al., 2013). The sequestration of RNA binding proteins into RNA foci, could alter the processing and expression of hundreds of distinct genes (Ling et al., 2013b, Polymenidou et al., 2012) resulting in markedly diverse forms of disease across different individuals. However, it remains unclear whether the sequestration of RBPs directly triggers the apoptotic machinery, or whether it is a secondary effect of mitigated or failed RNA metabolism, translation and transport dependent on normal RBP function.

1.5.8.3 RAN translation of G4C2

Immunoblotting and immunofluorescence detected the presence of polyGP proteins in C9ORF72 patient-derived iPSNs. The abundance of poly-GP signal was observed to be independent of RNA foci load and repeat length in these *C9ORF72* patient-derived iPSNs (Almeida et al., 2013). G4C2-derived DPRs were not observed in a *C9ORF72* patient-derived iPSN culture specifically containing motor neurons (Sareen et al., 2013). In contrast, a recent transfected non-neuronal cell model revealed that increasing levels of cytoplasmic DPRs correlate with increased cellular toxicity. They found that increased levels of poly-PR and poly-GP correlate with decreased cellular viability (Zu et al., 2013). DPR protein toxicity has been studied in various cellular models. However, the results clash with one another regarding the dipeptide that is the most toxic (May et al., 2014, Tao et al., 2015, Zhang et al., 2014, Yamakawa et al., 2014, Wen et al., 2014). Taken together, these experiments suggest that DPR accumulation causes cytotoxicity.

Recent studies have shown that distribution pattern of the DPR protein aggregates are homogenous among C9ORF72 patients regardless of the clinical phenotype. They are enhanced in the cerebellum neocortical regions and hippocampus while they have a moderate distribution in the moderate pathology in subcortical areas and minimal pathology in lower motor neurons. These studies show that there is no correlation DPR pathology and the degree of neurodegeneration. TDP-43 pathology is more prominent in areas of neurodegeneration. The distribution pattern of the DPRs is related to C9ORF72 mutations as evidenced by the presence of the G4C2 foci. The observed dissociation between DPR inclusion body load and neurodegeneration suggests that the DPR inclusions might be a protective response to cope with the soluble DPR protein (Gomez-Deza et al., 2015, Mackenzie et al., 2013, Schludi et al., 2015).

This evidence, however, does not preclude the possibility that soluble forms of the dipeptides, or variation in the distribution of the different types of dipeptides across brain tissue, could contribute to the clinical and/or pathological manifestations of C9+ disease.

1.5.9 TDP-43 and C9orf72

The C9ORF72 hexanucleotide repeat expansion has been linked to a high proportion of familial cases of ALS and FTLD-TDP as well as a proportion of sporadic cases. Pathological TDP-43 lesions were present in the frontal and temporal regions of the cerebral cortex, and in subcortical structures including striatum, hippocampus, basal ganglia, and substantia nigra. ALS patients with a C9orf72 repeat expansion have nuclear cytoplasmic inclusions (NCI) immunoreactive to TDP-43 present in the spinal cord. In addition to the TDP positive inclusions, there were unusual "star-shaped" inclusions in the hippocampus, neocortex, and basal ganglia that are also ubiquitin and p62 positive and TDP-43 negative (Al-Sarraj et al., 2011, Troakes et al., 2012). Recent studies have found that few dipeptides rarely co-localize with TDP-43 (Gomez-Deza et al., 2015, Cooper-Knock et al., 2015). Thus, TDP-43 pathology is closely associated with C9orf72 expansion mutation. Studies have shown that C9ORF72 repeat expansions in mice cause TDP-43 pathology, neuronal loss, and behavioural deficits. These mouse brains contained nuclear RNA foci, inclusions of poly(Gly-Pro), poly(Gly-Ala), and poly(Gly-Arg) dipeptide repeat proteins, as well as TDP-43 pathology. TDP-43 positive inclusions rarely co-localise with DPR inclusions and DPR inclusions precede TDP-43 pathology (Mackenzie et al., 2013). These mouse brains exhibited cortical neuron and cerebellar Purkinje cell loss, astrogliosis, and decreased weight; and behavioral abnormalities similar to clinical symptoms of c9FTD/ALS patients, including hyperactivity, anxiety, antisocial behaviour, and motor deficits (Chew et al., 2015). The formation of RNA foci by the G4C2 expansion repeats and the mis-regulation of RNA by TDP-43 suggest that RNA toxicity might be a mutual pathogenic mechanism leading to neurodegeneration. Motor defects seem to be a common phenotype in animal models overexpressing TDP-43 and G4C2 repeat expansions. The autophagy mechanism has been implicated with both these genes. The gene *SQSTM1*, encodes the autophagy receptor protein p62. Star shaped p62 positive TDP-43 negative inclusions are unique to *C9ORF72* and the DPRs co-localise with them. Expression of p62 reduces TDP-43 aggregation in an autophagy- and proteasome-dependent manner (Brady et al., 2011). TDP-43 is known to interact with SQSTM1 (Fecto et al., 2011). C9ORF72 plays an important role in the regulation of endosomal trafficking, and has been shown to

interact with Rab proteins that are involved in autophagy and endocytic transport (Farg et al., 2014). Thus, protein degradation pathways and autophagy pathways are also mechanisms that link these two genes. The G4C2 expansion repeats can sequester other RBPs including TDP-43. This suggests a possible mechanism by which early sequestration of TDP-43 could cause alterations in multiple proteins involved in neuronal development and function that could ultimately result in altered structural and/or network architecture that is vulnerable to diffuse cortical and subcortical damage. This would then be exacerbated by alterations in the cellular stress response due to altered stress granule dynamics. Further understanding of the molecular basis for both TDP-43 and C9ORF72 is required to gain insights into common biological mechanisms that could link both disorders into one disease continuum of overlapping clinical symptoms.

1.6 RNA processing, translation and mis-localization in neurons

Axonal mRNA translation plays a key role in cell polarity determination; axon elongation; synapse formation; injury response and pain regulation; cell survival, maintenance and regeneration. Studies link defects in axonal mRNA translocation to neurodegenerative disease like ALS (Jung et al., 2012). TDP-43 increases the number of stress granules, which reversibly sequester mRNAs and repress their translation (Volkening et al., 2009). Sustained translation of axonal mRNAs is required for axon maintenance, thereby decreased axonal mRNA translation caused by these mutations might contribute to axon degeneration in ALS.

TDP-43 is present in the cytoplasm where they are involved in diverse aspects of RNA metabolism, regulating the spatiotemporal fate of mRNA, i.e. subcellular localization, translation or degradation.TDP-43 is a mRNA binding protein (RBPs). Regulation of the localisation, stability, and translation of mRNAs is mediated in part by RBPs that bind to mRNAs in untranslated regions (3’-UTR and/or 5’-UTR) or coding regions of mRNA (Martin and Ephrussi, 2009). This phenomenon is especially prominent in neurons, in which specific mRNAs are selectively targeted to dendrites, synapses, axons, and growth cones. TDP-43 forms cytoplasmic mRNP granules that undergo bidirectional,

microtubule-dependent transport in neurons *in vitro* and *in vivo* and facilitate delivery of target mRNA to distal neuronal compartments. TDP-43 mutations impair this mRNA transport function *in vivo* and *in vitro*, including in stem cell-derived motor neurons from ALS patients. Thus, TDP-43 mutations that cause ALS lead to partial loss of a novel cytoplasmic function of TDP-43 (Alami et al., 2014). In neurons, TDP-43 is found in RNA transporting granules translocating to dendritic spines upon different neuronal stimuli (Lagier-Tourenne and Cleveland, 2009, Lagier-Tourenne et al., 2010). In addition, the loss of TDP-43 reduces dendritic branching as well as synaptic formation in *Drosophila* neurons(Feiguin et al., 2009). Collectively, these results suggest that TDP-43 could play a role in the modulation of neuronal plasticity by altering mRNA transport and local translation in neurons.

Cytoskeletal components such as actin, neurofilaments and microtubules play a key role in RNA localization, especially during transport of mRNAs and anchoring at target sites. Active transport of mRNAs along cytoskeletal filaments has been implicated as the major localization mechanism in most cells (de Heredia and Jansen, 2004).

TDP-43 directly interacts with the 3' UTR of the low molecular weight (68 kDa) neurofilament (NF-L) mRNA (Strong et al., 2007), stabilizing it and preventing its degradation. Conversely, in ALS the expression of the NF-L mRNA is suppressed and it is preferentially sequestered to stress granules (Strong et al., 2007, Volkening et al., 2009).

Studies have shown that TDP-43 is actively transported in motor neuron axons and is associated with several mRBPs like FMRP, IMP1 and HuD. Both FMRP and IMP1 have been described to inhibit the translation of bound mRNAs such as *PSD-95* and *β-actin*, although at the same time favouring their transport along neurites suggesting that TDP-43 may play a similar role in the regulation of its target mRNAs (Fallini et al., 2012). TDP-43, FMRP, IMP1, SMN and HuD, as well as the pathogenic variant of the ALS disease protein FUS, have all been shown to be components of stress granules-discrete cytoplasmic structures that assemble and silence mRNAs in response to environmental stress (Tolino et al., 2012). This suggests that these proteins may regulate common target mRNAs in response to stress. It has been speculated that aggregation of TDP-43 in the cytoplasm may lead to the co-aggregation and depletion

of other aggregation-prone mRBPs, thus leading to a general impairment of mRNA trafficking and/or regulation of mRNA stability.

TDP-43 plays an important role in mRNA transport, mRNA stability, and translation (Buratti and Baralle, 2010). TDP-43 also participates in regulating mRNA transport into neurites and local protein synthesis at synapses, two processes that are essential to neurons for a fast response to stimuli and cell survival. Thus, we speculate that mutant TDP-43 can affect RNA regulation of its targets and this aberrant RNA metabolism can be a direct cause of ALS/FTD. It is therefore important to recognise the mRNA targets of TDP-43 and see if mutant forms of TDP-43 can cause their aberrant metabolism which will provide us insights to the disease pathology and potentially identify therapeutic targets for the disease.

1.7 Aims of the Project

This project will directly investigate the molecular mechanisms underlying ALS/ FTLD with respect to two genes: *TDP-43* and *C9ORF72*.

1) To model the acute effects of TDP-43 *in vitro* using rat cortical neurons and to determine the cell-specific vulnerability of cortical neurons by over-expressing TDP-43 wild-type and mutant proteins
2) To observe if TDP-43 impairs different aspects of cytoskeletal function such as axon outgrowth, growth cone dynamics and axonal transport thereby implying that dysregulation of cytoskeletal components could play a key role in neurodegeneration.
3) To determine if TDP-43 causes mis-localization of cytoskeletal regulatory mRNAs thereby signifying the importance of TDP-43 mediated RNA misprocessing as a key mechanism in ALS/FTD
4) To determine the toxicity of G4C2 hexanucleotide expansion repeats and whether toxicity co-relates to repeat length.
5) To investigate the RNA foci toxicity mechanism and the dipeptide toxicity mechanisms of *C9ORF72 in vivo*.

Thus this project will offer key insights into whether cytoskeletal dysregulation, aberrant RNA metabolism and protein toxicity are major factors in pathogenic mechanism in ALS/FTD.

2 Materials and Methods

2.1 Materials

Table 2.1 Antibodies List

Primary Ab	**Host**	**Concentration**	**Company**
GFP	Chick	1:1000	Abcam
TDP-43	Rabbit	1: 1000	Cell Signalling
Neurofilament – H	Rabbit	1:1000	Millipore
Tyrosinated Tubulin	Rat	1:1000	Abcam
Glu-Tubulin	Rabbit	1:1000	Abcam
Secondary Ab	**Host**	**Concentration**	**Company**
Cy-3	Rabbit	1:1000	Life Technologies
Anti-chick 488		1:1000	Life Technologies
Anti rabbit 568		1:1000	Life Technologies
Anti rat 568		1:1000	Life Technologies

Table 2.2 cDNA list

Name of cDNA	**Company**	**Cat. No.**
β-actin	Plasmid Harvard Database	HsCD00326994
Kif2A	Plasmid Harvard Database	MmCD00311336
Map1B	Addgene	Plasmid # 44396
Map2	Plasmid Harvard Database	MmCD00320079
ND1-L	Plasmid Harvard Database	MmCD00311464
NFL	Plasmid Harvard Database	MmCD00316561

Table 2.3 Primers List

Primers	Sequence
β-actin Forward	GAC TGA CTG GAT CCA TGG ATG ACG AT
β-actin Reverse	GAC TGA CTC TCG AGA TCG TAC TCC TGC
Kif2A Forward	GAC TGA CTG GAT CCT TGA AAG GGG CAT GGC TA
Kif2A Reverse	GAC TGA CTC TCG AGA TTT TGT TCA CAG AGA AGT TTT
Map1B Forward	GAC TGA CTG GAT CCA ACC TTG ACA GAC ACA ATC TC
Map1B Reverse	GAC TGA CTC TCG AGT CAA AGA TGA GAC TGA GGT TA
Map2 Forward	GAC TGA CTG GAT CCT TCC CTC CCA AGA
Map2 Reverse	GAC TGA CTC TCG AGT CAC AAG CCC TG
ND1-L Forward	GAC TGA CTG GAT CCC ATT TTC CTT CAT GGG CG
ND1-L Reverse	GAC TGA CTC TCG AGG CAT TGC TCC TTG GTG AA
NFL Forward	GAC TGA CTG GAT CCG TAC TTT TCG ACC
NFL Reverse	GAC TGA CTC TCG AGC TCT TTC TTC TCT

Table 2.4 Linearization of Plasmid

Plasmid	RNA Polymerase	Restriction Enzyme
β-actin Sense	T7 (Roche)	Sac I
β-actin Anti-sense	SP6 (Roche)	Apa I
Kif2A Sense	T7	Sac I
Kif2A Anti-sense	SP6	Apa I
Map1B Sense	SP6	Apa I
Map1B Anti-sense	T7	Sal I
Map2 Sense	T7	Sal I
Map2 Anti-sense	SP6	Apa I
ND1-L Forward	T7	Spe I
ND1-L Anti-sense	SP6	Nco I
NFL Sense	SP6	Apa I

NFL Anti-sense	T7	Sal I

Table 2.5 Tissue Culture Reagents

Name of Reagent	**Company**
Poly-L-Lysine	Sigma- Aldrich
Laminin	Sigma- Aldrich
Hanks Balance Salt solution	Gibco (Thermo Fisher Scientific)
Neurobasal medium	Gibco (Thermo Fisher Scientific)
B-27	Gibco (Thermo Fisher Scientific)
Horse Serum	Sigma- Aldrich
Pen-Strep	Gibco (Thermo Fisher Scientific)
Glutamine	Gibco (Thermo Fisher Scientific)
Fluorsave	Calbiochem

Table 2.6 Kits

Kits	**Company**
Colorimetric TUNEL kit	Promega
RealTime-Glo™ MT Cell Viability Assay	Promega
Miniprep Kit	Qiagen
Maxiprep kit	Qiagen
Gel extraction kit	Qiagen
pGEM-T easy vector kit	Promega
One-Shot chemically competent E.Coli transformation kit	Thermo Fisher
Rat neuron Nucleofector kit	Lonza
DIG RNA Labelling Kit	Roche
NBT-BCIP	Roche

2.1.1 Recipes

Trypsin

Hanks Buffer – 19.8ml

BSA (fraction V) – 60mg

Trypsin – 40mg

1M $MgSO_4$ – 60µl

Trypsin Inhibitor

Hanks Buffer – 19.8ml

BSA (fraction V) – 60mg

Trypsin Inhibitor type II – 5mg

DNAse Type II – 1mg

1M $MgSO_4$ – 60µl

10x Tyrodes

NaCl -80g

D-Glucose – 10g

KCl -2g

$MgCl_2.6H_2O$ – 2g

$NaH_2PO_4.2H_2O$ – 0.5g

H_2O – Make up to 1 Litre. Autoclave and Filter.

NTMT

5M NaCl – 4ml

1M MgCl – 10ml

1M Tris pH 9.5 – 20ml

10% Tween-20 – 2ml

Levamisole - 100mg (Optional)

H_2O – Make up to 200ml

5x MABT

NaCl - 21.91g

Maleic Acid – 29.02g

NaOH – 18g

H_2O – Make up to 500ml. Adjust pH to 7.5 and Filter.

Add 0.1% Tween-20 on the day of use.

SSC

NaCl - 175.3g

Sodium citrate - 88.2g

H_2O – Make up to 1L. Adjust pH to 7 and Autoclave.

TE

0.5M EDTA – 2ml

Tris pH 7.5 – 4ml

H_2O – Make up to 10ml

2.2 Methods

2.2.1 Plasmids

The EGFP-tagged TDP-43 WT and mutant plasmids were obtained from Prof. Christopher Shaw's lab (IOPPN). The cDNA insert was cloned into the pEFGP-C1 (N-terminal GFP) vector at the XhoI and BamHI sites. Mutant forms of TDP-43 were those containing either the M337V familial mutation, or the Q331K sporadic mutation. Direct sequencing was used to confirm clone alignment and mutagenesis. pEGFP-C1 expression vector was used to express EGFP as a control.

The EGFP-tagged (G4C2)x plasmids were also obtained from Prof. ChristopherShaw's lab. 8x, 38x, 72x and 128x times G4C2 repeats were cloned into shuttle plasmid (pcDNAGateway directional TOPO expression vector, Invitrogen, kit K2440-20) using Xba1. The EGFP is on the 5' end.

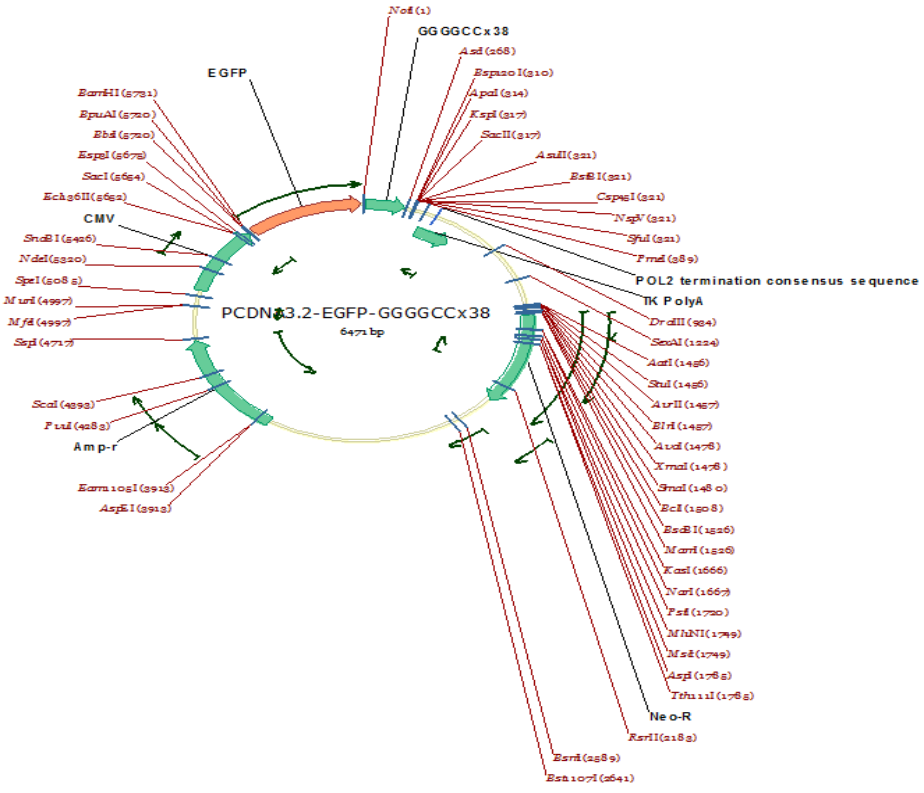

Figure 2.1 Plasmid map for EGFP-38x

The Dipeptide EGFP-WPRE was also obtained from Prof Chris Shaw's lab. The Dipeptides GA, GP, GR, PA and PR were tagged to EGFP-WPRE on the C-terminal. The repeats were synthesized from a scrambled hexanucleotide expansion carrying 125 repeats so as to eliminate the formation of the G4C2 RNA foci.

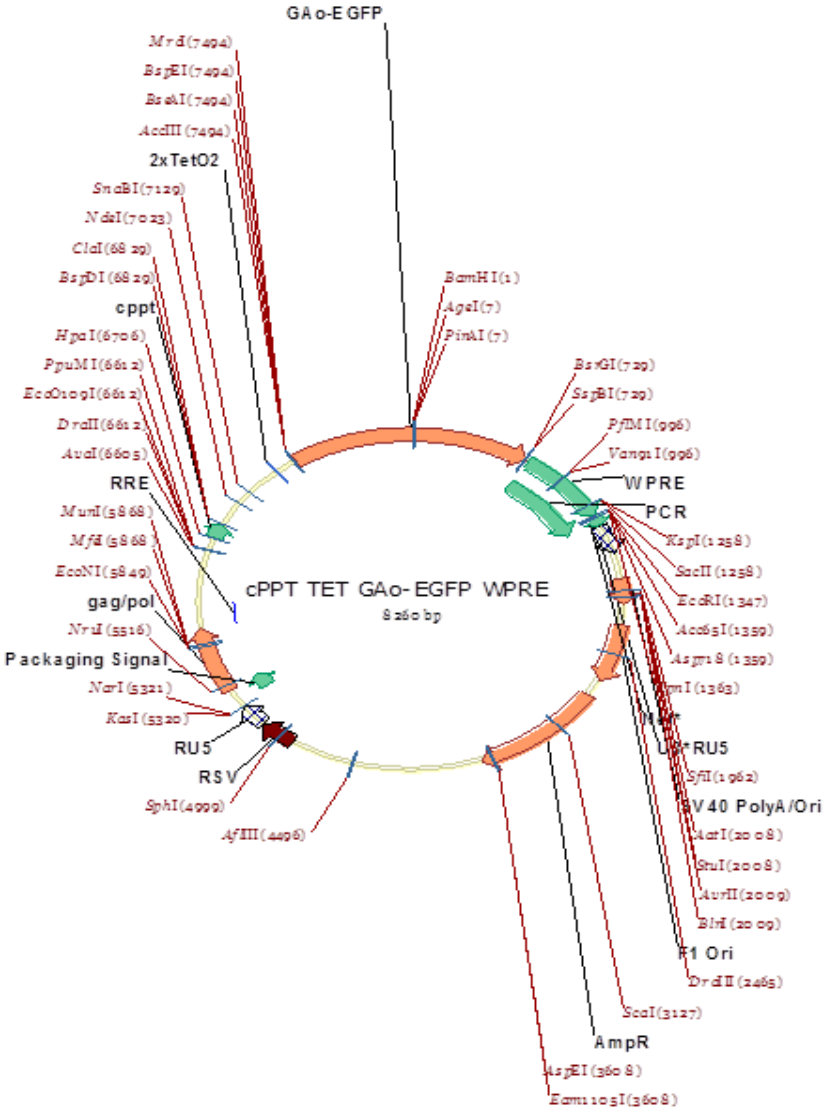

Figure 2.2 Plasmid Map for GA-EGFP-WPRE

2.2.2 Primary Rat cortical culture

2.2.2.1 Preparation of cover slips

13mm cover slips were soaked in concentrated Hydrochloric acid (Sigma) on a rocker plate for 1h and washed 2-3 times every half an hour in DEPC water (Elga water machine). The coverslips were then washed in 100% ethanol (VWR) for one hour and rinsed twice with DEPC water. The coverslips were spread out and allowed to dry over-night. The dried coverslips were baked at 220° C for 15 mins.

2.2.2.2 Preparation of Plates for Culture

Depending on the no. of cells to be cultured and the type of analysis, 24 well plates/ 6 well plates/ 96 well plates (Nunc) or confocal dishes (Ibidi) were prepared the day before the culture under the laminar airflow.

For 24 well plates, the autoclaved coverslips were added to each well followed by the addition of 400 µl of Poly-L-Lysine/well. The plates were then incubated for 2h at room temperature. After 2h, the poly-lysine was removed and the coverslips were rinsed once with 400 µl of cell culture grade PBS. The plates were then incubated over night with 100 µl of laminin inside the Co2 incubator.

For the 6 well plates/ 96 well plates/ confocal dishes, the poly- lysine and laminin were directly added to the wells without adding the autoclaved coverslips.

2.2.2.3 Tissue Culture

Freshly prepared culture medium (Neurobasal medium with 2% B-27, 2% horse serum, 1% glutamax and 1% Pen-strep), trypsin, trypsin inhibitor, Hanks solution was pre-equilibrated in the incubator before the dissection.

Rat cortices were dissected from the cerebral cortex of rats at embryonic day 18. Upon dissection, the cortical tissues were immediately transferred to a 15 ml falcon tube

containing ice cold Hanks buffer (HBSS). The cortices were equilibrated for 2 mins in HBSS and incubated with 1 ml of trypsin in 4 ml of HBSS for 15 mins in a 37°C water bath with intermittent shaking every 3 mins. After 15 mins, the trypsin solution was removed and 1 ml of trypsin inhibitor solution was added and the cortices were dissociated by tituration with a pipette until all pieces of the tissue were °homogenously dispersed. The dissociated cortices were then centrifuged for 5 mins at 1200 rpm. The supernatant was removed and the pellet was re-dissolved in 5 ml of pre-warmed HBSS and passed through a 70 µm filter and re-centrifuged for 5 mins at 1200 rpm. The pellet is re-dissolved in 2 ml of pre-warmed HBSS and the numbers of cells were counted using a haemocytometer.

For non-transfected cells, 80,000 cells from the cell suspension was centrifuged at 1800 rpm for 5 mins and the pellet was re-suspended in 400 µl of culture medium per well.

2.2.2.4 Amaxa Transfection

The neurons were transfected using the Amaxa machine with the Lonza rat neuron nucleofector solution according to the standard protocol. The required number of cells ($4 – 5 \times 10^6$ cells per plasmid construct) to be transfected was centrifuged at 1800 rpm for 5 mins. The cell pellet was resuspended in 100 µl of the nucleofector solution per construct along with 4 µg of DNA. The cell/DNA suspension was transferred into the Amaxa cuvette and transfected using the Amaxa machine using the O-003 program. 200 µl of pre-equilibrated culture medium was added immediately after the nucleofection and the transfected cells were plated at a density of 100,000 cells in 400µl of culture medium per well in a 24 well plate. Amaxa transfection has a good penetrance range with 70% target transfection efficiency.

For 6 well plates, the neurons were plated at a density of 1 million cells/well in 1 ml of culture medium and for confocal dishes, the neurons were plated at 160,000 cells per well in 1 ml of medium and for 96 well plates, the neurons were plated at different densities varying from 5000 to 15,000 cells/well in 50 µl of medium. The cells were incubated at 37°C with 5% CO_2 in a Binder incubator until analysis. For cultures that

were maintained in the incubators for over 48h, the medium was replaced every two days.

2.2.3 Immunohistochemistry

2.2.3.1 Fixation

The cultured cells were fixed with the same amount of 4% PFA / 4% PFA with 15% sucrose as the culture medium for 15 mins at room temperature. The coverslips with the fixed cells were washed twice with PBS-T (1X PBS + 0.1% Triton X-100) on a rocker plate. Specific antigen sites on the cells were then blocked using 0.5% BSA (Sigma) in PBS for 1h at room temperature.

2.2.3.2 Staining

After blocking, the cells were incubated with the recommended concentration of primary antibodies in 0.1% PBS-T with 0.5% FBS overnight on a rocker plate at 4°C. The following day, the cells incubated in primary antibodies were washed 3X times for 10 mins with PBS-T on a rocker plate at room temperature, followed by incubation with fluorescent secondary antibodies (recommended concentration) in PBS-T for 1 – 2h at room temperature on a rocker plate. After further washes (3 washes, 10 mins each with PBS-T), the coverslips were mounted on slides using fluorsave with Hoechst and left to dry overnight at room-temperature. The slides were protected from light after the addition of the secondary antibodies. A list of all the antibodies used and their concentrations are tabulated in the Materials chapter (Table 1).

2.2.4 TUNEL Toxicity Assay

Terminal Deoxynucleotidyl Transferase dUTP Nick End Labeling (TUNEL) detects fragmented DNA associated with cell apoptosis. The Promega DeadEnd colorimetric TUNEL system was used to assay apoptotic cells in both cultured cells and in tissue sections. Most of the reagents used in the protocol were a part of the TUNEL kit. It detects apoptosis by end- labelling and measuring nuclear DNA fragmentation. Biotinylated nucleotide is incorporated at the 3′-OH DNA ends using the Terminal

Deoxynucleotidyl Transferase, Recombinant, (rTdT) enzyme. Horseradish peroxidase-labeled streptavidin (Streptavidin HRP) is then bound to these biotinylated nucleotides, which are detected using the peroxidase substrate, hydrogen peroxide, and the stable chromogen, diaminobenzidine (DAB). Using this procedure, apoptotic nuclei are stained dark brown.

2.2.4.1 TUNEL assay on cultured neurons

Primary cortical cells were cultured and fixed at three different time points: 24h, 48h and 72h as mentioned above. 100 µl of 20 µg/ml of Proteinase K in 1x PBS- 0.1% T was added to each well and the cells were permeabilized for 5 mins. The Proteinase K solution was removed and the coverslips were washed twice with PBS-T with 2 mg/ml of glycine. The cells were then fixed for 5 mins with 4% PFA. After 5 mins of fixation, the cells were washed twice with PBS-T. The coverslips with the fixed cells were then equilibrated with 100 µl of Equilibration buffer per well for 10 mins at room temperature. The rTDT reaction mix was prepared by mixing 98 µl of equilibration buffer with 1 µl of rTDT and 1 µl of biotinylated nucleotide mix. 100 µl of the rTDT reaction mix was added to each well and the incubated at 37^{o}C for an hour. The plates were covered with a damp tissue to prevent excess evaporation. After an hour, the rTDT mixture was removed and 400 µl of 2x SSC was added to each of the wells and incubated at room temperature for 15 mins. The wells were washed twice for 5 mins with 1x PBS. The wells were incubated with 400 µl of 0.3% Hydrogen peroxide (Sigma) in 1X PBS. The cells were washed twice with 1x PBS for 5 mins. The Streptavidin HRP solution was diluted in 1x PBS (1:500). 100 µl of the diluted streptavidin solution was added to each well and incubated at room temperature for 30 mins. The cells were washed twice with 1x PBS for 5 mins. The DAB substrate was prepared as per the data sheet and 100 ul of the DAB substrate solution was added to each well and incubated for 10-15 mins. The DAB substrate is sensitive to light and the plates were kept covered after the addition of DAB. The wells were washed several times with water to wash away the DAB staining. The cells were fixed with 4% PFA for 10 mins and stained with the respective 1^{o} and 2^{o} antibodies using the immunostaining protocol.

2.2.4.2 TUNEL staining on chick embryonic sections

The TUNEL staining protocol for the embryonic sections on glass slides is the same as the staining protocol for cultured neurons. Using a PAP pen, a water repellent line was drawn around the edges of the slides containing the chick embryonic sections to prevent the reagents from spilling over. The fixing and the staining protocols are also the same as for the cultured cells.

2.2.4.3 TUNEL counting and Analysis

2.2.4.3.1 Cultured cortical neurons

The TUNEL positive cells appear as black dots and can be detected under a phase contrast. The number of TUNEL positive cells was manually counted from five different 0.24mm^2 fields from a 13mm^2 coverslip. The counted regions were imaged under phase (TUNEL) and also under blue fluorescence (Hoechst). Hoechst is a nuclear stain and will give us the number of total cells in the field. A total of 3 coverslips for each construct including the control transfection from three independent experiments was used to average the number of TUNEL positive cells and the significant difference was calculated using a one-way ANOVA coupled with the Dunn's multiple comparison test.

2.2.4.3.2 Embryonic sections

For electroporated chick embryonic spinal sections, the number of TUNEL positive cells along the entire transfected side of the spinal cords was manually counted. The TUNEL positive cells appear as black dots and can be detected under a phase contrast. Only sections with more than 50% transfection (as detected by the GFP staining) along the length of the spinal cords was used to count the number of apoptotic cells. A total of 75 embryos were electroporated for each construct and the data was analysed from 42 sections across at least 6 embryos from 3 sets of experiments. The graph was represented as a mean number of TUNEL positive cells and the significant difference was calculated using a one-way ANOVA coupled with the Dunn's multiple comparison test.

2.2.5 Promega Cell Viability Assay

In order to test the cell viability, rat cortical cultures transfected with the GFP control and the TDP-43 wild-type and mutant constructs were plated on white opaque walled 96 well plates using the methods described above. The transfected cells were placed at varying densities/ well: 5000, 8000, 10000 and 15,000 cells per well in 50 µl of culture medium. Cell viability was monitored using a continuous read format with the Promega RealTime-Glo™ MT Cell Viability Assay. All the reagents used in the protocol are a part of the kit. The RealTime-Glo™ MT Cell Viability Assay is a nonlytic, homogeneous, bioluminescent method to measure cell viability in real time using a simple, plate-based method. It determines the number of viable cells in culture by measuring the reducing potential of cells and thus metabolism (MT). The assay involves adding NanoLuc® luciferase and a cell-permeant prosubstrate, the MT Cell Viability Substrate, to cells in culture. Viable cells reduce the prosubstrate to generate a substrate for NanoLuc® luciferase. This substrate diffuses from cells into the surrounding culture medium, where it is rapidly used by the NanoLuc® Enzyme to produce a luminescent signal. The signal correlates with the number of viable cells, making the assay well suited for cytotoxicity studies.

The MT Cell Viability Substrate and NanoLuc® Enzyme were added to the culture medium at the dosage specified by the protocol. 50 µl of culture medium containing the MT substrate and the NanoLuc was added to each well with the plated cells after ~20h. The plates were re-incubated for about 4h and the first luminescence reading was taken at 24h after transfection using a luminescent plate reader . After the reading the plates were returned to the incubator and read again every 24h for a week. After every 72h, the medium was replaced with 100 µl of fresh culture medium containing the MT substrate and the NanoLuc.

The Luminometer parameters used to read the luminescence was as per the manufacturer's guidelines. The average relative light unit (RLU) from three different experiments, as measured by the luminometer was plotted for the different constructs against the different time-points.

2.2.6 Live Imaging of Cortical neurons

2.2.6.1 Phase Imaging

Rat cortical cells were transfected with the control EGFP and the TDP-43 wild-type and mutant plasmids as describe above and were plated on confocal dishes at a density of 160,000 cells per well in 1 ml of medium. The confocal dishes were incubated in a 5% CO_2 Binder incubator until imaging. The cells were imaged live at different time points (48h and 72h post transfection) using a Nikon Live imaging chamber microscope maintained at 37°C with 5% CO2. Transfected neurons – Identified using the GFP, were imaged at 60x with the DIC channel for 30 mins with 5 second intervals using the Nikon Elements software.

2.2.6.2 EB-3 Imaging

For Imaging EB3s, the rat cortical neurons were co-transfected with the GFP tagged control and TDP-43 wild-type and mutant plasmids alongside with EB3-RFP plasmid. Equal volumes of each of the respected plasmids (2 μg/μl) were used for co-transfection experiments. The co-transfected neurons were plated on confocal dishes at a density of 160,000 cells per well in 1 ml of medium. The confocal dishes were incubated in a 5% CO_2 Binder incubator until imaging. The cells were imaged live at different time points (48h and 72h post transfection) using a Nikon Live imaging chamber microscope maintained at 37°C with 5% CO2. Co-transfected neurons – Identified using the GFP and RFP, were imaged at 60x with the RFP channel for 5 mins with 2 second intervals using the Nikon Elements software.

2.2.7 In situ Hybridisation for Rat cortical cultures

2.2.7.1 Probe preparation

2.2.7.1.1 Re-cloning cDNA into pGEM-T easy vector

The cDNA sequences for β-actin, Kif 2A, Map1B, Map2, Nd1-L and NFL were obtained from Plasmid Harvard database. The forward and reverse primers were designed to be approximately 20 nucleotides in length with 45-55% GC content, complementary to unique, non-overlapping target mRNA sequences using data from the cDNA sequence and Oligocalc software (Northwestern university). The software assesses the properties of the designed primers in terms of melting temperature, GC content, secondary structure formation. The primers were used to amplify shorter region of sequences from the cDNA using a PCR. A list of the primers used is tabulated in the methods chapter. The PCR products were run on a 1% agarose (Sigma) gel and bands of the correct size were cut out and purified using the Qiagen gel extraction kit as per the manufacturer's protocol. The purified products were ligated into Promega pGEM-T easy vector as per their protocol. Restriction enzymes are not needed for this type of ligation as the pGEM-T vectors have 3´-T overhangs that attach to the deoxyadenosine at the 3' ends of the PCR product. The ligated products were transformed using the One Shot® TOP10 Chemically Competent E. coli kit as per the manufacturer's protocol. The transformed E.coli was plated on LB agar plates with X-Gal (Promega) and left to grow overnight. Around 5-6 white colonies for each construct were selected and processed using Qiagen Mini-prep kit as per the manufacturer's instructions. The mini-prep products were sent to Source Bioscience for sequencing. The sequencing helps in choosing the plasmids with the correct insert sequence and gives us information about the orientation of the insert so as to design the sense and anti-sense probes accordingly. Midi-prep of the chosen colonies was carried out according to the Qiagen protocol and the preps were linearized with different restriction enzymes to make the sense and anti-sense probes. The digest (10 µg of midi-prep product; 5 µl of restriction buffer; 2 µl of the restriction enzyme made up to 50 µl with DEPC water) was carried out for 2h at room-temperature. A list of the restriction enzymes used is tabulated under the materials section (Table 4).

2.2.7.1.2 Preparation of DNA template for RNA probe

50 µl of DEPC H_2O was added to the digest from the previous step. 100 µl of Phenol: Chloroform: Isoamyl alcohol (25:24:1) solution (Sigma) was added to the mix and centrifuged for 2 mins at 13,000 rpm. The upper phase was transferred to a new tube and 95 µl of pheno; chloroform: isoamyl alcohol solution was added and re-centrifuged. The upper-phase is transferred to a new tube. 225 µl of ice cold 100% Ethanol and 9 µl of 3M sodium acetate (pH 5.2) was added to the upper phase and incubated at -20^{o}C for 20 mins. The tubes were then centrifuged for 15 mins at 4^{o}C. The supernatant was removed and 150 µl of ice cold 70% Ethanol was added to the pellet and re-centrifuged for 15 mins at 4^{o}C. The supernatant was removed and the pellet was air-dried for 1-2 mins and then re-suspended in 20 ul of DEPC H_2O. The concentrations of the DNA templates were read using the Nanovue and tubes were stored at -20^{o}C.

2.2.7.1.3 Synthesis of RNA DIG labelled probes

To 1 µg of the DNA template: 2 µl of 10x Transcription buffer, 2 µl of the DIG RNA, 0.5 µl of RNA inhibitor, and 1 µl of the respective RNA polymerase (T7 or SP6, depending on sense or antisense orientation of insert) were added and made up to a total of 20 µl with Depc H_2O. This mixture was incubated at 37^{o}C for 2h. 50 µl of ice cold 100% Ethanol and 2 µl of 3M sodium acetate (pH 5.2) was added to the digest and incubated at -20^{o}C for 30 mins. The tubes were then centrifuged for 15 mins at 4^{o}C and the supernatant was discarded. The pellet was re-suspended in 150 µl of ice cold 70% Ethanol and re-centrifuged for 15 mins at 4^{o}C. The supernatant was discarded and the pellet was air dried at 60^{o}C for 15 seconds. The pellet was re-suspended in 25 µl of depc H_2O and the RNA concentration was measured using the nanovue. 25 µl of Formamide (Ambion) was added to the tubes and were stored at -20^{o}C.

2.2.7.2 In Situ Hybridisation

The protocol we used is a modification of the Springer mRNA FISH detection protocol for cultured neurons (Bassell, 2011). Rat cortical neurons were dissociated and cultured as described above (see primary rat culture). The cells were fixed with 4% DEPC PFA for 15 mins at room temperature at 24h, 48h and 72h post transfection. The fixed cells were washed twice in 1x DEPC PBS for 5 mins. The cells were permeabilized with 0.3% Triton X-100-X 100 (Sigma) in 1x DEPC PBS for 20 mins and equilibrated in 1x SSC with 40% formamide (Sigma) for 5 mins. The neurons were pre-hybridized in 200 µl (per well) of hybridization solution (50% formamide, 5x SSC, 5x Denhardts, 0.4 mg/ml Torula yeast RNA, 0.1 mg/ml of Bakers yeast) for 2h at 65°C in humidified chambers. The prepared probes (1 µg/ml) were added to the hybridisation solution and heated at 95°C for 5 mins. Hybridisation was performed by keeping cells overnight at 65°C in humidified chambers with the probe solution. The following day, cells were washed twice with 0.5x SSC, 40% Formamide and 0.1% Tween-20 (Sigma) solution for 30 mins at 65^{o}C. The cells were then blocked for 1h at room temperature with the blocking solution (1X MABT, 10% sheep serum, 10% Roche Boehringer blocking Reagent). After blocking, the cells were incubated overnight with Anti-DIG (1:3500, Roche) at 4^{o}C. The cells were washed with three to four times with 1x MABT every 10 mins. They were then washed twice with 1x NTMT buffer every 10 mins and developed with NBT-BCIP (Roche) in NTMT as per the manufacturer's dosage. The cells were developed in a dark room as NBT-BCIP is a light sensitive reaction. The reaction was stopped with TE buffer when the solution in the wells turned dark purple. The cells were washed a few times with 1x PBS to remove any background stain and were fixed in 4% PFA for 5 mins. The cells were then washed twice with 0.1% Triton X-100 in 1x PBS every 5 mins and then stained for 1^{o} and 2^{o} antibodies as per the immunohistochemistry protocol and fixed on slides using Fluorsave.

2.2.8 In ovo Electroporation

2.2.8.1 Incubation

During incubation, fertilized chick eggs were placed on their sides so that the embryo will be properly positioned for electroporation. The embryo will float on top of the yolk. A line was drawn across the surface of the side of the egg to indicate where the window should be made to allow best access to the embryo. The Eggs were incubated for 2.5 days (until HH14-15) in an egg incubator at 37^{o}C with < 45% humidity. Hamburger–Hamilton stages (HH) are a series of 46 chronological stages in chick development that are most commonly used for chicken staging.

2.2.8.2 Windowing

The surface of the eggs were sprayed with 70% ethanol and wiped. A pin-hole was made at the small end of the eggs with a needle. About 4ml of albumen was removed from each of the eggs using a 20 ml syringe with a 21-gauge 40 mm needle (Terumo neolus) through the pin-hole. The needle was inserted into the pin-hole at angle to avoid puncturing the yolk. A small strip of cello-tape was used to seal the pin-hole and reinforce the shell for windowing.

2.2.8.3 Electroporation Prep

1.5 mm glass capillary tubes (WPI) were pulled into microinjection pipettes with a pipette puller (Sutter Instrument P-87). Then 6 µl of DNA/fast-green solution was injected into the glass microinjection pipette using a 10 µl pipette fitted with a 20 µl microloader (Eppendorf). The microinjection pipette was then inserted into the pipette nozzle for the picopump (WPI pneumatic picopump PV860). The holding pressure was set to 3psi and the ejection pressure was set to 20 psi. The tip of the capillary was gently broken with the tweezers to create a tiny opening for the plasmid/fast-green solution to flow through (The tip of the capillary tube should be narrower than the neural tube).

The tyrodes solution should be prepared prior to electroporation and autoclaved before use. Tyrode's is a saline solution that is used to hydrate the embryo. 5 mg of Sodium bicarbonate and 200 µl of antibiotic Penicillin Streptomycin was added to 50 ml of 1x Tyrodes solution prior to electroporation. Indian ink is used to visualize the neural tube and was prepared by adding a few drops of Pelican Indian ink to the Tyrodes (1:10).

2.2.8.4 Electroporation

Using curved scissors, a small window was made around the marked line without disrupting the yolk. The eggs were carefully positioned under a light microscope (Zeiss Stemi SV6). To visualize the neural tube, the ink solution was injected with 26 gauge needle underneath the embryo (needle was inserted under the embryo from outside the blood ring. A sterile tungsten needle was used to remove a small part of the Vitelline membrane above the region of spinal cord to be electroporated. The tip of the capillary was inserted into the neural tube at a shallow angle and the plasmid solution (4 µg/µl in depc H_2O with 0.5% fastgreen) was injected in to the lumen of the neural tube until the dye spreads across the entire space, filling the anterior and posterior spinal canal. A few drops of Tyrodes solution was added over the embryo. Using two micromanipulators, the platinum electrodes were positioned on either side of the embryo, parallel to the spinal cord and gently pushed down so that the embryo was pressed up into the electric field of the electrodes and a square pulse at 20 mv was applied 5 times for 50 milliseconds at 1 second intervals. Bubbles along the electrodes are indicative of the current flow. The electrodes were carefully removed and a few drops of Tyrodes were added to the embryos and eggs were sealed with tape, making sure that there were no gaps or large creases that might let out moisture. The eggs were placed back in the incubator, window side up until the desired Hamburger-Hamilton (HH) stage.

2.2.8.5 Embryo Dissection and fixation

After either 24h or 48h post electroporation, the surviving embryos were removed from the eggs using forceps and placed in a petri-dish filled with 1x Tyrodes. Under the

light microscope, the outer amnion was carefully removed while keeping the limb-buds intact. The heart and other tissue organs were removed using the forceps. The embryos were checked for fluorescence along the neural tube using a fluorescence microscope (Leica MIG5FC). Embryos without fluorescence or with only superficial fluorescence were discarded. The remaining embryos were then decapitated and fixed overnight in 4% PFA.

2.2.8.6 Cryosection

Fixed embryos were washed 3 times with PBS-T every 30 mins each at room temperature and processed through ascending concentrations of sucrose (Sigma) (10%, 20%, 30%) for 1h each at room temperature. They were finally washed in 1:1 30% Sucrose: OCT for 30 mins at room temperature. Embryos were then embedded in OCT, flash-frozen in using liquid nitrogen and sectioned using a cryostat (LeicaMicrosystems) maintaining a thickness of 20 µm. The sections were fixed on super-frost slides (VWR).

2.2.9 Fluorescence In situ hybridisation

Cy3-labeled G2C4 ×8 RNA probes were synthesized by Integrated DNA Technologies and used as antisense probes. These probes were obtained from Prof. Christopher Shaw's group at the IOPPN. Using a PAP pen, a water repellent line was drawn around the sections so as to contain the reagents from spilling over. The sections were fixed with 4% DEPC PFA for 15 mins at room temperature. The fixed sections were washed twice with 1x DEPC PBS every 5 mins. The sections were permeabilized with 0.3% Triton X-100 (Sigma) in 1x DEPC PBS for 20 mins and equilibrated in 1x SSC with 40% formamide for 5 mins. The sections were pre-hybridized in 200 µl (per slide) of hybridization solution (50% formamide, 5x SSC, 5x Denhardts, 0.4 mg/ml Torula yeast RNA, 0.1 mg/ml of Bakers yeast) for 2h at 65°C in humidified chambers. The commercial probes (10 ng/µl) were added to the hybridisation solution and heated at 95°C for 5 mins. Hybridisation was performed overnight at 65°C in humidified chambers with the probe containing hybridization solution. The following day, sections were washed twice with 0.5x SSC, 40% Formamide and 0.1% Tween-20 solution for 30

mins at 65^{o}C. The sections were washed thrice with PBS-T (1x PBS + 0.1% Triton X-100) every 5 mins and were fixed with 4% PFA for 5 mins. For double immunostaining with FISH, sections were blocked in 1% BSA in PBS-T for 1h, and then sections were incubated with primary antibodies (Abcam chick anti-GFP, 1:1000) and secondary antibodies (anti-chick 488; anti-rabbit cy3-1:1000, Invitrogen; Hoechst 1:2000) as per the immunohistochemistry protocol. Nikon fluorescence and confocal systems were used for high-resolution imaging.

2.2.9.1 Semi-quantitative scoring of RNA foci

For electroporated chick embryonic spinal sections, the numbers of RNA foci along the entire transfected side of the spinal cords were manually counted. Only sections with more than 50% transfection (as detected by the GFP staining) along the length of the spinal cords was used to count the number of RNA foci. The data was analysed from ~20 sections across at least 3 embryos from 3 sets of experiments. Since the RNA foci appear as very tiny white dots, it is not possible to accurately count all the spots, Hence the number of RNA foci were counted based on three parameters: 0- 100, 100-200 and more than 200. The graph in figure 5.4 was broadly drawn to collectively represent these parameters.

2.2.10 Quantitative Analysis

2.2.10.1 Neurite length quantification

Neuron J, A plugin of Image J was used to quantify the neurite length. EGFP control and GFP tagged TDP-43 wild-type and mutant transfected neurons were labelled with anti-GFP and anti-neurofilament antibodies as per the immunohistochemistry protocol and were imaged using the Carl Zeiss Axioscope at 63x (24h and 48h) and 40x (72h). Volocity software was used for image processing. Using Neuron J, the longest axon along with its branches for each neuron was tracked for each neuron and measured. The measurements in pixels were converted into µm based on the objective used. A

total of ~100 neurons per construct were analysed from 3 independent experiments. The graphs were represented as mean length. The significant difference was calculated using a one-way Anova coupled with the Dunns multiple comparison test.

2.2.10.2 Growth cone Analysis

EGFP control and GFP tagged TDP-43 wild-type and mutant transfected neurons were labelled with anti-GFP and anti-tyrosinated tubulin antibodies as per the immunohistochemistry protocol and their growth cones imaged using the Carl Zeiss Axioscope at 63x. Volocity software was used for image processing. Image J was used to quantify the area of growth cone. The growth cones were thresholded to the same settings. Using the free-hand tool of image J, an outline was drawn around the thresholded growth cones and their area was measured in pixels. The pixel area was converted in to µm by calculating the scale on the 63x objective. A total of ~70 neurons per construct were analysed from 3 independent experiments. The graphs were drawn based on the average area and Standard error of mean. The significant difference was calculated using a one-way Anova coupled with the Dunns multiple comparison test.

2.2.10.3 Kymographs

To measure the velocity of the EB3s along the axons, we used kymographs. A kymograph displays position along a line over time. In a kymograph, the position of the EB3 along a single line is imaged at sequential time points and these lines are stacked together to make a 2D image. Image J was used to draw the kymographs. The EB3-RFP movies were converted into 8-bit files and opened in Image J as a stack. Using the line segment tool in Image J, the longest axon was traced from the edge of the cell-body till the tip of the growth cone on the first stack. Using the straighten plugin in Image J the width of the line drawn was adjusted such that it was equal to the width of the axon. The plugin straightens and stacks the line position through all the stacks. The intensity of the EB3s along the axons in the stack can be adjusted. From this stacked

image, the Kymograph was generated using the multiple kymograph plugin. Since EB3s are numerous and tiny, the kymographs generated have a lot of criss-crossing lines, making it hard to manually measure the velocity. Hence automated software was used to measure the velocity of the Kymograph. Kymoquant^{TM} measures orientation of kymograph by analysing ambiguous patterns (steepness of trace) thereof. It calculates the velocity based on the angle and tangent of the kymograph patterns. A total of 20 movies from 3 independent experiments were analysed. The graphs were drawn based on the average velocity in pixels/frame and standard error of mean. The significant difference was calculated using a one-way Anova coupled with the Dunns multiple comparison test.

3 *In vitro* modelling of TDP-43 pathogenicity using rat cortical neurons

3.1 Introduction

Neurodegeneration in the spinal cord and frontal and temporal cortices underlie both ALS and FTLD (Rowland and Shneider, 2001, Graff-Radford and Woodruff, 2007). It has been well established that mutations of TDP-43 are causal of ALS (Kabashi et al., 2008, Sreedharan et al., 2008). Previous studies in transgenic animal models have shown that over-expression of wild-type and mutant isoforms of TDP-43 is toxic and can cause neurodegeneration (Igaz et al., 2011, Wegorzewska et al., 2009, Xu et al., 2011).

TDP-43 is a highly conserved, ubiquitously expressed protein that was identified as the major protein component in the ubiquitinated cytoplasmic aggregates of patients with ALS and FTLD-U. TDP-43 is predominantly a nuclear protein, in patients with neurodegenerative TDP-43 proteinopathies, pathological TDP-43 is mis-localised to the cytoplasm as aggregates that are post-translationally modified (Neumann et al., 2006b, Arai et al., 2006). In degenerating neurons and in the brain and spinal cord of affected individuals, TDP-43 is depleted from the nucleus and accumulates in the cytoplasm as insoluble aggregates (Neumann et al, 2006b, Vance et al., 2009). The occurrence of pathological TDP-43 aggregates in other motor neuron diseases like Alzheimer's and Parkinsons disease suggests that the accumulation is an important molecular hallmark of the pathogenesis of many motor neuron diseases.

Transgenic mice overexpressing TDP-43 recapitulate key features of the disease such as TDP-43 fragmentation, cytoplasmic aggregation of TDP-43, neuronal loss, impaired motor functions and shortened life span. This suggests that neurotoxicity and aggregation might be related events. However, the mechanism behind the neurotoxicity is still unclear and a number of gain/ loss of function mechanisms have been studied in detail (Neumann et al., 2006b, Lagier-Tourenne and Cleveland, 2009, Strong, 2010).

Endogenous TDP-43, though predominantly nuclear, is found in lower levels in the cytoplasm. Under normal conditions, TDP-43 is shuttled continuously between the nucleus and the cytoplasm and this feature mediates its binding to other DNA/RNA and protein partners. Nuclear import and export of TDP-43 is regulated by its functional domains via a nuclear localisation domain (NLS) and a nuclear export

domain (NES). Several studies on cell lines and primary cultures have shown that disruption of these TDP-43 domains can perturb the trafficking of TDP-43, leading to the accumulation and sequestration of TDP-43 as cytoplasmic aggregates (Buratti and Baralle, 2009, Winton et al., 2008a).

Most studies have used transgenic animals and cell lines to investigate TDP-43 pathomechanisms (Wegorzewska and Baloh, 2011). Very few studies have been carried out using primary motor neurons, hippocampal neurons and cortical neurons to model the TDP-43 pathogenesis (Barmada et al., 2010, Fallini et al., 2012). With these models they have shown that TDP-43 is actively transported to axons and that the mis-localisation of both wild-type and mutant TDP-43 affects several features of axonal growth and is toxic to the neurons.

This chapter aims to model the pathogenicity of TDP-43 in primary rat cortical neurons *in vitro*. Since atrophy of the frontal and temporal cortex and neurodegeneration in the motor cortex and spinal cord underlie the pathology of ALS and FTLD, we chose primary cortical neurons to model the effects of TDP-43. Primary cortical neurons grown in a controlled environment offer the advantage of testing various cellular and molecular hypotheses under reproducible experimental conditions with minimal variations. We have previously used chick embryonic motor neurons *in vivo* and *in vitro* to model the acute effects of TDP-43, wherein we showed that TDP-43 mis-localisation coincides with the appearance of cytoplasmic aggregation, reduction in axonal length and cellular toxicity suggesting that TDP-43 dysregulation hinders the ability of spinal motor neurons to produce and maintain an axon, and that the disruption of cytoskeletal integrity may play a role in the pathogenesis of ALS and FTD-TDP (Tripathi et al., 2014). In order to corroborate with our previous studies, the same plasmids as those used in Tripathi et al., 2014 were used in this current study.

The primary cortical cultures were transfected with an EGFP tagged TDP-43 wild-type plasmid and two eGFP tagged TDP-43 missense mutations: M337V and Q331K. TDP-43 M337V is a familial mutation in which the amino acid valine is substituted for methionine at codon 337 in the C-terminal glycine rich region of TDP-43. TDP-43 Q331K is a sporadic mutation in which the amino acid glutamine is substituted for lysine at codon 331 in the C-terminal glycine rich region. EGFP plasmid was used as the

control for all transfection experiments. We have used these plasmids in our previous study (Tripathi et al., 2014) wherein we showed that TDP-43 wild-type and mutant proteins cause toxicity in chick embryonic motor neurons *in vivo*. Other studies have also utilised these mutants wherein they showed that TDP-43-Q331K and TDP-43-M337V provoke age-dependent, mutant-dependent, progressive motor axon degeneration and motor neuron death when expressed in mice at levels similar to endogenous TDP-43 (Arnold et al., 2013, Zhou et al., 2010).

This chapter aims to characterize the effects of EGFP- WT TDP-43 and mutants EGFP-TDP-43-M337V and EGFP -TDP-43 Q331K, on TDP-43 mis-localization and toxicity in cortical neurons over a period of time and to determine if a correlation exists between the two. Using cortical neurons and comparing results with spinal motor neurons would also help in understanding the selective vulnerability of the different neuronal types.

3.2 Results

3.2.1 TDP-43 mis-localises to the cytoplasm over time

Protein aggregation is a hallmark feature of ALS. We have previously shown that TDP-43 shows enhanced cytoplasmic mis-localization over time *in vivo* in chick spinal cord (Tripathi et al., 2014). In order to observe whether cortical cells have the same vulnerability as spinal motor neurons and to mimic the human neuronal TDP-43 aggregation in the cortex, rat cortical neurons were used *in vitro* in this study to recapitulate the salient features of TDP-43 pathogenicity.

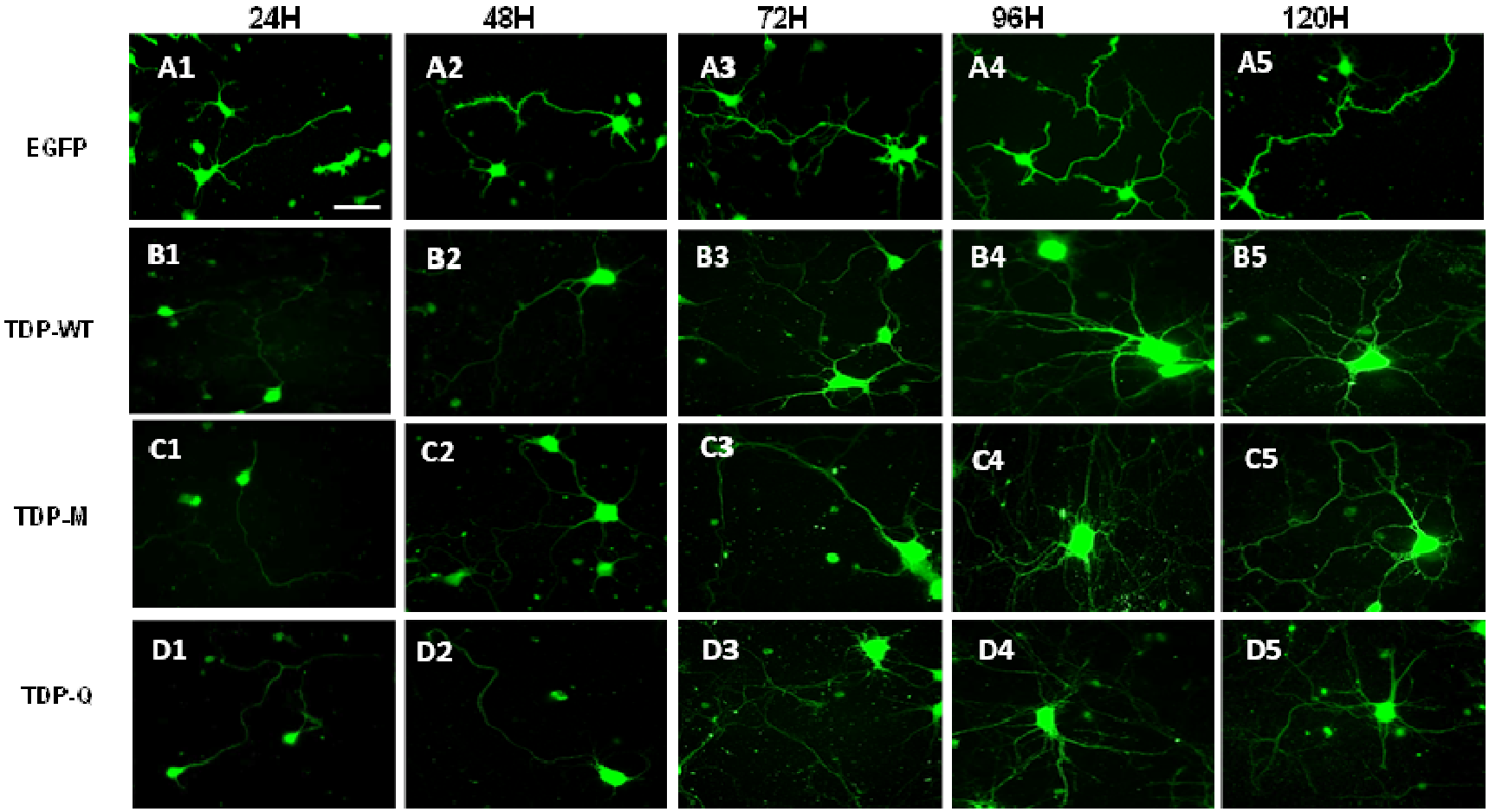

Figure 3.1 Tagged TDP-43 is re-distributed to the cytoplasm

Rat cortical neurons were transfected with EGFP control (A), and GFP tagged TDP-43 wild-type (TDP-WT) (B) and mutant isoforms TDP-43 M337V (TDP-M) (C) and TDP-43 Q331K (TDP-Q) (D) plasmids. The neurons were stained with anti-GFP primary and secondary antibodies and fixed at different time points (24H -120H). Compared to the EGFP controls (A1-A5), TDP-43 wild-type and mutant constructs show cytoplasmic re-distribution (B1-D5) over time. Scale bar = 10 µm

In order to evaluate TDP-43 mis-localisation and aggregation, cortical neurons were transfected with the control and TDP-43 wild-type and mutant constructs on day zero, fixed at various time points from 24 hours to 168 hours (Fig 3.1). Having standardized the Amaxa transfection protocol and the dosage of the constructs (4µg/1.5 million cells), a very good transfection efficiency of 70% for every 100,000 cells plated was consistently obtained. The fixed neurons were immunostained with antibodies to GFP to observe the expression patterns of the TDP-43 wild-type and mutant constructs, as the proteins were tagged to GFP.

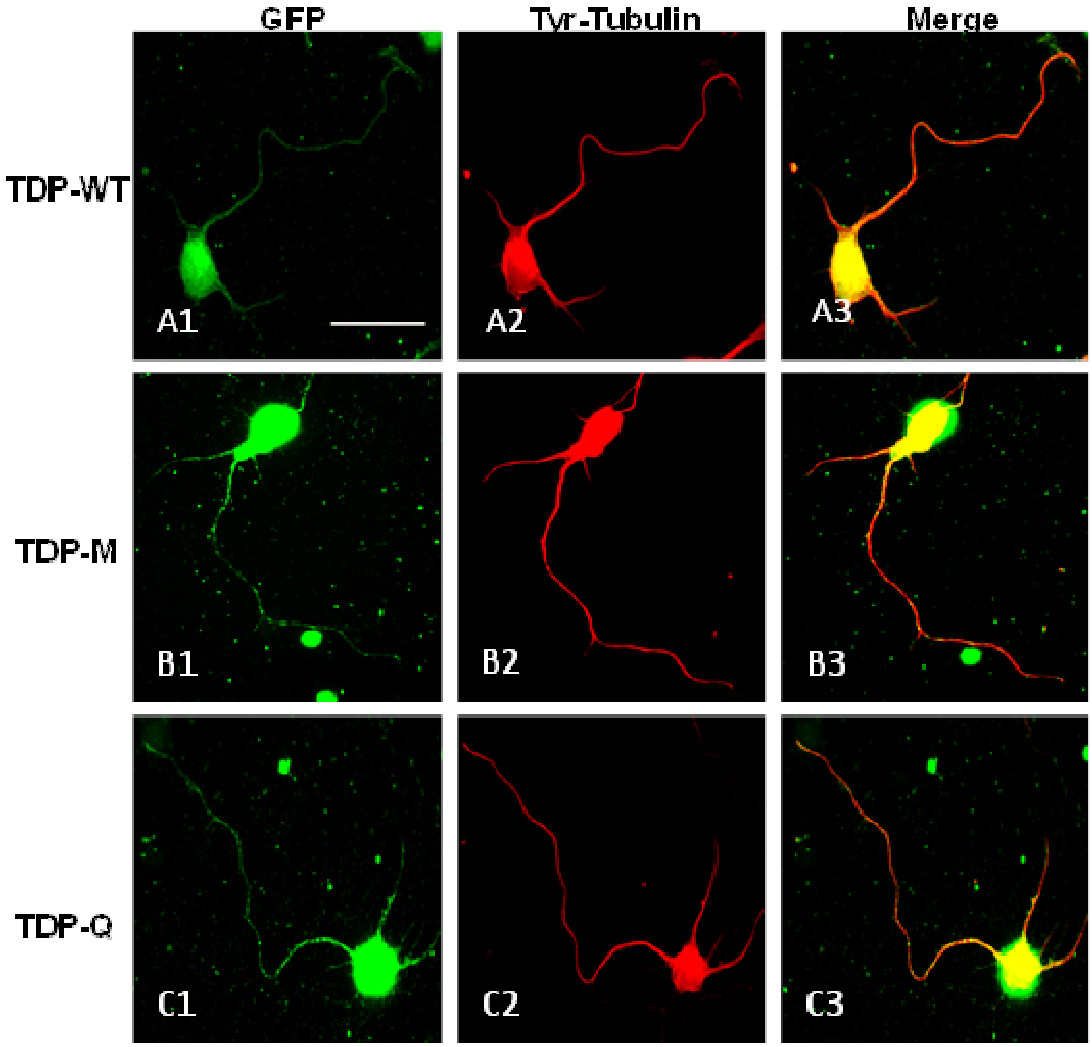

Figure 3.2 Tagged TDP-43 is mislocalised to the cytoplasm at 24H
Rat cortical neurons were transfected GFP tagged TDP-43 isoforms: TDP-WT (A); TDP-M (B); TDP-Q (C) and fixed after 24H in culture. The transfected neurons were immunostained with GFP (A1-C1) and tyrosinated (Tyr) tubulin (A2-C2) to mark the transfected cells and label the axons. Scale bar – 10 µm

At every time point, the GFP staining for the EGFP control transfection were seen through the entire neuron – nucleus, cell-body, axons and dendrites (Fig 3.1: A1- A5). Surprisingly, GFP expression for the TDP-43 wild-type and mutant isoforms was also seen ubiquitously over the entire neuron as early as 24 hours with progressive accumulation over time (Fig 3.1-3.6).

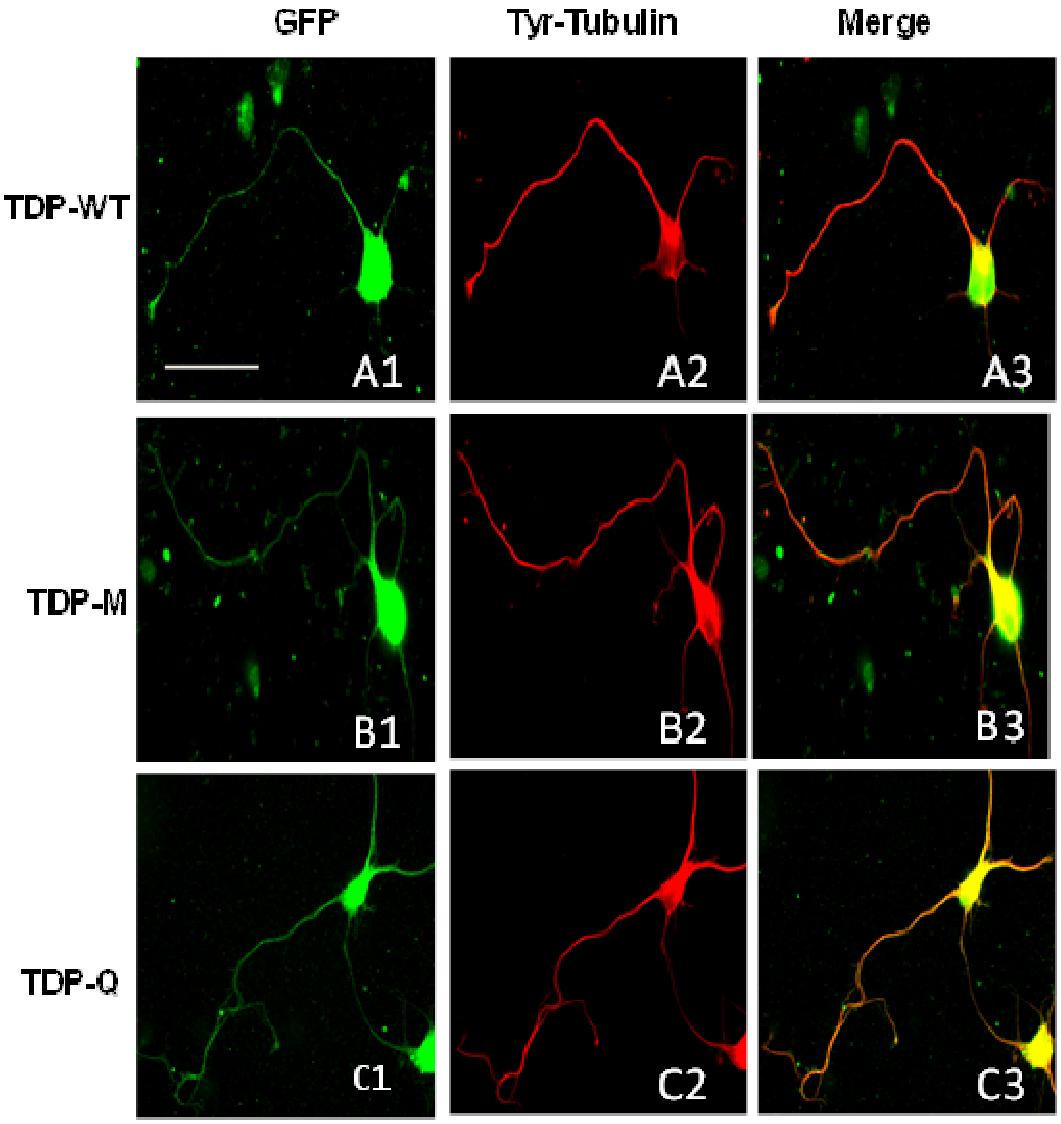

Figure 3.3 Tagged TDP-43 is mislocalised to the cytoplasm at 48H
Rat cortical neurons were transfected GFP tagged TDP-43 isoforms: TDP-WT (A); TDP-M (B); TDP-Q (C) and fixed after 48H in culture. The transfected neurons were immunostained with GFP (A1-C1) and tyrosinated (Tyr) tubulin (A2-C2) to mark the transfected cells and label the axons. Scale bar – 10 µm

At 24 hours and 48 hours, the GFP staining for the EGFP-WT TDP-43 appears less faint than the mutants, suggesting slower cytoplasmic re-distribution of wild-type TDP-43 compared to the mutant proteins (Fig 3.2-3.3).

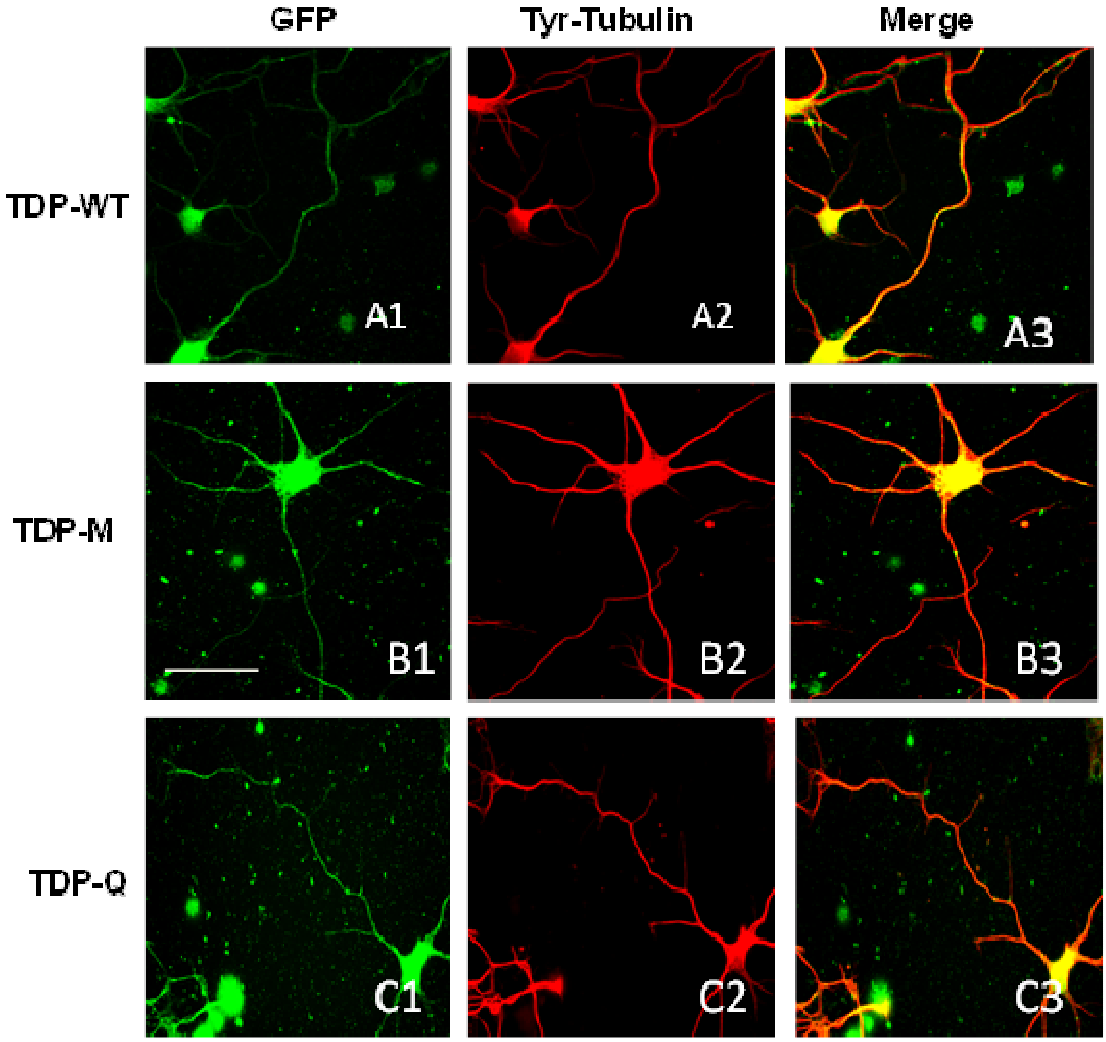

Figure 3.4 Tagged TDP-43 aggregates in the cytoplasm at 72H
Rat cortical neurons were transfected GFP tagged TDP-43 isoforms: TDP-WT (A); TDP-M (B); TDP-Q (C) and fixed after 72H in culture. The transfected neurons were immunostained with GFP (A1-C1) and tyrosinated (Tyr) tubulin (A2-C2) to mark the transfected cells and label the axons. Scale bar – 10 µm

The mis-localisation of TDP-43 into the axons is quickly followed by aggregation of TDP-43 in the cell body and axons. Distinct aggregates became very clear along the axons of the TDP-43 transfected neurons around 72 hours and the accumulation becomes increasingly granular over-time (Fig 3.4, Fig 3.6).

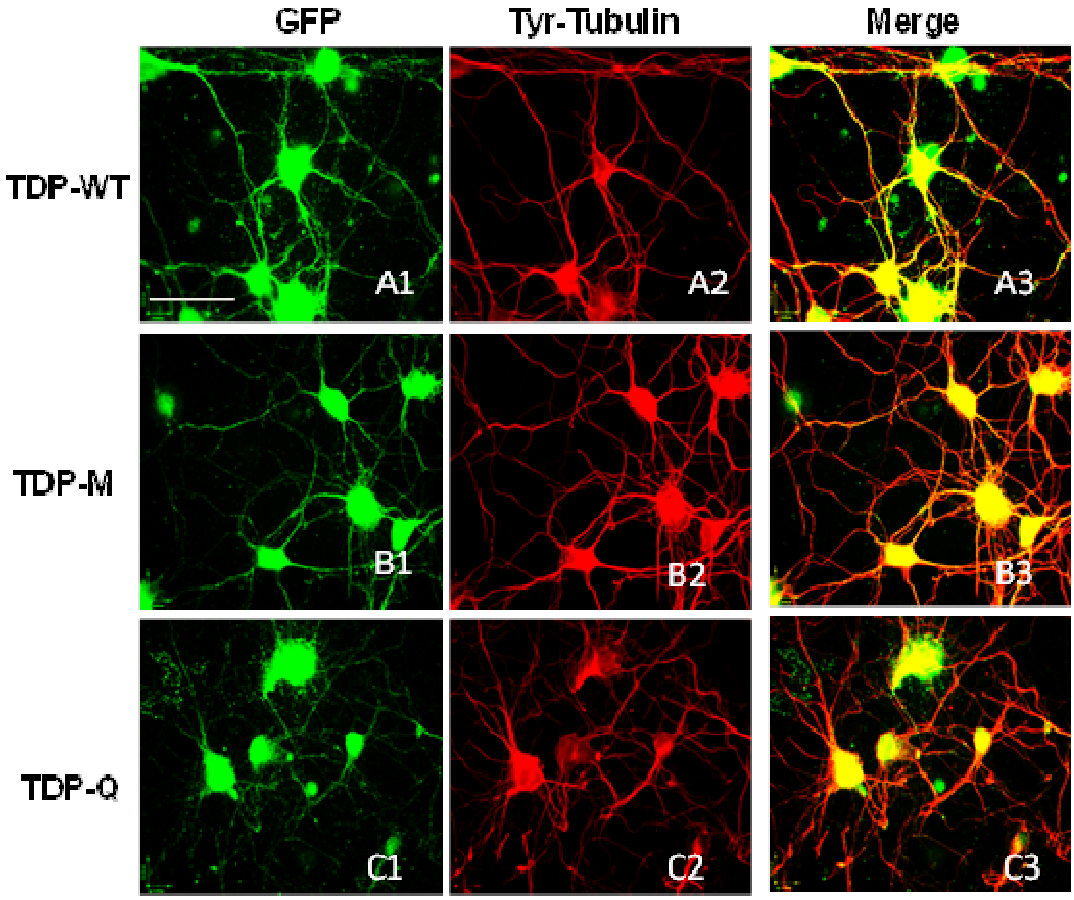

Figure 3.5 Cytoplasmic aggregation of Tagged TDP-43 increases over-time
Rat cortical neurons were transfected GFP tagged TDP-43 isoforms: TDP-WT (A); TDP-M (B); TDP-Q (C) and fixed after 144H in culture. The transfected neurons were immunostained with GFP (A1-C1) and tyrosinated (Tyr) tubulin (A2-C2) to mark the transfected cells and label the axons. Scale bar – 10 µm

At 144 hours, the aggregation of TDP-43 becomes more pronounced resulting in a dotted appearance of TDP-43 along the axons, as the aggregates spread out along the axon and becomes spaced apart (Fig 3.5). Compared to the TDP-43 mutants, EGFP-WT TDP-43 aggregates remain closer together, whereby their axons have a more intact appearance rather than the dotted appearance observed with the mutants. EGFP-TDP-43 Q331K has larger aggregates with more gaps between the aggregates compared to EGFP-TDP-43 M337V and EGFP WT-TDP-43 (Fig 3.1-3.6). These neurons were co-labelled with tyrosinated tubulin to observe the cytoskeletal integrity. Though the GFP expression appeared fragmented, the tubulin staining was intact (Fig 3.2-3.5).

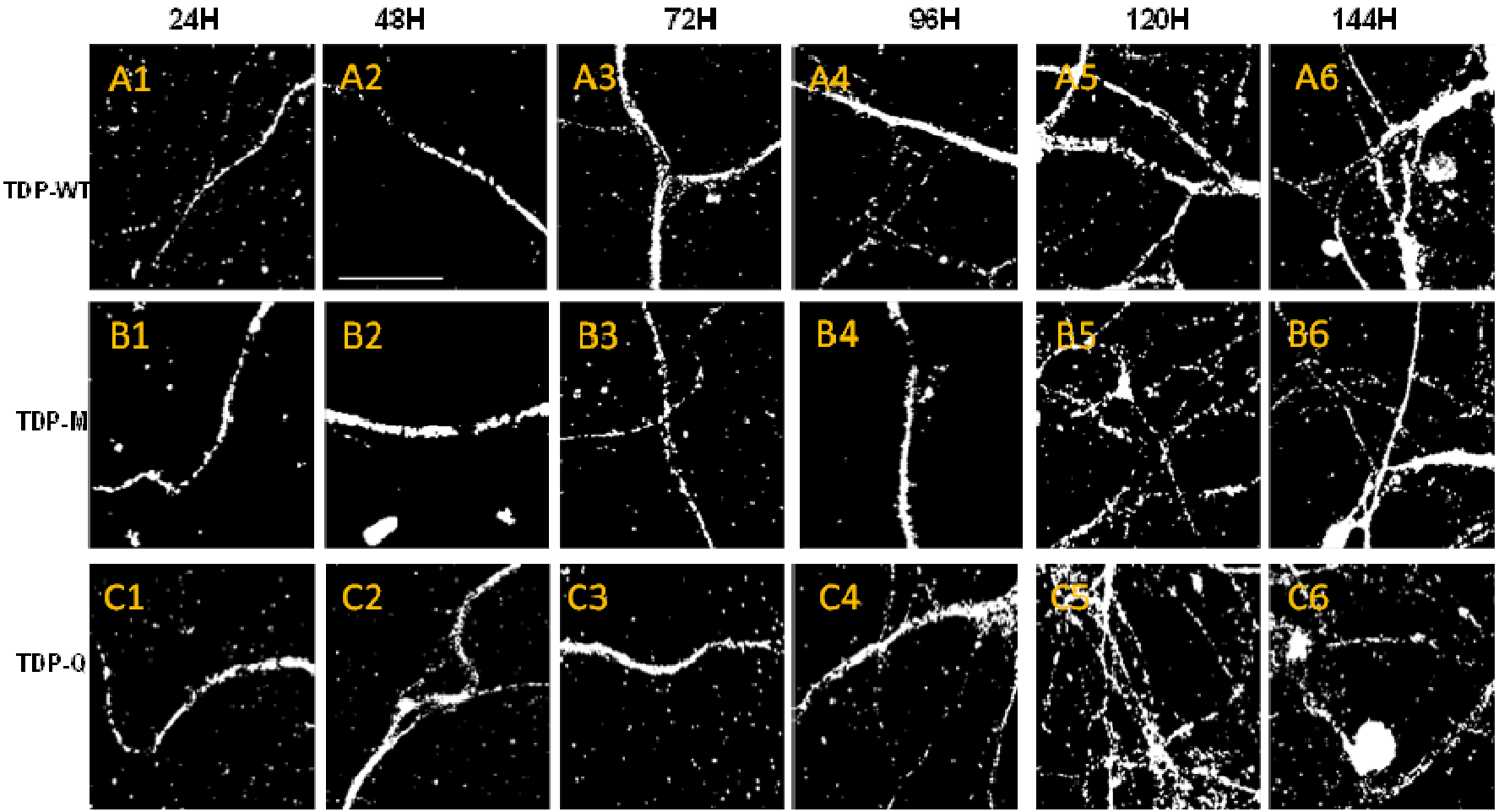

Figure 3.6 Tagged TDP-43 misclocalisation is followed by aggregation

Magnified images of axons from neurons transfected with GFP tagged TDP-43 isoforms. Monochromatic images of GFP antibody staining shows that TDP-43 is mislocalised to the axoplasm (A1-C2) and aggregates (A3-C6) in the cytoplasm. Scale bar = 10 µm

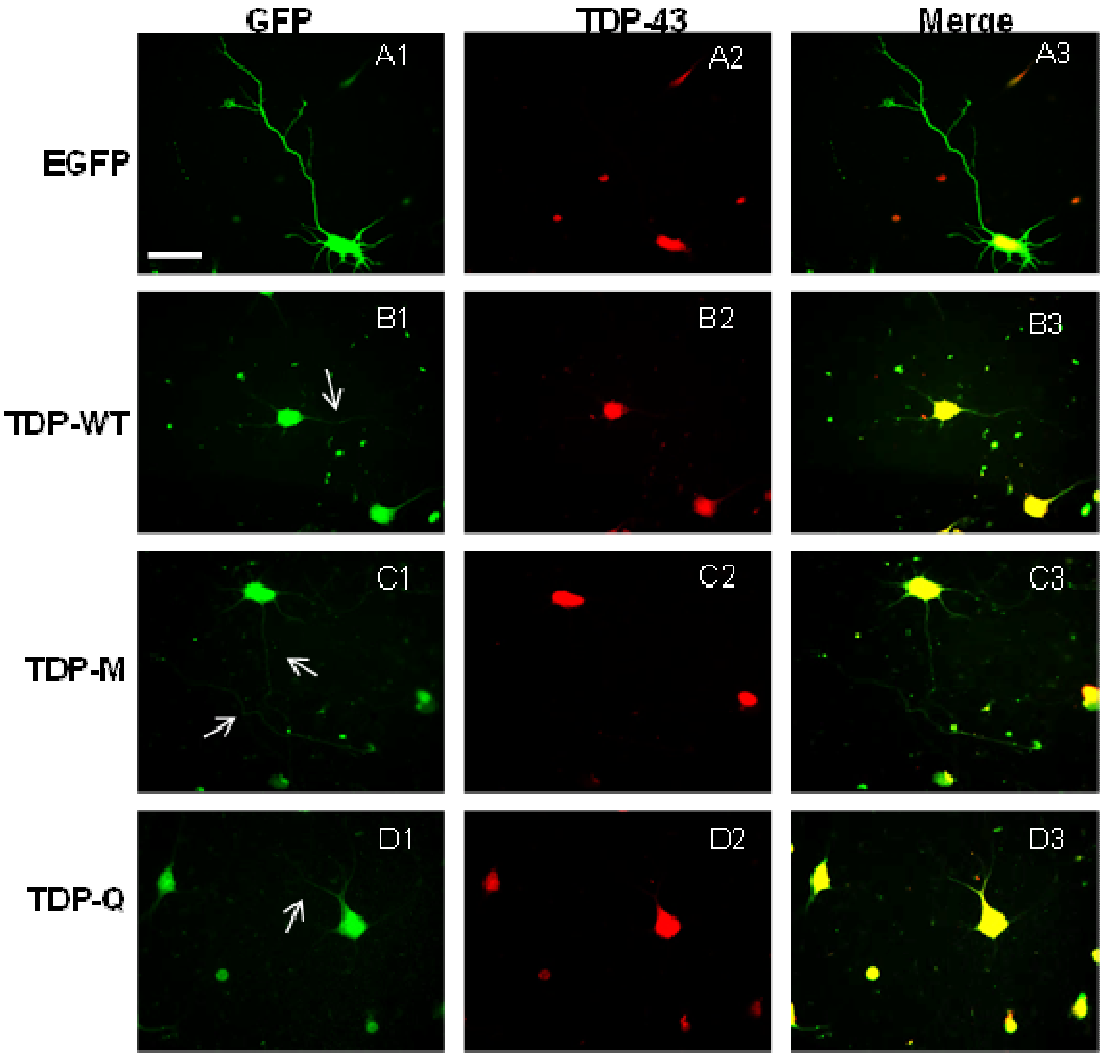

Figure 3.7 TDP-43 expression is nuclear at 24H
Rat cortical neurons were transfected with EGFP control and GFP tagged TDP-43 wildtype (TDP-WT) and mutant isoforms (TDP-M, TDP-Q). The neurons were stained with anti TDP-43 (Red) that detects endogenous levels of TDP-43 (A2-D2) and GFP (green) antibodies (A1-D1) after 24H in culture. Arrows show the axon path. Scale bar = 10 µm.

Neurons transfected with TDP-43 wild-type and mutant isoforms were double labelled with antibodies to GFP (green) and antibodies to TDP-43 (red) to detect the expression of tagged GFP and endogenous levels of TDP-43 (Fig 3.7 – Fig 3.9). At 24 hours, in contrast, to tagged TDP-43, anti TDP-43 was predominantly expressed in the nucleus with all the constructs (Fig 3.7). Post 24 hours, anti TDP-43 was re-distributed to the cytoplasm with progressive accumulation over time; similar to tagged TDP-43 (Fig 3.8 & 3.9).

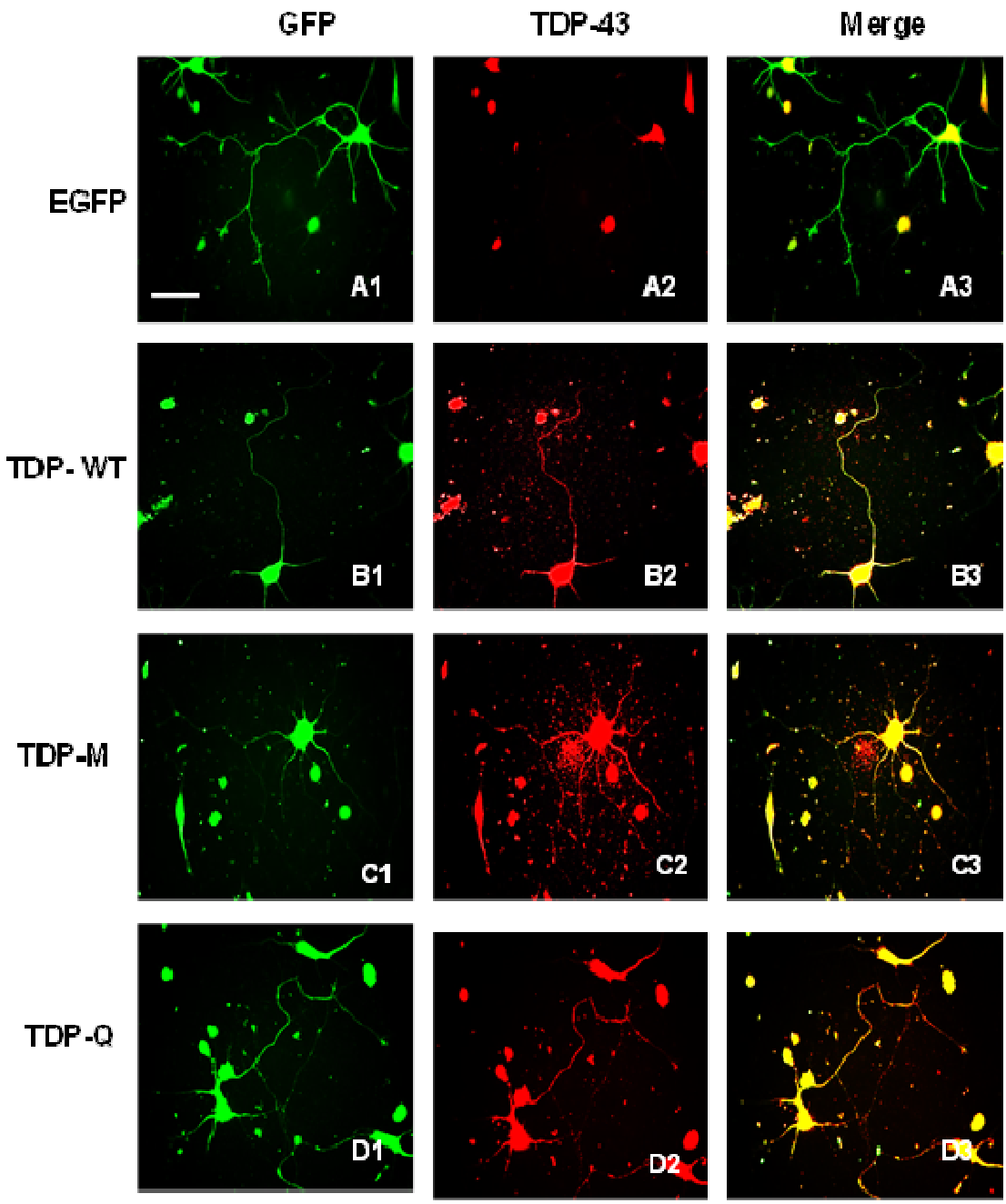

Figure 3.8 TDP-43 is mislocalised to the cytoplasm over time
Rat cortical neurons were transfected with GFP control and TDP-43 wild-type and mutant plasmids. The neurons were immunostained with GFP (green) and anti TDP-43 (red) after 72H in culture. GFP control neurons are stained throughout the axon with the GFP (A1) and only show a nuclear staining of anti TDP-43 (A2). Both the tagged TDP-43 (B1 –D1) and the anti TDP-43 (B2-D2) are mislocalised from the nucleus and distributed along the entire neuron when transfected with the TDP-43 plasmids. Scale bar = 10 µm.

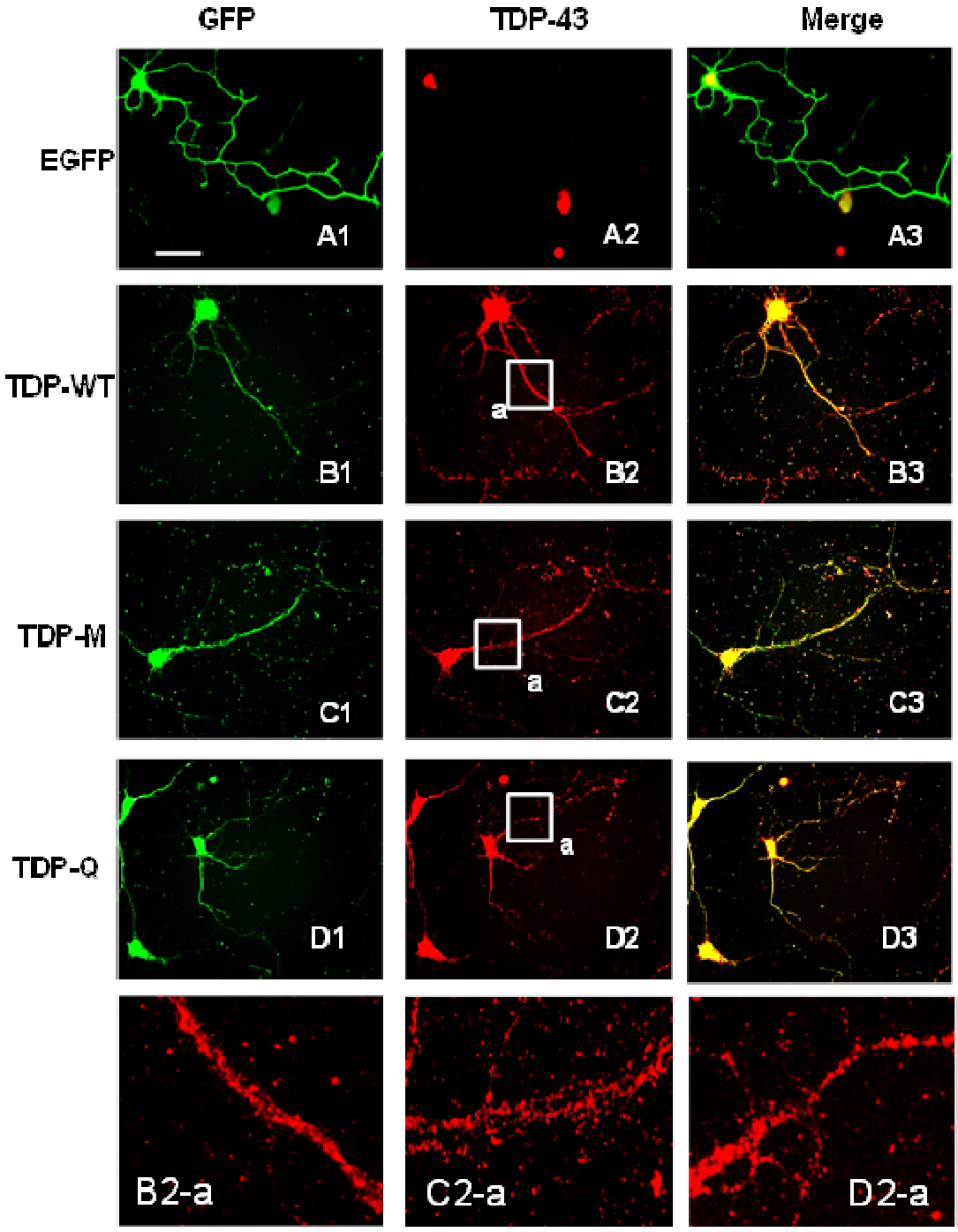

Figure 3.9 TDP-43 aggregates in the cytoplasm over-time
Rat cortical neurons were transfected with GFP control and TDP-43 wild-type and mutant plasmids. The neurons were immunostained with GFP (green) and anti TDP-43 (red) after 144H in culture. GFP control neurons show a nuclear staining of anti TDP-43 (A2). Both the tagged TDP-43 (B1 –D1) and the anti TDP-43 (B2-D2) are mislocalised from the nucleus and have a granular distribution when transfected with the TDP-43 plasmids. The aggregation is clearly seen in the inset (B2-a –D2-a). Scale bar = 10 µm

At all the time-points, the expression of TDP-43 remained nuclear in neurons transfected with EGFP control. In a similar fashion to tagged TDP-43, anti-TDP-43

aggregates became distinctly granular and spaced apart overtime. EGFP-TDP-43 Q331K aggregates were larger and widely spread whereas EGFP-WT TDP-43 was smaller and grouped together. EGFP-TDP-43 M337V aggregates are smaller and spaced apart having a fragmented appearance (Fig 3.8 – 3.9). Though TDP-43 was mis-localised to the cytoplasm and axons, the neurons still have a strong expression of both tagged TDP-43 (detected with antibodies to GFP) and TDP-43 (seen with antibodies specific to TDP-43) in the nucleus.

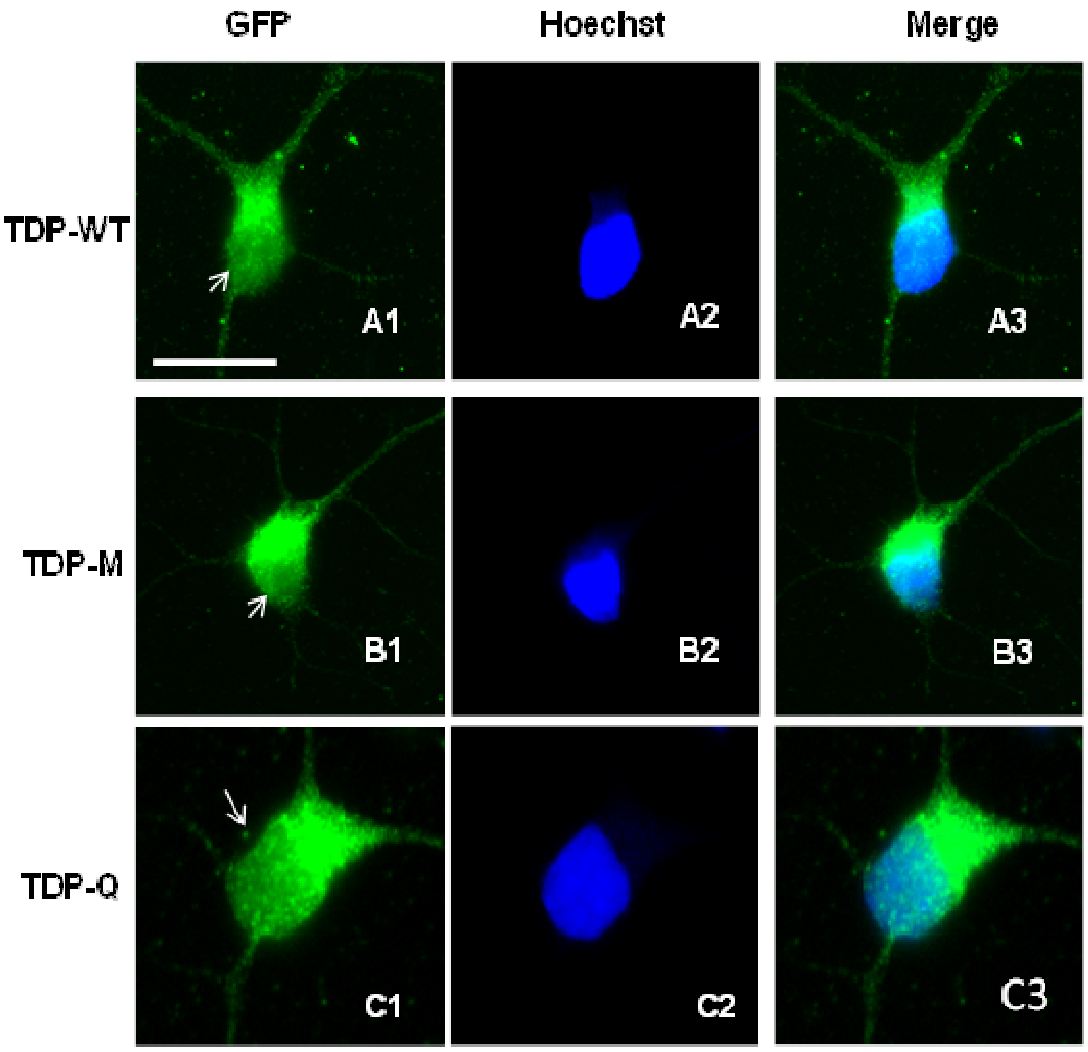

Figure 3.10 Nuclear clearing of tagged TDP-43

Rat cortical neurons were transfected with GFP control plasmid and GFP tagged TDP-43 wild-type and mutant plasmids. The cells were fixed at 144H post transfection and stained for GFP and Hoechst. Hoechst staining was used to identify the nucleus (A2 – C2). About 25% of transfected neurons (n=3) show a nuclear clearing of tagged GFP (A1 –C1). This reduction of nuclear GFP tagged TDP-43 can be seen along the arrows and is even more distinct in the merged images (A3 – C3). Scale bar = 10 µm.

However, between 96 hours – 144 hours post culture, around 10-15% of the neurons transfected with TDP-43 wild-type and mutant plasmids, show a nuclear clearing of tagged TDP-43 (Fig 3.10). No nuclear clearing of TDP-43 was seen using antibodies to TDP-43.

In Summary, TDP-43 wild-type and mutants are re-distributed to the axons over a period of time and the aggregation becomes more pronounced at later time points. The TDP-43 mutants when compared to the wild-type have a more pronounced mis-localisation and aggregation pattern. Also mis-localisation/aggregation of TDP-43 to the cytoplasm is not always accompanied by nuclear clearance.

3.2.2 Over-expression of Wild-type and Mutant isoforms of TDP-43 causes neurotoxicity in vitro in rat cortical neurons.

We have previously shown that over-expression of the wild-type and mutant isoforms of TDP-43 causes neurotoxicity *in vivo* in chick embryo spinal cord (Tripathi et al., 2014). In order to characterize TDP-43 mediated toxicity *in vitro,* primary rat cortical neurons were transfected with control EGFP and TDP-43 constructs as above. The cells were plated at an equal density between the different constructs. A general transfection efficiency of 70% was consistently observed with the different constructs. The cells were fixed at different time points post transfection.

The Promega TUNEL system was used to assay apoptotis in cultured cells. It detects apoptosis by end-labelling and measuring nuclear DNA fragmentation. The number of TUNEL positive cells was manually counted from five different 0.24mm^2 fields from a 13mm^2 coverslip plated with 70,000 transfected cells under a fluorescence/phase microscope. EGFP expressing neurons had few apoptotic cells throughout the different time points (Fig 3.11: A, E). The number of apoptotic cells in EGFP control was quite low and stable. In comparison, the number of apoptotic cells was significantly higher in neurons expressing EGFP- WT TDP-43 and TDP-43 mutant isoforms (EGFP-TDP-43 M337V, EGFP-TDP-43 Q331K) (Fig 3.11: B-E).

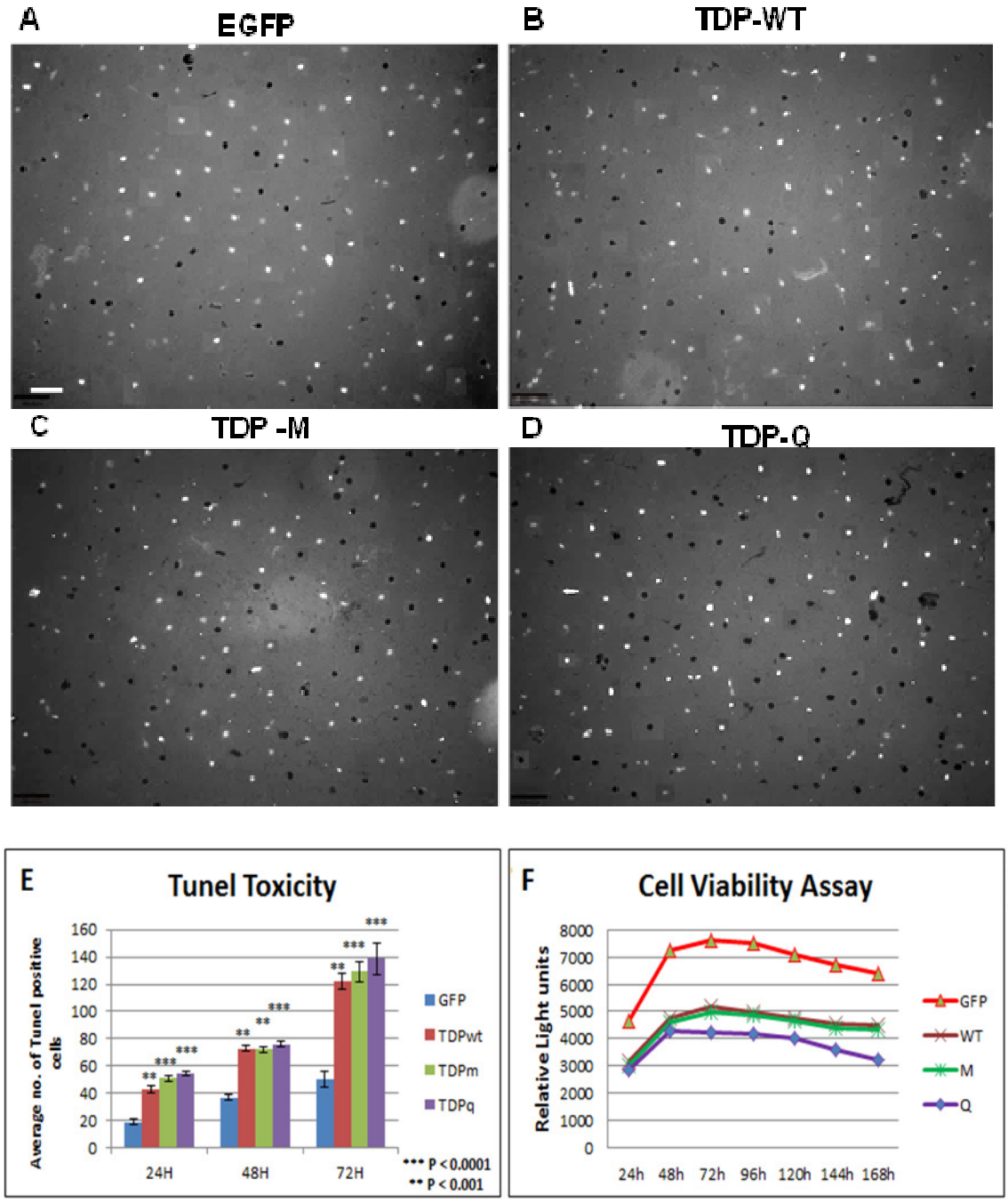

Figure 3.11 Overexpression of tagged TDP-43 is neurotoxic

Rat cortical neurons were transfected with EGFP control plasmid and GFP tagged TDP-43 wild-type and mutant plasmids. Panels A-D is a monochromatic merge of TUNEL positive cells (black dots) and Hoechst staining (white dots) after 72H in culture. The Hoechst staining represents the total number of cells while the TUNEL staining represents the dead cells. Scale bar = 10 µm. Panel E represents the average number of apoptotic cells quantified from five 0.24mm^2 fields, at 3 different time points (24H, 48H and 72H) post transfection (n=3). Data is presented as means and standard errors. Significance were compared by ANOVA (No significance: p > 0.05; *** P < 0.0001; ** P < 0.001- compared with EGFP control). Panel F is a semi quantitative analysis of the viability of transfected cells assessed by Promega real-time glo viability assay at different time points from 3 independent experiments.

At every time point, the neurons over-expressing the wild-type and mutant isoforms of TDP-43 showed a significant increase Fin the number of apoptotic cells compared to the neurons expressing control EGFP (ranging from: **p< 0.001 to ***p< 0.0001 - At 24 hours and 72 hours, EGFP vs. TDP-WT : **p< 0.001 ; EGFP vs. TDP-43 mutants: ***p< 0.0001; At 48 hours, EGFP vs. TDP-WT and TDP-M: **p< 0.001 ; EGFP vs. TDP-Q: ***p< 0.0001). There was no significant difference in toxicity between the TDP-43 wild-type and mutant constructs ($p > 0.05$). At 24 and 48h, TDP-43 wild-type and mutant constructs show double the amount of cell death when compared to the control EGFP and at 72h the number of apoptotic cells triple in comparison to EGFP (Fig 3.11: E).

To reciprocate cell toxicity to cell viability, a real time vialibility kit was used to. The Cell-Glo viability assay from Promega is a bioluminescent assay which is non-lytic and is used to determine cell viability in real time by measuring the metabolic activity of cells. The signal from the viable cells is read using a luminometer. The transfected cells to which the assay was added were grown in culture for a week, and their luminescent signal was read every 24 hours using a plate reader. The data obtained shows that the EGFP transfected control cells show greater viability than the TDP-43 transfected neurons (Fig 3.11: F). At 24 hours and 48 hours, the EGFP transfected control neurons show a ~1.5x difference in viability compared to the TDP-43 transfected neurons. Between 72 hours and 168 hours, EGFP transfected neurons show a ~two-fold increase in viability compared to the TDP-43 Q and a ~1.5 -1.3x difference compared to TDP-43 WT and TDP-43 M. Overall, the results obtained with the cell viability assay correlated with the increased apoptosis at the specified time points. Sporadic mutant EGFP- TDP-43 Q133K has the highest number of TUNEL positive cells and also the least number of viable cells. The viability curve for EGFP TDP-43 Q331k drops from 120 hours which correlates with the increased aggregation observed at the same time point. Over-expression of the TDP-43 wild-type plasmid and the familial mutant TDP-43 M337V are also toxic and show comparable levels of toxicity and viability.

In summary, TDP-43 wild-type (WT TDP-43) overexpression and the expression of the mutant isoforms: TDP-43 M337V and TDP-43 Q331K, caused substantial toxicity in primary cortical neurons *in vitro*. The level of toxicity in the neurons expressing wild-

type and mutant isoforms of TDP-43 increases over a period of time correlating with increase in TDP-43 aggregation. TDP-43 Q331K has the highest number of apoptotic cells and the lowest viability.

3.2.3 TDP-43 toxicity affects cytoskeletal integrity

While looking at TDP-43 aggregation in rat cortical neurons, from around 96 hours, ~25% of the TDP-43 transfected cells showed evidence of disintegration and cell death as reflected by cellular fragmentation and nuclear dissolution. TDP-43 cytotoxicity was marked by several morphological changes such as cell fragmentation, blebbing or rounding (Fig 3.12: A1-C1). In TDP-43 disintegrated neurons, we observed severe aggregation of TDP-43 and a complete collapse of the axonal integrity and structure. In these cells, TDP-43 fragmentation completely co-localises with tubulin fragmentation (Fig3.12). Thus, TDP-43 aggregation eventually leads to cellular fragmentation resulting in the disintegration of the axonal integrity causing neurodegeneration.

In summary, TDP-43 aggregation and collapse of the cytoskeletal structure precedes neuronal death and hence may be an important step towards neuronal toxicity.

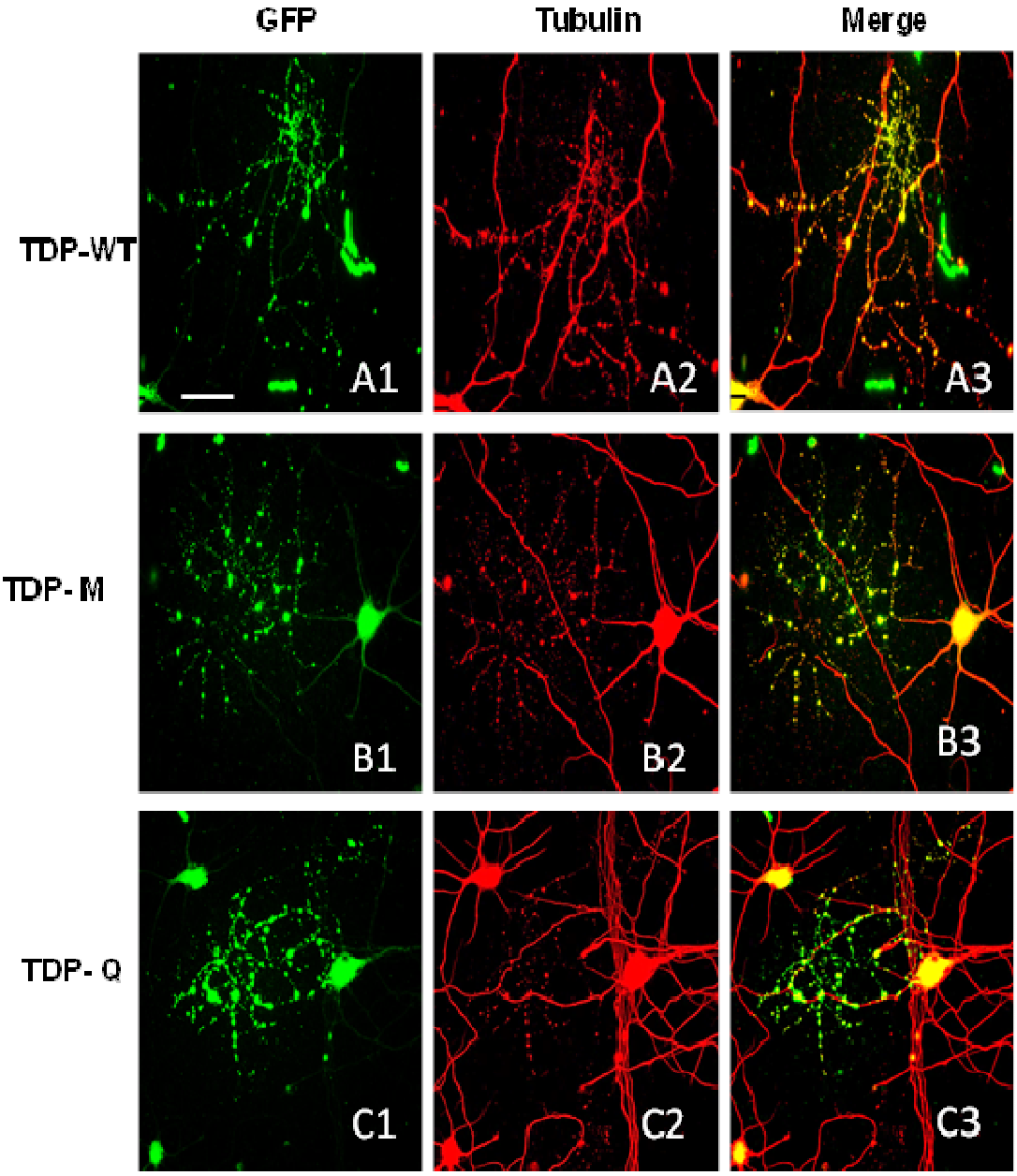

Figure 3.12 Tagged TDP-43 fragmentation co-localizes with tubulin

Rat cortical cells were transfected with GFP control plasmid and GFP tagged TDP-43 wild-type and mutant plasmids and fixed after 144H in culture. GFP staining identifies the transfected neurons (A1 – C1) and the tubulin staining was used to visualize the axonal integrity (A2 –C2). TDP- 43 induced axonal degeneration (A1 – C1) correlates with axonal fragmentation as evidenced by the fragmented tubulin (A2- C2). Panels A3- C3 shows that TDP-43 induced cytotoxicity co-localizes with axonal fragmentation (A3- C3). Scale bar = 10 µm

3.3 Discussions

Cortical degeneration is distinctive in ALS and in FTLD; hence in this chapter we used rat cortical neurons to model TDP-43 mediated neurodegeneration. We have previously used the chick spinal motor neurons *in vitro* and the chick spinal cord *in ovo* to model the pathogenicity of TDP-43 and here rat cortical neurons were used to recapitulate key features of TDP-43 pathogenesis and complement our previous findings.

The results presented in this chapter showed that over-expression of TDP-43 wild-type and mutant constructs, re-distributes EGFP-TDP-43 to the cytoplasm. The mis-localisation occurs as early as 24 hours post transfection and is progressively enhanced. TDP-43 mis-localisation precedes aggregation. TDP-43 wild-type and mutant aggregation is distinctly seen at 72 hours and the aggregation is enhanced over time. Mutants TDP-43 M337V and TDP-43 Q331K show an enhanced effect compared to the WT TDP-43. Toxicity by aggregation co-localised with fragmented tubulin implying that aggregation can lead to cell death by perturbing the cytoskeletal integrity. Anti TDP-43 staining corroborates the progressive mis-localisation and aggregation seen with tagged-TDP-43. Nuclear clearing of tagged TDP-43 is seen after 96 hours in a small minority of TDP-43 wild-type and mutant transfected neurons implying that nuclear clearing of TDP-43 is not necessary for TDP-43 pathogenesis. Over-expression of the TDP-43 wild-type and mutant constructs are toxic to cortical neurons and the number of apoptotic cells increase over time, suggesting a possible correlation between aggregation and toxicity.

3.3.1 TDP-43 mis-localises to the cytoplasm over-time

Aggregation of TDP-43 is a hallmark of ALS and ALS-FTLD. The results show that over-expression of TDP-43 wild-type and mutant proteins, re-distributes tagged TDP-43 to the cytoplasm. TDP-43 is mis-localised to the cytoplasm as early as 24 hours following transfection and the mis-localisation is enhanced over time. The WT-TDP-43 expression in the axons is fainter than the expression of TDP-43 M337V and TDP-43 Q331K at 24 hours and 48 hours. This implies that the mis-localisation of WT TDP-43

into the axons is slower than the mislocalisation of the TDP-43 mutants. The early mis-localisation of TDP-43 wild-type and mutant proteins in cortical neurons is interesting because in our previous study, spinal motor neurons transfected with the same TDP-43 wild-type and mutant plasmids showed that TDP-43 mis-localises and aggregates in the axons only at 72 hours post transfection. At 24 hours, TDP-43 wild-type and mutants remain predominantly nuclear in spinal motor neurons. One study showed that TDP-43 wild-type and mutant protein (TDP-43 A315T) was found to be re-distributed to the cytoplasm 24 hours after transfection in primary cortical neurons (Barmada et al., 2010) in a proportion of transfected cells (10-15%). Thus, cortical neurons show early mis-localisation of TDP-43 compared to spinal motor neurons. However, differing dosages and transfection efficiencies could also contribute to this difference. Brettschneider et al., 2012 studied the spread pattern of TDP-43 aggregates in the brain and spinal cords of ALS patient and suggested that TDP-43 pathology appears to start in the motor cortex at the top of the brain and radiate downward to the spinal cord. Thus, cortical neurons might be more sensitive to TDP-43 re-distribution than spinal motor neurons.

Aggregation of TDP-43 into distinct clumps along the axons can be clearly seen around 72 hours and the aggregation is progressively increased over time. At later time points (~120 hours), the aggregates of the TDP-43 M337V and TDP-43 Q331K are bigger in size and spaced widely apart along the axons whereas the aggregates of TDP-43 are smaller and closely placed whereby they appear intact as opposed to the fragmented appearance seen in the mutants. Comparatively, the aggregation is more severe in the spinal motor neurons at 72 hours. The aggregates looked bigger and widely spaced and reflected cellular fragmentation. Such an effect in cortical neurons was only seen at later time points indicating that the spinal motor neurons may be more susceptible to TDP-43 aggregation in comparison to the cortical neurons. A difference in aggregation between the wild-type and mutant constructs may be determined by detergent assays as Barmada and colleagues found that GFP fluorescence in the TDP-43 aggregation of the wild-type constructs was soluble whilst the GFP fluorescence in the TDP-A315T mutants were detergent resistant (Barmada et al., 2010).

Antibodies to TDP-43 that detect endogenous levels of TDP-43 showed that TDP-43 expression is predominantly nuclear in the EGFP control neurons at all the time points, whilst in the TDP-43 transfected neurons, it is predominantly nuclear at 24 hours and is thereafter mis-localised to the axons. The mis-localisation and aggregation of TDP-43 is enhanced over time in a similar fashion to tagged TDP-43. Over-expression of tagged TDP-43 constructs enhances the mis-localization of tagged TDP-43 followed by progressive aggregation of the tagged TDP-43 overtime. Thus, the re-distribution of TDP-43 to the axons may be the precursor to TDP-43 aggregation.

Post 96 hours in culture, ~ 15-20% of TDP-43 wild-type and mutant transfected neurons show nuclear clearing of tagged TDP-43. No nuclear clearing of TDP-43 was observed. One of the proposed disease mechanisms of TDP-43 is that nuclear depletion of TDP-43 might contribute to a loss of function mechanism. However, since we only see nuclear clearing in a minor proportion of transfected cells, we can speculate that nuclear clearing of TDP-43 might not be essential to TDP-43 neurotoxicity. Several studies have shown that nuclear depletion is not a requisite for TDP-43 neurotoxicity and that TDP-43 dependent degeneration can take place without nuclear depletion (Arnold et al., 2013).

The TDP-43 mis-localizaton and aggregation data complements our previous study which reported the mis-localization of TDP-43 *in vivo* and *in vitro* in chick spinal motor neurons. We also show that TDP-43 progressive pathology is not necessarily dependent on nuclear clearing of TDP-43 (loss of function mechanism). These results provide no evidence that nuclear depletion of TDP-43 is important for the toxicity of mutants but do indicate that the mis-localisation of TDP-43 is sufficient to induce neurotoxicity. However, the fact that these experiments were conducted in the presence of normal levels of endogenous TDP-43 limits our ability to completely avoid the likelihood that loss of nuclear TDP-43 is lethal.

3.3.2 Over-expression of wild-type and mutant isoforms of TDP-43 causes neurotoxicity in rat cortical neurons in vitro.

One of the key features underlying TDP-43 proteinopathies is neuronal loss. TDP-43 wild-type and mutant constructs are neurotoxic and the number of apoptotic cells increase over-time. Although there was no significant difference between the TDP-43 wild-type and mutant constructs, the mutant TDP-43 Q331K had the highest number of apoptotic cells across the different time points. This correlates with other studies on TDP-43, wherein ALS related TDP-43 mutants (A315T, N390S and G290A) caused substantial toxicity in rat cortical neurons (Barmada et al., 2010).

The toxicity data complements our TDP-43 toxicity study *in vivo* (Tripathi et al., 2014) wherein expression of the TDP-43 wild-type and mutant constructs at similar concentrations induced neurotoxicity with no significant difference between the wild-type and mutant constructs. Transgenic mice expressing TDP-43 Q331K and TDP-43 M337V showed progressive motor neuron death when compared to the WT TDP-43 (Arnold et al., 2013). Thus, both TDP-43 Q331K and TDP-43 M337V are toxic and the difference in the number of apoptotic cells vary in different cell-types and animal models.

Experiments in several transgenic models (*Drosophila*, *C.elegans*, Mice, zebrafish) have shown that over-expression of TDP-43 wild-type and mutant isoforms confers toxicity leading to premature death (Berthod and Gros-Louis, 2012). These studies suggest that the TDP-43 mutants are more neurotoxic than the wild-type and that effects are dose dependent. Thus, the lack of significant difference in the toxicity between the TDP-43 wild-type and mutant constructs could be due to the over-expression of these constructs.

The increased toxicity correlates with the progressive re-distribution/aggregation of TDP-43. The number of apoptotic cells in the TDP-43 wild-type and mutant transfected neurons increases over time. Between 96-168 hours, a small proportion of TDP-43 transfected neurons disintegrate as a result of severe TDP-43 aggregation. Neurodegeneration is marked by several morphological changes such as cell fragmentation, blebbing or rounding. The fragmentation of TDP-43 in the transfected

neurons (dead) co-localised with fragmented tubulin, showing that aggregation driven toxicity breaks down the neuronal cytoskeletal integrity. Thus, TDP-43 aggregation could also lead to neurotoxicity. However, since TDP-43 aggregation driven toxicity is only seen in a small percentage of cells, TDP-43 aggregation might not be the sole mechanism driving TDP-43 mediated neurodegeneration and could just be a risk factor for cell death. Studies have shown that cytoplasmic TDP-43 is associated with cell death in neurons expressing both WT-TDP-43 and mutant TDP-43 A315T (Barmada et al., 2014).

Thus, we have successfully modelled the TDP-43 pathology *in vitro* using rat cortical neurons. We have shown that cortical neurons are as susceptible to TDP-43 toxicity as spinal motor neurons under the same conditions. Both TDP-43 aggregation and neurotoxicity are progressive. However, this does not shed any light as to whether mis-localisation/aggregation is the primary trigger of toxicity or is just a consequence of other events.

4 TDP-43 disrupts cytoskeletal function through mRNA mislocalisation

4.1 Introduction

TDP-43 is a member of the heterogenous nuclear ribonucleoprotein (hnRNP) family and play important roles in multiple biological functions, including those that regulate RNA pathways. Experimental evidence has suggested that TDP-43 is a group of RBPs and as such shuttles between the nucleus and the cytoplasm and has clear nuclear and cytoplasmic functions (Ayala et al., 2008, Freibaum et al., 2010). TDP-43 is a component of heterogenous nuclear ribonucleoprotein (hnRNP) particles, which regulate splicing of pre-mRNA species (Polymenidou et al., 2011, Tollervey et al., 2011a). TDP-43 also binds to mRNA sequences, particularly within the 3' untranslated region, and affects mRNA stability and turnover (Buratti and Baralle, 2001, Ayala et al., 2008, Strong et al., 2007). TDP-43 is thought to play a part in mRNA trafficking (Wang et al., 2008b), as TDP-43 undergoes rapid nucleo–cytoplasmic shuttling and is localised within dendritic RNA granules. Several studies have suggested that TDP-43 mislocalisation to the cytoplasm and not the aggregation per se, is the cause of neurodegeneration (Barmada et al., 2010) as the cytoplasmic re-distribution may affect several roles of TDP-43. Many studies link defects in axonal mRNA translocation to neurodegenerative disease like ALS(Jung et al., 2012). TDP-43 increases the number of stress granules, which reversibly sequester mRNAs and repress their translation (Volkening et al., 2009). Sustained translation of axonal mRNAs is required for axon maintenance; thereby increased/decreased axonal mRNA translation caused by these mutations might contribute to axon degeneration in ALS.

Cytoskeletal components such as actin, neurofilaments and microtubules play a key role in RNA localization, especially during transport of mRNAs and anchoring at target sites. Active transport of mRNAs along cytoskeletal filaments has been implicated as the major localisation mechanism in most cells (de Heredia and Jansen, 2004). TDP-43 binds nearly one third of all genes (Tollervey et al., 2011a), many of which play critical roles in neuronal development, including components of the cytoskeleton and aberrant RNA metabolism of these genes could be a direct cause of ALS/FTLD. Studies have suggested that impairment in the post transcriptional regulation of mRNAs in the cytoplasm of motor neurons could play a major part in the pathogenesis of ALS (Fallini

et al., 2012). Thus, we propose that aberrant processing or trafficking of cytoskeletal RNAs which are normally bound to TDP-43 cause neuronal death.

There are many hypotheses that suggest that TDP-43 brings about neuronal death by dysregulation of cytoskeletal components (Wang et al., 2008). Studies have reported that TDP-43 plays an important role in regulation of axon growth (Fallini et al., 2012, Fiesel and Kahle, 2011). We have previously shown that TDP-43 regulates axon outgrowth and the integrity of the cytoskeleton, and that dysfunction of TDP-43 contributes to the pathology of ALS (Tripathi et al., 2014). TDP-43 isolated from a cytoplasmic fraction of the human brain revealed that it binds to the 3'UTR of several mRNA targets thereby suggesting that it plays an important role in mRNA stability and transport (Tollervey et al., 2011). For example, TDP-43 directly interacts with the 3'UTR of neurofilament light chain (68 kDa) mRNA and stabilizes it, preventing its degradation (Strong et al., 2007). TDP-43 associates with *futsch* mRNA in a complex *in vivo* and regulates its localization and translation in *Drosophila* motor neurons (Coyne et al., 2014). TDP-43 also plays an important role in axonal transport. TDP-43 itself is actively transported between the nucleus and the cytoplasm (Fallini et al., 2012) and as a part of the hnRNP complex it facilitates the transport of other molecules along the axons. TDP-43 plays an important role in the anterograde axonal transport of target mRNA from the soma to the distal axons and mutations in TDP-43 disrupt this transport function, contributing to ALS toxicity (Alami et al., 2014). Polymenidou et al., 2011 showed that levels of 601 mRNAs and splicing patterns of 965 mRNAs were altered following TDP-43 reduction in the adult nervous system. Other studies have shown that induced knockdown of TDP-43 in mouse embryonic stem cells (ESCs), results in reduced mRNA levels for proteins involved in processes such as RNA metabolism, cell signaling, cell cycle regulation, axon guidance, and long-term potentiation (Chiang et al., 2010).

Thus, taking into account all of these previous studies and our findings, we propose that TDP-43 affects the subcellular localisation of a key range of cytoskeletal mRNA species, whose mis-localization can cause defective cytoskeletal dynamics, synaptogenesis/synapse maintenance and neuronal death.

In this chapter the hypothesis that TDP-43 overexpression leads to the misregulation of mRNAs encoding regulators of the cytoskeleton and their protein products was investigated. The effects of TDP-43 overexpression on axonal growth, cytoskeletal integrity, axonal transport and subcellular localization of putative target mRNAs in primary rat cortical neurons were analysed. Neuronal cultures, immunohistochemistry, live imaging and *in situ* hybridisation were the methods employed to investigate the effects of TDP-43.

Data from previous studies showed that TDP-43 binds to/regulates the cytoskeletal targets ACTB (Sephton et al., 2011) MAP1B (Coyne et al., 2014), NFL (Strong et al., 2007). UV-CLIP studies have also shown that TDP-43 associates with other kinesin and microtubule associated families of proteins such as KIF7 and Mapt (Sephton et al., 2011). FUS targets mRNAs such as β-actin and Nd1-L (Da Cruz, 2011). TDP-43 and FUS share many common pathophysiological characteristics and have common downstream RNA targets (Honda, 2013). Since β-actin and ND1-L play important roles in cytoskeletal function, we have selected these targets to see if TDP-43 disrupts their mRNA distribution thereby sharing common pathophysiological RNA metabolism cascades with FUS. Probes for these targets were used to determine the effects of TDP-43 on cytoskeletal components. Also these markers target the different neuronal compartments like growth cones, axons and dendrites. TDP-43 plasmids used for transfection were those used in chapter 1, i.e. EGFP-WT TDP-43, EGFP TDP-43 M337V, EGFP TDP-43 Q331K and EGFP control.

4.2 Results

4.2.1 TDP-43 affects axonal growth *in vitro*

We have previously shown that over-expression of TDP-43 wild-type and mutant isoforms impair axonal growth in chick spinal motor neurons *in vitro* and *in vivo* (Tripathi et al., 2014). In order to characterize the effects of TDP-43 on axon outgrowth using an *in vitro* cortical model, I recapitulated experiments using rat cortical neurons. The cells were fixed at 3 different time points post transfection and were stained with anti-GFP antibodies. The cells were then imaged using a fluorescent microscope and

the length of 100 healthy neurons per transfection per experiment (n =3) were measured using neuron J. The criteria for analysing axonal length were that healthy neurons that did not display any sign of blebbing or distress due to transfection or fixation and that which contained a full, uninterrupted axon that was at least thrice the length of the cell body.

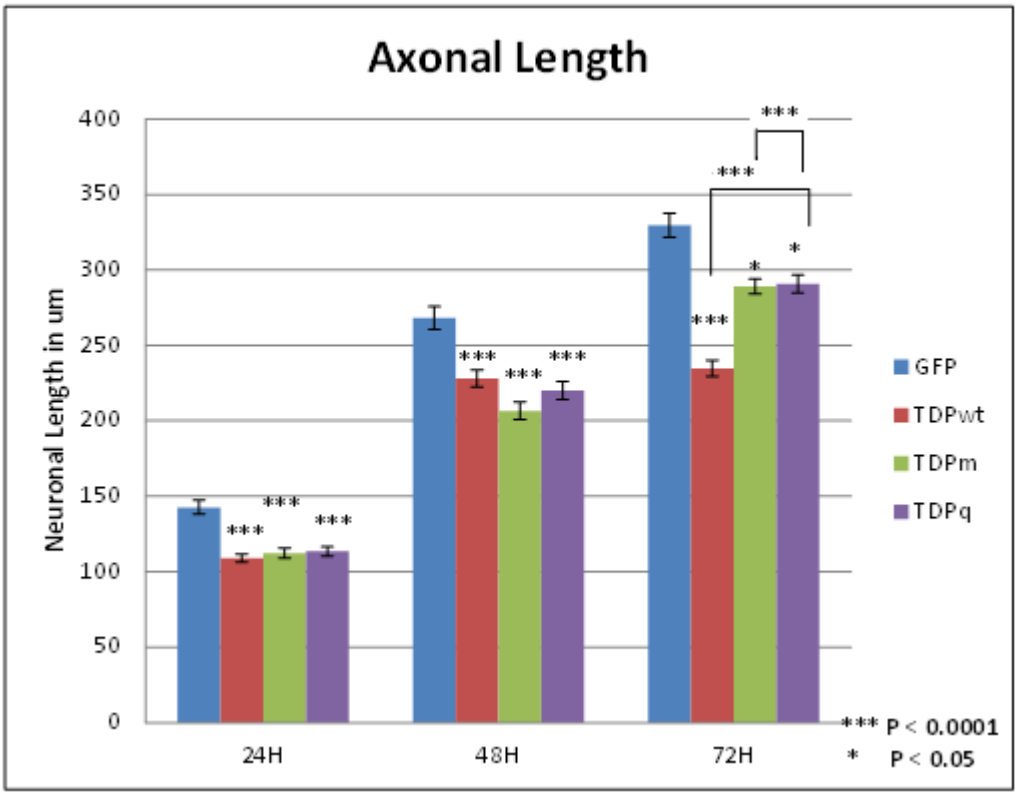

Figure 4.1 Tagged TDP-43 affects axonal growth *in vitro*
Rat cortical cells were transfected with GFP control plasmid and GFP tagged TDP-43 wild-type and mutant plasmids. Quantification of axonal length using Neuron J indicates a reduction in neurite length with TDP-43 over-expression compared to the EGFP control at three different time-points (n=3; 100 neurons per experiment). Healthy neurons with defined axons were analysed. Data is presented as means and standard errors. Significance were compared by ANOVA (No significance: p > 0.05; *** P < 0.0001; * P < 0.05). The asterisks above the bars are in comparison with the control EGFP.

Quantification suggested that control EGFP transfected neurons had the longest lengths at all the time points whereas TDP-43 transfected neurons (wild-type and mutants) show a reduction in neuronal length compared to the eGFP transfected controls (Fig 4.1). At 24 hours and 48 hours post transfection, a significant reduction in the length of neurites for all the three TDP-43 plasmid constructs (Fig 4.1: ***P< 0.0001 for WT TDP-43, TDP- 43 M337V and TDP- 43 Q331K vs. EGFP) was observed with no significant difference (P > 0.05) between wild-type and mutant isoforms.

However, at 72 hours post transfection, there was a drastic difference in neurite length between the wild-type (WT TDP-43) and the mutant isoforms: TDP-43 M337V and TDP-43 Q331K (Fig 4.1 - ***P < 0.0001 for both TDP-43 M and TDP-43 Q vs. the WT TDP-43. At 72 hours, the neurite length for the mutant isoforms: TDP -43 M337V and TDP-43 Q331K was reduced, but only by a small yet significant difference (Fig 4.1: P < 0.05 for TDP-43 mutants vs EGFP) relative to EGFP control. However, in contrast to the earlier time points, the TDP-43 wild-type plasmid shows a drastic reduction in neurite length compared to EGFP (Fig 4.1: P < 0.0001 for WT TDP-43 vs. EGFP). Thus, it seems that though all the three TDP-43 constructs affect axonal growth, over-expression of the wild-type TDP-43 seems to have a more drastic effect at a later time point. Thus, the rat cortical neurons have the same selective vulnerability to TDP-43 as the spinal motor neurons. This data suggest that the expression of TDP-43 wild-type and mutant isoforms impairs axon outgrowth *in vitro*

4.2.2 TDP-43 transfected neurons have smaller growth cones

While live imaging rat cortical neurons transfected with TDP-43 wild-type and mutant isoforms, a stalling phenotype for the TDP-43 transfected neurons was observed that was absent in the control EGFP transfections (data not shown). This prompted us to assay growth cone dynamics in neurons transfected with TDP-43 constructs.

Rat cortical neurons were transfected with the EGFP and TDP-43 plasmids as before and fixed at different time points (24 hours, 48 hours and 72 hours) in culture. The transfected neurons were immunostained with antibodies to GFP in order to identify the transfected neurons and tyrosinated tubulin antibody was used to label the growth cones. At the onset of axonal outgrowth the tyrosinated tubulin antibody labels the minor neurites, the axon, and its growth cone.

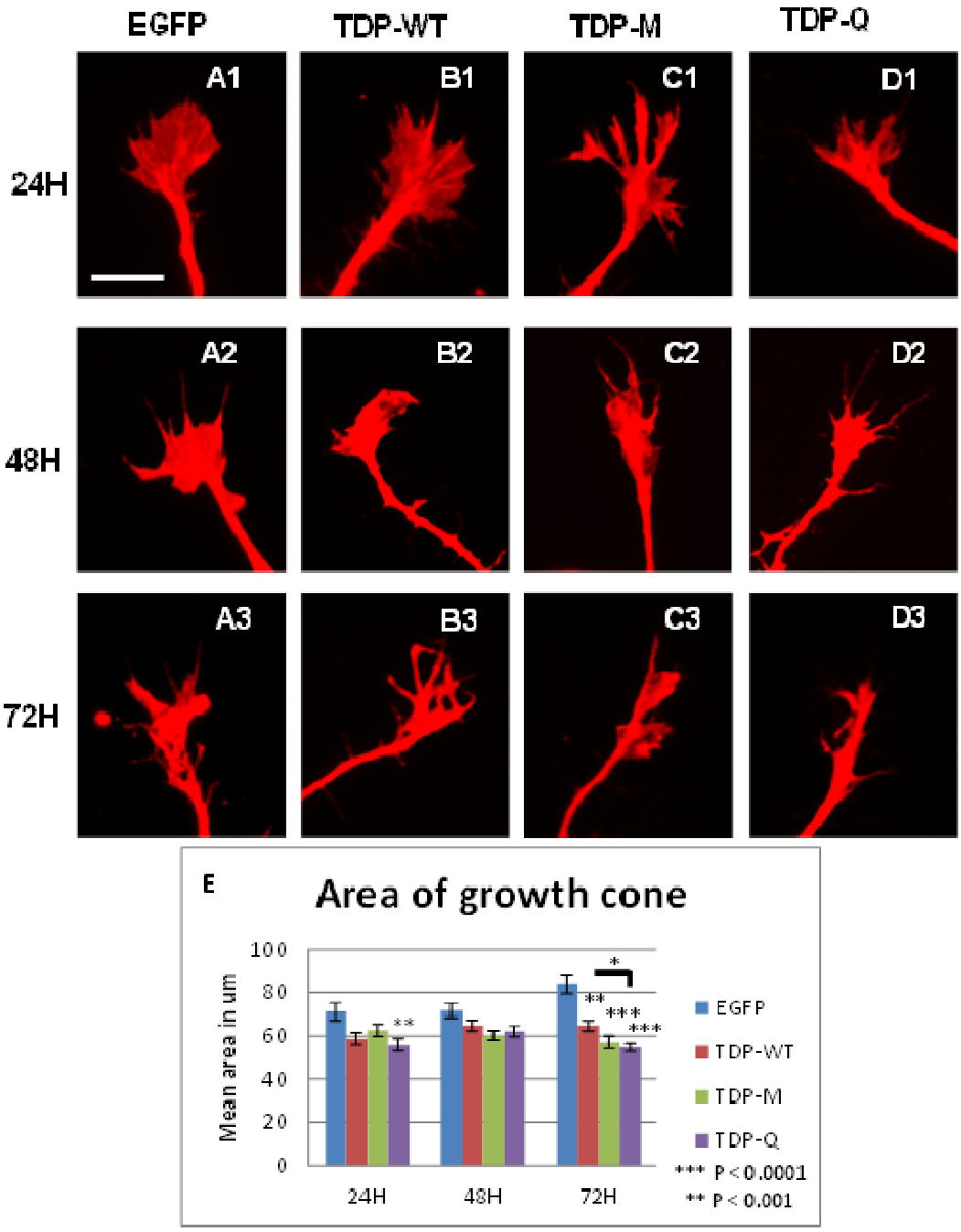

Figure 4.2 Tagged TDP-43 transfected neurons have smaller growth cones

Rat cortical cells were transfected with EGFP control plasmid and GFP tagged TDP-43 wild-type and mutant plasmids and fixed at different time points. Transfected neurons were immunostained with Tyrosinated tubulin (red) and the area of the growth cones were measured using Image J. Panels A-D represent the growth cones at the different time points for the different constructs. Panel E represents the mean area of tyrosinated tubulin from 70 neurons per construct per experiment, at 3 different time points (24H, 48H and 72H) post transfection (n=3). Data is presented as means and standard errors. Significance were compared by ANOVA (No significance: $p > 0.05$; *** $P < 0.0001$; ** $P < 0.001$). The asterisks above the bars are in comparison with the control EGFP.

At 24 hours and 48 hours, EGFP control neurons have a characteristic 'palm' appearance with many filapodia extensions displayed in a radial pattern whereas at 72 hours, the 'palm' appearance while still evident is slightly narrowed (Fig 4.2: A1-A3). WT TDP-43 has widespread 'palm' morphology at 24 hours similar to the EGFP control. However, after 48 hours, the 'palm' shape thins out and becomes narrower over time (72 hours) with longer filopodia (Fig 4.2: B1-B3). TDP-43 M337V has narrow growth cone morphology with longer filopodia at 24 hours that becomes progressively thinner at 48 hours and is almost lost at 72 hours. The filopodia look retracted at the later time points giving a collapsed appearance (club shaped with few filopodia) to the growth cone (Fig 4.2: C1-C3). TDP-43 Q331K transfected neurons have narrow palm shaped growth cones with many short fiopodia at 24 hours and while they mostly retain the narrow palm morphology at 48 hours, the growth cones have very few filopodia. At 72 hours, they lose the palm domain and the filopodia has a drawn in-retracted pattern (Fig 4.2: D1-D3). The growth cone area for 70 neurons per construct from 3 independent experiments were measured using image J and analysed (Fig 4.2: E) using a one-way Anova to calculate the significant differences. Quantification suggested that TDP-43 transfected neurons have smaller growth cones than the control neurons. However, this reduction was not significant at all-time points ($P > 0.05$). TDP-43 M337V (***$P<0.0001$) and WT TDP-43 (**$P<0.001$) had significantly smaller growth cones compared to EGFP control at 72 hours but not for the other time points. Growth cones of TDP- 43 Q331K transfected neurons were significantly smaller compared to the EGFP controls at 24 hours (**$P<0.001$) and 48h (***$P<0.0001$) and also significantly smaller compared to the TDP-WT neurons at 72 hours (*$P<0.05$). There was no significant difference compared to TDP-43 M337V ($p > 0.05$) at any of the time points. Thus, TDP- 43 Q331K mutant transfected neurons had the smallest growth cones compared to the other constructs.

4.2.3 TDP-43 affects anterograde transport

The data obtained so far converges on the possibility that TDP-43 associates either directly or indirectly with proteins that affect different aspects such as cytoskeletal integrity, axonal outgrowth, and growth cone dynamics. Several studies have proposed

that TDP-43 is a highly mobile protein (Fallini et al., 2012) and can form mRNP complexes with its target mRNA/proteins and facilitates their transport bi-directionally along the axons in a microtubule dependent manner (Alami et al., 2014). Since TDP-43 affects growth cone dynamics, suggesting an underlying effect of TDP-43 on microtubule stability, we were intrigued to see if TDP-43 also affects anterograde transport of microtubule plus tip proteins.

EB3 is a microtubule associated protein that binds to the plus end of microtubules and regulates and promotes microtubule dynamics and growth (Straube and Merdes, 2007). Rat cortical neurons were co-transfected with GFP tagged TDP-43 constructs and EB3-RFP and live imaged after 48 hours and 72 hours in culture. EB3 proteins, termed 'comets' move rapidly in an anterograde manner to the growing tips of axons (Fig 15: F). Kymographs were drawn for 10 neurons per construct per experiment (n=3) using Image J. A kymograph is a graphical representation of spatial position over time with time along the X-axis and distance along the Y-axis.

A visual difference can be seen in the number of EB3 plus end tracking proteins (+ TIPS) between EGFP control and the TDP-43 neurons at both the time points. The TDP-43 plasmids have a lesser number of +TIPs when compared to the control at 48 hours and 72 hours. The number of +TIPS reduces even more at 72 hours compared to the 48 hours for the TDP-43 transfected neurons (Fig 4.3: A1-D2) The kymographs of the TDP-43 transfected cells show lots of blank spaces that relates to the loss of the EB3s. Thus, at a later time point, the number of EB3s in the TDP-43 transfected neurons are more stationary (indicated by the vertical lines in the kymograph background) or reduced in number.

The velocity of the EB3 +TIPS for the different transfected cells, at different time points were automatically quantified using the Kymoquant plugin of Image J. The graph was drawn based on the average velocity and standard error of the mean. The TDP-43 transfected neurons have a lower EB3 velocity when compared to the EGFP control at both 48 hours and 72 hours. The EB3 velocities of the wid-type and mutant TDP-43 constructs decrease at 72 hours from their velocities at 48 hours. Though the velocities differ between the constructs and the control, there was no significance in this difference at either time points when calculated using a one-way Anova or a Mann

Whitney test. Higher ‘n’ numbers need to be quantified to observe a significant trend (Fig 4.3 E).

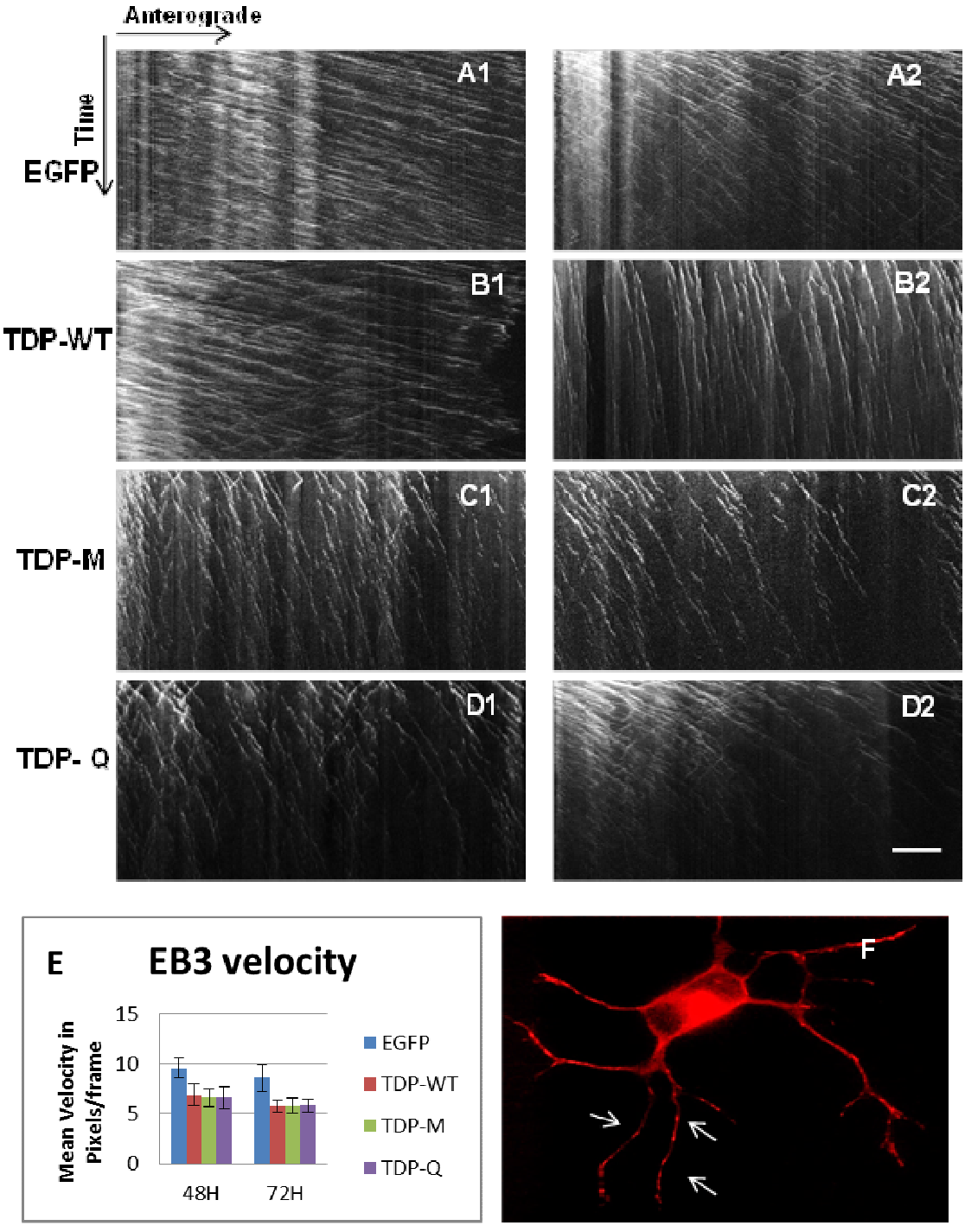

Figure 4.3 Tagged TDP-43 affects anterograde transport
Rat cortical cells were co-transfected with EB3-RFP and EGFP control and GFP tagged TDP-43 wild-type and mutant plasmids and live imaged for 10 mins with 5 sec intervals at 48H and 72H. EB3s move in an anterograde manner towards the growing ends of axon. Control neuron transfected with EB3-RFP at 48H (F). Kymographs of co-transfected neurons at 48 and 72H .Time along the X-axis and distance along the Y-axis (A1 –D2). Scale bar = 10 µm. Quantification of velocity of EB3-RFP comets in the axons of co-transfected neurons (E). Graphs represent means and standard error of *n* = 3. No significant difference was observed.

Thus, TDP-43 transfected neurons have reduced numbers of EB3s with reduced velocities when compared to the control EGFP transfected neurons. This indicates that TDP-43 can directly or indirectly impair axonal transport.

4.2.4 TDP-43 affects subcellular mislocalisation of its target mRNA

TDP-43 plays an important role in regulating RNA metabolism at multiple levels such as transcription, splicing, transport and stability. Studies have shown that TDP-43 impairs axonal transport (defective trafficking) of its target mRNA (Alami et al., 2014) and can bind to the 3' UTR of its target mRNA (Buratti et al., 2001). Our data so far suggests that the cytoskeleton is a target of TDP-43 dysfunction. *In situ* hybridization was carried out so as to study the expression and intracellular distribution of the putative cytoskeletal mRNA targets of TDP-43.

Actins are highly conserved proteins that are involved in cell motility, structure, and integrity. Kif2A is a plus end-directed motor required for normal mitotic progression. Plus end-directed microtubule-dependent motor required for normal brain development and may regulate microtubule dynamics during axonal growth. Map1B and Map2 belong to the microtubule-associated protein family. The proteins of this family are thought to be involved in microtubule assembly, which is an essential step in neurogenesis. Phosphorylated MAP1B may play a role in the cytoskeletal changes that accompany neurite extension. They might also be involved in nucleating microtubule polymerization and in stabilizing microtubules. The exact function of MAP2 is unknown but MAPs may stabilize the microtubules against depolymerization. Nd1-L acts as an actin cytoskeleton stabilizer. Neurofilaments comprise the axoskeleton and they functionally maintain the neuronal caliber. They may also play a role in intracellular transport to axons and dendrites.

The TDP-43 and control neurons were treated with DIG labelled sense and antisense probes for FoxG1, β-actin, Kif2A, Map1B, Map2, ND1-L and NFL. The sense probes had no expression and the anti-sense probes for the various mRNA were differentially expressed in terms of region and levels.

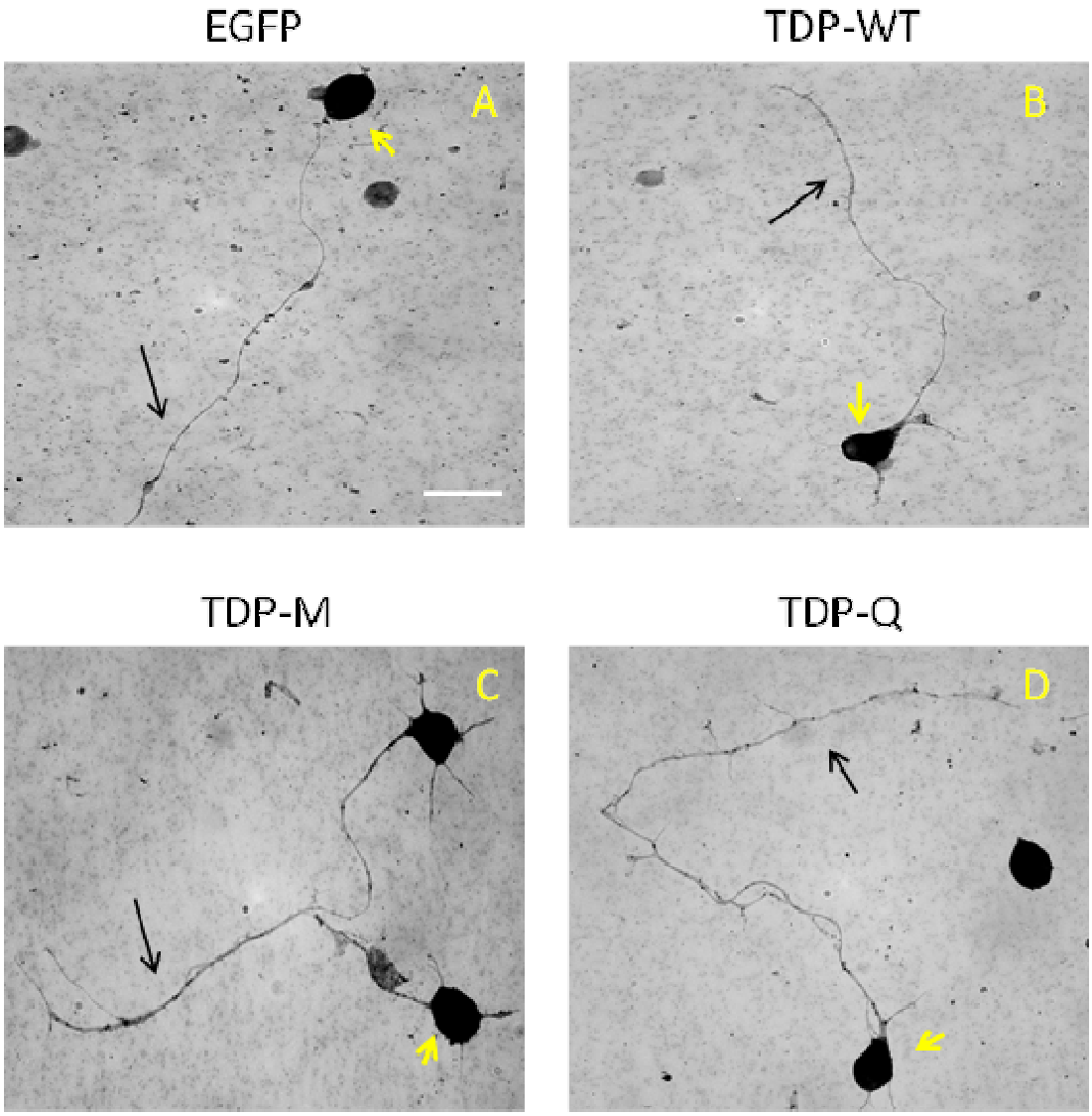

Figure 4.4 *FoxG1* control mRNA is evenly expressed
Rat cortical neurons were transfected with TDP-43 wild-type and mutant plasmids and fixed after 72H in culture. *In situ* hybridisation was performed using the DIG-labelled *FoxG1* anti-sense probe and the neurons were imaged using DIC filter. Control EGFP and TDP-43 transfected neurons expressed the probe through-out the neuron. Yellow arrows indicate the cell-body and the black arrows point out the axons. Scale Bar = 10 µm.

FoxG1, a transcription factor expressed in all cortical cells was used as a control probe and was expressed equally through-out the neurons in all the transfected cells, both control and TDP-43 neurons (Fig 4.4).

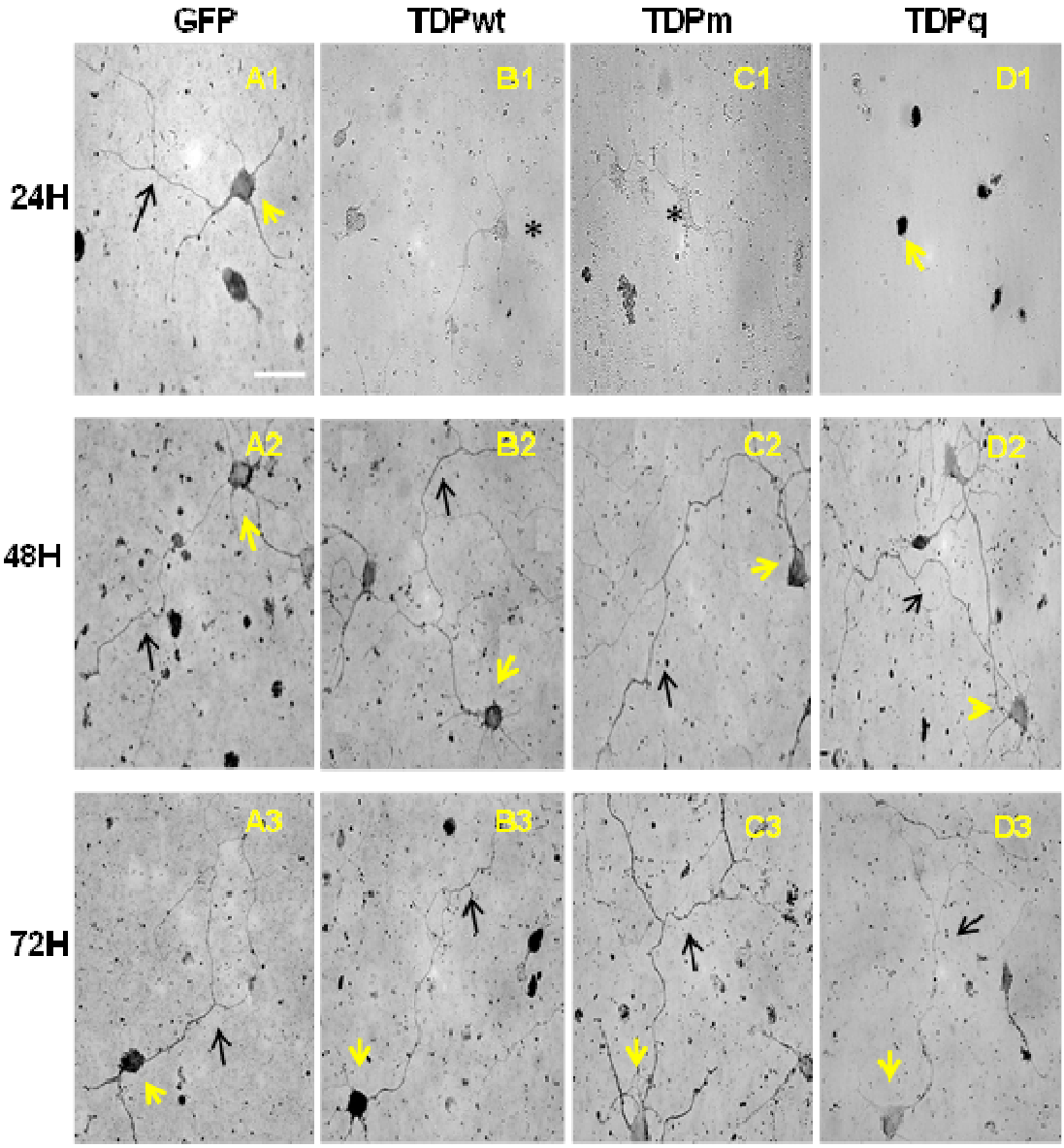

Figure 4.5 TDP-43 affects subcellular mislocalisation of *β-actin*
Rat cortical neurons were transfected with TDP-43 wild-type and mutant plasmids and fixed at different time-points (24H, 48H,72H). *In situ* hybridisation was performed using the DIG-labelled *β-actin* anti-sense probe and the neurons were imaged using DIC filter. Expression pattern of *β-actin* varies between the different constructs and the different time-points. Yellow arrows indicate the cell-body and the black arrows point out the axons Scale Bar = 10 µm.

β-actin is evenly expressed along the entire neurons in the EGFP control at all the time points. At 72 hours, there is an increased expression of β-actin in the cell body. The WT-TDP-43 and TDP-43 M337V have similar expression patterns wherein at 24 hours; there is no expression of β-actin followed by an even expression throughout the neuron at 48 hours and 72 hours. There is a slight increase of β-actin mRNA expression in the cell body of the WT TDP-43 transfected at 72 hours similar to EGFP control. In

TDP-43 Q331K transfected cells, there is an increased nuclear expression at 24 hours with no expression in the axons, followed by an even expression throughout the neuron at 48 hours which progressively becomes fainter at 72 hours (Fig 4.5).

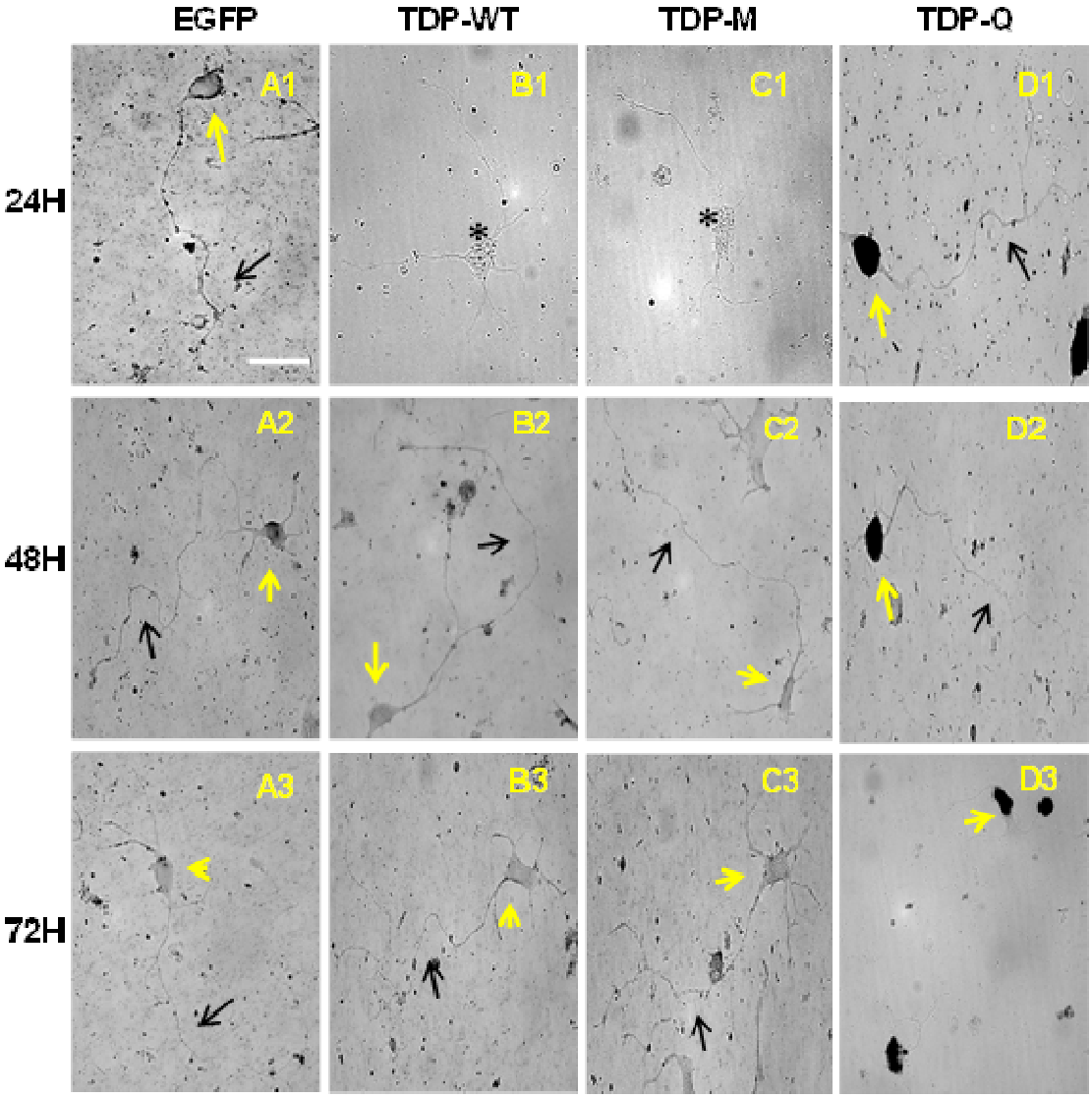

Figure 4.6 TDP-43 affects subcellular mislocalisation of *Kif2A*
Rat cortical neurons were transfected with TDP-43 wild-type and mutant plasmids and fixed at different time-points (24H, 48H,72H). *In situ* hybridisation was performed using the DIG-labelled *Kif2A* anti-sense probe and the neurons were imaged using DIC filter. Expression pattern of *Kif2A* varies between the different constructs and the different time-points. Yellow arrows indicate the cell-body and the black arrows point out the axons Scale Bar = 10 µm.

Kif2A is evenly expressed along the entire neuron in the EGFP control at all the time points. The WT-TDP-43 and TDP-43 M337V have similar expression patterns wherein at 24 hours; there is no expression of Kif2A followed by an even expression throughout the neuron at 48 hours and 72 hours. In TDP-43 Q331K transfected cells, the

expression is seen throughout the neuron with increased nuclear expression at 24 hours. The mRNA expression in the axons becomes faint at 48 hours and completely fades away at 72 hours. Increased nuclear expression is seen throughout the time-points (Fig 4.6).

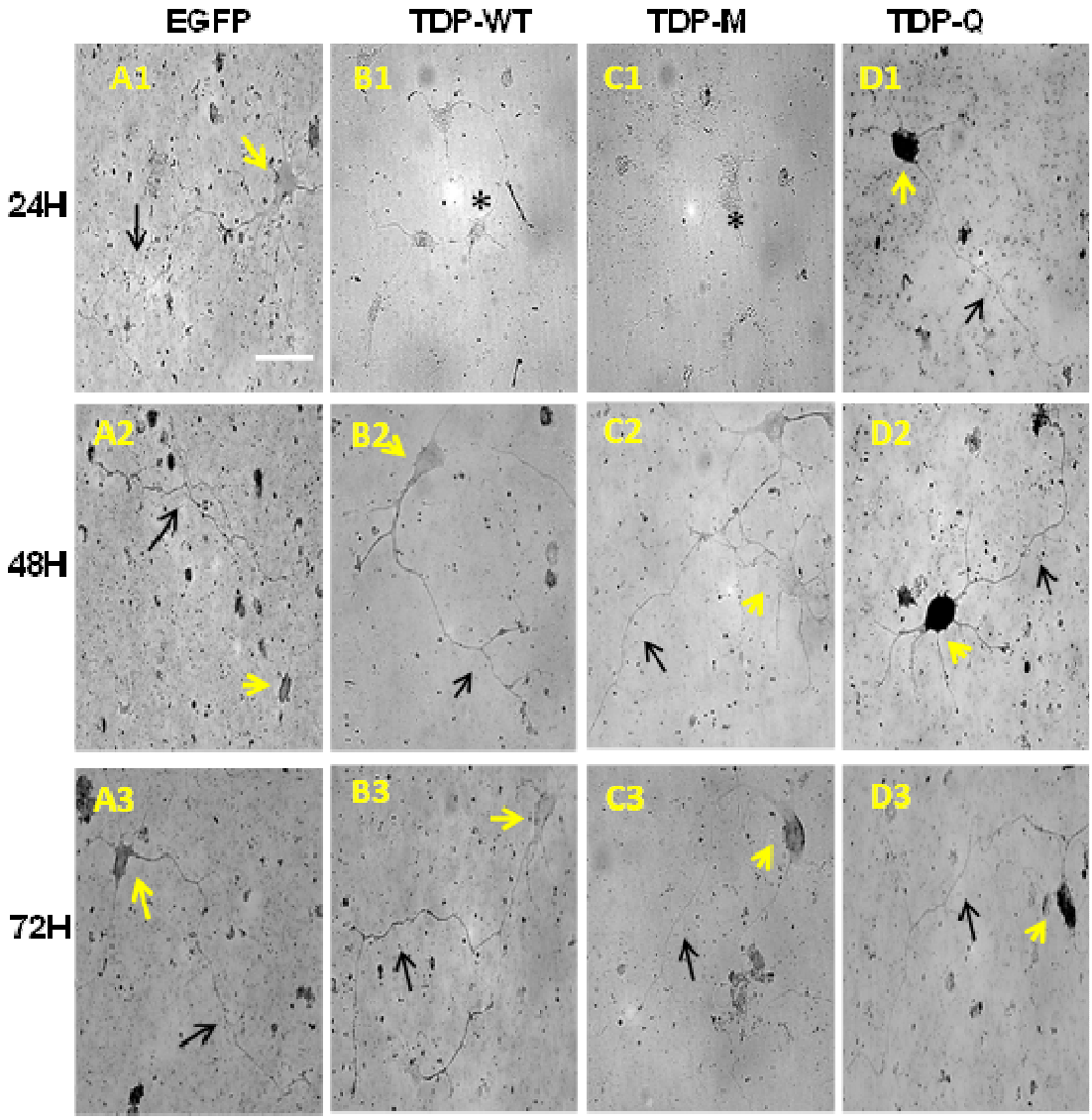

Figure 4.7 TDP-43 affects subcellular mislocalisation of *Map1B*
Rat cortical neurons were transfected with TDP-43 wild-type and mutant plasmids and fixed at different time-points (24H, 48H, 72H). *In situ* hybridisation was performed using the DIG-labelled *Map1B* anti-sense probe and the neurons were imaged using DIC filter. Expression pattern of *Map1B* varies between the different constructs and the different time-points. Yellow arrows indicate the cell-body and the black arrows point out the axons Scale Bar = 10 µm.

Map1B is evenly expressed along the entire neuron in the EGFP control at all the time points. The WT-TDP-43 and TDP-43 M337V have similar expression patterns at 24 hours and 48 hours, wherein there is no expression of Map1B followed by an even

expression throughout the neuron at 48 hours. At 72 hours, WT-TDP-43 has the same expression pattern seen at 48 hours whereas for the TDP-43 M337V, the expression is faint along the axon with a faint increase in nuclear expression. In TDP-43 Q331K transfected cells, the expression is seen throughout the neuron with increased expression in the cell-body throughout the time-points (Fig 4.7).

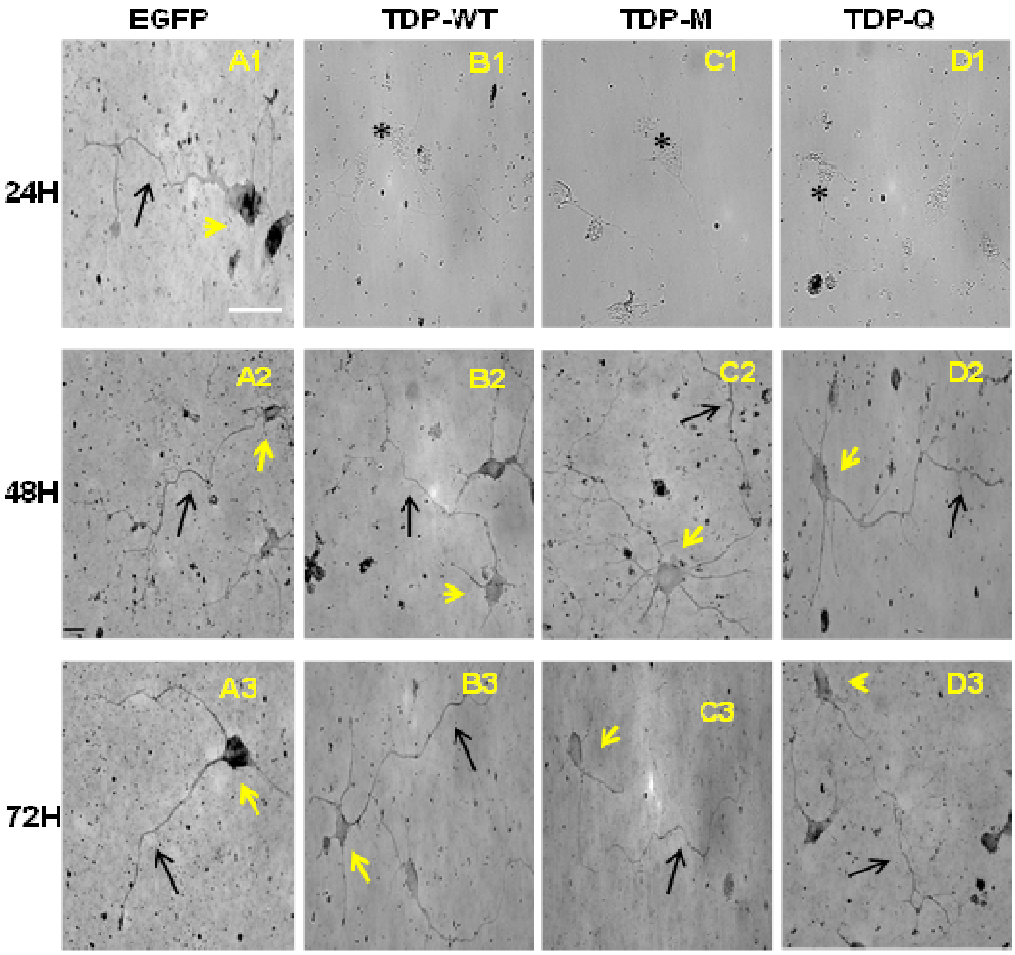

Figure 4.8 TDP-43 affects subcellular mislocalisation of *Map2*
Rat cortical neurons were transfected with TDP-43 wild-type and mutant plasmids and fixed at different time-points (24H, 48H, 72H). *In situ* hybridisation was performed using the DIG-labelled *Map2* anti-sense probe and the neurons were imaged using DIC filter. Expression pattern of *Map2* varies between the different constructs and the different time-points. Yellow arrows indicate the cell-body and the black arrows point out the axons Scale Bar = 10 µm.

Map2 is expressed along the entire neuron with an increased nuclear expression in the EGFP control at all the time points. The WT-TDP-43, TDP-43 M337V and TDP-43 Q331K have similar expression patterns wherein at 24 hours; there is no expression of Map2 followed by an even expression throughout the neuron at 48 hours and 72 hours (Fig 4.8).

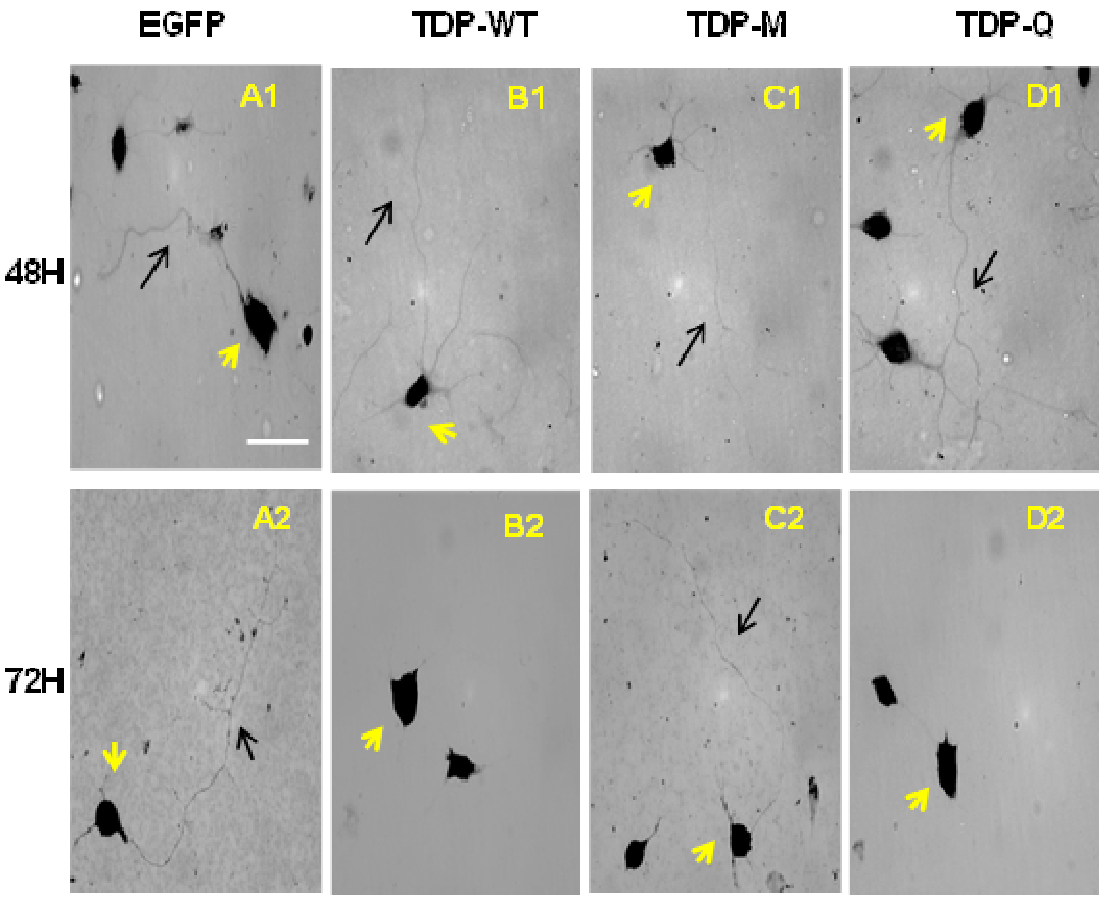

Figure 4.9 TDP-43 affects subcellular mislocalisation of *Nd1-L*
Rat cortical neurons were transfected with TDP-43 wild-type and mutant plasmids and fixed at different time-points (48H, 72H). *In situ* hybridisation was performed using the DIG-labelled *Nd1-L* anti-sense probe and the neurons were imaged using DIC filter. Expression pattern of *Nd1-L* varies between the different constructs and the different time-points. Yellow arrows indicate the cell-body and the black arrows point out the axons Scale Bar = 10 µm.

ND1-L is expressed along the entire neuron with an increased expression in the cell body in EGFP controls at all the time points. The WT-TDP-43 and TDP-43 Q331K have similar levels of expression wherein at 48 hours; the expression is seen throughout the neuron with increased cell body expression. The expression along the axons fades away at 72 hours leaving an increased expression in the cell-body. For TDP-43 M337V, the expression is faint along the axons with increased cell body expression at both the time points (Fig 4.9).

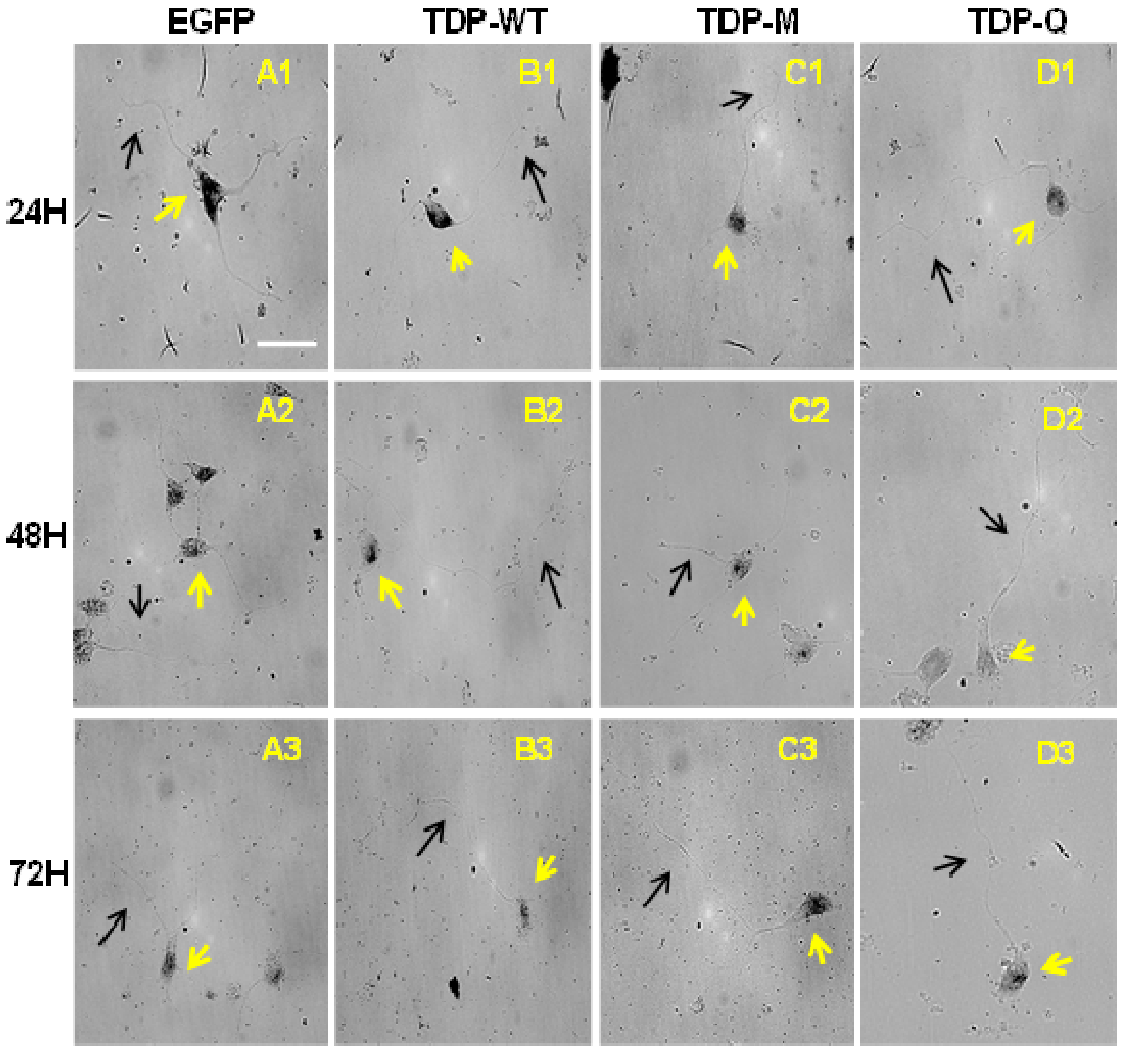

Figure 4.10 TDP-43 affects subcellular mislocalisation of *NFL*
Rat cortical neurons were transfected with TDP-43 wild-type and mutant plasmids and fixed at different time-points (24H, 48H, 72H). *In situ* hybridisation was performed using the DIG-labelled *NFL* anti-sense probe and the neurons were imaged using DIC filter. Expression pattern of *NFL* varies between the different constructs and the different time-points. Yellow arrows indicate the cell-body and the black arrows point out the axons Scale Bar = 10 µm.

NFL is expressed along the entire neuron with an increased expression in the cell body in EGFP transfected neuron at 24 hours. At 48 hours and 72 hours, the expression fades along the nucleus and cell body with a slightly increased nuclear expression. The WT-TDP-43 transfected neurons show an increased cell body expression with a faint expression along the axons at 24 hours. At 48 hours and 72 hours, the expression fades away in the axons with a slight expression in the nucleus. The expression pattern for all the time points is the same for TDP-43 M337V neurons, wherein a faint expression is seen along the axons with a slight increase in nuclear expression. TDP-43 Q331K has a faint expression along the neurons at 24 hours which is very faint at 48 hours. At 72

hours, the expression along the axons remains faint with a slight increase in nuclear expression (Fig 4.10).

Thus, TDP-43 affects the subcellular localisation of its target mRNA compared to EGFP control mRNA expression. The WT- TDP-43 and TDP-43 M337V follow similar patterns of expression wherein mostly there is a delay in expression of their target mRNA (no expression at 24 hours) followed by expression throughout the neuron in most cases (expression seen throughout the neuron at 48 hours) that is either maintained at a later time point or fades away in the axons with increased nuclear expression (72 hours). TDP-43 Q331K mostly has an over-expression in the cell-body with faint or no expression along the axons at later time-points. Thus, the subcellular mRNA mislocalisation is characterized by i) delay in expression ii) over-expression in the cell-body or iii) loss of nuclear expression'.

In summary, our results have shown several phenotypes for cytoskeletal dysregulation by TDP-43. Axonal outgrowth, growth cone dynamics, anterograde transport and subcellular localisation are all affected indicating that TDP-43 may play multiple roles in the regulation of cytoskeletal. All of these phenotypes indicate that the underlying functional mechanisms may be related to regulation of various mRNAs involved in several aspects of cytoskeletal function whose transport, stability and splicing may be regulated by TDP-43. Thus cytoskeletal dysfunction could be an important process leading to neurodegeneration.

4.3 Discussions

Our previous studies have shown that the cytoskeleton is a target of TDP-43 dysfunction (Tripathi et al., 2014). Taking into account our previous findings and other research publications, rat cortical neurons were used to investigate the effects of TDP-43 on several axonal functions like growth, transport and mRNA localisation.

The findings from this chapter showed that TDP-43 wild-type and mutant proteins have shorter neurite lengths implying that axon growth is impaired. TDP-43 wild-type and mutant proteins have smaller growth cones and exhibit a stalling phenotype

suggesting that growth cone dynamics are altered either directly or indirectly by TDP-43. TDP-43 wild-type and mutants affect anterograde transport of EB3s signifying the role of TDP-43 in axonal transport. TDP-43 wild-type and mutant proteins mis-localise subcellular cytoskeletal mRNA targets implying that mis-regulation of its target RNA binding partners could play an important role in TDP-43 mediated neurodegeneration.

4.3.1 TDP-43 affects axonal growth *in vitro*

Axon outgrowth and the continuous regulation of axon growth are key steps during axon guidance and regeneration. TDP-43 has been implicated as the local regulator of axon growth suggesting that translation regulation in the axons during this process may be broadly crucial for the health and survival of motor neurons. Several studies suggest that TDP-43 affects axonal outgrowth (Kabashi et al., 2010). However, the results of these findings are divided in that some suggest that TDP-43 wild-type significantly reduces neurite length compared to the mutants (Fallini et al., 2012) while others suggest that the TDP-43 mutants have a greater reduction effect (Kabashi et al.,2010). These studies show that both over-expression and deletion of TDP-43 resulted in locomotive defects caused by short motor neuron axons that have premature and excessive branching (Hornberg and Holt, 2013). Studies have shown that TDP-43 acts a negative regulator of axon growth since over-expression of WT-TDP-43 decreases neurite length and branching whereas knock-down of TDP-43 caused a slight increase in axonal length (Fallini et al., 2012). However, other studies in zebrafish embryos and mouse neuroblastoma cells show that depletion of TDP-43 impairs axonal length (Kabashi et al., 2010, Hornberg and Holt, 2013). Motor dysfunction in *Drosophila* caused by the deletion of the TBPH (TDP-43 ortholog), could only be rescued by introduction of the WT TDP-43 while the TDP-43 mutants expressed at the same levels showed no effects suggesting the importance of the wild-type construct in a loss of function role (Alami et al., 2014). This implies that TDP-43 plays an important role in regulating mRNAs involved in axonal fate and may play different roles in different neuronal population and species. Thus, the expression levels of TDP-43 plays an important role in the regulation of axon outgrowth. Any alteration/perturbations of

the protein levels could result in impairment of axonal growth eventually leading to neurodegeneration.

According to our analysis, TDP-43 transfected neurons show a significant reduction in neurite length compared to EGFP control neurons. At 24 hours and 48 hours there was no significant difference between the wild-type and mutant constructs but at 72 hours, TDP- 43 wild-type transfected neurons were significantly shorter in length compared to the TDP-43 mutant neurons. This data is consistent with previous findings wherein over-expression of the full length TDP-43 wild-type caused a significant reduction in axon outgrowth in primary motor neurons when compared to the mutants TDP – M337V and TDP-Q382T (Fallini et al., 2012). Our results also complement our previous findings wherein TDP-43 causes premature truncation and de-fasciculation of axons *in vivo* and reduces neurite outgrowth in chick spinal motor neurons *in vitro*. Axonal outgrowth defects are phenotypic as they are not the sole cause of neurodegeneration. Thus, it is suggestive that bigger defective mechanism (mis-processing of RNA, axonal maintenance, plasticity, and defective NMJs) may underlie such phenotypes that might lead to neurodegeneration. Thus, we show that over-expression of TDP-43 wild-type and mutant proteins affects axonal outgrowth and cortical neurons have the same vulnerability as motor neurons and are sensitive to the alteration of TDP-43 protein levels.

4.3.2 TDP-43 induces axonal stalling and the transfected neurons have smaller growth cones

Time lapse movies of cortical neurons transfected with TDP-43 wild-type and mutant constructs show a stalling phenotype of growth cones characterized by retracting filopodia with no forward movement at 72 hours post transfection compared to the EGFP controls which showed active growth cone dynamics with forward movement (Data not shown). We have previously shown that over-expression of TDP-43 wild-type and mutant isoforms cause premature truncation and debundling/de-fasciculation of axons *in vivo* in chick spinal cord in the periphery. This stalling of the growth cones fits in with our current and previous results wherein we observe that TDP-43 affects axonal outgrowth. Changes in growth cone morphology, motility, and direction of

growth depend on changes in the organization of the actin and microtubule cytoskeleton (Dent et al., 2011). Thus, we stained the growth cones of TDP-43 transfected neurons with antibodies to tyrosinated tubulin and measured their area. Our results suggested that the TDP-43 transfected neurons have smaller growth cones when compared to EGFP control. Studies have also shown that knock down of TDP-43 in SH-SY5Y cells produced abnormal growth cone structures (Fiesel et al., 2011).

Growth cone dynamics are complex and are mediated by intracellular signalling pathways that link guidance cues/receptors to the cytoskeleton. Studies of vertebrate and invertebrate growth cones suggest that common mechanisms regulate growth cone behaviour and axon branching and that these mechanisms play an important role during response to axonal injury (Dent et al., 2003). We know that TDP-43 regulates axonal branching and axonal outgrowth (Kabashi et al., 2010, Fallini et al., 2012, Tripathi et al., 2014). TDP-43 also plays an important role in mediating the response of the neuronal cytoskeleton to neuronal injury (Swarup et al., 2012). Proteomic studies on growth cones revealed that about 1% of all growth cone proteins are putative RNA RBPs. The single largest group of RBPs, were the heterogenous nuclear ribonucleoprotein (hnRNPs) family of RBPs that vary greatly in function and structure. Growth cone collapse and Map1B mRNA translation in response to sema3a is attenuated in axons depleted of FMRP, suggesting a role for FMRP in axon guidance (Hornberg and Holt, 2013). FMRP has been known to repress the translation of bound mRNAs like β-actin whilst supporting their transport along neurites. Studies have shown that TDP-43 co-localises with FMRP and is speculated to regulate mRNA in a similar fashion (Fallini et al., 2012) thereby implicating a role for TDP-43 in axon guidance. Thus, TDP-43 being a part of the hnRNP complex could affect growth cone dynamics through aberrant processing, mis-regulation/mis-splicing of target proteins (β-actin, MAP1B and Sema) that play an important role in growth cone dynamics and function.

Microtubules and actin microfilament interactions play an important role in growth cone dynamics and axon outgrowth, thus, we speculate that TDP-43 interacts with microtubules and microfilaments and impaired interactions may contribute to phenotypes eventually leading to neurodegeneration.

4.3.3 TDP-43 affects anterograde transport

Deficits in axonal transport have been proposed to contribute to neurodegeneration. In SOD1 G93A mice retrograde axonal transport defects were the earliest observed phenotypes implying that axonal transport deficits may be a key pathogenic event in ALS and an early indicator of motor neuron degeneration (Bilsland et al., 2010). Mutations in kinesin motor family (KIF) and dynein heavy chain have been implicated in neuronal degeneration. Several lines of evidence suggest that deficits in both anterograde and retrograde transport contribute to ALS pathogenesis (Millecamps and Julien, 2013).

End binding proteins like EB3s have been shown to associate specifically with the ends of growing microtubules, thereby regulating microtubule dynamics and the binding of microtubules to protein complexes, organelles and membranes. We used EB3s to visualize microtubule dynamics and organization and to see if TDP-43 impairs these interactions. We show that TDP-43 affects EB3 plus tip dynamics. The wild-type and mutant TDP-43 reduces the number and the speed of the EB3s *in vitro*. The kymographs show that TDP-43 transfected neurons have more stationary EB3s than the EGFP control. The speed of the EB3s displacement reflects microtubule growth rates (Stepanova et al., 2003). EB3s play an important role in promoting microtubule stability and growth. Axon extension requires assembly and reorganization of microtubules, neurofilaments and actins (Dent et al., 2003). Thus, reduced EB3 velocity reduces microtubule growth rates which in turn might affect axonal outgrowth. The reduction of EB3 velocity in the TDP-43 wild-type and mutant transfected neurons correlates with the reduced neurite lengths. Previous studies have shown that TDP-43 regulates Kinesin family of proteins (Tollervey et al., 2011a) and microtubule associated proteins (Coyne et al., 2014). Thus, we speculate that TDP-43 affects microtubule dynamics and axonal transport of cargos through mis-regulation of its microtubule targets.

Pathomechanisms of sporadic ALS include oxidative stress, glutamate toxicity and mitochondrial impairment all of which is inter-related by defects of their transport along the axons. Both TDP-43 and SOD1 mice models exhibit mitochondrial transport

defects (Magrane et al., 2014) suggesting that they are common denominators of different genetic forms of the ALS, though the mechanisms behind the transport defects are not clear. SOD1 mutants also affect dynein and KIF5 mediated retrograde and anterograde axonal transport (Shi et al., 2010). Thus, we speculate that TDP-43 can regulate microtubule dynamics and motor proteins thereby affecting transport of cargos along the axons eventually leading to neurodegeneration.

4.3.4 TDP-43 affects subcellular mis-localisation of its target mRNA

Localisation and translation of mRNAs play a key role in axonal survival and regeneration. Subcellular mRNA trafficking has been demonstrated as a mechanism to control protein distribution. However, the mechanism behind the re-distribution of cargos/targets is not very well known.

Our data suggests that TDP-43 alters the levels of expression and affects the distribution of its target mRNA. TDP-43 mutants and the wild-type differently distribute target mRNAs compared to the EGFP control. WT-TDP-43and TDP-43 M337V had similar patterns of expression/ localisation wherein, there was delayed expression of the construct (no expression at 24 hours), reduction of expression in the axon and enhancement of expression in the cell body. TDP-43 Q331K mostly shows an ectopic cell body expression at 24 hours, over-expression in the cell body with faint or no axonal expression. Thus, depending on the mRNA targets, the TDP-43 wild-type and mutants isoforms show a loss of axonal expression, increased nuclear expression or delayed expression. These expression patterns could signify inhibition of local translocation and translation.

TDP-43 regulates Futsch mRNA expression at the NMJ in *Drosophila.* TDP-43 inhibits the localisation and translation of Futsch mRNA by reducing its expression in the NMJ and increasing its expression in the cell body (Coyne et al., 2014). Expression of Map1B is seen throughout the neurons in EGFP control whereas with the WT-TDP-43 and TDP-43 M337V, expression of Map1B is seen throughout the neuron after a delayed period wherein no expression is seen. TDP-43 is expressed throughout the neuron with an increased nuclear expression. At 72 hours, the expression in the axons is quite faint

with increased nuclear expression implying that TDP-43 Q331K can inhibit local translation of Map1B along the axons. The 72 hour time point also coincides with TDP-43 aggregation. TDP-43 M337V starts to show an increase in nuclear expression implying that over time it might function in a manner similar to TDP-43 Q331K.

TDP-43 is not known to directly affect Map2 but it is known to be associated with Mapt (microtubule associated protein-tau). Map2 also belongs to the microtubule associated protein family. MAPs are differentially distributed in neuronal processes; adult form of MAP-2 is almost exclusively in perikarya and dendrites while Tau is predominantly compartmentalized to axons and plays an important role in dendritic and axonal stability. The expression of Map2 in the TDP-43 wild-type and mutants proteins is delayed at 24 hours followed by normal expression throughout the neuron at later time points. However, when compared to EGFP control, the expression is weaker in the TDP-43 constructs. This coincides with the shorter neurite lengths and lesser dendritic branching seen in TDP-43 transfected spinal and cortical neurons (Tripathi et al., 2014).

In EGFP transfected controls, β-actin is expressed throughout the neuron with progressive increase in expression in the cell body. After a delay, WT TDP-43 is expressed along the neurons but at later time point, the expression increases in the cell body and becomes weaker in the axons. TDP-43 M337V shows a delay in expression after which it is evenly expressed in the neurons. TDP-43 Q331K has increased expression in the cell body at 24 hours which is then expressed evenly throughout the neuron and becomes fainter over time. β-actin in a RNA target of TDP-43 (Sephton et al., 2011). β-actin is also a housekeeping gene and plays an important role in maintaining the cytoskeletal integrity.

In EGFP control, Kif2a is expressed throughout the neuron. In comparison, after a delay, Kif2a is evenly expressed in WT-TDP-43 and TDP-43 M337V. TDP-43 Q331K is expressed throughout the neuron with increased expression in the cell body. The axonal expression fades over time. TDP-43 is known to regulate the splicing of Kif2a (Tollervey et al., 2011a). Kif2a plays an important role in axonal branching. The expression seems to fade over time for TDP-43 Q331K.

Nd1-L is an actin stabilizing protein that is a cargo transcript for FUS (Lagier-Tourenne et al., 2010). TDP-43 regulates FUS. Thus, we used Nd1-L to see if TDP-43 affects its localisation and expression. Nd1-L is highly expressed in the cell body for all the constructs, but the expression in the axons fades at 72 hours for WT-TDP-43 and TDP-43 Q331K while it becomes faint for TDP-43 M337V. In comparison EGFP control neurons have increased expression in the in the nucleus with a steady expression in the axons. Thus, the expression levels seem to be reduced by TDP-43 wild-type and mutant isoforms.

TDP-43 is known to bind to the 3'UTR of Nfl and stabilizes its mRNA (Strong et al., 2007). Studies have shown that TDP-43 affects Nfl trafficking in neurons (Alami et al., 2014). In control EGFP, expression is seen throughout the neuron at 24 hours, after which the expression in the axons become faint with increased nuclear expression. The TDP-43 wild-type and mutant isoforms show very faint expression along the neurons at all the time points and reduced nuclear expression. NFL plays an important role in maintaining the neuronal structure. The expression levels seem to be reduced by TDP-43 wild-type and mutant isoforms.

Thus, TDP-43 affects the expression and localisation of the cytoskeletal mRNAs. However, it is important to note that though these interactions can be assayed *in vitro,* it might not have such a physiological effect *in vivo,* given, the complex nature of RNA processing. The expression patterns also depend on the time-frames as the effects can be progressive over time. Studies have shown that TDP-43 affects NFL mRNA trafficking after about 9 days in culture (Alami et al., 2014). Thus, it will be interesting to see the expression patterns at later time points.

TDP-43 mutant Q seems to have the most adverse effects when compared to the other TDP-43 constructs. Some of the mRNA targets accumulated in/restricted to the nucleus/cell body with no axonal expression or a low level of axonal expression. Restriction of the mRNA distribution to the cell body suggests impaired axonal transport or impaired mRNA splicing/translation mechanism while low levels of axonal expression compared to the control could imply down regulation of the target mRNA. Thus, the mis-localization of subcellular mRNA in TDP-43 transfected neurons highlight the importance of TDP-43 mediated mRNA localisation and regulation.

To conclude, our data suggest that TDP-43 regulates the integrity of the cytoskeleton by binding to and processing different cytoskeletal mRNA targets, and that dysfunction of TDP-43 contributes to the pathology of ALS. Axonal outgrowth, growth cone dynamics, microtubule dependent axonal transport, and subcellular cytoskeletal mRNA distribution are all affected by TDP-43. All of these impairments may be inter-related and the sequence of mechanisms leading to TDP-43 mediated neurodegeneration is not very clear. We speculate that aberrant trafficking and mis-regulation of mRNA/protein targets of TDP-43 play a key role in the pathology of ALS.

5 C9ORF72 toxicity: RNA vs. RAN

5.1 Introduction

The mechanism by which C9orf72 G4C2 hexanucleotide expansion repeats cause neurodegeneration is unknown. Several mechanisms have been proposed including both gain and loss of function. Possible mechanisms of neurodegeneration include loss of C9orf72 protein and function, RNA toxicity, and toxicity from the DPR proteins, but which of these is the major pathogenic mechanism is not yet certain.

Renton et al., 2011 and DeJesus-Hernandez et al., 2011 demonstrated that large GGGGCC hexanucleotide expansion repeats (700-1600) within the *C9ORF72* is the most common cause of chromosome 9p21-linked ALS, FTD and ALS-FTD. They associated the G4C2 repeat sizes with the presence or absence of 'risk' haplotype, concluding that a cut-off of thirty repeats is commonly used to differentiate between pathogenic and non-pathogenic repeat sizes since the maximum size of the repeats in the controls were around ~23. Decreased levels of C9orf72 transcript in the expanded repeat carriers, suggest a loss of protein function due to haplo-insufficiency (DeJesus-Hernandez et al., 2011, Renton et al., 2011). Rademaker's group identified RNA foci generated by the G4C2 repeat expansion to be a key factor in the disease mechanism. RNA foci are intracellular accumulation of expanded nucleotide repeats. They proposed that GC-rich mRNA could cause disease by recruiting and sequestering RNA-binding proteins into the foci, leading to aberrant splicing of RNAs favouring a toxic RNA gain of function mechanism. Repeat associated non-ATG translation of the G4C2 repeats resulting in the aggregation of dipeptide proteins (Mori et al., 2013a) is another key mechanism favouring the gain of function mechanism.

Thus, taking into account the previous studies, we used chick embryos to model the G4C2 RNA and protein toxicity. We have previously used the chick embryonic system to model acute effects of TDP-43 wherein we showed that over-expression of TDP-43 wild-type and mutant constructs caused neurotoxicity accompanied by striking defects in axon outgrowth implying that cytoskeletal dysregulation may play a role in ALS and FTD-TDP pathogenesis (Tripathi et al., 2014). Here we use similar techniques to model the G4C2 toxicity.

The aim of this study was to evaluate the toxic effects of G4C2 repeat lengths on spinal cord and motor neurons in particular and to establish the effect of repeat number on pathology in a specific spinal cord model. This study also aims to assess the dipeptide toxicity and to analyse the RNA toxicity vs. the dipeptide toxicity, as a mechanism of *C9ORF72*. Results arising from this study could provide preliminary information to consolidate the role of *C9ORF72* in ALS and investigate whether the expansion acts through a gain of function mechanism that is dependent on either RNA or protein toxicity or a consolidation of the two.

In order to investigate the relationship between repeat number and the severity of the disease, we used EGFP tagged constructs with four different repeat numbers 8x, 38x, 72x and 128x. These constructs contained only the G4C2 DNA sequence so as to look at the RNA mediated toxicity. Since the cut-off repeat number for 'risk' haplotype was reported at 30x (Renton et al., 2011), 8x is considered to be non-pathological and used as a positive control whilst the 38x, 72x and 128x repeats are considered pathological. The G4C2 repeats were cloned into pcDNA EGFP expression vector where EGFP is at the 5' end followed by the G4C2 repeats. The constructs were designed with the capability to be transcribed but not translated through conventional ATG-initiated mechanisms.

To investigate the protein toxicity, we used the five different sense (GA-EGFP, GR-EGFP, GP-EGFP) and anti-sense (PA-EGFP, PR-EGFP) dipeptides constructs tagged with WPRE. These synthetic constructs, encoding 125 repeats, contained a mixture of alternative codons with reduced GC content to prevent instability observed with repetitive GGGGCC-based constructs. Thus, changing the original hexanucleotide repeat sequence, but maintaining the DPR protein sequence, allowed us to focus on protein toxicity rather than GGGGCC or CCCCGG RNA toxicity. The dipeptides were tagged with the EGFP at the C-terminus and were inserted into a cPPT TET construct with WPRE sequence. The woodchuck hepatitis virus post-transcriptional regulatory element (WPRE) is a DNA sequence used to elevate the expression of the cDNA encoding EGFP in a transgene, promoter and vector-independent manner.

5.2 Results

5.2.1 Longer G4C2 repeats causes neurotoxicity *in vivo*

In order to determine whether expanded G4C2 transcripts might be toxic, EGFP–G4C2 repeat constructs (8x, 38x, 72x and 128x), were electroporated into the spinal cord at embryonic day 2.5 (E2.5). Empty EGFP plasmid was electroporated as the control. The electroporated embryos were re-incubated for 24hours, until E3.5 and were fixed, sectioned on a cryostat and immunostained with antibodies to GFP to determine the expression of the injected constructs. The sections were treated with TUNEL kit to determine the number of apoptotic cells. TUNEL positive cells appear as black dots. A total of 75 embryos were electroporated for each construct and the data was analysed from 42 sections across at least 6 embryos from 3 sets of experiments.

Initially, plasmid DNA constructs were injected at a final concentration of 2 µg/µl. However, with this concentration of DNA, no apoptosis was detected with any of the G4C2 repeat constructs (data not shown). Hence we increased the final concentration of DNA to 4 µg/µl. Only spinal cords with more than 50% of transfected cells were analysed for TUNEL.

EGFP and EGFP-8x electroporated embryos have very few TUNEL positive cells on the electroporated side with no TUNEL positive cells on the control side. EGFP-38x, EGFP-72x and EGFP-128x showed TUNEL positive cells on the electroporated side and the non-electroporated side suggesting that the G4C2 mediates toxicity spreads contralaterally. The EGFP-72x had smaller apoptotic cells, whereas the TUNEL positive cells of EGFP-38x looked more clumped up and bigger and the EGFP-128x TUNEL positive cells were of an average size (Fig 5.1: C2-a – E2-a).

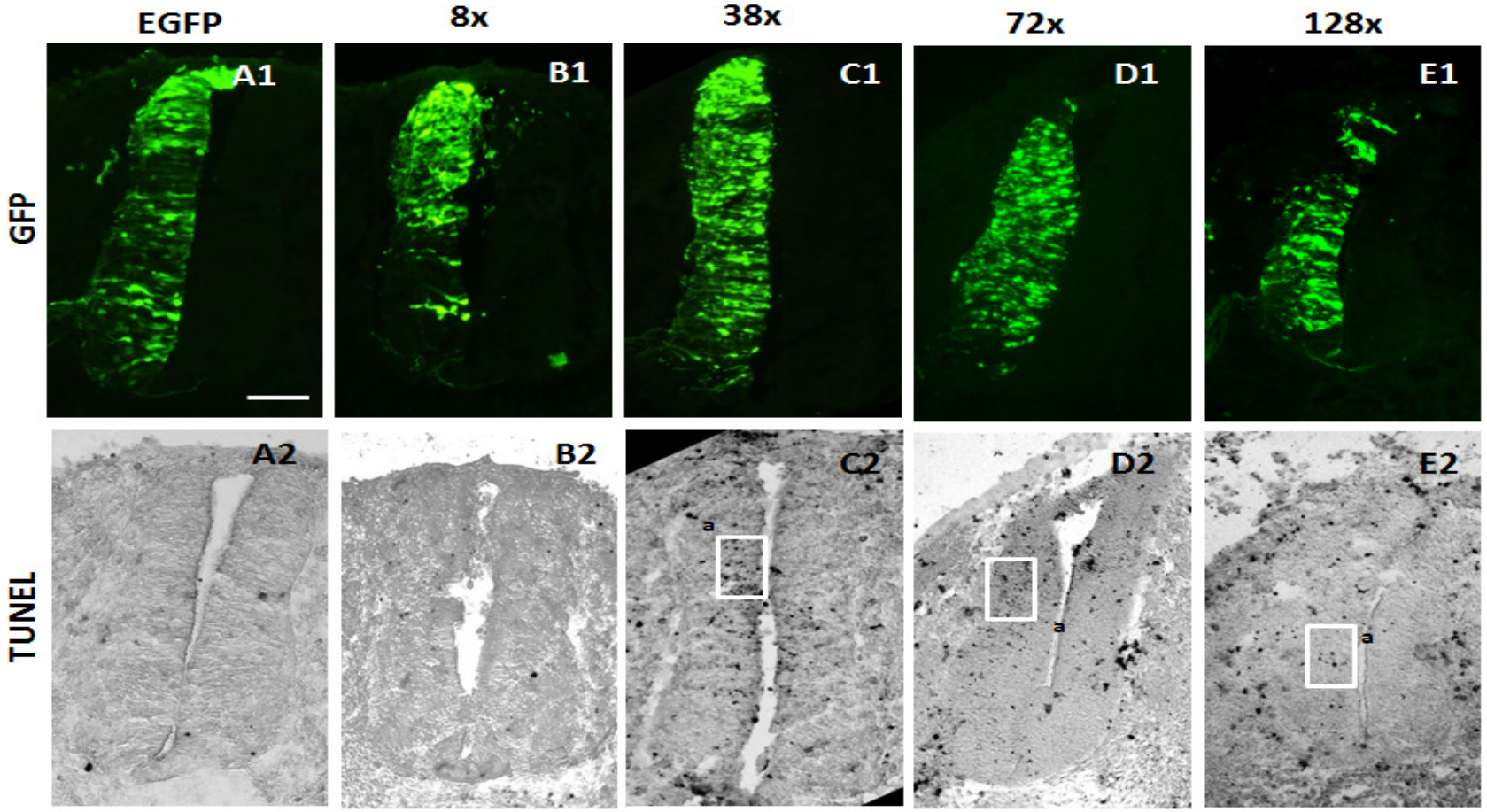

Figure 5.1 Longer G4C2 expansion repeats are toxic:

Transverse section of the spinal cord at HH 20. HH 15/16 stage chick embryos were electroporated *in ovo* with the EGFP tagged G4C2 expansion repeats (A1-E1) and assayed after 24H for TUNEL staining to mark apoptotic cells. TUNEL stained nuclei appear as black dots. The spinal cords electroporated with EGFP and 8x show very few TUNEL positive cells (A2-B2) when compared to the 38x (C2), 72x (D2) and 128x (E2). The boxed regions (C2- E2: a) are enlarged in the next figure. Scale bar = 100 µm.

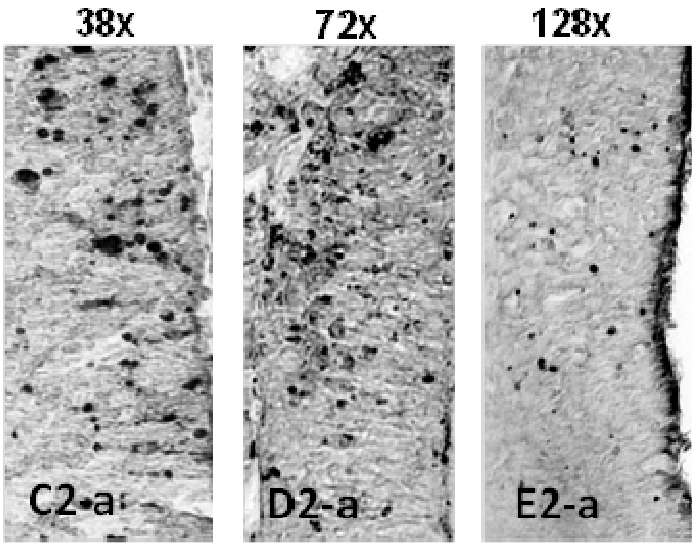

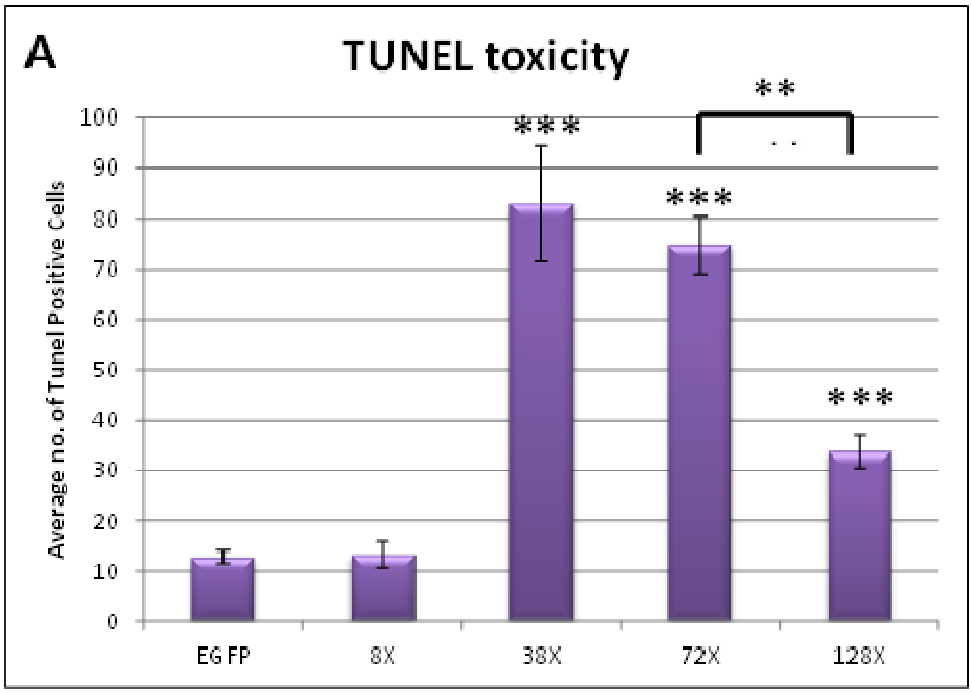

Figure 5.2 G4C2 toxicity graph
Panels C2-E2: a - are magnified images of the boxed regions from panels C2-E2 in Fig 21. They show the TUNEL toxicity in the longer repeats (38x, 72x and 128x). TUNEL positive cells appear as black dots. A) Graph representing the average number of TUNEL positive cells on the electroporated side after electroporation of EGFP tagged G4C2 repeats (8x, 38x,72x and 128x). Data is based on average and standard error of mean. Significant difference was calculated using the one –way anova and Dunn's comparison. 38x, 72x and 128x repeats are significantly different to both EGFP and 8x (*P<0.0001). There is a significant difference between 128x and 72x (**P<0.001).**

Electroporation with the EGFP and EGFP-8x resulted in very few TUNEL positive cells with no significant difference between them (Fig 5.1: A2-B2; Fig 5.2: A). In comparison, embryos electroporated with the EGFP-38x, EGFP-72x and EGFP-128x repeats showed higher numbers of apoptotic cells (Fig 23: C2-E2; Fig 24: C2-a –E2-a). A quantitative

comparison of the average number of apoptotic cells between the higher repeat lengths showed that EGFP-38x had an 8-fold increase in the number of apoptotic cells (***P<0.0001), while EGFP-72x repeats showed a 7-fold increase in apoptosis (***P<0.0001) and the EGFP-128x showed a three-fold increase (***P<0.0001) compared to EGFP and EGFP-8x (Fig 5.2: A). There was no significant difference between EGFP-38x and EGFP-72x (P>0.05) and between EGFP-38x and EGFP-128X. However, there was a slight significant difference between EGFP-72x and EGFP-128x (**P<0.001).

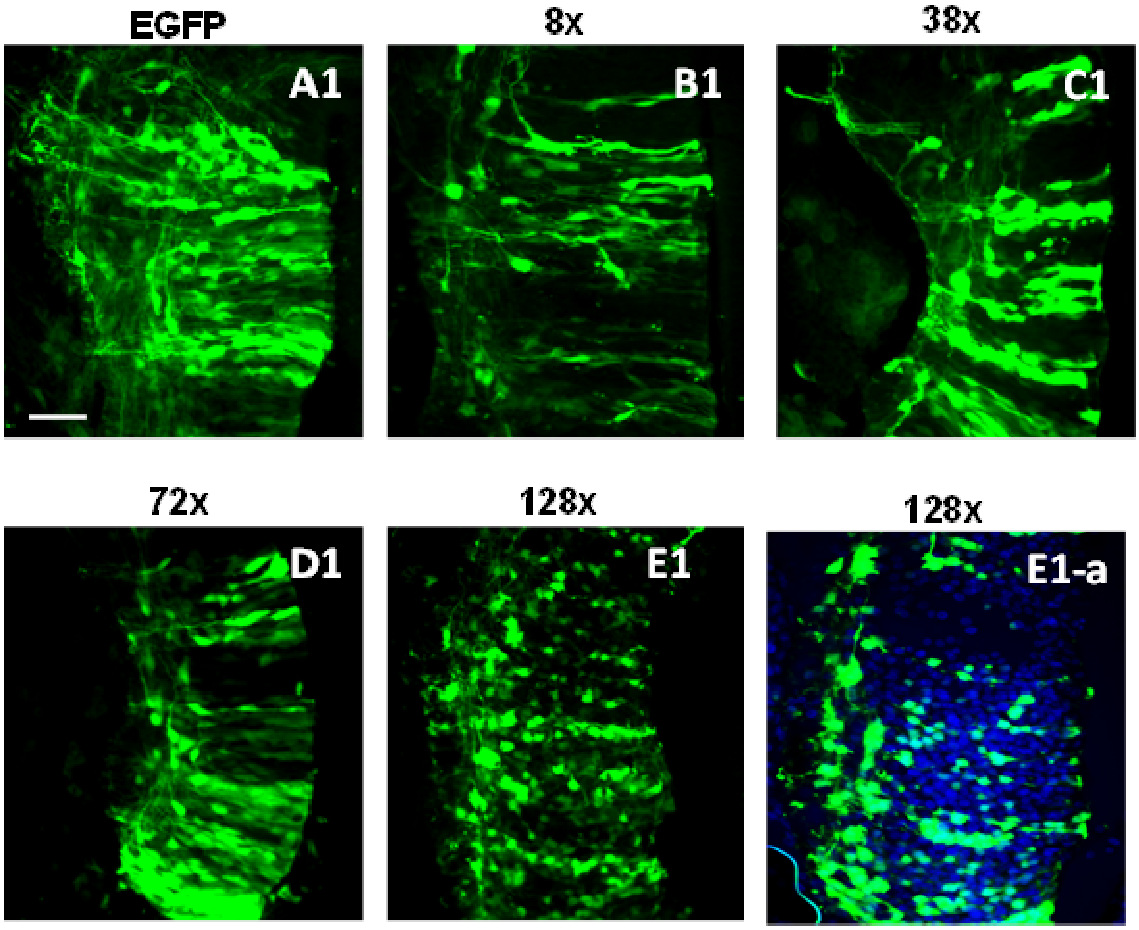

Figure 5.3 Expression of 128x is mostly nuclear
Representative images from embryos electroporated with EGFP-tagged G4C2 repeat expansions and control EGFP constructs in the spinal cord. EGFP control (A1), along with the 8x (B1), 38x (C1) and 72x (D1) are expressed along the entire neurons whilst the 128x is mostly expressed only in the cell body. E1-a) 128x transfected spinal section double labelled with anti-GFP and Hoechst. Scale bar = 100µm.

Magnified images of the GFP staining on spinal sections transfected with the G4C2 repeats, showed that anti-GFP expression was seen throughout the neurons in the spinal cord transfected with EGFP control, EGFP-8x, EGFP-38x, EGFP-72x. However, the

sections of the cord injected with EGFP-128x, show GFP expression only in the nucleus with very few cells showing axonal staining of GFP (Fig 5.3). The Hoechst staining on these sections show that there are lots of gaps in the nuclear staining (Fig 5.3: E1-a). Thus, the differential expression of EGFP-128x suggests that the construct may confer neurotoxicity but the cells might be cleared off at an earlier time point.

Thus, the longer G4C2 hexanucleotide expansion repeats confer neurotoxicity in chick spinal cords *in vivo*.

5.2.2 G4C2 hexanucleotide expansions form intranuclear RNA foci *in vivo*

One of the key RNA gain-of function mechanisms associated with the G4C2 repeat mediated neurodegeneration is the presence of intra-nuclear RNA foci containing G4C2 repeats in the tissues of ALS and FTLD patients (DeJesus-Hernandez et al., 2011). The prevalence of these RNA foci in chick embryos electroporated with the EGFP tagged G4C2 repeats was analysed. Chick embryos were electroporated with the same repeat constructs at E2.5 and re-incubated for 24 hours post electroporation. The embryos were sectioned and assayed for the presence of the RNA foci using a cy3 tagged G4C2 probe by fluorescent *in situ* hybridisation. The G4C2 positive RNA foci were completely absent in the control EGFP and EGFP-8x expressing spinal sections but were abundantly found in cells expressing the longer repeats; EGFP-38x, EGFP-72x and EGFP-128x (Fig 5.4). The RNA foci of the EGFP-38x repeats were bigger in size compared to the dotted appearance seen with EGFP-72x and EGFP-128x electroporations (Fig 5.4: C1-a –E1a). The foci numbers were manually counted from ~ 20 sections across 3 embryos from 3 independent experiments. A semi-quantitative analysis of the number of RNA foci, showed that EGFP-38x sections have less than 120 RNA foci whereas the EGFP-72x and the EGFP-128x have more than 250 foci. Therefore, longer G4C2 hexanucleotide expansion repeats can form more RNA foci *in vivo* in chick embryos.

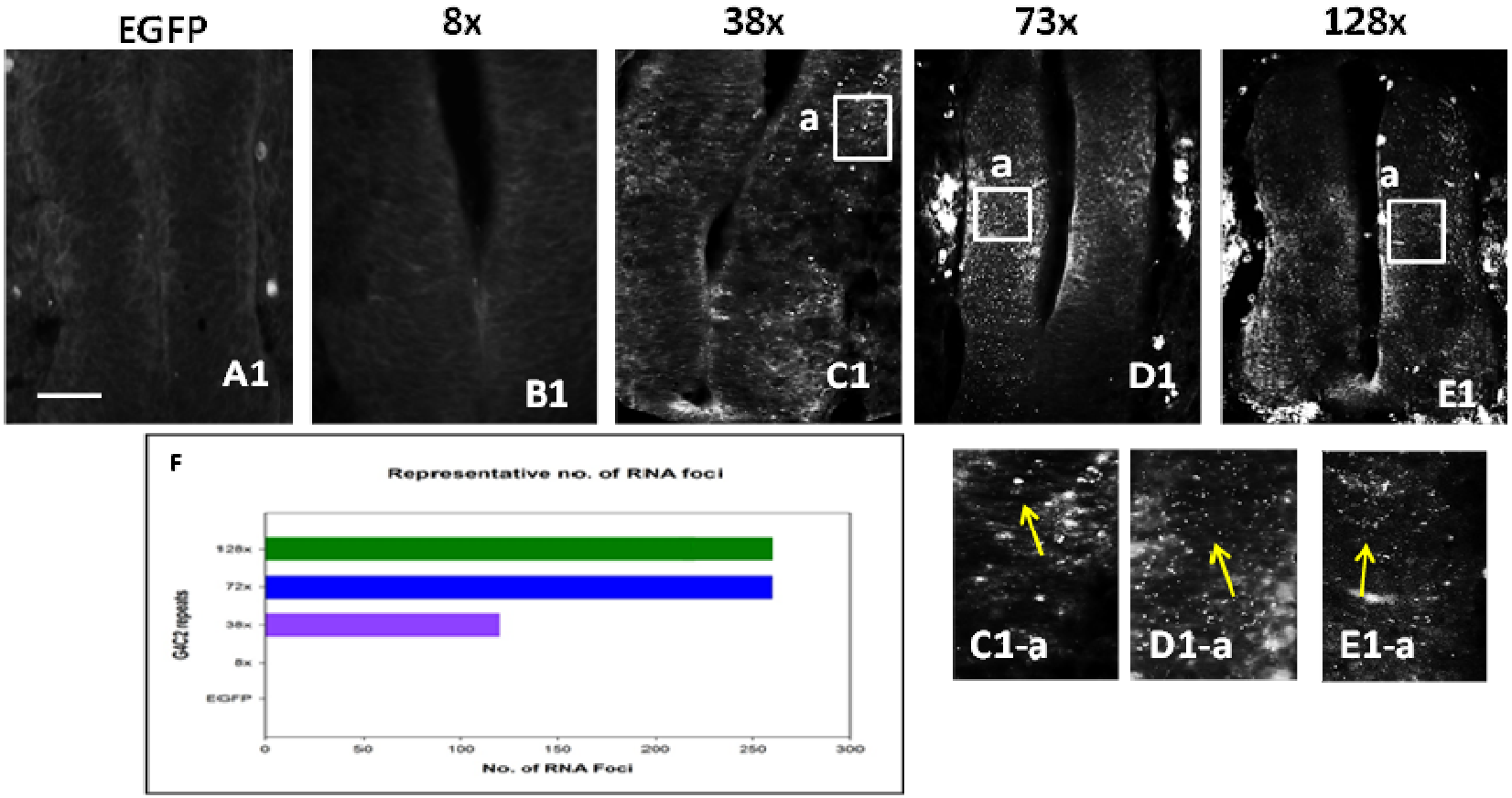

Figure 5.4 Longer G4C2 repeats form more RNA foci

Transverse sections of the spinal cord at HH 20 in monochrome. HH15/16 stage chick embryos were electroporated *in ovo* with the EGFP tagged G4C2 expansion repeats and hybridised after 24H with a Cy3 tagged G4C2 probe (A1-E1). G4C2 RNA foci are seen as tiny white dots (Indicated by yellow arrows). EGFP control (A1) and 8x (B1) show a complete absence of RNA foci compared to the 38x (C1), 72x (D1), 128x (E1) constructs that show a high number of G4C2 foci. Panels C1-a to E1-a are inset of the boxed area from the corresponding panels C1-E1. F) Semi-quantitative analysis of the number of foci. 38x constructs roughly have < 120 foci whereas both 72x and 128x constructs have more than > 250. Scale bar = 100 µm

5.2.3 G4C2 hexanucleotide expansion repeats affect motor neurons

ALS is characterized by a specific loss in motor neurons and so it is important to establish whether cell death relating to transfection specifically affects motor neurons. In order to determine if the G4C2 hexanucleotide repeat expansions affects motor neurons, chick embryos were electroporated at E2.5 with the EGFP tagged repeat expansions and control EGFP. The embryos were harvested 24 hours after the injection and sectioned and immuno-stained with antibodies to GFP and motor-neuron specific Islet-1 antibodies (Fig 5.5; Fig 5.6: A2-a - B2-b). The number of motor neurons on the electroporated side and the control non-electroporated side were manually counted for each construct. The number of motor neurons were counted from a total of 8 sections per construct from 1 experiment. These results are preliminary data and since the 'n' numbers were not sufficient, a semi-quantitative graph was drawn to represent the average number of motor neurons on the control and the electroporated sides (Fig 5.6: F) and the percentage difference in the number of motor neurons between the control and the electroporated sides is shown (Fig 5.6: G). EGFP control and EGFP-8x electroporated embryos showed very little difference in the number of motor neurons between the control and the electroporated sides (~ < 10%). EGFP-38x, EGFP-72x and EGFP-128x electroporated embryos had less number of neurons on the electroporated side compared to the control side (~>23%). EGFP-128x electroporated spinal cords have lesser number of motor neurons on the control side when compared to the other constructs. This implies that EGFP-128x affects the contralateral region. Thus, motor neurons are susceptible to the G4C2 hexanucleotide repeat mediated toxicity.

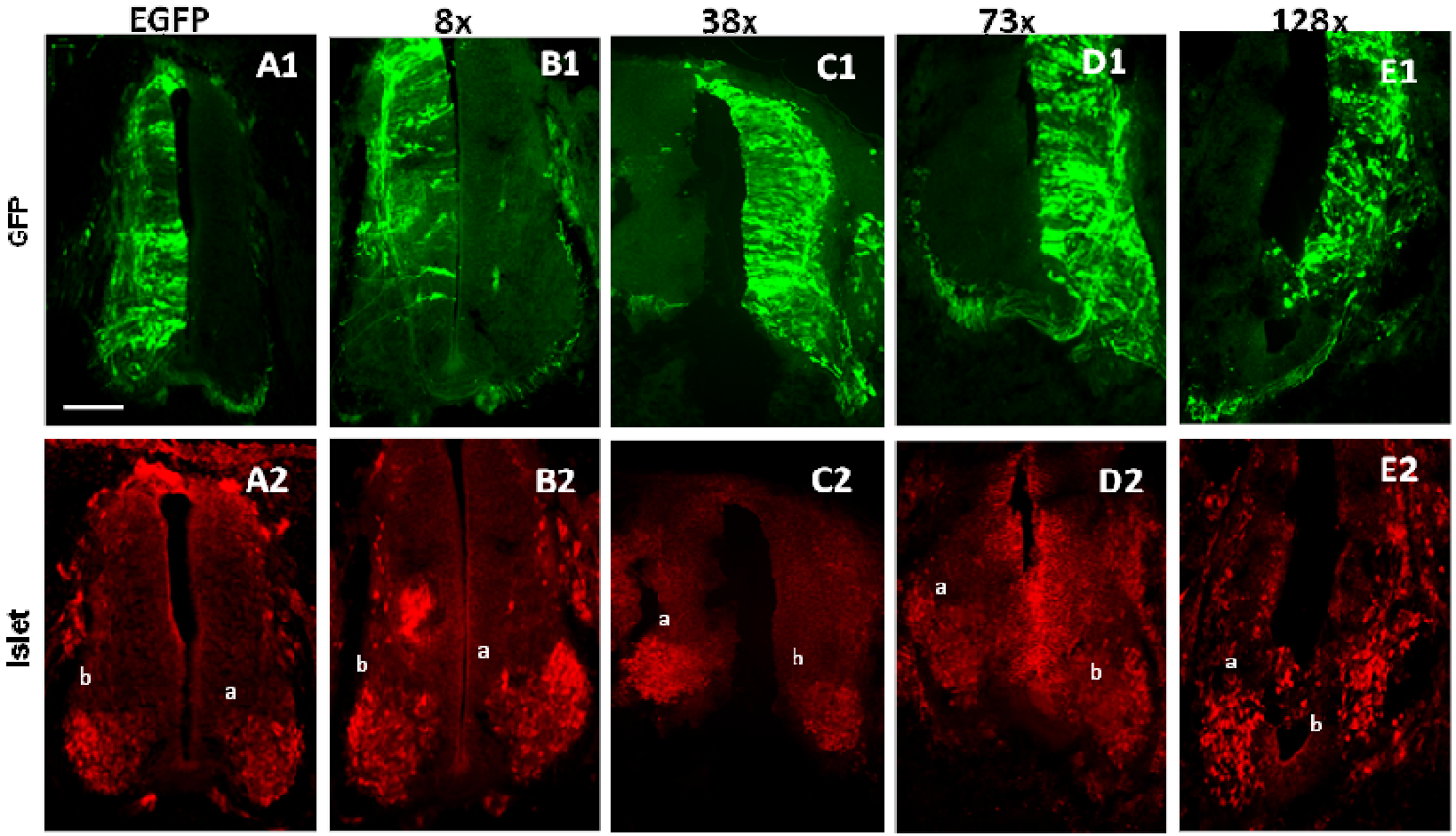

Figure 5.5 G4C2 repeats affect motor neurons

Transverse sections of the spinal cord at the forelimb level at HH stage 25. HH15/16 stage chick embryos were electroporated *in ovo* with the EGFP tagged G4C2 expansion repeats (A1-E1) and assayed after 48H for islet -1 immunostaining as a marker for motor neurons (A2-E2). a) motor neurons on the control side. b) motor neurons on the electroporated side. Scale bar = 100 µm

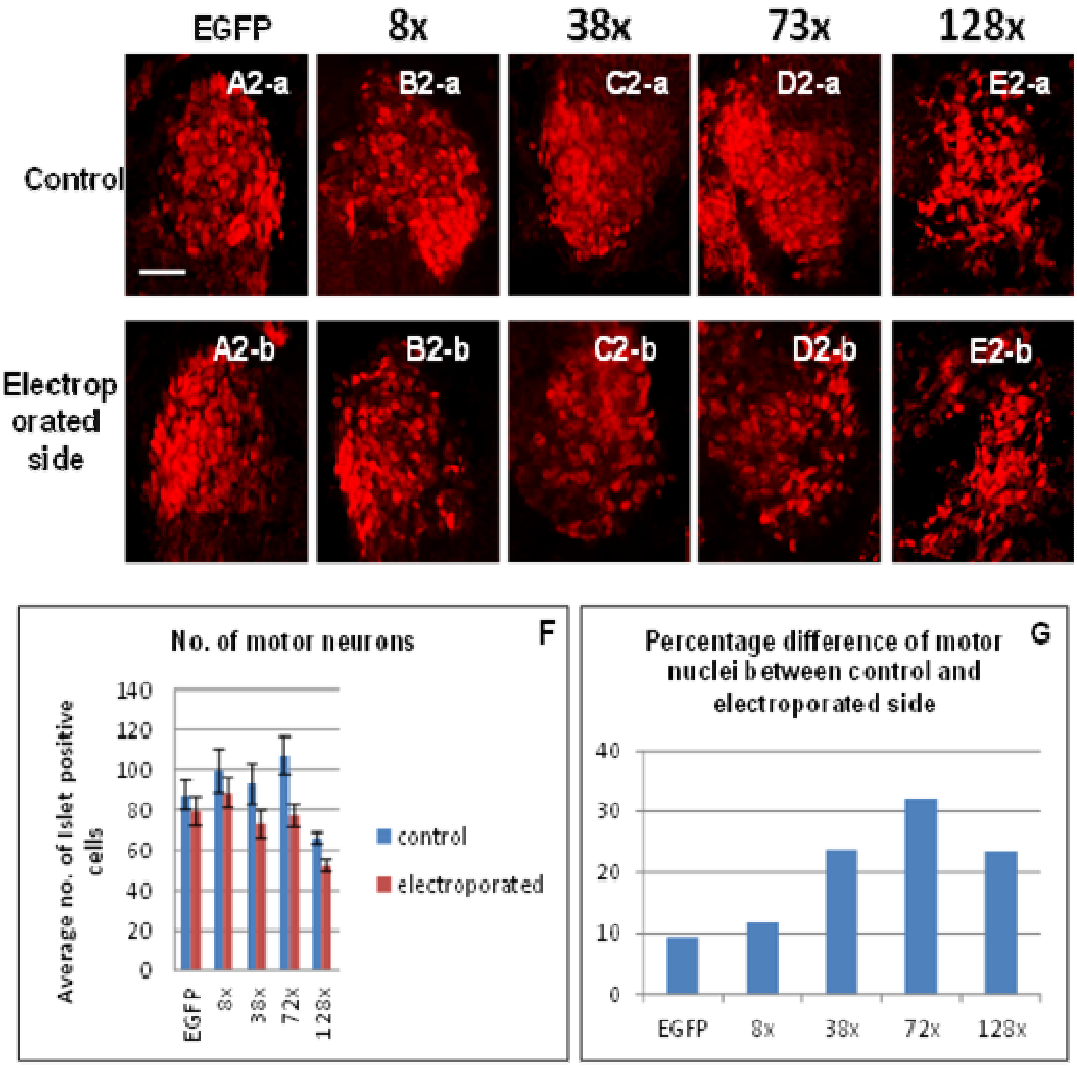

Figure 5.6 Longer G4C2 repeats have lesser motor neurons

Representative images from embryos electroporated with EGFP tagged G4C2 expansion repeats and control EGFP, immunostained with Islet-1 as a marker for motor neurons. Panels A2-a to E2-a are magnified images of the motor neurons from the corresponding control side of the spinal cord from fig 25 whilst panels A2-b to E2-b are magnified images of the motor neurons from the electroporated side of the cord from fig 25. F) Semi quantitative analysis of the number of motor neurons on the control side vs. the electroporated side. G) Semi-quantitative analysis showing the percentage difference between the number of motor nuclei on the control side and the number of motor nuclei on the electroporated side. 18 sections across 3 independent experiments were analysed for each construct. Scale bar = 100 µm.

5.2.4 Longer G4C2 hexanucleotide expansion repeats perturb axonal projections

ALS is characterized by a loss of motor control thus, the motor axon projections that innervate these muscles are particularly relevant to ALS. We have previously shown that over-expressing two different mutant forms of TDP-43 *in ovo* (Q331K, and M337V), caused disruption of the motor projection integrity (Tripathi et al., 2014). Hence, after observing a reduction in the number of motor neurons with the longer repeat constructs, we looked at the effects of the G4C2 repeats on the motor axon projections at the branchial level.

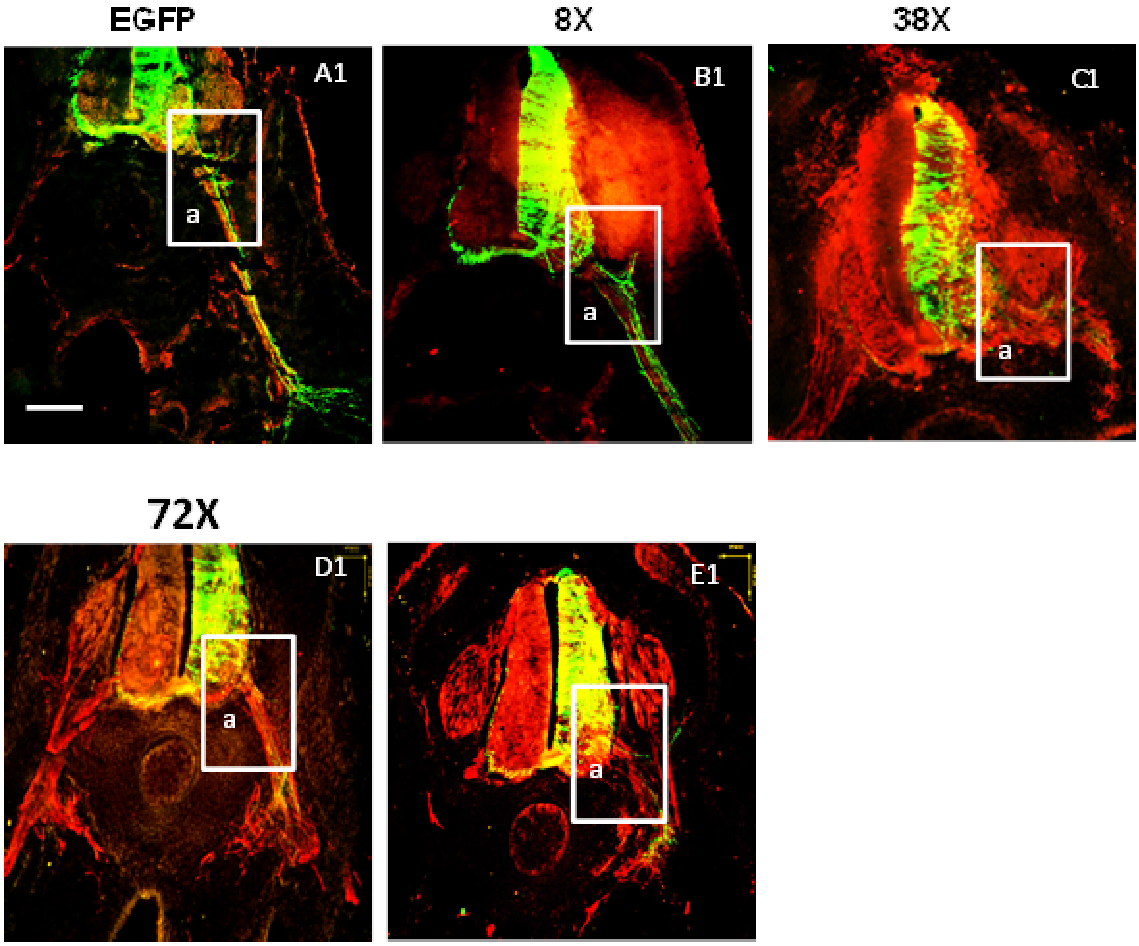

Figure 5.7 Longer G4C2 expansion repeats cause axonal defects
Representative transverse sections (forelimb level) from embryos electroporated with EGFP control and EGFP tagged G4C2 repeats. Panels A1–E1 show entire spinal cords demonstrating unilateral expression of EGFP-tagged constructs (green) at E4.5; sections are stained for EGFP (green) and neurofilament (3A10; red). 38x, 72x and 128x electroporated sections show defects in axonal projections when compared to EGFP and 8x constructs. Inset of boxed areas (a) of the corresponding panels are magnified in fig 28. Scale bar = 100 µm.

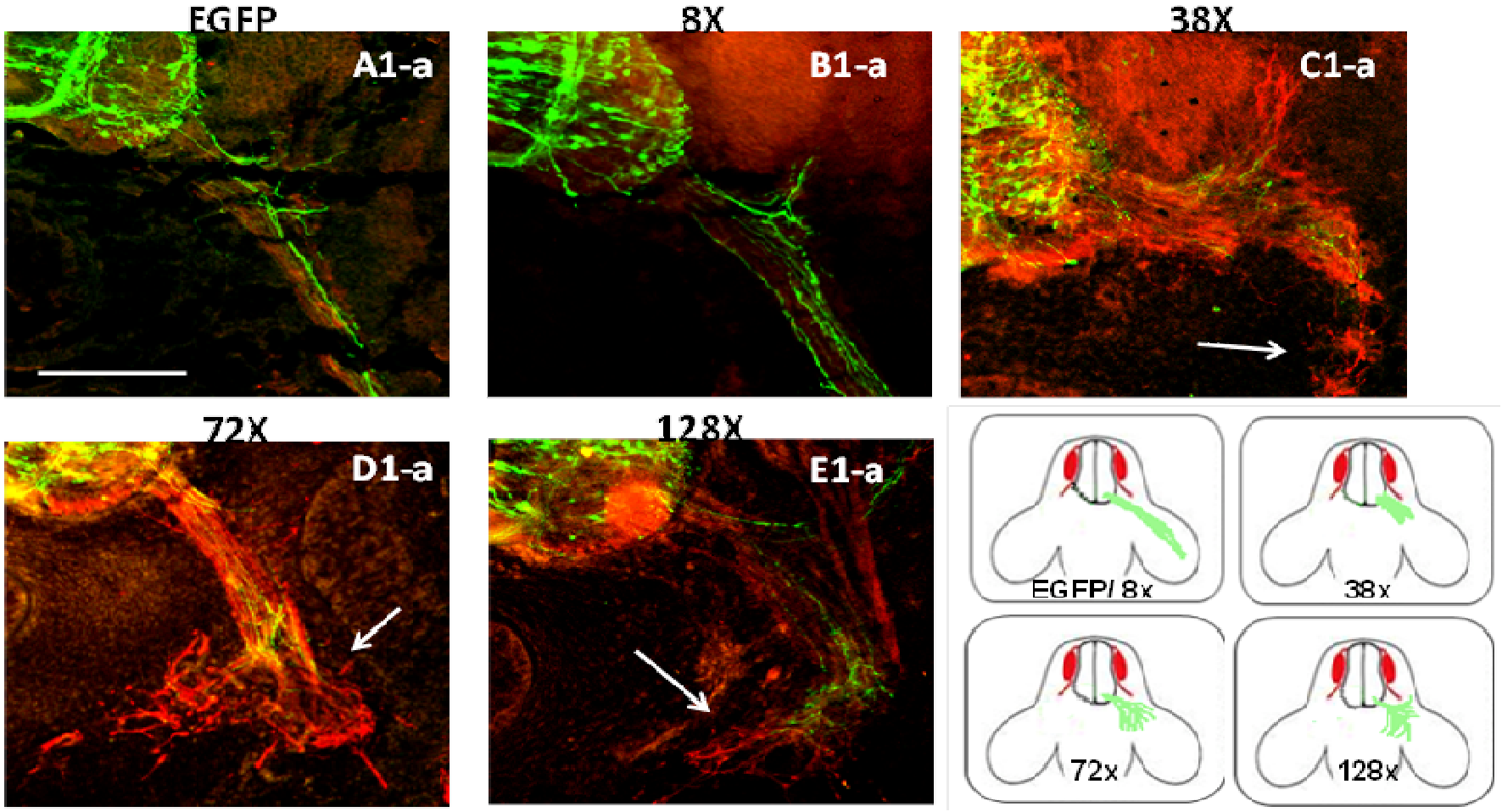

Figure 5.8 G4C2 hexanucleotide repeats cause premature truncation of axons

Representive sections from inset of fig 27; Sections are stained for GFP (green) and neurofilament (red). Axonal projections from ventral motor neurons electroporated with the longer G4C2 repeats (38x, 72x and 128x) show aberrant truncation and fasciculation (C1-a- E1-a) compared to the EGFP (A1-a) and 8x (B1-a) constructs. Scale bar = 100 µm.

The G4C2 repeat transfected sections (48 hours post electroporation – E4.5) were stained with 3A10 (neurofilament associated antigen) and antibodies to GFP to analyse the spinal motor projection. EGFP control and EGFP-8x electroporated embryos extend motor axons into the limb buds. However, over-expression of the longer G4C2 repeats: EGFP-38x, EGFP-72x and EGFP-128x showed various abnormal phenotypes like debundling/defasciculation and truncation as they extend into the periphery (Fig 5.7; Fig 5.8). Spinal motor axons are arranged in close bundles called fascicles. The perturbation of this arrangement is called defasciculation. The motor axons of EGFP-38x, EGFP-72x and EGFP-128x electroporations were aberrantly truncated and de-fasciculated (Fig 5.8: C1-a – E1-a; indicated by arrows). The three longer hexanucleotide repeats (38x, 72x, 128x) show abnormal axon projection defects. Thus we speculate that the G4C2 hexanucleotide expansion repeats impair normal motor neuron outgrowth.

5.2.5 Dipeptides cause toxicity in chick spinal cord *in vivo*

Microsatellite expansions can initiate non-ATG translations, and produce a series of unexpected repeat proteins that may affect various properties of the cell. RAN translation of the G4C2 hexanucleotide RNA can produce both sense and anti-sense dipeptides: GlyPro (GP), GlyArg (GR), GlyAla (GA), ProArg(PA) and ProAla(PA) (Ash et al., 2013; Mori et al., 2013) by non-canonical translation of its G-quadruple complex tertiary structures. In order to determine if dipeptide repeat proteins can contribute to the C9orf72 mediated toxicity, the GA-EGFP-WPRE, GP-EGFP-WPRE, GR-EGFP-WPRE, PA-EGFP-WPRE and PR-EGFP-WPRE constructs were electroporated into the spinal cord of E2.5 chick embryos as a final concentration of 4 µg/µl. The electroporated embryos were then re-incubated for 24 hours, cryo-sectioned and immunostained with antibodies to GFP to determine the expression of the injected constructs (Fig 5.9). A total of 36 embryos were electroporated for each construct and the data were analysed from 35 sections across at least 6 embryos from 3 sets of experiments. The sections were treated with the TUNEL kit to assay apoptosis. TUNEL positive cells appear as black dots. Control electroporations were performed with EGFP.

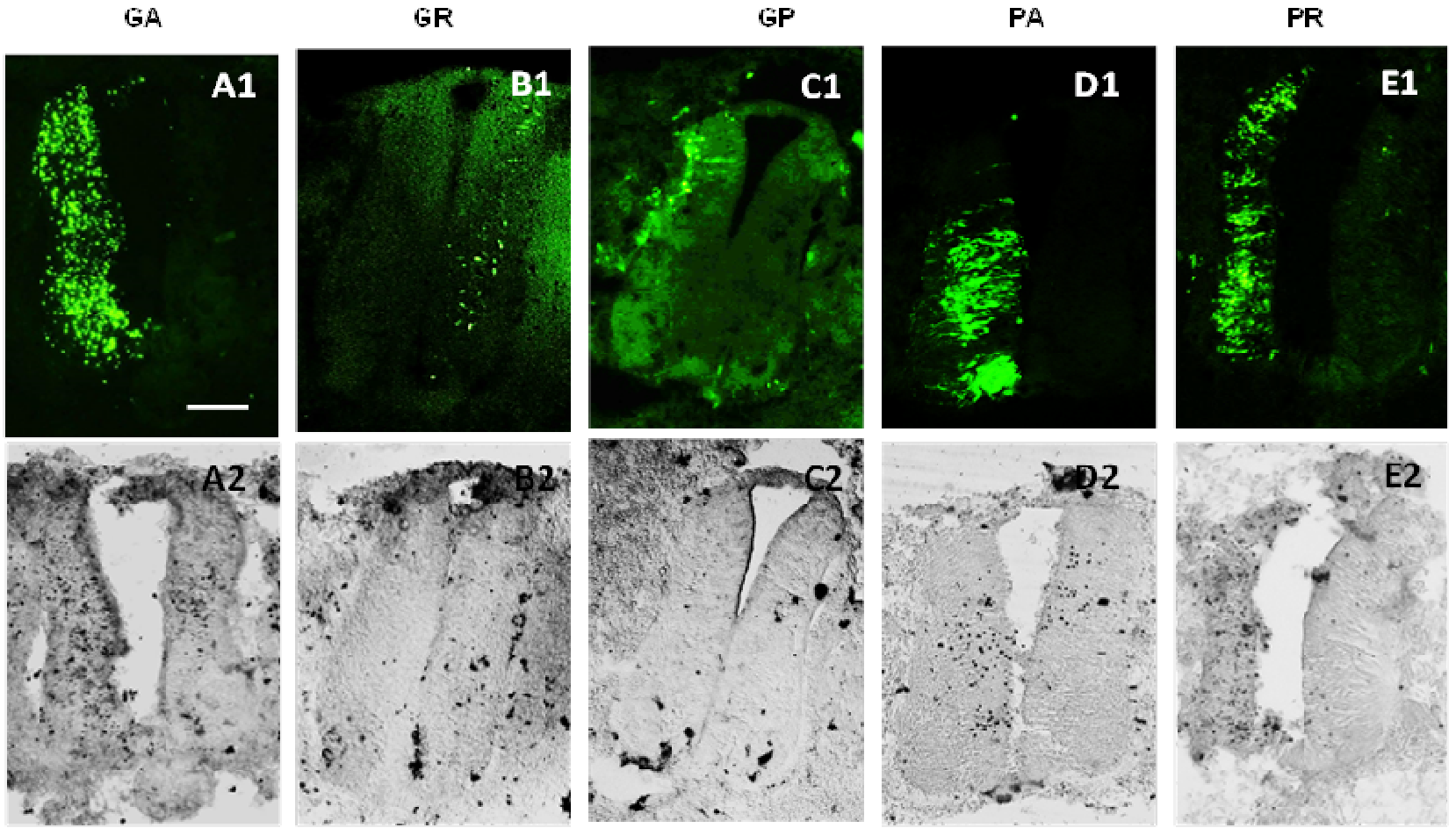

Figure 5.9 Dipeptides are toxic

Sections of the spinal cord at HH stage 20. HH14/15 stage chick embryos were electroporated *in ovo* with the EGFP-WPRE tagged sense (GA-EGFP-WPRE, GP-EGFP-WPRE and GR-EGFP-WPRE) and anti-sense dipeptides (PA-EGFP-WPRE and PR-EGFP-WPRE) (A1-E1) and assayed after 24H for TUNEL staining to mark for apoptotic cells (A2-E2). TUNEL stained nuclei appear as black dots. Scale bar = 100 µm.

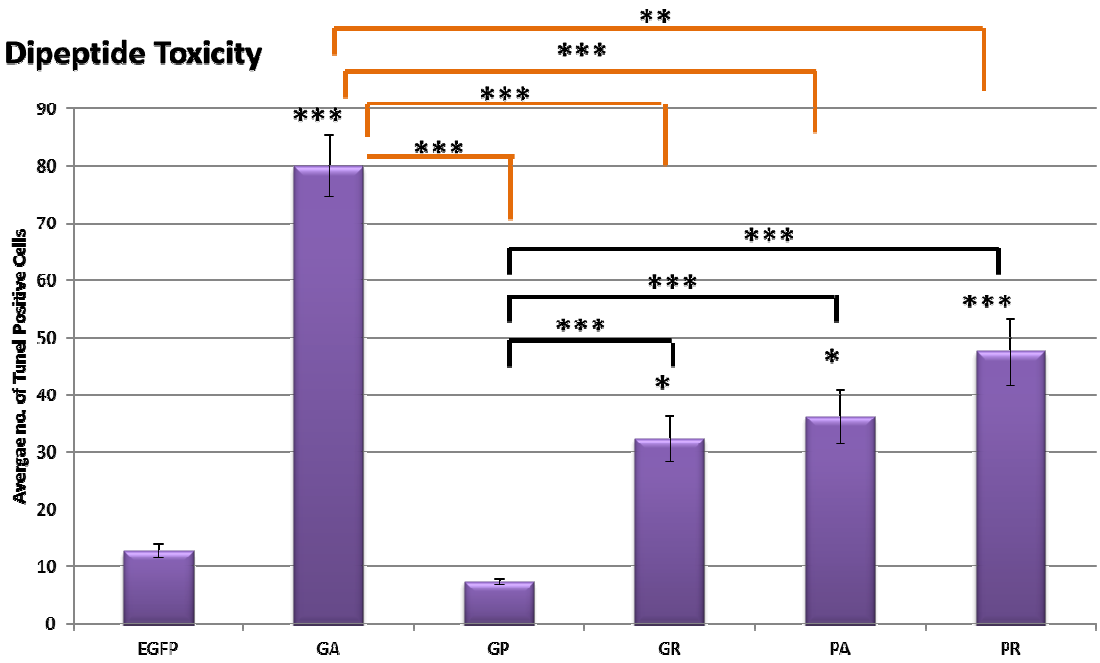

Figure 5.10 GA is the most toxic dipeptide
Graph representing the average number of TUNEL positive cells after electroporation of EGFP-WPRE tagged sense (GA, GP, GR) and anti-sense constructs (PA, PR). EGFP was used as the control. A total of 75 embryos were electroporated for each construct and the data was analysed from 42 sections across at least 6 embryos from 3 sets of experiments. Data is based on average and standard error of mean. Significant difference was calculated using the one –way anova and Dunn's comparison. The significant difference between the dipeptides was compared to EGFP and amongst themselves. GA-EGFP-WPRE is the most toxic and is significantly different from all the other dipeptides (*P< 0.0001, **P<0.001, *P<0.05) whilst GP-EGFP-WPRE has the least toxicity and is significantly different from the other constructs. There is no significant difference between EGFP and GP-EGFP-WPRE; and between GR-EGFP-WPRE, PA-EGFP-WPRE and PR-EGFP-WPRE (P>0.05).**

The expression levels of the different dipeptides vary *in vivo* wherein GA-EGFP-WPRE, PA-EGFP-WPRE and PR-EGFP-WPRE constructs had a 50-75% transfection efficiency while GP-EGFP-WPRE, GR-EGFP-WPRE had very low levels of expression (< 30%). A western blot of these constructs showed that all of the five protein constructs have the same level of expression and are equally expressed in cell lines (data not shown; experiment performed by Dr.Younbok Lee, personal communication). Thus, the expression levels of GP-EGFP-WPRE, GR-EGFP-WPRE may vary *in vivo* due to the various biological barriers that are not reflected *in vitro*.

Embryos electroporated with the EGFP and the GP-EGFP-WPRE dipeptides showed very little toxicity with no significant difference (P>0.05) between them. GR-EGFP-WPRE (*P<0.05), GA-EGFP-WPRE (*P<0.05) and PR-EGFP-WPRE (***P<0.0001) showed a three to five fold toxicity when compared to EGFP and GP (Fig 5.10). GP-EGFP-WPRE

had the least number of apoptotic cells amongst the dipeptides and was significantly lower compared to all the other dipeptides (***P<0.0001). GA-EGFP-WPRE electroporated embryos showed the highest number of apoptotic cells with a 6-fold and 10-fold increase compared to EGFP and GP-EGFP-WPRE (***P<0.0001). The number of apoptotic cells in GA-EGFP-WPRE was significantly higher compared to the other dipeptide constructs (Fig 5.10: ***P<0.0001 for GA-EGFP-WPRE vs. GR-EGFP-WPRE and GA-EGFP-WPRE vs. PA-EGFP-WPRE; **P<0.001 for GA-EGFP-WPRE vs. PR-EGFP-WPRE). There was no significant difference between GR-EGFP-WPRE, PA-EGFP-WPRE and PR-EGFP-WPRE (p>0.05). Thus, over-expression of the dipeptides causes varying degrees of neuro-toxicity in the chick embryo spinal cord with GA being the most toxic and GP being the least toxic.

Magnified images of the GFP staining on spinal sections transfected with the dipeptide repeats, showed differential expression for the different dipeptides. GA-EGFP-WPRE expression was completely nuclear. The EGFP staining appears to be aggregated in the nucleus. PR-EGFP-WPRE, GP-EGFP-WPRE, GR-EGFP-WPRE were expressed in the cell. GR-EGFP-WPRE was expressed in the cytoplasm of the cell body and not in the nucleus. PA-EGFP-WPRE expression was seen throughout the neuron (Fig 5.11). This difference in expression pattern might explain the varying toxicity exhibited by the dipeptides. The aggregation of GA-EGFP-WPRE in the nucleus could confer its toxicity.

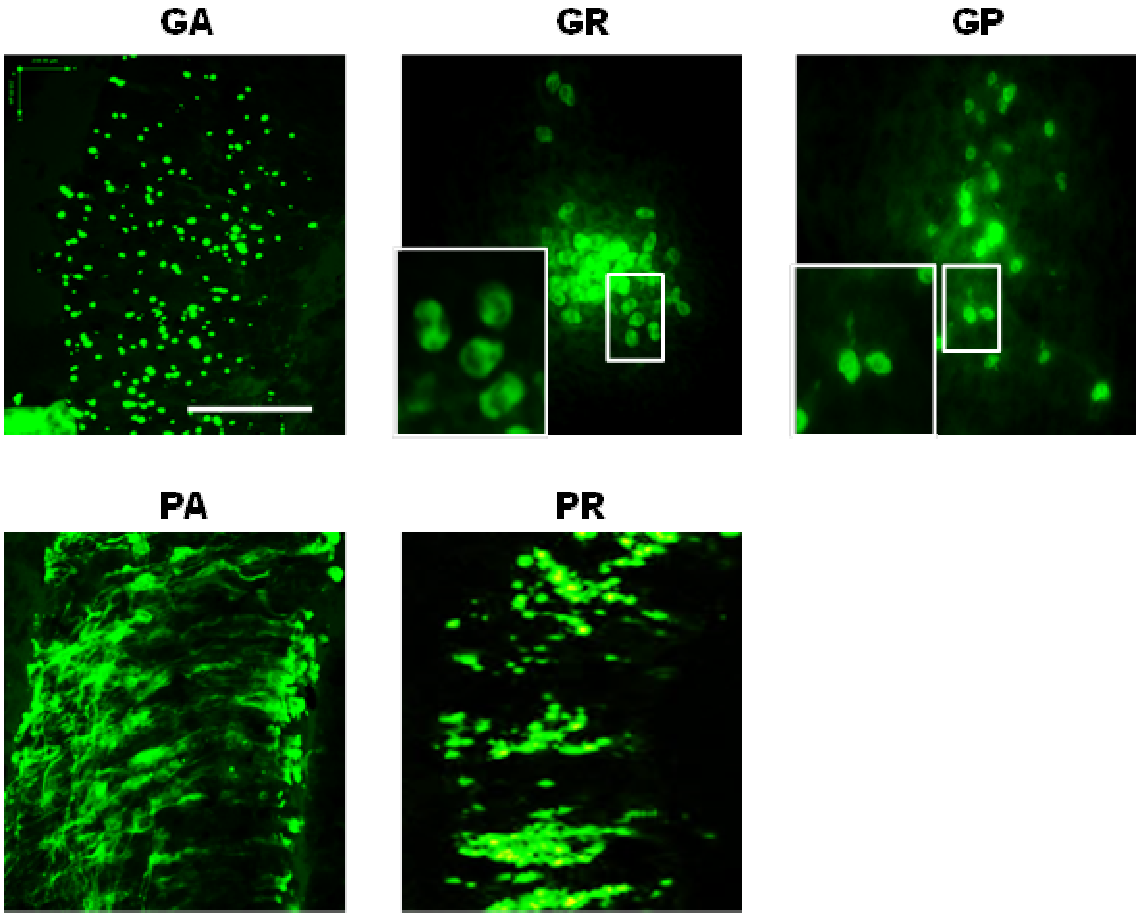

Figure 5.11 The dipeptides are differentially expressed
Representative images from embryos electroporated with EGFP-WPRE tagged sense and anti-sense dipeptides and control EGFP constructs in the spinal cord. GA-EGFP-WPRE and PR-EGFP-WPRE are expressed in the nucleoli. PA-EGFP-WPRE is expressed along the entire neuron. GR-EGFP-WPRE and GP-EGFP-WPRE are expressed in the cell body (magnified in inset). Scale bar = 100 µm.

Thus both the G4C2 hexanucleotide expansion repeats (RNA toxicity) and the dipeptides (protein toxicity) confer neurotoxicity in vivo in chick spinal cord. In order to determine which of the two was more toxic, the dipeptide toxicity was compared to the EGFP-128x toxicity since the dipeptides were synthesised from constructs encoding ~ 125x repeats. The average number of TUNEL positive cells for the EGFP-128x construct was about ~ 35, whereas the average number of TUNEL positive cells for GA-EGFP-WPRE was ~80. GA-EGFP-WPRE shows ~2 fold increase compared to the EGFP-128x. Except for GP-EGFP-WPRE which was the least toxic, all the other dipeptides have an equal or greater number of TUNEL positive cells compared to the EGFP-128x. GR-EGFP-WPRE and PA-EGFP-WPRE have approximately the same number of TUNEL positive cells as EGFP-128x whilst PR-EGFP-WPRE has a slightly higher average number

of TUNEL positive cells compared to EGFP. This shows that the dipeptides are more toxic than the RNA mediated toxicity.

In summary, we show that over-expression of both the longer G4C2 hexanucleotide expansion repeats and the dipeptides confer neurotoxicity *in vivo* in the chick. The longer G4C2 hexanucleotide repeat expansions form more RNA foci. Over-expression of the longer repeats affect motor neurons and motor axon projections. Similar phenotypes were observed with the over-expression of TDP-43 wild-type and mutant isoforms (Tripathi et al., 2014), suggesting that a common mechanism might link *C9ORF72* and *TDP-43* to ALS and FTLD.

5.3 Discussions

The mechanism of neurotoxicity in C9orf72 disease is unknown. In order to better understand neurotoxicity in C9orf72 disease, chick embryos were used to model the RNA based toxicity and the dipeptide repeat toxicity.

The observations from this work showed that the longer G4C2 repeats cause toxicity *in vivo* in chick spinal cords. Longer G4C2 hexanucleotide expansion repeats form more RNA foci. The longer repeats affect motor neurons and have defective axonal projections. The sense and anti-sense dipeptides also cause toxicity *in vivo* with GA-EGFP-WPRE being the most toxic and GP-RGFP-WPRE being the least toxic. All the dipeptides are differentially expressed with some being expressed only in the nucleus, with others being expressed in the cell-body or cytoplasm of the neuronwhilst one is expressed throughout the neuron. The differential expression might explain their varying toxicity as GA-EGFP-WPRE has an aggregation like expression that might account for this dipeptide being the most toxic.

5.3.1 Longer G4C2 hexanucleotide repeats confer neurotoxicity

G4C2 repeat length is important in establishing its pathogenicity (DeJesus-Hernandez et al., 2011, Renton et al., 2011). The number of G4C2 repeat length sufficient to produce pathological phenotypes varies in different animal and cellular models indicating that the C9ORF72 hexanucleotide repeat expansion may be unstable. This

instability may be particularly relevant for sporadic ALS, where the apparent random nature of the disease in the community could be a consequence of stochastic expansion in the number of repeats (Renton et al., 2011). The exact number of repeats and hence the precise threshold for disease is still unclear due to difficulties in accurately handling and sequencing DNA with such high GC contents.

Over-expression of longer G4C2 repeats is toxic when compared to control EGFP and EGFP-8x repeat length. This toxicity is dose-dependent as electroporation of the same constructs at lower concentrations (2 µg/µl) showed fewer number of apoptotic cells. EGFP-38x repeats and EGFP-72x G4C2 repeats had the most toxicity with no significant difference between them. The EGFP-128x G4C2 repeats were also toxic, but the number of apoptotic cells was significantly lower than the EGFP-72x repeats. GFP expression of EGFP-128x repeats is expressed along the neurons. However, there were a lot of gaps in the Hoechst staining, indicating missing cells and the cells appeared unhealthy and did not project any axons. This implies that the EGFP-128x constructs might be toxic but the cells are being cleared off at an earlier time point.

Studies have also shown that repeat length as short as ~22 can cause symptoms of FTD and that the length number could vary between tissues (Gómez-Tortosa et al., 2013). Also varying repeat lengths in various organisms have shown to produce different levels of toxicity. These wide variations and differential dosage could explain the difference in toxicity.

Our results complement other studies that relate the cellular toxicity of hexanucleotide repeat expansion directly with G4C2 repeat length, indicating that the longer the repeat, the more toxic its nature (Lee et al., 2013b).

5.3.2 G4C2 hexanucleotide expansions form intranuclear RNA foci *in vivo*

RNA foci were first observed in the frontal cortex and spinal cord of C9orf72 patients (DeJesus-Hernandez et al., 2011) and a number of studies have presented evidence for the presence of both sense and antisense intra-nuclear RNA foci in disease-relevant CNS regions of C9orf72 patients, including frontal cortex, cerebellum, hippocampus,

and spinal neurons as well as in non-neuronal cells (Gendron et al., 2013, Lagier-Tourenne et al., 2013, Mizielinska and Isaacs, 2014, Zu et al., 2011). Evidence from cellular and *in vivo* studies indicates that longer G4C2 repeats lead to the nuclear retention of transcripts, forming RNA foci that are RNase resistant and potently toxic (Lee et al., 2013b). Through fluorescent *in situ* hybridisation using G4C2 probes, we detected the presence of RNA foci in embryos electroporated with the longer repeats (EGFP-38x, EGFP-72x, EGFP-128x). EGFP control and the EGFP-8x repeats transfected tissues did not show any RNA foci. A manual quantification of the number of RNA foci showed that EGFP-128x and EGFP-72x had more foci (>250) than the EGFP-38x (<120). Also the EGFP-128x, showed a number of RNA foci on the contralateral side, indicating that the toxicity spreads. This data complements other findings wherein repeat length-dependent formation of RNA foci have been observed in numerous cell types, primary neurons and zebrafish embryos ectopically expressing G4C2 repeat sequences (Lee et al., 2013b). Thus, we show that expression of EGFP-38x, EGFP-72x and EGFP-128x G4C2 repeats *in vivo* form intranuclear RNA foci that co-relate with the length-dependent G4C2 toxicity. Studies suggest these RNA foci sequester RNA binding proteins (Todd and Paulson, 2010) and that the foci-bound RNA binding proteins cannot regulate their RNA targets and that this impaired RNA metabolism leads to neurodegeneration.

5.3.3 G4C2 hexanucleotide repeats affect motor neurons and motor axon projections

Chick embryos injected with the G4C2 longer repeats (EGFP-38x, EGFP-72x, EGFP-128x) show a reduction in the number of motor neurons. The EGFP-128x had less number of motor neurons on the control side to begin with. This implies that the long repeats affect motor neurons on the control side as well as the electroporated side. This correlates with the contralateral spread of RNA foci. EGFP-72x had the least number of motor neurons on the electroporated side when compared to the control side.

The longer repeats also exhibit abnormal motor defects such as defasciculation/ debundling and truncation. We have observed similar phenotypes *in vivo* in chick embryos injected with the TDP-43 wild-type and mutant constructs (Tripathi et al.,

2014). Though it is not certain whether the relationship between motor projections morphology and pathology is causative or symptomatic, the results nevertheless establish that changes in motor axon projection are a useful indication of ALS-like pathology in the chick model systems. This pattern indicates that expression of the expansion alone is sufficient to produce ALS-like pathology that is related to repeat length. The defasciculation and truncation of motor neurons is thought to be caused by mis-regulation of the cytoskeleton. Patients with C9orf72 repeat expansion mutations show several unique pathological features, one such wherein C9ORF72 expansion cases show a combination of FTLD-TDP and classical ALS with abnormal accumulation of TDP-43 into neuronal and oligodendroglial inclusions consistently seen in the frontal and temporal cortex, hippocampus and pyramidal motor system (Mackenzie et al., 2013). *C9ORF72* repeat expansions in mice cause TDP-43 pathology, neuronal loss, and behavioural deficits (Chew et al., 2015). Several studies including ours contribute to the growing evidence that TDP-43 can regulate the neuronal cytoskeleton through its binding with NFL (strong et al., 2007); MAP1B (Coyne et al., 2014) and that the mis-regulation of TDP-43 is a key step in the ALS pathomechanism. Since similar motor defecit phenotypes are observed with the G4C2 hexanucleotide repeats, we propose that there might be a shared pathogenic mechanism common to both TDP-43 and C9orf72. We speculate that C9orf72 mediated G4C2 RNA foci can sequester TDP-43 and aberrant RNA processing through mis-regulation of TDP-43 contributes to ALS pathology.

5.3.4 Dipeptides cause toxicity in chick spinal cord *in vivo*

Another proposed mechanism for neurodegeneration in G4C2 repeat mutation in C9orf72 is the RAN translation of the G4C2 repeats resulting in the accumulation of sense and anti-sense dipeptide repeats. Our results show that over-expression of the dipeptide repeats in chick spinal cord cause neurotoxicity. GA-EGFP was found to be the most toxic while GP-EGFP had the least toxicity. The variability in the level of GFP-DPR expression *in vivo* may be due to arginine rich sequences. A magnified image of the GFP expression of the dipeptides shows that they are differentially expressed. GA-EGFP is expressed only in the nucleus while PR-EGP and GP-EGFP are expressed in the

cell body. GR-EGFP expression is perinuclear and PA-EGFP is expressed throughout the neurons. The differential localisation of the dipeptides may contribute to their toxicity.

Over-expression models have been invaluable tools to study neurodegenerative diseases but abnormally high levels of the aggregating proteins could also complicate the interpretation. Though several groups have worked on the toxicity of the dipeptide repeats, the results as to which dipeptide is the most toxic are conflicting with some suggesting that GR is the most toxic (Kwon et al., 2014, Mizielinska et al., 2014) while others suggest that GA is the most toxic (Zhang et al., 2014, May et al., 2014). However, studies have suggested that poly GA is the main aggregating species in FTLD-UPS and that p62 co-localizes more abundantly with GA and to a lesser extent with GR and GP (Mori et al., 2013a). A recent study has implied that the presence of the DPR might not be a relevant factor in the pathogenic mechanism because DPR inclusions are rarely found in the spinal cord and are almost absent from motor neurons in C9orf72 mutant ALS and are unlikely to cause their degeneration (Gomez-Deza et al., 2015). While there is no doubt that DPR pathology is a highly specific pathological feature in C9ORF72 expansion carriers, its pathomechanistic relevance is less clear and further investigation about their distribution patterns, selective vulnerability and solubility are needed to understand their role in ALS pathology.

When the dipeptide toxicity was compared to the EGFP-128x repeat mediated toxicity, it was found that the dipeptides conferred more toxicity than the EGFP-128x. All of the dipeptides except GP-EGFP had an equal or greater number of TUNEL positive cells compared to EGFP-128x. GA-EGFP which is the most toxic dipeptide had a 2 fold increase in toxicity compared to EGFP-128x. However, studies have shown that dipeptides are rarely found (Gomez-Deza et al., 2015) and only very long G4C2 hexanucleotide expansion repeats can produce detectable amounts of dipeptides (Mori et al., 2013a). DPR pathology is a direct consequence of the G4C2 hexanucleotide expansion repeat and it is G4C2 expansion repeats that form RNA foci that may sequester other RBPs. Thus, it appears that the two mechanisms might be related *in vivo* and cannot be separately distinguished.

Thus, we have efficiently modelled the RNA and the dipeptide toxicity of the C9orf72 mutant G4C2 hexanucleotide expansion repeats *in vivo* using the chick system.

Although the mechanisms underlying the toxicity of the G4C2 mutants are not fully understood, we propose that RNA toxicity and protein sequestration may disrupt RNA processing and lead to neurodegeneration. The toxicity due to RNA foci and RAN translation are not mutually exclusive to ALS, and their relative contribution to repeat-associated neurodegenerative disorders requires further investigation.

6 Conclusions and Future Directions

6.1 Conclusions

ALS is a devastating neurodegenerative disorder that results in the loss of all voluntary movement and is fatal in the majority of cases. It is a multi-systems disease with genetic variability affecting several pathways. The exact mechanisms underlying ALS have not been pinned down but several speculative mechanisms have been proposed that lead to neurodegeneration.

The focus of this study was mainly to shed some light on the mechanisms underlying ALS with respect to *TDP-43* and *C9orf72*. Both *TDP-43* and *C9orf72* are major players in ALS because the hexanucleotide repeat expansion in *C9orf72* is the most common genetic variant of ALS and FTLD and TDP-43 inclusions are a hallmark feature of ALS and FTLD. Our previous study focused on the toxicity of TDP-43 *in vivo* in chick embryonic spinal cord, wherein we observed that TDP-43 wild-type and mutants mis-localize to the cytoplasm over time and that over-expression of TDP-43 is neurotoxic. The study also showed that TDP-43 affects motor axon morphology and reduced axonal outgrowth of motor neurons implying that the cytoskeleton is a target of TDP-43 dysfunction (Tripathi et al., 2014).

We have shown that TDP-43 mis-localises and aggregates *in vitro* in cortical cultures and that the re-distribution is more enhanced compared to the TDP-43 mis-localisation in spinal motor neurons. Over-expression of TDP-43 wild-type and mutant proteins is toxic to cortical neurons and both aggregation and toxicity progresses with time. This is evident by the fact that apoptosis occurs only in a proportion of the transfected cells implying that at least a proportion of cortical neurons which express TDP-43 wild-type and mutant isoforms can extend axons and function normally. Though TDP-43 aggregation can cause toxicity, the role of TDP-43 aggregation in neurodegeneration is still not clear. Studies have shown that TDP-43 mis-localisation rather than aggregation confers toxicity (Barmada et al., 2010). TDP-43 mediated apoptosis breaks down the neuronal cytoskeleton suggesting that loss of cytoskeletal structure is integral to TDP-43 pathology.

Rat cortical cells transfected with TDP-43 wild-type and mutant proteins show varying phenotypes related to cytoskeletal functions. TDP-43 impairs axon outgrowth, growth

cone dynamics, anterograde transport and subcellular localisation of target mRNAs. TDP-43 affects axonal outgrowth in cortical neurons suggesting a link between TDP-43 and axon maintenance. Our data is in conjunction with other studies, showing that over-expression of wild-type in transgenic mice impairs axonal growth (Fallini et al., 2012) and affects the regenerative response following nerve injury (Swarup et al., 2012). TDP-43 transfected neurons have smaller growth cones and exhibit a stalling phenotype implying a defect in microtubule/actin dynamics. TDP-43 affects microtubule-dependent anterograde transport of EB3s. TDP-43 transfected neurons show a reduction in numbers and in the speed of EB3s which reflects slower microtubule dynamics that correlate with the observed shorter neurite length and growth cone stalling.

RNA transport and local translation are critical for the development and function of polarized cells in diverse organisms. RNA-binding proteins (RBPs) are the local regulators of translation and they play an important role in growth, guidance, and synapse formation in developing axons. TDP-43 as a RBP regulates RNA metabolism at multiple levels, including transcription, RNA splicing, mRNA transport and stability. TDP-43 is known to regulate and bind to the 3'UTR of cytoskeletal mRNAs such as: *Map1B* (Coyne et al., 2014), *β-actin* (Wang et al., 2008, Ayala et al., 2011) and *NFL* (Strong et al., 2007) implicating its importance in axonal functions such axon outgrowth, synapse formation, axon growth and branching. (Fallini et al., 2012, Kabashi et al., 2010, Godena et al., 2011, Lin et al., 2011). Studies have shown that TDP-43 impairs axonal transport of mRNA granules like *NFL* and that plays an important role in cytoskeletal structure. TDP-43 mis-localises the distribution of *β-actin*, Kif2a, *Map1B*, *Map2*, *Nd1-L* and *NFL* and affects their expression. A change in expression occurs around 72 hours, correlating with toxicity and aggregation. The changes in expression of cytoskeletal mRNA can be associated with the observed cytoskeletal phenotypes. Thus, mis-regulation of target RNA by TDP-43 is an important step in ALS pathogenesis.

TDP-43 auto-regulates its own levels and several studies have shown that the level of TDP-43 is important as perturbations in the levels of cytoplasmic/axonal TDP-43 can affect several processes such as mRNA transport and stabilityand mRNA splicing. Thus,

cytoplasmic mis-localisation and autoregulation of TDP-43 are key concepts that affect several other regulation processes. Axonal mRNA transport is considered to be a key feature in RBPs mediated neurodegeneration. Axonal mRNA transport is a necessity for local translation. Genetic linkage studies have found a new risk gene in ALS called TUB4A (tubulin alpha 4a), which further implicates defects in the cellular transport system as a cause of the disease (Smith et al., 2014). Motor neuron loss is the characteristic trait of ALS. Dysregulation of cytoskeletal function and structure causes neuronal disintegration and damage. Thus, cytoskeletal proteins could be used as biomarkers to predict cell death. We speculate that impairment in the mRNA regulation of its binding partners may contribute to neurodegeneration via dysregulation of the axonal cytoskeleton.

In vivo findings provide experimental evidence that longer G4C2 repeats form more RNA foci that correlate with toxicity. The repeat length is important for formation of RNA foci and dipeptides but the relevance between repeat length and toxicity is not clear as the results are varied. This could be due to the instability of the longer repeats. The data complements other studies that show that cellular toxicity is associated with the nuclear retention of transcripts containing 38x, 72x and 128x repeats and the appearance of RNA foci (Lee et al., 2013). Studies have shown that only very long repeats of the G4C2 hexanucleotide expansion can produce the dipeptide repeats which are otherwise quite rare in distribution (Mori et al., 2013a), thereby attesting the importance of repeat length in the C9orf72 pathology. Longer G4C2 hexanucleotide expansion repeats affect motor neurons. They also show aberrant truncations and de-fasciculation of the axon projections *in vivo*. This data is consistent with the motor defects (locomotive behaviour) seen in the G4C2 transgenic mice (Chew et al., 2015).

We have shown that the dipeptides like the G4C2 foci are also toxic. Though the dipeptides appear to be more toxic than the repeats, the fact that dipeptides are rarely found in the spinal cord of patients (Gomez-Deza et al., 2015) implies that the observed toxic effects are only due to the over-expression of the dipeptides. On the other hand, the longer G4C2 repeats show deficit motor axon phenotype and motor neuron degeneration similar to TDP-43, indicating that RNA toxicity might play a bigger

role in the *C9ORF72* mechanism. However, the mechanisms behind this toxicity are not fully understood but have led to the speculation that both protein aggregation (Dipeptides) and RNA mis-processing (RNA foci) play an important role in ALS pathology.

Studies have shown that dipeptide inclusions can rarely co—localize with TDP-43 (Gomez-Deza et al., 2015) and that C9ORF72 cases all have widespread TDP-43 neuropathology in brain areas that show atrophy. These findings link TDP-43 and C9orf72 pathology but it still remains to be seen as to how TDP-43 pathology fits in with *C9ORF72*. TDP-43 wild-type and mutant proteins confer neurotoxicity and cause premature truncation and defasiculation of axons *in vivo* (Tripathi et al., 2014), similar to the toxicity and axon projection defects seen with the longer G4C2 repeats. FTLD and ALS cases with C9ORF72 expansions showed TDP-43-positive neuronal and glial inclusions and a higher proportion of nuclear RNA foci in frontal cortex and spinal cord neurons (Cooper-Knock et al., 2012). Thus the toxicity and motor defects caused by the G4C2 hexanucleotide repeats and TDP-43 *in vivo* in the spinal cord of the chick can be related to the spinal cord pathology in patients. This suggests that a common mechanism might link the two, wherein C9ORF72 RNA foci could sequester TDP-43, which is a RBP, resulting in motor deficits and toxicity.

Many advances have been made in the field of ALS that have brought to light new research information on complex genetic and environmental factors involved in ALS. Several research groups have been working on understanding the molecular mechanisms in ALS, finding appropriate biomarkers, developing new therapies, starting new clinical trials. Projects are being set up to share data across countries so as to set up the largest collection of ALS data. This open access to a large amount of data will help researchers analyse large amounts of information on the disease, drawing on clinical, chemical, genetic, protein, historical and biological information from ALS patients across the world. New technology, better models of study and collaborative research have changed our understanding of ALS. Researchers all over the world are working on finding a cure and translating research into significant therapies. The field of ALS has made a lot of progress with many more possibilities yet to be ascertained.

6.2 Limitations of the model system

In this study, we have used both *in vivo* and *in vitro* systems to model different aspects of TDP-43 and C9orf72 pathology. These models provide excellent possibilities for further characterisation and understanding of the mechanisms of FTD/ALS pathogenesis as well as for testing emerging therapeutic approaches. *In vitro* studies provide useful information regarding cellular and molecular mechanisms in a specific cell-type manner while, experiments in whole living animal models reflect more closely the human disease. Using these model systems, multiple cellular pathways have been identified including, protein misfolding, RNA processing, oxidative stress, excitotoxicity, axonal transport, mitochondrial dysfunction and abnormal secretion of proteins. Nevertheless, how accurately these animal models replicate all ALS clinical symptoms of the human illness remains unanswered. The animal and cellular models lack the proof of their relevance to the ALS human disease. Only partial patient phenotypes are observed and not all models define clear neurodegeneration. There are confounding variables in the interpretation of these models: the presence of the endogenous non-mutated protein, variations in the expression level of the transgene, type of mutation and the species used. There are multiple–pathways that are simultaneously affected, leaving no clear demarcation between cause and symptoms. The major drawbacks of cell cultures are the need to perform cell extraction from embryos for each new experiment. In addition, cells cultured on plastic dishes cannot recapitulate the *in vivo* environment and some results obtained *in vitro* may not be reproducible *in vivo* because of the complex interactions developed in the nervous system. Furthermore, another disadvantage of using primary cells from embryos is that some features of the adult phenotype may not be expressed at this early stage (Park, et al., 2004). The current models do not take into account aging phenomenon and susceptibility factors which might account for the large variability of the onset of appearance of the symptoms. Therefore, an integrative model that links both genetic and environmental factors to reproduce the chronic progressive motor neuron death and the main characteristics of the disease is still needed.

6.3 Future Directions

When TDP-43 variants were expressed in cortical neurons, we also found several hallmark features of ALS, including cytoplasmic aggregates, cell death and several cytoskeletal functional defects affecting axonal outgrowth, growth cone dynamics, axonal transport and the distribution of subcellular target mRNA. It would be interesting to expand on these defects and focus on how TDP-43 mis-regulates the cytoskeletal mRNA/proteins related to the various cytoskeletal functions by co-localization experiments using live imaging to visualize the re-distribution and quantify the rate of transport. Growing cortical neurons in compartmentalized chambers and looking at the distribution of subcellular mRNA in the nuclear vs. distal vs. proximal regions of the axons and carrying out similar experiments in motor neurons to address the issue of cell specificity would also be important. We would also like to do a western blot of TDP-43 transfected wild-type and mutant neurons and check for the expression levels of the different cytoskeletal proteins to check for upregulation/downregulation. We would also like to see if TDP-43 affects protein synthesis by transfecting neurons with mRNAs tagged with a fluorescent protein, Kaede, to follow the rate of recovery of de novo protein synthesis. In order to check if TDP-43 and C9orf72 share common mechanisms of neurodegeneration, we would like to co-electroporate chick embryos with G4C2 longer repeats and TDP-43 wild-type and mutant constructs to analyse toxicity, patterns of distribution and axon projection defects. Dipeptide repeats are rarely found in the spinal cord and are completely absent in motor neurons (Gomez-Deza et al., 2015). The motor axon projections should be analysed and checked for motor neuron toxicity in chick embryos over-expressing the dipeptide repeats in the spinal cord. These experiments would help us characterise the role of TDP-43 and C9orf72 in ALS pathology and shed more light on the RNA mis-processing mechanisms leading to neurodegeneration.

References

1. ABHYANKAR, M. M., UREKAR, C. & REDDI, P. P. 2007. A Novel CpG-free Vertebrate Insulator Silences the Testis-specific SP-10 Gene in Somatic Tissues ROLE FOR TDP-43 IN INSULATOR FUNCTION. *Journal of Biological Chemistry,* 282**,** 36143-36154.

2. ACHI, E. Y. & RUDNICKI, S. A. 2012. ALS and Frontotemporal Dysfunction: A Review. *Neurol Res Int,* 2012**,** 806306.

3. AKIMOTO, C., VOLK, A. E., VAN BLITTERSWIJK, M., VAN DEN BROECK, M., LEBLOND, C. S., LUMBROSO, S., CAMU, W., NEITZEL, B., ONODERA, O. & VAN RHEENEN, W. 2014. A blinded international study on the reliability of genetic testing for GGGGCC-repeat expansions in C9orf72 reveals marked differences in results among 14 laboratories. *Journal of medical genetics,* 51**,** 419-424.

4. AL-SARRAJ, S., KING, A., TROAKES, C., SMITH, B., MAEKAWA, S., BODI, I., ROGELJ, B., AL-CHALABI, A., HORTOBAGYI, T. & SHAW, C. E. 2011. p62 positive, TDP-43 negative, neuronal cytoplasmic and intranuclear inclusions in the cerebellum and hippocampus define the pathology of C9orf72-linked FTLD and MND/ALS. *Acta Neuropathol,* 122**,** 691-702.

5. ALAMI, N. H., SMITH, R. B., CARRASCO, M. A., WILLIAMS, L. A., WINBORN, C. S., HAN, S. S., KISKINIS, E., WINBORN, B., FREIBAUM, B. D. & KANAGARAJ, A. 2014. Axonal transport of TDP-43 mRNA granules is impaired by ALS-causing mutations. *Neuron,* 81**,** 536-543.

6. ALMEIDA, S., GASCON, E., TRAN, H., CHOU, H. J., GENDRON, T. F., DEGROOT, S., TAPPER, A. R., SELLIER, C., CHARLET-BERGUERAND, N. & KARYDAS, A. 2013. Modeling key pathological features of frontotemporal dementia with C9ORF72 repeat expansion in iPSC-derived human neurons. *Acta neuropathologica,* 126**,** 385-399.

7. ARAI, T., HASEGAWA, M., AKIYAMA, H., IKEDA, K., NONAKA, T., MORI, H., MANN, D., TSUCHIYA, K., YOSHIDA, M. & HASHIZUME, Y. 2006. TDP-43 is a component of ubiquitin-positive tau-negative inclusions in frontotemporal lobar degeneration and amyotrophic lateral sclerosis. *Biochemical and biophysical research communications,* 351**,** 602-611.

8. ARNOLD, E. S., LING, S.-C., HUELGA, S. C., LAGIER-TOURENNE, C., POLYMENIDOU, M., DITSWORTH, D., KORDASIEWICZ, H. B., MCALONIS-DOWNES, M., PLATOSHYN, O. & PARONE, P. A. 2013. ALS-linked TDP-43 mutations produce aberrant RNA splicing and adult-onset motor neuron disease without aggregation or loss of nuclear TDP-43. *Proceedings of the National Academy of Sciences,* 110**,** E736-E745.

9. ASH, P. E., BIENIEK, K. F., GENDRON, T. F., CAULFIELD, T., LIN, W.-L., DEJESUS-HERNANDEZ, M., VAN BLITTERSWIJK, M. M., JANSEN-WEST, K., PAUL, J. W. & RADEMAKERS, R. 2013. Unconventional translation of C9ORF72 GGGGCC expansion generates insoluble polypeptides specific to c9FTD/ALS. *Neuron,* 77**,** 639-646.

10. ATKINSON, R. A., FERNANDEZ-MARTOS, C. M., ATKIN, J. D., VICKERS, J. C. & KING, A. E. 2015. C9ORF72 expression and cellular localization over mouse development. *Acta neuropathologica communications,* 3**,** 1.

11. AVILA, J., LUCAS, J. J., PEREZ, M. & HERNANDEZ, F. 2004. Role of tau protein in both physiological and pathological conditions. *Physiol Rev,* 84**,** 361-84.

12. AYALA, Y. M., DE CONTI, L., AVENDANO-VAZQUEZ, S. E., DHIR, A., ROMANO, M., D'AMBROGIO, A., TOLLERVEY, J., ULE, J., BARALLE, M., BURATTI, E., et al. 2011. TDP-43 regulates its mRNA levels through a negative feedback loop. *EMBO J,* 30**,** 277-88.

13. AYALA, Y. M., ZAGO, P., D'AMBROGIO, A., XU, Y.-F., PETRUCELLI, L., BURATTI, E. & BARALLE, F. E. 2008. Structural determinants of the cellular localization and shuttling of TDP-43. *Journal of cell science,* 121**,** 3778-3785.

14. BAK, T. H. 2010. Motor neuron disease and frontotemporal dementia: One, two, or three diseases? *Annals of Indian Academy of Neurology,* 13**,** 81.

15. BALOH, R. H. 2011. TDP-43: the relationship between protein aggregation and neurodegeneration in amyotrophic lateral sclerosis and frontotemporal lobar degeneration. *FEBS J,* 278**,** 3539-49.

16. BARMADA, S. J., SERIO, A., ARJUN, A., BILICAN, B., DAUB, A., ANDO, D. M., TSVETKOV, A., PLEISS, M., LI, X. & PEISACH, D. 2014. Autophagy induction enhances TDP43 turnover and survival in neuronal ALS models. *Nature chemical biology,* 10**,** 677-685.

17. BARMADA, S. J., SKIBINSKI, G., KORB, E., RAO, E. J., WU, J. Y. & FINKBEINER, S. 2010. Cytoplasmic mislocalization of TDP-43 is toxic to neurons and enhanced by a mutation associated with familial amyotrophic lateral sclerosis. *J Neurosci,* 30**,** 639-49.

18. BECK, J., POULTER, M., HENSMAN, D., ROHRER, J. D., MAHONEY, C. J., ADAMSON, G., CAMPBELL, T., UPHILL, J., BORG, A., FRATTA, P., et al. 2013. Large C9orf72 hexanucleotide repeat expansions are seen in multiple neurodegenerative syndromes and are more frequent than expected in the UK population. *Am J Hum Genet,* 92**,** 345-53.

19. BELZIL, V. V., BAUER, P. O., PRUDENCIO, M., GENDRON, T. F., STETLER, C. T., YAN, I. K., PREGENT, L., DAUGHRITY, L., BAKER, M. C. & RADEMAKERS, R. 2013. Reduced C9orf72 gene expression in c9FTD/ALS is caused by histone trimethylation, an epigenetic event detectable in blood. *Acta neuropathologica,* 126**,** 895-905.

20. BENAJIBA, L., LE BER, I., CAMUZAT, A., LACOSTE, M., THOMAS-ANTERION, C., COURATIER, P., LEGALLIC, S., SALACHAS, F., HANNEQUIN, D. & DECOUSUS, M. 2009. TARDBP mutations in motoneuron disease with frontotemporal lobar degeneration. *Annals of neurology,* 65**,** 470-473.

21. BERTHOD, F. & GROS-LOUIS, F. 2012. *In Vivo and In Vitro Models to Study Amyotrophic Lateral Sclerosis*, Citeseer.

22. BIGIO, E. H., WU, J. Y., DENG, H.-X., BIT-IVAN, E. N., MAO, Q., GANTI, R., PETERSON, M., SIDDIQUE, N., GEULA, C. & SIDDIQUE, T. 2013. Inclusions in frontotemporal lobar degeneration with TDP-43 proteinopathy (FTLD-TDP) and amyotrophic lateral sclerosis (ALS), but not FTLD with FUS proteinopathy (FTLD-FUS), have properties of amyloid. *Acta neuropathologica,* 125**,** 463.

23. BILSLAND, L. G., SAHAI, E., KELLY, G., GOLDING, M., GREENSMITH, L. & SCHIAVO, G. 2010. Deficits in axonal transport precede ALS symptoms in vivo. *Proc Natl Acad Sci U S A,* 107**,** 20523-8.

24. BOEVE, B. F., BOYLAN, K. B., GRAFF-RADFORD, N. R., DEJESUS-HERNANDEZ, M., KNOPMAN, D. S., PEDRAZA, O., VEMURI, P., JONES, D., LOWE, V. & MURRAY, M. E. 2012. Characterization of frontotemporal dementia and/or amyotrophic lateral sclerosis associated with the GGGGCC repeat expansion in C9ORF72. *Brain,* 135**,** 765-783.

25. BORRONI, B., GHEZZI, S., AGOSTI, C., ARCHETTI, S., FENOGLIO, C., GALIMBERTI, D., SCARPINI, E., DI LUCA, M., BRESOLIN, N., COMI, G. P., et al. 2008. Preliminary evidence that VEGF genetic variability confers susceptibility to frontotemporal lobar degeneration. *Rejuvenation Res,* 11**,** 773-80.

26. BORRONI, B., GRASSI, M., AGOSTI, C., COSTANZI, C., ARCHETTI, S., FRANZONI, S., CALTAGIRONE, C., DI LUCA, M., CAIMI, L. & PADOVANI, A. 2006. Genetic correlates of behavioral endophenotypes in Alzheimer disease: role of COMT, 5-HTTLPR and APOE polymorphisms. *Neurobiol Aging,* 27**,** 1595-603.

27. BORRONI, B., GRASSI, M., AGOSTI, C., PREMI, E., ARCHETTI, S., ALBERICI, A., BELLELLI, G., CAIMI, L., DI LUCA, M. & PADOVANI, A. 2010. Establishing short-term prognosis in Frontotemporal Lobar Degeneration spectrum: role of genetic background and clinical phenotype. *Neurobiol Aging,* 31**,** 270-9.

28. BOSE, J. K., WANG, I.-F., HUNG, L., TARN, W.-Y. & SHEN, C.-K. J. 2008. TDP-43 overexpression enhances exon 7 inclusion during the survival of motor neuron pre-mRNA splicing. *Journal of Biological Chemistry,* 283**,** 28852-28859.

29. BOXER, A. L., MACKENZIE, I. R., BOEVE, B. F., BAKER, M., SEELEY, W. W., CROOK, R., FELDMAN, H., HSIUNG, G.-Y. R., RUTHERFORD, N. & LALUZ, V. 2010. Clinical, neuroimaging and neuropathological features of a new chromosome 9p-linked FTD-ALS family. *Journal of Neurology, Neurosurgery & Psychiatry***,** jnnp. 2009.204081.

30. BOXER, A. L. & MILLER, B. L. 2005. Clinical features of frontotemporal dementia. *Alzheimer Disease & Associated Disorders,* 19**,** S3-S6.

31. BRADY, O. A., MENG, P., ZHENG, Y., MAO, Y. & HU, F. 2011. Regulation of TDP-43 aggregation by phosphorylation andp62/SQSTM1. *Journal of neurochemistry,* 116**,** 248-259.

32. BRAUN, R. J., SOMMER, C., CARMONA-GUTIERREZ, D., KHOURY, C. M., RING, J., BÜTTNER, S. & MADEO, F. 2011. Neurotoxic 43-kDa TAR DNA-binding protein (TDP-43) triggers mitochondrion-dependent programmed cell death in yeast. *Journal of Biological Chemistry,* 286**,** 19958-19972.

33. BRETTSCHNEIDER, J., VAN DEERLIN, V. M., ROBINSON, J. L., KWONG, L., LEE, E. B., ALI, Y. O., SAFREN, N., MONTEIRO, M. J., TOLEDO, J. B., ELMAN, L., et al. 2012. Pattern of ubiquilin pathology in ALS and FTLD indicates presence of C9ORF72 hexanucleotide expansion. *Acta Neuropathol,* 123**,** 825-39.

34. BRUIJN, L. I., MILLER, T. M. & CLEVELAND, D. W. 2004. Unraveling the mechanisms involved in motor neuron degeneration in ALS. *Annu. Rev. Neurosci.,* 27**,** 723-749.

35. BUCHMAN, V. L., COOPER-KNOCK, J., CONNOR-ROBSON, N., HIGGINBOTTOM, A., KIRBY, J., RAZINSKAYA, O. D., NINKINA, N. & SHAW, P. J. 2013. Simultaneous and independent detection of C9ORF72 alleles with low and high number of GGGGCC repeats using an optimised protocol of Southern blot hybridisation. *Molecular neurodegeneration,* 8**,** 1-6.

36. BURATTI, E. & BARALLE, F. E. 2001. Characterization and Functional Implications of the RNA Binding Properties of Nuclear Factor TDP-43, a Novel Splicing Regulator ofCFTR Exon 9. *Journal of Biological Chemistry,* 276**,** 36337-36343.

37. BURATTI, E. & BARALLE, F. E. 2009. The Molecular Links Between TDP-43 Dysfunction and Neurodegeneration. *Advances in genetics,* 66**,** 1-34.

38. BURATTI, E. & BARALLE, F. E. 2010. The multiple roles of TDP-43 in pre-mRNA processing and gene expression regulation. *RNA biology,* 7**,** 420-429.

39. BURATTI, E., BRINDISI, A., GIOMBI, M., TISMINETZKY, S., AYALA, Y. M. & BARALLE, F. E. 2005. TDP-43 Binds Heterogeneous Nuclear Ribonucleoprotein A/B through Its C-terminal Tail AN IMPORTANT REGION FOR THE INHIBITION OF CYSTIC FIBROSIS TRANSMEMBRANE CONDUCTANCE REGULATOR EXON 9 SPLICING. *Journal of Biological Chemistry,* 280**,** 37572-37584.

40. BURATTI, E., DE CONTI, L., STUANI, C., ROMANO, M., BARALLE, M. & BARALLE, F. 2010. Nuclear factor TDP-43 can affect selected microRNA levels. *FEBS journal,* 277**,** 2268-2281.

41. BURATTI,E. & BARALLE, F. E. 2012. TDP-43: gumming up neurons through protein–protein and protein–RNA interactions. Trends in Biochemical Sciences, 37, 237 - 247.

42. BYRNE, S., HEVERIN, M., ELAMIN, M., WALSH, C. & HARDIMAN, O. 2014. Intermediate repeat expansion length in C9orf72 may be pathological in amyotrophic lateral sclerosis. *Amyotrophic Lateral Sclerosis and Frontotemporal Degeneration,* 15**,** 148-150.

43. CARRI, M. T., VALLE, C., BOZZO, F. & COZZOLINO, M. 2015. Oxidative stress and mitochondrial damage: importance in non-SOD1 ALS. *Front Cell Neurosci,* 9**,** 41.

44. CHEN, S., SAYANA, P., ZHANG, X. & LE, W. 2013. Genetics of amyotrophic lateral sclerosis: an update. *Mol Neurodegener,* 8**,** 28.

45. CHEN, S., ZHANG, X., SONG, L. & LE, W. 2012. Autophagy dysregulation in amyotrophic lateral sclerosis. *Brain Pathology,* 22**,** 110-116.

46. CHEW, J., GENDRON, T. F., PRUDENCIO, M., SASAGURI, H., ZHANG, Y.-J., CASTANEDES-CASEY, M., LEE, C. W., JANSEN-WEST, K., KURTI, A. & MURRAY, M. E. 2015. C9ORF72 repeat expansions in mice cause TDP-43 pathology, neuronal loss, and behavioral deficits. *Science,* 348**,** 1151-1154.

47. CHIANG, P.-M., LING, J., JEONG, Y. H., PRICE, D. L., AJA, S. M. & WONG, P. C. 2010. Deletion of TDP-43 down-regulates Tbc1d1, a gene linked to obesity, and alters body fat metabolism. *Proceedings of the National Academy of Sciences,* 107**,** 16320-16324.

48. CIRULLI, E. T., LASSEIGNE, B. N., PETROVSKI, S., SAPP, P. C., DION, P. A., LEBLOND, C. S., COUTHOUIS, J., LU, Y. F., WANG, Q., KRUEGER, B. J., et al. 2015. Exome sequencing in amyotrophic lateral sclerosis identifies risk genes and pathways. *Science,* 347**,** 1436-41.

49. CIURA, S., LATTANTE, S., LE BER, I., LATOUCHE, M., TOSTIVINT, H., BRICE, A. & KABASHI, E. 2013. Loss of function of C9orf72 causes motor deficits in a zebrafish model of amyotrophic lateral sclerosis. *Annals of neurology,* 74**,** 180-187.

50. CLEARY, J. D. & RANUM, L. P. 2013. Repeat-associated non-ATG (RAN) translation in neurological disease. *Hum Mol Genet,* 22**,** R45-51.

51. COOPER-KNOCK, J., HEWITT, C., HIGHLEY, J. R., BROCKINGTON, A., MILANO, A., MAN, S., MARTINDALE, J., HARTLEY, J., WALSH, T. & GELSTHORPE, C. 2012. Clinico-pathological features in amyotrophic lateral sclerosis with expansions in C9ORF72. *Brain,* 135**,** 751-764.

52. COOPER-KNOCK, J., KIRBY, J., HIGHLEY, R. & SHAW, P. J. 2015. The Spectrum of C9orf72-mediated Neurodegeneration and Amyotrophic Lateral Sclerosis. *Neurotherapeutics,* 12**,** 326-39.

53. COOPER, T. A., WAN, L. & DREYFUSS, G. 2009. RNA and disease. *Cell,* 136**,** 777-793.

54. COYLE-GILCHRIST, I. T., DICK, K. M., PATTERSON, K., VAZQUEZ RODRIQUEZ, P., WEHMANN, E., WILCOX, A., LANSDALL, C. J., DAWSON, K. E., WIGGINS, J., MEAD, S., et al. 2016. Prevalence, characteristics, and survival of frontotemporal lobar degeneration syndromes. *Neurology*.

55. COYNE, A. N., SIDDEGOWDA, B. B., ESTES, P. S., JOHANNESMEYER, J., KOVALIK, T., DANIEL, S. G., PEARSON, A., BOWSER, R. & ZARNESCU, D. C. 2014. Futsch/MAP1B mRNA is a translational target of TDP-43 and is neuroprotective in a Drosophila model of amyotrophic lateral sclerosis. *J Neurosci,* 34**,** 15962-74.

56. CRONIN, S., HARDIMAN, O. & TRAYNOR, B. J. 2007. Ethnic variation in the incidence of ALS: a systematic review. *Neurology,* 68**,** 1002-7.

57. CRUTS, M., GIJSELINCK, I., VAN DER ZEE, J., ENGELBORGHS, S., WILS, H., PIRICI, D., RADEMAKERS, R., VANDENBERGHE, R., DERMAUT, B. & MARTIN, J.-J. 2006. Null mutations in progranulin cause ubiquitin-positive frontotemporal dementia linked to chromosome 17q21. *Nature,* 442**,** 920-924.

58. DA CRUZ, S. & CLEVELAND, D. W. 2011. Understanding the role of TDP-43 and FUS/TLS in ALS and beyond. *Curr Opin Neurobiol*, 21, 904-19.

59. DE HEREDIA, M. L. & JANSEN, R.-P. 2004. mRNA localization and the cytoskeleton. *Current opinion in cell biology,* 16**,** 80-85.

60. DEJESUS-HERNANDEZ, M., MACKENZIE, I. R., BOEVE, B. F., BOXER, A. L., BAKER, M., RUTHERFORD, N. J., NICHOLSON, A. M., FINCH, N. A., FLYNN, H., ADAMSON, J., et al. 2011. Expanded GGGGCC hexanucleotide repeat in noncoding region of C9ORF72 causes chromosome 9p-linked FTD and ALS. *Neuron,* 72**,** 245-56.

61. DENG, H.-X., CHEN, W., HONG, S.-T., BOYCOTT, K. M., GORRIE, G. H., SIDDIQUE, N., YANG, Y., FECTO, F., SHI, Y. & ZHAI, H. 2011. Mutations in UBQLN2 cause dominant X-linked juvenile and adult-onset ALS and ALS/dementia. *Nature,* 477**,** 211-215.

62. DENT, E. W., GUPTON, S. L. & GERTLER, F. B. 2011. The growth cone cytoskeleton in axon outgrowth and guidance. *Cold Spring Harb Perspect Biol,* 3.

63. DENT, E. W., TANG, F. & KALIL, K. 2003. Axon Guidance by Growth Cones and Branches: Common Cytoskeletal and Signaling Mechanisms. *The Neuroscientist,* 9**,** 343-353.

64. DEWEY, C. M., CENIK, B., SEPHTON, C. F., JOHNSON, B. A., HERZ, J. & YU, G. 2012. TDP-43 aggregation in neurodegeneration: are stress granules the key? *Brain research,* 1462**,** 16-25.

65. DIAPER, D. C., ADACHI, Y., LAZAROU, L., GREENSTEIN, M., SIMOES, F. A., DI DOMENICO, A., SOLOMON, D. A., LOWE, S., ALSUBAIE, R. & CHENG, D. 2013a. Drosophila TDP-43 dysfunction in glia and muscle cells cause cytological and behavioural phenotypes that characterize ALS and FTLD. *Human molecular genetics***,** ddt243.

66. DIAPER, D. C., ADACHI, Y., SUTCLIFFE, B., HUMPHREY, D. M., ELLIOTT, C. J., STEPTO, A., LUDLOW, Z. N., VANDEN BROECK, L., CALLAERTS, P., DERMAUT, B., et al. 2013b. Loss and gain of Drosophila TDP-43 impair synaptic efficacy and motor control leading to age-related neurodegeneration by loss-of-function phenotypes. *Hum Mol Genet,* 22**,** 1539-57.

67. DONNELLY, C. J., ZHANG, P.-W., PHAM, J. T., HAEUSLER, A. R., MISTRY, N. A., VIDENSKY, S., DALEY, E. L., POTH, E. M., HOOVER, B. & FINES, D. M. 2013. RNA toxicity from the ALS/FTD C9ORF72 expansion is mitigated by antisense intervention. *Neuron,* 80**,** 415-428.

68. DORMANN, D., CAPELL, A., CARLSON, A. M., SHANKARAN, S. S., RODDE, R., NEUMANN, M., KREMMER, E., MATSUWAKI, T., YAMANOUCHI, K. & NISHIHARA, M. 2009. Proteolytic processing of TAR DNA binding protein-43 by caspases produces C-terminal fragments with disease defining properties independent of progranulin. *Journal of neurochemistry,* 110**,** 1082-1094.

69. FALLINI, C., BASSELL, G. J. & ROSSOLL, W. 2012. The ALS disease protein TDP-43 is actively transported in motor neuron axons and regulates axon outgrowth. *Hum Mol Genet,* 21**,** 3703-18.

70. FARG, M. A., SUNDARAMOORTHY, V., SULTANA, J. M., YANG, S., ATKINSON, R. A., LEVINA, V., HALLORAN, M. A., GLEESON, P. A., BLAIR, I. P. & SOO, K. Y. 2014. C9ORF72, implicated in amytrophic lateral sclerosis and frontotemporal dementia, regulates endosomal trafficking. *Human molecular genetics***,** ddu068.

71. FECTO, F., YAN, J., VEMULA, S. P., LIU, E., YANG, Y., CHEN, W., ZHENG, J. G., SHI, Y., SIDDIQUE, N. & ARRAT, H. 2011. SQSTM1 mutations in familial and sporadic amyotrophic lateral sclerosis. *Archives of neurology,* 68**,** 1440-1446.

72. FEIGUIN, F., GODENA, V. K., ROMANO, G., D'AMBROGIO, A., KLIMA, R. & BARALLE, F. E. 2009. Depletion of TDP-43 affects Drosophila motoneurons terminal synapsis and locomotive behavior. *FEBS letters,* 583**,** 1586-1592.

73. FERRARI, R., KAPOGIANNIS, D., HUEY, E. D. & MOMENI, P. 2011. FTD and ALS: a tale of two diseases. *Curr Alzheimer Res,* 8**,** 273-94.

74. FIESEL, F. C. & KAHLE, P. J. 2011. TDP-43 and FUS/TLS: cellular functions and implications for neurodegeneration. *FEBS Journal,* 278**,** 3550-3568.

75. FIESEL, F. C., SCHURR, C., WEBER, S. S. & KAHLE, P. J. 2011. TDP-43 knockdown impairs neurite outgrowth dependent on its target histone deacetylase 6. *Mol Neurodegener,* 6**,** 64.

76. FILIPPI, M., AGOSTA, F. & FERRARO, P. M. 2016. Charting Frontotemporal Dementia: From Genes to Networks. *J Neuroimaging,* 26**,** 16-27.

77. FRATTA, P., POULTER, M., LASHLEY, T., ROHRER, J. D., POLKE, J. M., BECK, J., RYAN, N., HENSMAN, D., MIZIELINSKA, S., WAITE, A. J., et al. 2013. Homozygosity for the C9orf72 GGGGCC repeat expansion in frontotemporal dementia. *Acta Neuropathol,* 126**,** 401-9.

78. FREIBAUM, B. D., CHITTA, R. K., HIGH, A. A. & TAYLOR, J. P. 2010. Global analysis of TDP-43 interacting proteins reveals strong association with RNA splicing and translation machinery. *Journal of proteome research,* 9**,** 1104-1120.

79. FURUKAWA, Y. 2012. *Protein aggregates in pathological inclusions of amyotrophic lateral sclerosis*, Citeseer.

80. GENDRON, T. F., BIENIEK, K. F., ZHANG, Y.-J., JANSEN-WEST, K., ASH, P. E., CAULFIELD, T., DAUGHRITY, L., DUNMORE, J. H., CASTANEDES-CASEY, M. & CHEW, J. 2013. Antisense transcripts of the expanded C9ORF72 hexanucleotide repeat form nuclear RNA foci and undergo repeat-associated non-ATG translation in c9FTD/ALS. *Acta neuropathologica,* 126**,** 829-844.

81. GENDRON, T. F. & PETRUCELLI, L. 2011. Rodent models of TDP-43 proteinopathy: investigating the mechanisms of TDP-43-mediated neurodegeneration. *J Mol Neurosci,* 45**,** 486-99.

82. GESER, F., LEE, V. M. Y. & TROJANOWSKI, J. Q. 2010. Amyotrophic lateral sclerosis and frontotemporal lobar degeneration: A spectrum of TDP-43 proteinopathies. *Neuropathology,* 30**,** 103-112.

83. GESER, F., MARTINEZ-LAGE, M., KWONG, L. K., LEE, V. M.-Y. & TROJANOWSKI, J. Q. 2009a. Amyotrophic lateral sclerosis, frontotemporal dementia and beyond: the TDP-43 diseases. *Journal of neurology,* 256**,** 1205-1214.

84. GESER, F., MARTINEZ-LAGE, M., ROBINSON, J., URYU, K., NEUMANN, M., BRANDMEIR, N. J., XIE, S. X., KWONG, L. K., ELMAN, L. & MCCLUSKEY, L. 2009b. Clinical and pathological continuum of multisystem TDP-43 proteinopathies. *Archives of Neurology,* 66**,** 180-189.

85. GIORDANA, M. T., FERRERO, P., GRIFONI, S., PELLERINO, A., NALDI, A. & MONTUSCHI, A. 2011. Dementia and cognitive impairment in amyotrophic lateral sclerosis: a review. *Neurological Sciences,* 32**,** 9-16.

86. GIORDANA, M. T., PICCININI, M., GRIFONI, S., DE MARCO, G., VERCELLINO, M., MAGISTRELLO, M., PELLERINO, A., BUCCINNÀ, B., LUPINO, E. & RINAUDO, M. T. 2010.

TDP-43 redistribution is an early event in sporadic amyotrophic lateral sclerosis. *Brain pathology,* 20**,** 351-360.

87. GITCHO, M. A., BALOH, R. H., CHAKRAVERTY, S., MAYO, K., NORTON, J. B., LEVITCH, D., HATANPAA, K. J., WHITE, C. L., BIGIO, E. H. & CASELLI, R. 2008. TDP-43 A315T mutation in familial motor neuron disease. *Annals of neurology,* 63**,** 535-538.

88. GITLER, A. D. & SHORTER, J. 2011. RNA-binding proteins with prion-like domains in ALS and FTLD-U. *Prion,* 5**,** 179-187.

89. GODENA, V. K., ROMANO, G., ROMANO, M., APPOCHER, C., KLIMA, R., BURATTI, E., BARALLE, F. E. & FEIGUIN, F. 2011. TDP-43 regulates Drosophila neuromuscular junctions growth by modulating Futsch/MAP1B levels and synaptic microtubules organization. *PloS one,* 6**,** e17808.

90. GOEDERT, M., GHETTI, B. & SPILLANTINI, M. G. 2012. Frontotemporal dementia: implications for understanding Alzheimer disease. *Cold Spring Harb Perspect Med,* 2**,** a006254.

91. GOEDERT, M. & SPILLANTINI, M. G. 2001. Tau gene mutations and neurodegeneration. *Biochem Soc Symp***,** 59-71.

92. GOMEZ-DEZA, J., LEE, Y.-B., TROAKES, C., NOLAN, M., AL-SARRAJ, S., GALLO, J.-M. & SHAW, C. E. 2015. Dipeptide repeat protein inclusions are rare in the spinal cord and almost absent from motor neurons in C9ORF72 mutant amyotrophic lateral sclerosis and are unlikely to cause their degeneration. *Acta neuropathologica communications,* 3**,** 1.

93. GÓMEZ-TORTOSA, E., GALLEGO, J., GUERRERO-LÓPEZ, R., MARCOS, A., GIL-NECIGA, E., SAINZ, M. J., DÍAZ, A., FRANCO-MACÍAS, E., TRUJILLO-TIEBAS, M. J. & AYUSO, C. 2013. C9ORF72 hexanucleotide expansions of 20–22 repeats are associated with frontotemporal deterioration. *Neurology,* 80**,** 366-370.

94. GORNO-TEMPINI, M., HILLIS, A., WEINTRAUB, S., KERTESZ, A., MENDEZ, M., CAPPA, S., OGAR, J., ROHRER, J., BLACK, S., BOEVE, B., et al. 2011. Classification of primary progressive aphasia and its variants. *Neurology,* 76**,** 1006-14.

95. GRAFF-RADFORD, N. R. & WOODRUFF, B. K. 2007. Frontotemporal dementia. *Semin Neurol,* 27**,** 48-57.

96. GREENWAY, M. J., ANDERSEN, P. M., RUSS, C., ENNIS, S., CASHMAN, S., DONAGHY, C., PATTERSON, V., SWINGLER, R., KIERAN, D. & PREHN, J. 2006. ANG mutations segregate with familial and'sporadic'amyotrophic lateral sclerosis. *Nature genetics,* 38.

97. GUO, W., CHEN, Y., ZHOU, X., KAR, A., RAY, P., CHEN, X., RAO, E. J., YANG, M., YE, H. & ZHU, L. 2011. An ALS-associated mutation affecting TDP-43 enhances protein aggregation, fibril formation and neurotoxicity. *Nature structural & molecular biology,* 18**,** 822-830.

98. HALES, C. M. & HU, W. T. 2013. From frontotemporal lobar degeneration pathology to frontotemporal lobar degeneration biomarkers. *Int Rev Psychiatry,* 25**,** 210-20.

99. HARMS, M. B., CADY, J., ZAIDMAN, C., COOPER, P., BALI, T., ALLRED, P., CRUCHAGA, C., BAUGHN, M., LIBBY, R. T. & PESTRONK, A. 2013. Lack of C9ORF72 coding mutations supports a gain of function for repeat expansions in amyotrophic lateral sclerosis. *Neurobiology of aging,* 34**,** 2234. e13-2234. e19.

100. HASEGAWA, M., ARAI, T., NONAKA, T., KAMETANI, F., YOSHIDA, M., HASHIZUME, Y., BEACH, T. G., BURATTI, E., BARALLE, F. & MORITA, M. 2008. Phosphorylated TDP-43 in frontotemporal lobar degeneration and amyotrophic lateral sclerosis. *Annals of neurology,* 64**,** 60-70.

101. HE, Y. & SMITH, R. 2009. Nuclear functions of heterogeneous nuclear ribonucleoproteins A/B. *Cellular and molecular life sciences,* 66**,** 1239-1256.

102. HE, Z. & BATEMAN, A. 2003. Progranulin (granulin-epithelin precursor, PC-cell-derived growth factor, acrogranin) mediates tissue repair and tumorigenesis. *J Mol Med (Berl),* 81**,** 600-12.

103. HODGES, J. R. 2001. Frontotemporal dementia (Pick's disease): clinical features and assessment. *Neurology,* 56**,** S6-S10.

104. HONDA, D., ISHIGAKI, S., IGUCHI, Y., FUJIOKA, Y., UDAGAWA, T., MASUDA, A., OHNO, K., KATSUNO, M. & SOBUE, G. 2013. The ALS/FTLD-related RNA-binding proteins TDP-43 and FUS have common downstream RNA targets in cortical neurons. *FEBS Open Bio*, 4, 1-10.

105. HORNBERG, H. & HOLT, C. 2013. RNA-binding proteins and translational regulation in axons and growth cones. *Front Neurosci,* 7**,** 81.

106. HORTOBÁGYI, T., CAIRNS, N. J., HORTOBÁGYI, T. & CAIRNS., N. J. 2000. *Amyotrophic lateral sclerosis and frontotemporal lobar degeneration*

107. *Neuropathology of Neurodegenerative Diseases*, Cambridge University Press.

108. HOSLER, B. A., SIDDIQUE, T., SAPP, P. C., SAILOR, W., HUANG, M. C., HOSSAIN, A., DAUBE, J. R., NANCE, M., FAN, C. & KAPLAN, J. 2000. Linkage of familial amyotrophic lateral sclerosis with frontotemporal dementia to chromosome 9q21-q22. *Jama,* 284**,** 1664-1669.

109. IGAZ, L. M., KWONG, L. K., CHEN-PLOTKIN, A., WINTON, M. J., UNGER, T. L., XU, Y., NEUMANN, M., TROJANOWSKI, J. Q. & LEE, V. M.-Y. 2009. Expression of TDP-43 C-terminal fragments in vitro recapitulates pathological features of TDP-43 proteinopathies. *Journal of Biological Chemistry,* 284**,** 8516-8524.

110. IGAZ, L. M., KWONG, L. K., LEE, E. B., CHEN-PLOTKIN, A., SWANSON, E., UNGER, T., MALUNDA, J., XU, Y., WINTON, M. J., TROJANOWSKI, J. Q., et al. 2011. Dysregulation of the ALS-associated gene TDP-43 leads to neuronal death and degeneration in mice. *J Clin Invest,* 121**,** 726-38.

111. IGUCHI, Y., KATSUNO, M., NIWA, J., TAKAGI, S., ISHIGAKI, S., IKENAKA, K., KAWAI, K., WATANABE, H., YAMANAKA, K., TAKAHASHI, R., et al. 2013. Loss of TDP-43 causes age-dependent progressive motor neuron degeneration. *Brain,* 136**,** 1371-82.

112. ISKEN, O. & MAQUAT, L. E. 2007. Quality control of eukaryotic mRNA: safeguarding cells from abnormal mRNA function. *Genes & development,* 21**,** 1833-3856.

113. ITTNER, A., KE, Y. D., EERSEL, J. V., GLADBACH, A., GÖTZ, J. & ITTNER, L. M. 2011. Brief update on different roles of tau in neurodegeneration. *IUBMB life,* 63**,** 495-502.

114. JANG, J.-H., KWON, M.-J., CHOI, W. J., OH, K.-W., KOH, S.-H., KI, C.-S. & KIM, S. H. 2013. Analysis of the C9orf72 hexanucleotide repeat expansion in Korean patients with familial and sporadic amyotrophic lateral sclerosis. *Neurobiology of aging,* 34**,** 1311. e7-1311. e9.

115. JANSSENS, J. & VAN BROECKHOVEN, C. 2013a. Pathological mechanisms underlying TDP-43 driven neurodegeneration in FTLD-ALS spectrum disorders. *Hum Mol Genet,* 22**,** R77-87.

116. JANSSENS, J. & VAN BROECKHOVEN, C. 2013b. Pathological mechanisms underlying TDP-43 driven neurodegeneration in FTLD–ALS spectrum disorders. *Hum Mol Genet,* 22**,** R77-87.

117. JOHNSON, B. S., MCCAFFERY, J. M., LINDQUIST, S. & GITLER, A. D. 2008. A yeast TDP-43 proteinopathy model: Exploring the molecular determinants of TDP-43 aggregation and cellular toxicity. *Proc Natl Acad Sci U S A,* 105**,** 6439-44.

118. JUNG, H., YOON, B. C. & HOLT, C. E. 2012. Axonal mRNA localization and local protein synthesis in nervous system assembly, maintenance and repair. *Nat Rev Neurosci,* 13**,** 308-24.

119. KABASHI, E., LIN, L., TRADEWELL, M. L., DION, P. A., BERCIER, V., BOURGOUIN, P., ROCHEFORT, D., HADJ, S. B., DURHAM, H. D. & VELDE, C. V. 2010. Gain and loss of function of ALS-related mutations of TARDBP (TDP-43) cause motor deficits in vivo. *Human molecular genetics,* 19**,** 671-683.

120. KABASHI, E., VALDMANIS, P. N., DION, P., SPIEGELMAN, D., MCCONKEY, B. J., VELDE, C. V., BOUCHARD, J.-P., LACOMBLEZ, L., POCHIGAEVA, K. & SALACHAS, F. 2008. TARDBP mutations in individuals with sporadic and familial amyotrophic lateral sclerosis. *Nature genetics,* 40**,** 572-574.

121. KATIRJI, B., KAMINSKI, H. J. & RUFF, R. L. 2013. *Neuromuscular disorders in clinical practice*, Springer Science & Business Media.

122. KAWAHARA, Y. & MIEDA-SATO, A. 2012. TDP-43 promotes microRNA biogenesis as a component of the Drosha and Dicer complexes. *Proceedings of the National Academy of Sciences,* 109**,** 3347-3352.

123. KIERNAN, M. C., VUCIC, S., CHEAH, B. C., TURNER, M. R., EISEN, A., HARDIMAN, O., BURRELL, J. R. & ZOING, M. C. 2011. Amyotrophic lateral sclerosis. *The Lancet,* 377**,** 942-955.

124. KIM, H. J., KIM, N. C., WANG, Y.-D., SCARBOROUGH, E. A., MOORE, J., DIAZ, Z., MACLEA, K. S., FREIBAUM, B., LI, S. & MOLLIEX, A. 2013. Mutations in prion-like domains in hnRNPA2B1 and hnRNPA1 cause multisystem proteinopathy and ALS. *Nature,* 495**,** 467-473.

125. KIMONIS, V. E., FULCHIERO, E., VESA, J. & WATTS, G. 2008. VCP disease associated with myopathy, Paget disease of bone and frontotemporal dementia: review of a unique disorder. *Biochim Biophys Acta,* 1782**,** 744-8.

126. KIMONIS, V. E. & WATTS, G. D. 2005. Autosomal dominant inclusion body myopathy, Paget disease of bone, and frontotemporal dementia. *Alzheimer Dis Assoc Disord,* 19 Suppl 1**,** S44-7.

127. KING, O. D., GITLER, A. D. & SHORTER, J. 2012. The tip of the iceberg: RNA-binding proteins with prion-like domains in neurodegenerative disease. *Brain research,* 1462**,** 61-80.

128. KINSLEY, L. & SIDDIQUE, T. 2012. Amyotrophic lateral sclerosis overview.

129. KRAEMER, B. C., SCHUCK, T., WHEELER, J. M., ROBINSON, L. C., TROJANOWSKI, J. Q., LEE, V. M. & SCHELLENBERG, G. D. 2010. Loss of murine TDP-43 disrupts motor function and plays an essential role in embryogenesis. *Acta neuropathologica,* 119**,** 409-419.

130. KUO, P.-H., DOUDEVA, L. G., WANG, Y.-T., SHEN, C.-K. J. & YUAN, H. S. 2009. Structural insights into TDP-43 in nucleic-acid binding and domain interactions. *Nucleic acids research,* 37**,** 1799-1808.

131. KWON, I., XIANG, S., KATO, M., WU, L., THEODOROPOULOS, P., WANG, T., KIM, J., YUN, J., XIE, Y. & MCKNIGHT, S. L. 2014. Poly-dipeptides encoded by the C9orf72 repeats bind nucleoli, impede RNA biogenesis, and kill cells. *Science,* 345**,** 1139-1145.

132. KWONG, L. K., URYU, K., TROJANOWSKI, J. Q. & LEE, V. M. 2008. TDP-43 proteinopathies: neurodegenerative protein misfolding diseases without amyloidosis. *Neurosignals,* 16**,** 41-51.

133. LA SPADA, A. R. & TAYLOR, J. P. 2010. Repeat expansion disease: progress and puzzles in disease pathogenesis. *Nature Reviews Genetics,* 11**,** 247-258.

134. LAAKSOVIRTA, H., PEURALINNA, T., SCHYMICK, J. C., SCHOLZ, S. W., LAI, S.-L., MYLLYKANGAS, L., SULKAVA, R., JANSSON, L., HERNANDEZ, D. G. & GIBBS, J. R. 2010. Chromosome 9p21 in amyotrophic lateral sclerosis in Finland: a genome-wide association study. *The Lancet Neurology,* 9**,** 978-985.

135. LAGIER-TOURENNE, C., BAUGHN, M., RIGO, F., SUN, S., LIU, P., LI, H.-R., JIANG, J., WATT, A. T., CHUN, S. & KATZ, M. 2013. Targeted degradation of sense and antisense C9orf72 RNA foci as therapy for ALS and frontotemporal degeneration. *Proceedings of the National Academy of Sciences,* 110**,** E4530-E4539.

136. LAGIER-TOURENNE, C. & CLEVELAND, D. W. 2009. Rethinking ALS: the FUS about TDP-43. *Cell,* 136**,** 1001-4.

137. LAGIER-TOURENNE, C., POLYMENIDOU, M. & CLEVELAND, D. W. 2010. TDP-43 and FUS/TLS: emerging roles in RNA processing and neurodegeneration. *Hum Mol Genet,* 19**,** R46-64.

138. LE BER, I., VAN DER ZEE, J., HANNEQUIN, D., GIJSELINCK, I., CAMPION, D., PUEL, M., LAQUERRIERE, A., DE POOTER, T., CAMUZAT, A., VAN DEN BROECK, M., et al. 2007.

Progranulin null mutations in both sporadic and familial frontotemporal dementia. *Hum Mutat,* 28**,** 846-55.

139. LEE, E. B., LEE, V. M.-Y. & TROJANOWSKI, J. Q. 2012. Gains or losses: molecular mechanisms of TDP43-mediated neurodegeneration. *Nature Reviews Neuroscience,* 13**,** 38-50.

140. LEE, Y.-B., CHEN, H.-J., PERES, J. N., GOMEZ, J., SARDONE, V., NISHIMURA, A. L., SCOTTER, E., VANCE, C., ŠTALEKAR, M., ADACHI, Y., et al. 2013a. Expanded G4C2 repeats linked to C9ORF72 ALS and FTD form length-dependent RNA foci, sequester RNA binding proteins and are neurotoxic. *Molecular Neurodegeneration,* 8**,** O14.

141. LEE, Y. B., CHEN, H. J., PERES, J. N., GOMEZ-DEZA, J., ATTIG, J., STALEKAR, M., TROAKES, C., NISHIMURA, A. L., SCOTTER, E. L., VANCE, C., et al. 2013b. Hexanucleotide repeats in ALS/FTD form length-dependent RNA foci, sequester RNA binding proteins, and are neurotoxic. *Cell Rep,* 5**,** 1178-86.

142. LEFEBVRE, S., BÜRGLEN, L., REBOULLET, S., CLERMONT, O., BURLET, P., VIOLLET, L., BENICHOU, B., CRUAUD, C., MILLASSEAU, P. & ZEVIANI, M. 1995. Identification and characterization of a spinal muscular atrophy-determining gene. *Cell,* 80**,** 155-165.

143. LI, Y., RAY, P., RAO, E. J., SHI, C., GUO, W., CHEN, X., WOODRUFF, E. A., 3RD, FUSHIMI, K. & WU, J. Y. 2010. A Drosophila model for TDP-43 proteinopathy. *Proc Natl Acad Sci U S A,* 107**,** 3169-74.

144. LIACHKO, N. F., GUTHRIE, C. R. & KRAEMER, B. C. 2010. Phosphorylation promotes neurotoxicity in a Caenorhabditis elegans model of TDP-43 proteinopathy. *The Journal of Neuroscience,* 30**,** 16208-16219.

145. LIN, M. T. & BEAL, M. F. 2006. Mitochondrial dysfunction and oxidative stress in neurodegenerative diseases. *Nature,* 443**,** 787-95.

146. LING, J. P., PLETNIKOVA, O., TRONCOSO, J. C. & WONG, P. C. 2015. TDP-43 repression of nonconserved cryptic exons is compromised in ALS-FTD. *Science,* 349**,** 650-655.

147. LING, S.-C., ALBUQUERQUE, C. P., HAN, J. S., LAGIER-TOURENNE, C., TOKUNAGA, S., ZHOU, H. & CLEVELAND, D. W. 2010. ALS-associated mutations in TDP-43 increase its stability and promote TDP-43 complexes with FUS/TLS. *Proceedings of the National Academy of Sciences,* 107**,** 13318-13323.

148. LING, S.-C., POLYMENIDOU, M. & CLEVELAND, D. W. 2013a. Converging mechanisms in ALS and FTD: disrupted RNA and protein homeostasis. *Neuron,* 79**,** 416-438.

149. LING, S. C., POLYMENIDOU, M. & CLEVELAND, D. W. 2013b. Converging mechanisms in ALS and FTD: disrupted RNA and protein homeostasis. *Neuron,* 79**,** 416-38.

150. LISCIC, R. M., GRINBERG, L. T., ZIDAR, J., GITCHO, M. A. & CAIRNS, N. J. 2008. ALS and FTLD: two faces of TDP-43 proteinopathy. *Eur J Neurol,* 15**,** 772-80.

151. LIU-YESUCEVITZ, L., BILGUTAY, A., ZHANG, Y.-J., VANDERWYDE, T., CITRO, A., MEHTA, T., ZAARUR, N., MCKEE, A., BOWSER, R. & SHERMAN, M. 2010. Tar DNA binding protein-43 (TDP-43) associates with stress granules: analysis of cultured cells and pathological brain tissue. *PloS one,* 5**,** e13250.

152. LIU, W., MILLER, B. L., KRAMER, J. H., RANKIN, K., WYSS-CORAY, C., GEARHART, R., PHENGRASAMY, L., WEINER, M. & ROSEN, H. J. 2004. Behavioral disorders in the frontal and temporal variants of frontotemporal dementia. *Neurology,* 62**,** 742-748.

153. LOGROSCINO, G., TRAYNOR, B. J., HARDIMAN, O., CHIO, A., MITCHELL, D., SWINGLER, R. J., MILLUL, A., BENN, E. & BEGHI, E. 2010. Incidence of amyotrophic lateral sclerosis in Europe. *J Neurol Neurosurg Psychiatry,* 81**,** 385-90.

154. LOMEN-HOERTH, C., MURPHY, J., LANGMORE, S., KRAMER, J. H., OLNEY, R. K. & MILLER, B. 2003. Are amyotrophic lateral sclerosis patients cognitively normal? *Neurology,* 60**,** 1094-7.

155. MACKENZIE, I. R. 2007. The neuropathology of FTD associated with ALS. *Alzheimer Disease & Associated Disorders,* 21**,** S44-S49.

156. MACKENZIE, I. R., ARZBERGER, T., KREMMER, E., TROOST, D., LORENZL, S., MORI, K., WENG, S.-M., HAASS, C., KRETZSCHMAR, H. A. & EDBAUER, D. 2013. Dipeptide repeat protein pathology in C9ORF72 mutation cases: clinico-pathological correlations. *Acta neuropathologica,* 126**,** 859-879.

157. MACKENZIE, I. R., BAKER, M., PICKERING-BROWN, S., HSIUNG, G. Y., LINDHOLM, C., DWOSH, E., GASS, J., CANNON, A., RADEMAKERS, R., HUTTON, M., et al. 2006. The neuropathology of frontotemporal lobar degeneration caused by mutations in the progranulin gene. *Brain,* 129**,** 3081-90.

158. MACKENZIE, I. R., NEUMANN, M., BIGIO, E. H., CAIRNS, N. J., ALAFUZOFF, I., KRIL, J., KOVACS, G. G., GHETTI, B., HALLIDAY, G., HOLM, I. E., et al. 2009. Nomenclature for neuropathologic subtypes of frontotemporal lobar degeneration: consensus recommendations. *Acta Neuropathol,* 117**,** 15-8.

159. MAGRANE, J., CORTEZ, C., GAN, W. B. & MANFREDI, G. 2014. Abnormal mitochondrial transport and morphology are common pathological denominators in SOD1 and TDP43 ALS mouse models. *Hum Mol Genet,* 23**,** 1413-24.

160. MAJOUNIE, E., RENTON, A. E., MOK, K., DOPPER, E. G., WAITE, A., ROLLINSON, S., CHIO, A., RESTAGNO, G., NICOLAOU, N., SIMON-SANCHEZ, J., et al. 2012. Frequency of the C9orf72 hexanucleotide repeat expansion in patients with amyotrophic lateral sclerosis and frontotemporal dementia: a cross-sectional study. *Lancet Neurol,* 11**,** 323-30.

161. MANN, D. M., ROLLINSON, S., ROBINSON, A., CALLISTER, J. B., THOMPSON, J. C., SNOWDEN, J. S., GENDRON, T., PETRUCELLI, L., MASUDA-SUZUKAKE, M. & HASEGAWA, M. 2013. Dipeptide repeat proteins are present in the p62 positive inclusions in patients with frontotemporal lobar degeneration and motor neurone disease associated with expansions in C9ORF72. *Acta neuropathologica communications,* 1**,** 1.

162. MARTIN, K. C. & EPHRUSSI, A. 2009. mRNA localization: gene expression in the spatial dimension. *Cell,* 136**,** 719-730.

163. MARUYAMA, H., MORINO, H., ITO, H., IZUMI, Y., KATO, H., WATANABE, Y., KINOSHITA, Y., KAMADA, M., NODERA, H. & SUZUKI, H. 2010. Mutations of optineurin in amyotrophic lateral sclerosis. *Nature,* 465**,** 223-226.

164. MASSMAN, P. J., SIMS, J., COOKE, N., HAVERKAMP, L. J., APPEL, V. & APPEL, S. 1996. Prevalence and correlates of neuropsychological deficits in amyotrophic lateral sclerosis. *Journal of Neurology, Neurosurgery & Psychiatry,* 61**,** 450-455.

165. MAY, S., HORNBURG, D., SCHLUDI, M. H., ARZBERGER, T., RENTZSCH, K., SCHWENK, B. M., GRASSER, F. A., MORI, K., KREMMER, E., BANZHAF-STRATHMANN, J., et al. 2014. C9orf72 FTLD/ALS-associated Gly-Ala dipeptide repeat proteins cause neuronal toxicity and Unc119 sequestration. *Acta Neuropathol,* 128**,** 485-503.

166. MERCADO, P. A., AYALA, Y. M., ROMANO, M., BURATTI, E. & BARALLE, F. E. 2005. Depletion of TDP 43 overrides the need for exonic and intronic splicing enhancers in the human apoA-II gene. *Nucleic acids research,* 33**,** 6000-6010.

167. MEYER, K., FERRAIUOLO, L., MIRANDA, C. J., LIKHITE, S., MCELROY, S., RENUSCH, S., DITSWORTH, D., LAGIER-TOURENNE, C., SMITH, R. A. & RAVITS, J. 2014. Direct conversion of patient fibroblasts demonstrates non-cell autonomous toxicity of astrocytes to motor neurons in familial and sporadic ALS. *Proceedings of the National Academy of Sciences,* 111**,** 829-832.

168. MILLECAMPS, S. & JULIEN, J. P. 2013. Axonal transport deficits and neurodegenerative diseases. *Nat Rev Neurosci,* 14**,** 161-76.

169. MIZIELINSKA, S., GRÖNKE, S., NICCOLI, T., RIDLER, C. E., CLAYTON, E. L., DEVOY, A., MOENS, T., NORONA, F. E., WOOLLACOTT, I. O. & PIETRZYK, J. 2014. C9orf72 repeat expansions cause neurodegeneration in Drosophila through arginine-rich proteins. *Science,* 345**,** 1192-1194.

170. MIZIELINSKA, S. & ISAACS, A. M. 2014. C9orf72 amyotrophic lateral sclerosis and frontotemporal dementia: gain or loss of function? *Curr Opin Neurol,* 27**,** 515-23.

171. MORI, F., TANJI, K., ZHANG, H.-X., NISHIHIRA, Y., TAN, C.-F., TAKAHASHI, H. & WAKABAYASHI, K. 2008. Maturation process of TDP-43-positive neuronal cytoplasmic inclusions in amyotrophic lateral sclerosis with and without dementia. *Acta neuropathologica,* 116**,** 193-203.

172. MORI, K., ARZBERGER, T., GRÄSSER, F. A., GIJSELINCK, I., MAY, S., RENTZSCH, K., WENG, S.-M., SCHLUDI, M. H., VAN DER ZEE, J. & CRUTS, M. 2013a. Bidirectional transcripts of the expanded C9orf72 hexanucleotide repeat are translated into aggregating dipeptide repeat proteins. *Acta neuropathologica,* 126**,** 881-893.

173. MORI, K., LAMMICH, S., MACKENZIE, I. R., FORNÉ, I., ZILOW, S., KRETZSCHMAR, H., EDBAUER, D., JANSSENS, J., KLEINBERGER, G. & CRUTS, M. 2013b. hnRNP A3 binds to GGGGCC repeats and is a constituent of p62-positive/TDP43-negative inclusions in the hippocampus of patients with C9orf72 mutations. *Acta neuropathologica,* 125**,** 413-423.

174. MORITA, M., AL-CHALABI, A., ANDERSEN, P., HOSLER, B., SAPP, P., ENGLUND, E., MITCHELL, J., HABGOOD, J., DE BELLEROCHE, J. & XI, J. 2006. A locus on chromosome 9p confers susceptibility to ALS and frontotemporal dementia. *Neurology,* 66**,** 839-844.

175. MÜNCH, C., ROSENBOHM, A., SPERFELD, A. D., UTTNER, I., RESKE, S., KRAUSE, B. J., SEDLMEIER, R., MEYER, T., HANEMANN, C. O. & STUMM, G. 2005. Heterozygous R1101K mutation of the DCTN1 gene in a family with ALS and FTD. *Annals of neurology,* 58**,** 777-780.

176. MURRAY, M. E., DEJESUS-HERNANDEZ, M., RUTHERFORD, N. J., BAKER, M., DUARA, R., GRAFF-RADFORD, N. R., WSZOLEK, Z. K., FERMAN, T. J., JOSEPHS, K. A., BOYLAN, K. B., et al. 2011. Clinical and neuropathologic heterogeneity of c9FTD/ALS associated with hexanucleotide repeat expansion in C9ORF72. *Acta Neuropathol,* 122**,** 673-90.

177. NEARY, D., SNOWDEN, J. S., GUSTAFSON, L., PASSANT, U., STUSS, D., BLACK, S., FREEDMAN, M., KERTESZ, A., ROBERT, P. H., ALBERT, M., et al. 1998. Frontotemporal lobar degeneration: a consensus on clinical diagnostic criteria. *Neurology,* 51**,** 1546-54.

178. NEUMANN, M., KWONG, L. K., LEE, E. B., KREMMER, E., FLATLEY, A., XU, Y., FORMAN, M. S., TROOST, D., KRETZSCHMAR, H. A. & TROJANOWSKI, J. Q. 2009a. Phosphorylation of S409/410 of TDP-43 is a consistent feature in all sporadic and familial forms of TDP-43 proteinopathies. *Acta neuropathologica,* 117**,** 137-149.

179. NEUMANN, M., KWONG, L. K., SAMPATHU, D. M., TROJANOWSKI, J. Q. & LEE, V. M.-Y. 2007. TDP-43 proteinopathy in frontotemporal lobar degeneration and amyotrophic lateral sclerosis: protein misfolding diseases without amyloidosis. *Archives of Neurology,* 64**,** 1388-1394.

180. NEUMANN, M., RADEMAKERS, R., ROEBER, S., BAKER, M., KRETZSCHMAR, H. A. & MACKENZIE, I. R. 2009b. A new subtype of frontotemporal lobar degeneration with FUS pathology. *Brain,* 132**,** 2922-2931.

181. NEUMANN, M., SAMPATHU, D. M., KWONG, L. K., TRUAX, A. C., MICSENYI, M. C., CHOU, T. T., BRUCE, J., SCHUCK, T., GROSSMAN, M. & CLARK, C. M. 2006a. Ubiquitinated TDP-43 in frontotemporal lobar degeneration and amyotrophic lateral sclerosis. *Science,* 314**,** 130-133.

182. NEUMANN, M., SAMPATHU, D. M., KWONG, L. K., TRUAX, A. C., MICSENYI, M. C., CHOU, T. T., BRUCE, J., SCHUCK, T., GROSSMAN, M., CLARK, C. M., et al. 2006b. Ubiquitinated TDP-43 in frontotemporal lobar degeneration and amyotrophic lateral sclerosis. *Science,* 314**,** 130-3.

183. NISHIMURA, A. L., MITNE-NETO, M., SILVA, H. C., RICHIERI-COSTA, A., MIDDLETON, S., CASCIO, D., KOK, F., OLIVEIRA, J. R., GILLINGWATER, T. & WEBB, J. 2004. A mutation in the vesicle-trafficking protein VAPB causes late-onset spinal muscular atrophy and amyotrophic lateral sclerosis. *The American Journal of Human Genetics,* 75**,** 822-831.

184. NONAKA, T., MASUDA-SUZUKAKE, M., ARAI, T., HASEGAWA, Y., AKATSU, H., OBI, T., YOSHIDA, M., MURAYAMA, S., MANN, D. M. & AKIYAMA, H. 2013. Prion-like properties of pathological TDP-43 aggregates from diseased brains. *Cell reports,* 4**,** 124-134.

185. ONYIKE, C. U. 2011. What is the life expectancy in frontotemporal lobar degeneration? *Neuroepidemiology,* 37**,** 166-7.

186. OU, S., WU, F., HARRICH, D., GARCÍA-MARTÍNEZ, L. F. & GAYNOR, R. B. 1995. Cloning and characterization of a novel cellular protein, TDP-43, that binds to human immunodeficiency virus type 1 TAR DNA sequence motifs. *Journal of virology,* 69**,** 3584-3596.

187. PEARSON, J. P., WILLIAMS, N. M., MAJOUNIE, E., WAITE, A., STOTT, J., NEWSWAY, V., MURRAY, A., HERNANDEZ, D., GUERREIRO, R. & SINGLETON, A. B. 2011. Familial frontotemporal dementia with amyotrophic lateral sclerosis and a shared haplotype on chromosome 9p. *Journal of neurology,* 258**,** 647-655.

188. PIGUET, O., HALLIDAY, G. M., REID, W. G., CASEY, B., CARMAN, R., HUANG, Y., XUEREB, J. H., HODGES, J. R. & KRIL, J. J. 2011. Clinical phenotypes in autopsy-confirmed Pick disease. *Neurology,* 76**,** 253-9.

189. POLYMENIDOU, M. & CLEVELAND, D. W. 2011. The seeds of neurodegeneration: prion-like spreading in ALS. *Cell,* 147**,** 498-508.

190. POLYMENIDOU, M., LAGIER-TOURENNE, C., HUTT, K. R., BENNETT, C. F., CLEVELAND, D. W. & YEO, G. W. 2012. Misregulated RNA processing in amyotrophic lateral sclerosis. *Brain Res,* 1462**,** 3-15.

191. POLYMENIDOU, M., LAGIER-TOURENNE, C., HUTT, K. R., HUELGA, S. C., MORAN, J., LIANG, T. Y., LING, S.-C., SUN, E., WANCEWICZ, E. & MAZUR, C. 2011. Long pre-mRNA depletion and RNA missplicing contribute to neuronal vulnerability from loss of TDP-43. *Nature neuroscience,* 14**,** 459-468.

192. RAVITS, J., APPEL, S., BALOH, R. H., BAROHN, R., RIX BROOKS, B., ELMAN, L., FLOETER, M. K., HENDERSON, C., LOMEN-HOERTH, C. & MACKLIS, J. D. 2013. Deciphering amyotrophic lateral sclerosis: what phenotype, neuropathology and genetics are telling us about pathogenesis. *Amyotrophic Lateral Sclerosis and Frontotemporal Degeneration,* 14**,** 5-18.

193. RECHTMAN, L., JORDAN, H., WAGNER, L., HORTON, D. K. & KAYE, W. 2015. Racial and ethnic differences among amyotrophic lateral sclerosis cases in the United States. *Amyotroph Lateral Scler Frontotemporal Degener,* 16**,** 65-71.

194. RENTON, A. E., MAJOUNIE, E., WAITE, A., SIMON-SANCHEZ, J., ROLLINSON, S., GIBBS, J. R., SCHYMICK, J. C., LAAKSOVIRTA, H., VAN SWIETEN, J. C., MYLLYKANGAS, L., et al. 2011. A hexanucleotide repeat expansion in C9ORF72 is the cause of chromosome 9p21-linked ALS-FTD. *Neuron,* 72**,** 257-68.

195. RIEDL, L., MACKENZIE, I. R., FÖRSTL, H., KURZ, A. & DIEHL-SCHMID, J. 2014. Frontotemporal lobar degeneration: current perspectives. *Neuropsychiatr Dis Treat,* 10**,** 297-310.

196. RINGHOLZ, G. M., APPEL, S. H., BRADSHAW, M., COOKE, N. A., MOSNIK, D. M. & SCHULZ, P. E. 2005. Prevalence and patterns of cognitive impairment in sporadic ALS. *Neurology,* 65**,** 586-90.

197. RIORDAN, J. R. 2008. CFTR function and prospects for therapy. *Annu. Rev. Biochem.,* 77**,** 701-726.

198. RITSON, G. P., CUSTER, S. K., FREIBAUM, B. D., GUINTO, J. B., GEFFEL, D., MOORE, J., TANG, W., WINTON, M. J., NEUMANN, M. & TROJANOWSKI, J. Q. 2010. TDP-43 mediates degeneration in a novel Drosophila model of disease caused by mutations in VCP/p97. *The Journal of Neuroscience,* 30**,** 7729-7739.

199. ROSEN, D. R., SIDDIQUE, T., PATTERSON, D., FIGLEWICZ, D. A., SAPP, P., HENTATI, A., DONALDSON, D., GOTO, J., O'REGAN, J. P. & DENG, H.-X. 1993. Mutations in Cu/Zn superoxide dismutase gene are associated with familial amyotrophic lateral sclerosis. *Nature,* 362**,** 59-62.

200. ROSSI, F. H., FRANCO, M. C. & ESTEVEZ, A. G. 2013. Pathophysiology of Amyotrophic Lateral Sclerosis.

201. ROWLAND, L. P. & SHNEIDER, N. A. 2001. Amyotrophic lateral sclerosis. *New England Journal of Medicine,* 344**,** 1688-1700.

202. RUTHERFORD, N. J., ZHANG, Y.-J., BAKER, M., GASS, J. M., FINCH, N. A., XU, Y.-F., STEWART, H., KELLEY, B. J., KUNTZ, K. & CROOK, R. J. 2008. Novel mutations in TARDBP (TDP-43) in patients with familial amyotrophic lateral sclerosis. *PLoS Genet,* 4**,** e1000193.

203. SAREEN, D., O'ROURKE, J. G., MEERA, P., MUHAMMAD, A., GRANT, S., SIMPKINSON, M., BELL, S., CARMONA, S., ORNELAS, L. & SAHABIAN, A. 2013. Targeting RNA foci in iPSC-derived motor neurons from ALS patients with a C9ORF72 repeat expansion. *Science translational medicine,* 5**,** 208ra149-208ra149.

204. SCHLUDI, M. H., MAY, S., GRÄSSER, F. A., RENTZSCH, K., KREMMER, E., KÜPPER, C., KLOPSTOCK, T., ARZBERGER, T., EDBAUER, D. & ALLIANCE, B. B. B. 2015. Distribution of dipeptide repeat proteins in cellular models and C9orf72 mutation cases suggests link to transcriptional silencing. *Acta neuropathologica,* 130**,** 537-555.

205. SEPHTON, C. F., CENIK, B., CENIK, B. K., HERZ, J. & YU, G. 2012. TDP-43 in central nervous system development and function: clues to TDP-43-associated neurodegeneration. *Biol Chem,* 393**,** 589-94.

206. SEPHTON, C. F., CENIK, C., KUCUKURAL, A., DAMMER, E. B., CENIK, B., HAN, Y., DEWEY, C. M., ROTH, F. P., HERZ, J., PENG, J., et al. 2011. Identification of neuronal RNA targets of TDP-43-containing ribonucleoprotein complexes. *J Biol Chem,* 286**,** 1204-15.

207. SEPHTON, C. F., GOOD, S. K., ATKIN, S., DEWEY, C. M., MAYER, P., HERZ, J. & YU, G. 2010. TDP-43 is a developmentally regulated protein essential for early embryonic development. *Journal of Biological Chemistry,* 285**,** 6826-6834.

208. SHAN, X., CHIANG, P.-M., PRICE, D. L. & WONG, P. C. 2010. Altered distributions of Gemini of coiled bodies and mitochondria in motor neurons of TDP-43 transgenic mice. *Proceedings of the National Academy of Sciences,* 107**,** 16325-16330.

209. SHAW, P. 2005. Molecular and cellular pathways of neurodegeneration in motor neurone disease. *Journal of Neurology, Neurosurgery & Psychiatry,* 76**,** 1046-1057.

210. SHI, P., STROM, A. L., GAL, J. & ZHU, H. 2010. Effects of ALS-related SOD1 mutants on dynein- and KIF5-mediated retrograde and anterograde axonal transport. *Biochim Biophys Acta,* 1802**,** 707-16.

211. SHODAI, A., MORIMURA, T., IDO, A., UCHIDA, T., AYAKI, T., TAKAHASHI, R., KITAZAWA, S., SUZUKI, S., SHIROUZU, M. & KIGAWA, T. 2013. Aberrant assembly of RNA recognition motif 1 links to pathogenic conversion of TAR DNA-binding protein of 43 kDa (TDP-43). *Journal of Biological Chemistry,* 288**,** 14886-14905.

212. SKIBINSKI, G., PARKINSON, N. J., BROWN, J. M., CHAKRABARTI, L., LLOYD, S. L., HUMMERICH, H., NIELSEN, J. E., HODGES, J. R., SPILLANTINI, M. G., THUSGAARD, T., et al. 2005. Mutations in the endosomal ESCRTIII-complex subunit CHMP2B in frontotemporal dementia. *Nat Genet,* 37**,** 806-8.

213. SMITH, B. N., TICOZZI, N., FALLINI, C., GKAZI, A. S., TOPP, S., KENNA, K. P., SCOTTER, E. L., KOST, J., KEAGLE, P., MILLER, J. W., et al. 2014. Exome-wide rare variant analysis identifies TUBA4A mutations associated with familial ALS. *Neuron,* 84**,** 324-31.

214. SNOWDEN, J. S., HARRIS, J., RICHARDSON, A., ROLLINSON, S., THOMPSON, J. C., NEARY, D., MANN, D. M. & PICKERING-BROWN, S. 2013. Frontotemporal dementia with amyotrophic lateral sclerosis: a clinical comparison of patients with and without repeat expansions in C9orf72. *Amyotrophic Lateral Sclerosis and Frontotemporal Degeneration,* 14**,** 172-176.

215. SNOWDEN, J. S., NEARY, D. & MANN, D. M. 1996. *Fronto-Temporal Lobar Degenertaion*, Churchill Livingstone.

216. SNOWDEN, J. S., NEARY, D. & MANN, D. M. 2002. Frontotemporal dementia. *Br J Psychiatry,* 180**,** 140-3.

217. SREEDHARAN, J., BLAIR, I. P., TRIPATHI, V. B., HU, X., VANCE, C., ROGELJ, B., ACKERLEY, S., DURNALL, J. C., WILLIAMS, K. L. & BURATTI, E. 2008. TDP-43 mutations in familial and sporadic amyotrophic lateral sclerosis. *Science,* 319**,** 1668-1672.

218. STALLINGS, N. R., PUTTAPARTHI, K., LUTHER, C. M., BURNS, D. K. & ELLIOTT, J. L. 2010. Progressive motor weakness in transgenic mice expressing human TDP-43. *Neurobiology of disease,* 40**,** 404-414.

219. STEINACKER, P., HENDRICH, C., SPERFELD, A. D., JESSE, S., VON ARNIM, C. A., LEHNERT, S., PABST, A., UTTNER, I., TUMANI, H. & LEE, V. M.-Y. 2008. TDP-43 in cerebrospinal fluid of patients with frontotemporal lobar degeneration and amyotrophic lateral sclerosis. *Archives of neurology,* 65**,** 1481-1487.

220. STEPANOVA, T., SLEMMER, J., HOOGENRAAD, C. C., LANSBERGEN, G., DORTLAND, B., DE ZEEUW, C. I., GROSVELD, F., VAN CAPPELLEN, G., AKHMANOVA, A. & GALJART, N. 2003. Visualization of microtubule growth in cultured neurons via the use of EB3-GFP (end-binding protein 3-green fluorescent protein). *The Journal of neuroscience,* 23**,** 2655-2664.

221. STEPTO, A., GALLO, J.-M., SHAW, C. E. & HIRTH, F. 2014a. Modelling C9ORF72 hexanucleotide repeat expansion in amyotrophic lateral sclerosis and frontotemporal dementia. *Acta neuropathologica,* 127**,** 377-389.

222. STEPTO, A., GALLO, J. M., SHAW, C. E. & HIRTH, F. 2014b. Modelling C9ORF72 hexanucleotide repeat expansion in amyotrophic lateral sclerosis and frontotemporal dementia. *Acta Neuropathol,* 127**,** 377-89.

223. STOICA, R., DE VOS, K. J., PAILLUSSON, S., MUELLER, S., SANCHO, R. M., LAU, K. F., VIZCAY-BARRENA, G., LIN, W. L., XU, Y. F., LEWIS, J., et al. 2014. ER-mitochondria associations are regulated by the VAPB-PTPIP51 interaction and are disrupted by ALS/FTD-associated TDP-43. *Nat Commun,* 5**,** 3996.

224. STRAUBE, A. & MERDES, A. 2007. EB3 regulates microtubule dynamics at the cell cortex and is required for myoblast elongation and fusion. *Current Biology,* 17**,** 1318-1325.

225. STRONG, M. J. 2001. Progress in clinical neurosciences: the evidence for ALS as a multisystems disorder of limited phenotypic expression. *The Canadian Journal of Neurological Sciences,* 28**,** 283-298.

226. STRONG, M. J. 2008. The syndromes of frontotemporal dysfunction in amyotrophic lateral sclerosis. *Amyotroph Lateral Scler,* 9**,** 323-38.

227. STRONG, M. J. 2010. The evidence for altered RNA metabolism in amyotrophic lateral sclerosis (ALS). *Journal of the neurological sciences,* 288**,** 1-12.

228. STRONG, M. J., LOMEN-HOERTH, C., CASELLI, R. J., BIGIO, E. H. & YANG, W. 2003. Cognitive impairment, frontotemporal dementia, and the motor neuron diseases. *Annals of neurology,* 54**,** S20-S23.

229. STRONG, M. J., VOLKENING, K., HAMMOND, R., YANG, W., STRONG, W., LEYSTRA-LANTZ, C. & SHOESMITH, C. 2007. TDP43 is a human low molecular weight neurofilament (hNFL) mRNA-binding protein. *Mol Cell Neurosci,* 35**,** 320-7.

230. SUZUKI, N., MAROOF, A. M., MERKLE, F. T., KOSZKA, K., INTOH, A., ARMSTRONG, I., MOCCIA, R., DAVIS-DUSENBERY, B. N. & EGGAN, K. 2013. The mouse C9ORF72 ortholog is enriched in neurons known to degenerate in ALS and FTD. *Nature neuroscience,* 16**,** 1725-1727.

231. SWARUP, V., AUDET, J. N., PHANEUF, D., KRIZ, J. & JULIEN, J. P. 2012. Abnormal regenerative responses and impaired axonal outgrowth after nerve crush in TDP-43 transgenic mouse models of amyotrophic lateral sclerosis. *J Neurosci,* 32**,** 18186-95.

232. TAO, Z., WANG, H., XIA, Q., LI, K., LI, K., JIANG, X., XU, G., WANG, G. & YING, Z. 2015. Nucleolar stress and impaired stress granule formation contribute to C9orf72 RAN translation-induced cytotoxicity. *Human molecular genetics***,** ddv005.

233. TIAN, T., HUANG, C., TONG, J., YANG, M., ZHOU, H. & XIA, X. 2011. TDP-43 potentiates alpha-synuclein toxicity to dopaminergic neurons in transgenic mice.

234. TODD, P. K. & PAULSON, H. L. 2010. RNA-mediated neurodegeneration in repeat expansion disorders. *Annals of neurology,* 67**,** 291-300.

235. TOLINO, M., KÖHRMANN, M. & KIEBLER, M. A. 2012. RNA-binding proteins involved in RNA localization and their implications in neuronal diseases. *European Journal of Neuroscience,* 35**,** 1818-1836.

236. TOLLERVEY, J. R., CURK, T., ROGELJ, B., BRIESE, M., CEREDA, M., KAYIKCI, M., KÖNIG, J., HORTOBÁGYI, T., NISHIMURA, A. L. & ŽUPUNSKI, V. 2011a. Characterizing the RNA targets and position-dependent splicing regulation by TDP-43. *Nature neuroscience,* 14**,** 452-458.

237. TOLLERVEY, J. R., CURK, T., ROGELJ, B., BRIESE, M., CEREDA, M., KAYIKCI, M., KONIG, J., HORTOBAGYI, T., NISHIMURA, A. L., ZUPUNSKI, V., et al. 2011b. Characterizing the RNA targets and position-dependent splicing regulation by TDP-43. *Nat Neurosci,* 14**,** 452-8.

238. TRIPATHI, V. B., BASKARAN, P., SHAW, C. E. & GUTHRIE, S. 2014. Tar DNA-binding protein-43 (TDP-43) regulates axon growth in vitro and in vivo. *Neurobiol Dis,* 65**,** 25-34.

239. TROAKES, C., MAEKAWA, S., WIJESEKERA, L., ROGELJ, B., SIKLÓS, L., BELL, C., SMITH, B., NEWHOUSE, S., VANCE, C. & JOHNSON, L. 2012. An MND/ALS phenotype associated with C9orf72 repeat expansion: Abundant p62-positive, TDP-43-negative inclusions in cerebral cortex, hippocampus and cerebellum but without associated cognitive decline. *Neuropathology,* 32**,** 505-514.

240. TSAI, C.-P., SOONG, B.-W., TU, P.-H., LIN, K.-P., FUH, J.-L., TSAI, P.-C., LU, Y.-C., LEE, I.-H. & LEE, Y.-C. 2012. A hexanucleotide repeat expansion in C9ORF72 causes familial and sporadic ALS in Taiwan. *Neurobiology of aging,* 33**,** 2232. e11-2232. e18.

241. TSAI, K.-J., YANG, C.-H., FANG, Y.-H., CHO, K.-H., CHIEN, W.-L., WANG, W.-T., WU, T.-W., LIN, C.-P., FU, W.-M. & SHEN, C.-K. J. 2010. Elevated expression of TDP-43 in the forebrain of mice is sufficient to cause neurological and pathological phenotypes mimicking FTLD-U. *The Journal of experimental medicine,* 207**,** 1661-1673.

242. TSAO, W., JEONG, Y. H., LIN, S., LING, J., PRICE, D. L., CHIANG, P.-M. & WONG, P. C. 2012. Rodent models of TDP-43: recent advances. *Brain research,* 1462**,** 26-39.

243. UDAN, M. & BALOH, R. H. 2011. Implications of the prion-related Q/N domains in TDP-43 and FUS. *Prion,* 5**,** 1-5.

244. VAN BLITTERSWIJK, M., DEJESUS-HERNANDEZ, M., NIEMANTSVERDRIET, E., MURRAY, M. E., HECKMAN, M. G., DIEHL, N. N., BROWN, P. H., BAKER, M. C., FINCH, N. A. & BAUER, P. O. 2013. Association between repeat sizes and clinical and pathological characteristics in carriers of C9ORF72 repeat expansions (Xpansize-72): a cross-sectional cohort study. *The Lancet Neurology,* 12**,** 978-988.

245. VAN BLITTERSWIJK, M., DEJESUS-HERNANDEZ, M. & RADEMAKERS, R. 2012a. How do C9ORF72 repeat expansions cause ALS and FTD: can we learn from other non-coding repeat expansion disorders? *Current opinion in neurology,* 25**,** 689.

246. VAN BLITTERSWIJK, M., DEJESUS-HERNANDEZ, M. & RADEMAKERS, R. 2012b. How do C9ORF72 repeat expansions cause amyotrophic lateral sclerosis and frontotemporal dementia: can we learn from other noncoding repeat expansion disorders? *Curr Opin Neurol,* 25**,** 689-700.

247. VAN BLITTERSWIJK, M., MULLEN, B., WOJTAS, A., HECKMAN, M. G., DIEHL, N. N., BAKER, M. C., DEJESUS-HERNANDEZ, M., BROWN, P. H., MURRAY, M. E. & HSIUNG, G.-

Y. R. 2014. Genetic modifiers in carriers of repeat expansions in the C9ORF72 gene. *Molecular neurodegeneration,* 9**,** 1-10.

248. VAN DEERLIN, V. M., LEVERENZ, J. B., BEKRIS, L. M., BIRD, T. D., YUAN, W., ELMAN, L. B., CLAY, D., WOOD, E. M., CHEN-PLOTKIN, A. S. & MARTINEZ-LAGE, M. 2008. TARDBP mutations in amyotrophic lateral sclerosis with TDP-43 neuropathology: a genetic and histopathological analysis. *The Lancet Neurology,* 7**,** 409-416.

249. VAN DER ZEE, J., GIJSELINCK, I., DILLEN, L., VAN LANGENHOVE, T., THEUNS, J., ENGELBORGHS, S., PHILTJENS, S., VANDENBULCKE, M., SLEEGERS, K. & SIEBEN, A. 2013. A Pan-European Study of the C9orf72 Repeat Associated with FTLD: Geographic Prevalence, Genomic Instability, and Intermediate Repeats. *Human mutation,* 34**,** 363-373.

250. VAN EERSEL, J., KE, Y. D., GLADBACH, A., BI, M., GÖTZ, J., KRIL, J. J. & ITTNER, L. M. 2011. Cytoplasmic accumulation and aggregation of TDP-43 upon proteasome inhibition in cultured neurons. *PLoS One,* 6**,** e22850.

251. VAN RHEENEN, W., VAN BLITTERSWIJK, M., HUISMAN, M. H., VLAM, L., VAN DOORMAAL, P. T., SEELEN, M., MEDIC, J., DOOIJES, D., DE VISSER, M. & VAN DER KOOI, A. J. 2012. Hexanucleotide repeat expansions in C9ORF72 in the spectrum of motor neuron diseases. *Neurology,* 79**,** 878-882.

252. VANACOVA, S. & STEFL, R. 2007. The exosome and RNA quality control in the nucleus. *EMBO reports,* 8**,** 651-657.

253. VANCE, C., AL-CHALABI, A., RUDDY, D., SMITH, B. N., HU, X., SREEDHARAN, J., SIDDIQUE, T., SCHELHAAS, H. J., KUSTERS, B. & TROOST, D. 2006. Familial amyotrophic lateral sclerosis with frontotemporal dementia is linked to a locus on chromosome 9p13. 2–21.3. *Brain,* 129**,** 868-876.

254. VANCE, C., ROGELJ, B., HORTOBÁGYI, T., DE VOS, K. J., NISHIMURA, A. L., SREEDHARAN, J., HU, X., SMITH, B., RUDDY, D. & WRIGHT, P. 2009. Mutations in FUS, an RNA processing protein, cause familial amyotrophic lateral sclerosis type 6. *Science,* 323**,** 1208-1211.

255. VOIGT, A., HERHOLZ, D., FIESEL, F. C., KAUR, K., MÜLLER, D., KARSTEN, P., WEBER, S. S., KAHLE, P. J., MARQUARDT, T. & SCHULZ, J. B. 2010. TDP-43-mediated neuron loss in vivo requires RNA-binding activity. *PloS one,* 5**,** e12247.

256. VOLKENING, K., LEYSTRA-LANTZ, C., YANG, W., JAFFEE, H. & STRONG, M. J. 2009. Tar DNA binding protein of 43 kDa (TDP-43), 14-3-3 proteins and copper/zinc superoxide dismutase (SOD1) interact to modulate NFL mRNA stability. Implications for altered RNA processing in amyotrophic lateral sclerosis (ALS). *Brain research,* 1305**,** 168-182.

257. WALLING, A. D. 1999. Amyotrophic lateral sclerosis: Lou Gehrig's disease. *Am Fam Physician,* 59**,** 1489-96.

258. WANG, H.-Y., WANG, I.-F., BOSE, J. & SHEN, C.-K. J. 2004. Structural diversity and functional implications of the eukaryotic TDP gene family. *Genomics,* 83**,** 130-139.

259. WANG, I.-F., WU, L.-S. & SHEN, C. J. 2008a. TDP-43: an emerging new player in neurodegenerative diseases. *Trends in molecular medicine,* 14**,** 479-485.

260. WANG, I., WU, L. S., CHANG, H. Y. & SHEN, C. K. J. 2008b. TDP-43, the signature protein of FTLD-U, is a neuronal activity-responsive factor. *Journal of neurochemistry,* 105**,** 797-806.

261. WEGORZEWSKA, I. & BALOH, R. H. 2011. TDP-43-based animal models of neurodegeneration: new insights into ALS pathology and pathophysiology. *Neurodegener Dis,* 8**,** 262-74.

262. WEGORZEWSKA, I., BELL, S., CAIRNS, N. J., MILLER, T. M. & BALOH, R. H. 2009. TDP-43 mutant transgenic mice develop features of ALS and frontotemporal lobar degeneration. *Proc Natl Acad Sci U S A,* 106**,** 18809-14.

263. WEN, X., TAN, W., WESTERGARD, T., KRISHNAMURTHY, K., MARKANDAIAH, S. S., SHI, Y., LIN, S., SHNEIDER, N. A., MONAGHAN, J., PANDEY, U. B., et al. 2014. Antisense proline-arginine RAN dipeptides linked to C9ORF72-ALS/FTD form toxic nuclear aggregates that initiate in vitro and in vivo neuronal death. *Neuron,* 84**,** 1213-25.

264. WIJESEKERA, L. C. & LEIGH, P. N. 2009. Amyotrophic lateral sclerosis. *Orphanet J Rare Dis,* 4**,** 3.

265. WILSON, C., GRACE, G., MUNOZ, D., HE, B. & STRONG, M. J. 2001. Cognitive impairment in sporadic ALS A pathologic continuum underlying a multisystem disorder. *Neurology,* 57**,** 651-657.

266. WINTON, M. J., IGAZ, L. M., WONG, M. M., KWONG, L. K., TROJANOWSKI, J. Q. & LEE, V. M.-Y. 2008a. Disturbance of nuclear and cytoplasmic TAR DNA-binding protein (TDP-43) induces disease-like redistribution, sequestration, and aggregate formation. *Journal of Biological Chemistry,* 283**,** 13302-13309.

267. WINTON, M. J., IGAZ, L. M., WONG, M. M., KWONG, L. K., TROJANOWSKI, J. Q. & LEE, V. M. 2008b. Disturbance of nuclear and cytoplasmic TAR DNA-binding protein (TDP-43) induces disease-like redistribution, sequestration, and aggregate formation. *J Biol Chem,* 283**,** 13302-9.

268. WINTON, M. J., VAN DEERLIN, V. M., KWONG, L. K., YUAN, W., WOOD, E. M., YU, C.-E., SCHELLENBERG, G. D., RADEMAKERS, R., CASELLI, R. & KARYDAS, A. 2008c. A90V TDP-43 variant results in the aberrant localization of TDP-43 in vitro. *FEBS letters,* 582**,** 2252-2256.

269. WOJCIECHOWSKA, M. & KRZYZOSIAK, W. J. 2011. Cellular toxicity of expanded RNA repeats: focus on RNA foci. *Human molecular genetics,* 20**,** 3811-3821.

270. WOJCIECHOWSKA, M., OLEJNICZAK, M., GALKA-MARCINIAK, P., JAZUREK, M. & KRZYZOSIAK, W. J. 2014. RAN translation and frameshifting as translational challenges at simple repeats of human neurodegenerative disorders. *Nucleic acids research,* 42**,** 11849-11864.

271. WU, L.-S., CHENG, W.-C. & SHEN, C.-K. J. 2012. Targeted depletion of TDP-43 expression in the spinal cord motor neurons leads to the development of amyotrophic

lateral sclerosis-like phenotypes in mice. *Journal of Biological Chemistry,* 287**,** 27335-27344.

272. XI, Z., ZHANG, M., BRUNI, A. C., MALETTA, R. G., COLAO, R., FRATTA, P., POLKE, J. M., SWEENEY, M. G., MUDANOHWO, E., NACMIAS, B., et al. 2015. The C9orf72 repeat expansion itself is methylated in ALS and FTLD patients. *Acta Neuropathol,* 129**,** 715-27.

273. XI, Z., ZINMAN, L., MORENO, D., SCHYMICK, J., LIANG, Y., SATO, C., ZHENG, Y., GHANI, M., DIB, S. & KEITH, J. 2013. Hypermethylation of the CpG island near the G 4 C 2 repeat in ALS with a C9orf72 expansion. *The American Journal of Human Genetics,* 92**,** 981-989.

274. XIAO, S., SANELLI, T., DIB, S., SHEPS, D., FINDLATER, J., BILBAO, J., KEITH, J., ZINMAN, L., ROGAEVA, E. & ROBERTSON, J. 2011. RNA targets of TDP-43 identified by UV-CLIP are deregulated in ALS. *Molecular and Cellular Neuroscience,* 47**,** 167-180.

275. XU, Y. F., ZHANG, Y. J., LIN, W. L., CAO, X., STETLER, C., DICKSON, D. W., LEWIS, J. & PETRUCELLI, L. 2011. Expression of mutant TDP-43 induces neuronal dysfunction in transgenic mice. *Mol Neurodegener,* 6**,** 73.

276. XU, Z., POIDEVIN, M., LI, X., LI, Y., SHU, L., NELSON, D. L., LI, H., HALES, C. M., GEARING, M. & WINGO, T. S. 2013. Expanded GGGGCC repeat RNA associated with amyotrophic lateral sclerosis and frontotemporal dementia causes neurodegeneration. *Proceedings of the National Academy of Sciences,* 110**,** 7778-7783.

277. XU, Z. S. 2012. Does a loss of TDP-43 function cause neurodegeneration? *Mol Neurodegener,* 7**,** 27.

278. YAMAKAWA, M., ITO, D., HONDA, T., KUBO, K.-I., NODA, M., NAKAJIMA, K. & SUZUKI, N. 2014. Characterization of the dipeptide repeat protein in the molecular pathogenesis of c9FTD/ALS. *Human molecular genetics***,** ddu576.

279. YANG, C., TAN, W., WHITTLE, C., QIU, L., CAO, L., AKBARIAN, S. & XU, Z. 2010. The C-terminal TDP-43 fragments have a high aggregation propensity and harm neurons by a dominant-negative mechanism. *PloS one,* 5**,** e15878.

280. ZAGO, S., POLETTI, B., MORELLI, C., DORETTI, A. & SILANI, V. 2011. Amyotrophic lateral sclerosis and frontotemporal dementia (ALS-FTD). *Archives italiennes de biologie,* 149**,** 39-56.

281. ZHANG, Y.-J., JANSEN-WEST, K., XU, Y.-F., GENDRON, T. F., BIENIEK, K. F., LIN, W.-L., SASAGURI, H., CAULFIELD, T., HUBBARD, J. & DAUGHRITY, L. 2014. Aggregation-prone c9FTD/ALS poly (GA) RAN-translated proteins cause neurotoxicity by inducing ER stress. *Acta neuropathologica,* 128**,** 505-524.

282. ZHANG, Y.-J., XU, Y.-F., COOK, C., GENDRON, T. F., ROETTGES, P., LINK, C. D., LIN, W.-L., TONG, J., CASTANEDES-CASEY, M. & ASH, P. 2009. Aberrant cleavage of TDP-43 enhances aggregation and cellular toxicity. *Proceedings of the National Academy of Sciences,* 106**,** 7607-7612.

283. ZHANG, Y. J., XU, Y. F., DICKEY, C. A., BURATTI, E., BARALLE, F., BAILEY, R., PICKERING-BROWN, S., DICKSON, D. & PETRUCELLI, L. 2007. Progranulin mediates caspase-dependent cleavage of TAR DNA binding protein-43. *J Neurosci,* 27**,** 10530-4.

284. ZHOU, H., HUANG, C., CHEN, H., WANG, D., LANDEL, C. P., XIA, P. Y., BOWSER, R., LIU, Y.-J. & XIA, X. G. 2010. Transgenic rat model of neurodegeneration caused by mutation in the TDP gene. *PLoS Genet,* 6**,** e1000887.

285. ZU, T., GIBBENS, B., DOTY, N. S., GOMES-PEREIRA, M., HUGUET, A., STONE, M. D., MARGOLIS, J., PETERSON, M., MARKOWSKI, T. W. & INGRAM, M. A. 2011. Non-ATG–initiated translation directed by microsatellite expansions. *Proceedings of the National Academy of Sciences,* 108**,** 260-265.

286. ZU, T., LIU, Y., BAÑEZ-CORONEL, M., REID, T., PLETNIKOVA, O., LEWIS, J., MILLER, T. M., HARMS, M. B., FALCHOOK, A. E. & SUBRAMONY, S. 2013. RAN proteins and RNA foci from antisense transcripts in C9ORF72 ALS and frontotemporal dementia. *Proceedings of the National Academy of Sciences,* 110**,** E4968-E4977.